Ketocarotenoid production in *Solanum lycopersicum*; biosynthesis and sequestration

Esther Ruth Lewis

This thesis was submitted for the degree of Doctor of Philosophy at Royal Holloway, University of London, March 2020

Declaration of Authorship

I, Esther Ruth Lewis, hereby declare that the work presented in this thesis is the original work of the author unless otherwise stated. Original material used in the production of this thesis has not been previously submitted either in part or whole for a degree of any description from any institution.

Signed: 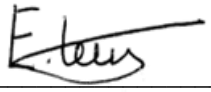

Date: 30/03/2020

Abstract

Carotenoids are natural pigments with important antioxidant properties. Commercially they have been exploited across multiple industrial sectors, including aquaculture, health supplements, and food-related industries. Currently carotenoids are produced predominantly by chemical synthesis using precursors from the petrochemical industry. The unfavourable environmental impact of these procedures means new sustainable production platforms are being sought with rapidity. The production of ketocarotenoids is especially desirable, with industries such as aquaculture reliant on their pigmentation and antioxidant effects.

Previous work has led to the biosynthesis of ketocarotenoids and ketocarotenoid esters in tomato fruit. The bacterial genes carotenoid hydroxylase (*Crt*Z) and oxygenase (*Crt*W) have been combined with the overexpression of lycopene β-cyclase (*cyc-b*). The present study focusses on improvement of the previous approach to ketocarotenoid production, firstly by addition of beta carotene hydroxylase (*Crt*R-*b2*), and secondly using a single, multigene construct designed for ketocarotenoid production. The addition of *Crt*R-*b2* has increased the amount of astaxanthin produced within tomato fruit to 650 μg/g. However, the complexity of the background means each generation has a complicated segregation pattern, and the resulting screening is laborious. Therefore, an alternative approach is desirable. The use of a single, multigene construct has been employed to transform *Crt*W, *Crt*R-*b2* and an alternative cyclase, lycopene beta-cyclase (*lcy*) into tomato. Stable transformation of this multigene construct resulted in a T_0 generation which accumulated predominantly lycopene, however the ketocarotenoids astaxanthin and phoenicoxanthin were also produced.

Esterification plays an important role in the bioavailability and sequestration of the ketocarotenoids. As carotenoid esterification does not normally occur in tomato fruit, the gene responsible for this process is unknown. The pale yellow petal (*pyp*) gene has previously been identified as an important acyltransferase in tomato flower, with mutants displaying a paler petal phenotype and a lack of carotenoid esters. In this work the ketocarotenoid producing genotype has been genetically crossed with the *pyp*-1 mutant line in order to elucidate the potential role of *pyp* in esterification of ketocarotenoids. The presence of the *pyp* mutation in ketocarotenoid producing fruit caused a complete absence of carotenoid esters, this corroborates that the *pyp* gene is necessary and involved in the esterification of ketocarotenoids in fruit.

Acknowledgements

I would like to thank everyone who has helped me through my Ph.D., from academic help, to answering my stupid questions, to keeping my morale high. I would like to say a very special thank you to Paul Fraser, who offered me this opportunity and has given me his support and knowledge which have helped me to achieve this. Without his sense of humour, I would never have been 'Esther who works on esters'.

To everyone else in the Fraser group, I would like to say thank you. You have all helped in one way or another and have been a great pool of knowledge. You have also made the Ph.D. process much more enjoyable, making morning tea and lunchtime a fun respite from the hard work. In particular, I would not have been able to accomplish this without Genny Enfissi or Marilise Nogueira, who have both offered constant encouragement and expertise.

Finally, I would like to thank those who have helped me more personally. Thank you to my parents, Shirley Lewis and Glenn Lewis, who have encouraged me through my education and been there when I need them. I would also like to thank my partner, Jacob Dunstan who has always supported me and understood the challenges faced.

Contents

List of figures

List of tables

Abbreviations

5'UTR	5’ untranslated region
ABA	abscisic acid
AMDIS	automated mass spectral deconvolution and identification system
ANOVA	analysis of variance
APCI	atmospheric pressure chemical ionisation
BCO	beta-carotene 15,15'-monooxygenase
BHY	beta-carotene hydroxylase
BKT	carotenoid oxygenase
CaMV	cauliflower mosaic virus
CAS	CRISPR associated protein
CBFD	carotenoid beta-ring 4-dehydrogenase
CCD	carotenoid cleavage dioxygenase
CDS	coding region
CM	Chylomicron
CRISPR	clustered regularly interspaced short palindromic repeats
CRTB	phytoene synthase
CRTE	geranylgeranyl pyrophosphate synthase
CRTI	phytoene desaturase
CRTISO	carotene isomerase
CRTO	carotenoid oxygenase
CRTR	carotenoid reductase
CRTR-B1/2	beta-carotene hydroxylase
CRTS	astaxanthin synthase
CRTW (W)	carotenoid oxygenase
CRTY	lycopene beta-cyclase
CRTZ (Z)	carotenoid hydroxylase
CYC-B	lycopene beta cyclase
DAG	Diacylglycerol
DET1	de-etiolated1
DGDG	Digalactosyldiacylglycerol
DMAPP	dimethylallyl pyrophosphate
DMS	dimethyl sulphate
DNA	deoxyribonucleic acid
dNTP	deoxynucleotide triphosphates
DXP	1-deoxy-D-xylulose
EMS	ethyl methansulphonate
EU	European Union
FPP	farnesyl pyrophosphate
GA3P	glyceraldehyde-3-phosphate
GBSS	granule bound starch synthase

GC/MS	gas chromatography mass spectroscopy
GDSL	Gly-Asp-Ser-Leu esterase/lipase
GGPP	geranylgeranyl pyrophosphate
GGPPS	geranylgeranyl diphosphate synthase
GM	genetic modification
GPP	geranyl pyrophosphate
GWAS	genome wide association study
HBFD	4-hydroxy-beta-ring 4-dehydrogenase
HF	high fidelity
HMG-CoA	3-hydroxy-3-methylglutaryl CoA
HPLC	high-performance liquid chromatography
HR	homologous repair
HRM	high resolution melt
IDI	isopentneyl pyrophosphate isomerase
IPI	isopentenyl diphosphate isomerase
IPP	isopentenyl diphosphate
IPTG	isopropyl beta-D-1-thiogalactopyranoside
LB	Lucia broth
LC/MS	liquid chromatography mass spectroscopy
LCY-b	beta-cyclase
LCY-e	epsilon-cyclase
LD	linkage disequilibrium
LDL	low density lipoprotein
LHC	light harvesting complex
LMW	low molecular weight
LPAT	lysophospholipid acyltransferase
MAG	Monoacylglycerol
MEOX	methoxyamine hydrochloride
MEP	methyleryhritol phosphate
MGDG	Monogalactosyldiacylglycerol
MoClo	modular cloning toolkit
MPS	multipurpose sampler
MS	Murashige and Skoog
MSD	mass selective detector
MSTFA	N-methyl-N-(trimethylsilyl) trifluoroacetamide
MVA	Mevalonic
NCED	nine-*cis*-epoxycarotenoid dioxygenases
NHEJ	non-homologous end joining
NIST	National Institute of Standards and Technology
NMR	nuclear magnetic resonance
NTG	N-methyl-N′-nitro-N-nitroso-guanidine
NXS	neoxanthin synthase

PAM	protospacer adjacent motif
PAR	photosynthetically active radiation
PCA	principal component analysis
PCR	polymerase chain reaction
PDA	photo diode array
PDS	phytoene desaturase
PE	Phosphotidylethanolamine
PES	phytyl ester synthase
PG	Phosphatidylcholine
PPC2	phosphoenolpyruvate carboxylase
PSII	photosystem II
PSY	phytoene synthase
PYP	pale yellow petal acyltransferase
qPCR	quantitative (real time) PCR
QTL	quantitative trait loci
Q-TOF	quantitive time of flight
RBC	Rubisco
RI	high beta-carotene background
RNA	ribonucleic acid
ROS	reactive oxygene species
RT	reverse transcripton
SNP	single nucleotide polymorphism
SP	signalling peptide
SPME	solid-phase microextraction
TAG	Triacylglycerol
TCA	tricarboxylic acid
TILLING	targeting induced local lesions in genomes
TLC	thin layer chromatography
Tm	melting temperature
TPRP	tomato pro-rich promoter
UBQ	Ubiquitin
UPLC	ultra-high-performance liquid chromatography
UU/U0/00	various zygosities for the overexpression of *Crt*R-*b2*
UV	Ultraviolet
VAD	vitamin A deficiency
VDE	violaxanthin de-epoxidase
VLDL	very low density lipoprotein
XAT	xanthophyll acyltransferase
YEB	yeast extract beef
ZDS	zeta-carotene desaturase
ZEP	zeaxanthin epoxidase
ZISO	zeta-carotene isomerase

Chapter I:
Introduction

1.1 *Solanum lycopersicum*

1.1.1 Solanaceae family

The Solanaceae family contains more than 3000 species, including many notable crops; tomato, pepper, tobacco, potato and aubergine, which can be found all over the world. The family is very diverse, both in morphology and geographical location (Knapp, 2002; Mueller, *et al.*, 2005). Within the family there are several genera, with tomato, aubergine and potato belonging to *Solanum*. Due to the wide range of diversity seen in *Solanum*, it contains many plants useful for their pharmaceutical and medical properties as well as containing important food crops (Kaunda & Zhang, 2019). Tomatoes themselves originate from South America, and it was here that the domestication process begun. After arriving into Europe and North America they underwent concentrated domestication to create the cultivated tomato, *S. lycopersicum* (Bai, 2007). Along with the domestic variety, there are 12 other wild varieties which provide a pool of genetic diversity that is a potential source of desirable traits for future crop development. The genetic diversity within the cultivated *S. lycopersicum* is minimal and has resulted in a relatively small genome with few gene duplication events (Bergougnoux, 2014); these features make tomato ideal as a model organism.

1.1.2 Global market

Tomato is one of the most widely consumed fruits. It is grown worldwide, either outside, or if the climate doesn't allow for field production, under controlled glasshouse conditions. Recently tomato production in Asia has overtaken that from Europe and America (Bergougnoux, 2014), however the single biggest producer remains the Netherlands which produces 0.5 million kg per hectare per year (FAOSTAT, 2017). Tomatoes are versatile, and are consumed in many forms; raw, cooked, paste, juice and dried. This versatility may be responsible for the 182 million tons produced each year (Quinet, *et al.*, 2019). Their popularity is also, in part, due to them often being viewed as a health food. Tomatoes are naturally rich in carotenoids and vitamins, with lycopene being a major constituent of their beneficial bioactive compounds (Viuda-Martos, *et al.*, 2014).

1.1.3 Scientific resources

With tomatoes providing a rich source of carotenoids, the engineering to alter and improve them over many years has provided a large pool of resources. The tomato genome has been fully sequenced by 14 countries over eight years (Tomato Genome Consortium, 2012). There have also been several iterations since the first release in 2012 (SGN, 2014), with the latest build (SL4.0) released in 2019. With the advent of new technologies the annotations of the genomes will only continue to improve (Sun, *et al.*, 2019). Tomato has the most extensively researched proteome of the Solanaceae family (Ghatak, *et al.*, 2017).

The diversity of growing conditions for tomatoes has allowed for its use as a model crop. Since tomatoes are grown worldwide, including in artificial conditions, they can be grown and studied with ease. Environmental conditions can be altered, and various stresses applied within a contained environment. Unlike many plants, such as tobacco, the growth cycle of tomato is relatively short. Tomatoes reach maturation and fruit set approximately two months after germination. They can also be indeterminate allowing for a constant supply of fruit. Tomatoes are amenable to genetic modification; plants can regenerate from callus allowing for a stable transformation. Grafting is also viable on tomatoes, as is regeneration from side shoots. Furthermore, tomatoes are rich in secondary metabolites including carotenoids. Tomato fruit accumulates lycopene, and therefore provide a good platform for the enhancement of carotenoid production. All of these traits make tomatoes a practical organism for research.

1.2 Carotenoids

1.2.1 Structure

Carotenoids represent a wide range of molecules, most of which are comprised of 40 carbons, however the higher carotenoids contain 45 or 50 carbons (Maoka, 2020). C40 carotenoids are synthesised from eight isopentenyl diphosphate (IPP) units (Britton, *et al.*, 2004). There are around 850 naturally occurring carotenoids, and there are more that have been chemically synthesised, but not yet found in nature. A long hydrocarbon chain provides the polyene chain backbone of carotenoids (Figure 1-1) with other elements sometimes featuring on the end groups, such as in the oxygen containing xanthophylls, i.e. violaxanthin. Carotenes are carotenoids which are pure hydrocarbons, such as beta-carotene, and there have been

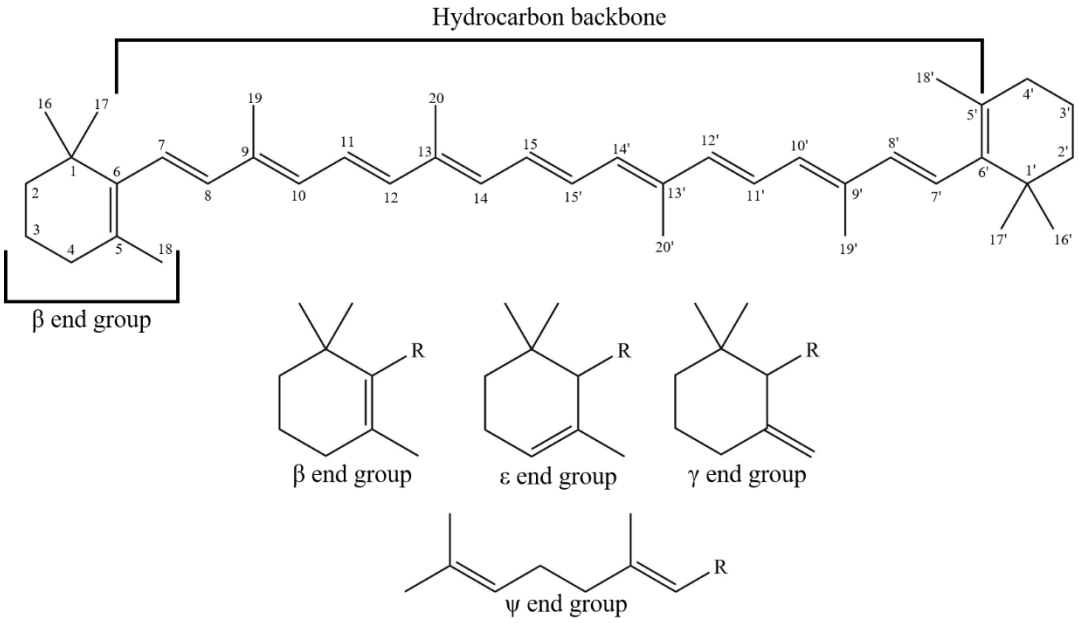

Figure 1-1. Example carotenoid structure
The structure above shows beta-carotene, with two β rings attached to the hydrocarbon backbone. The other end groups which are observed in plants are also shown, R represents the carotenoid backbone.

approximately 50 found so far in nature (Maoka, 2020). The backbone and end groups can also vary, the chain can be straight, or cyclisation can provide various ring sizes, most commonly five or six membered rings. The conformation of the ring provides multiple isomers, with the position of the double bond dictating the isomer observed. There are four end groups observed in higher plants (Figure 1-1). Carotenoids can undergo further modifications, such as breakdown into smaller compounds called apocarotenoids. Carotenoids can also undergo other modifications, such as esterification with fatty acids or sugars or conjugation with proteins. The carotenoids are often coloured and provide pigmentation across a range of organisms. Carotenoids are synthesised in bacteria, fungi, algae and plants, but are not commonly made *de novo* in animals.

1.2.2 Biosynthesis and sequestration

1.2.2.1 Formation of phytoene

The initial building block for carotenoids is the IPP unit. Within plants there are two routes for the biosynthesis of IPP, via acetyl-coA in the mevalonic (MVA) pathway and via methylerythritol in the methylerythritol phosphate (MEP) pathway (Eisenreich, *et al.*, 1998). The MVA pathway is commonly seen across multiple organism and occurs in the cytoplasm

whereas the MEP pathway is limited to cyanobacteria and plants and is localised to the plastid (Eisenreich, *et al.*, 2001; Hemmerlin, *et al.*, 2012) (Figure 1-2). The discovery of the MEP pathway occurred after there were discrepancies in radiolabelling experiments which indicated an alternative process for the synthesis of IPP, or its isomer dimethylallyl pyrophosphate (DMAPP) (Rohmer, 1993).

To proceed from IPP to carotenoids, there are several reaction steps (Figure 1-3) which take place to combine the IPP, or DMAPP units into longer isoprenoids. Firstly, 'head to tail' condensation reactions occur to join the five carbon building blocks together to form isoprene units such as the C10 geranyl pyrophosphate (GPP) and C20 geranylgeranyl pyrophosphate (GGPP) (Fraser & Bramley, 2004). This is then followed by 'head to head' condensation reactions of the GGPP units to form the colourless C40 molecule, phytoene. This is carried out by the enzyme phytoene synthase (PSY) and represents the first committed step in carotenoid formation.

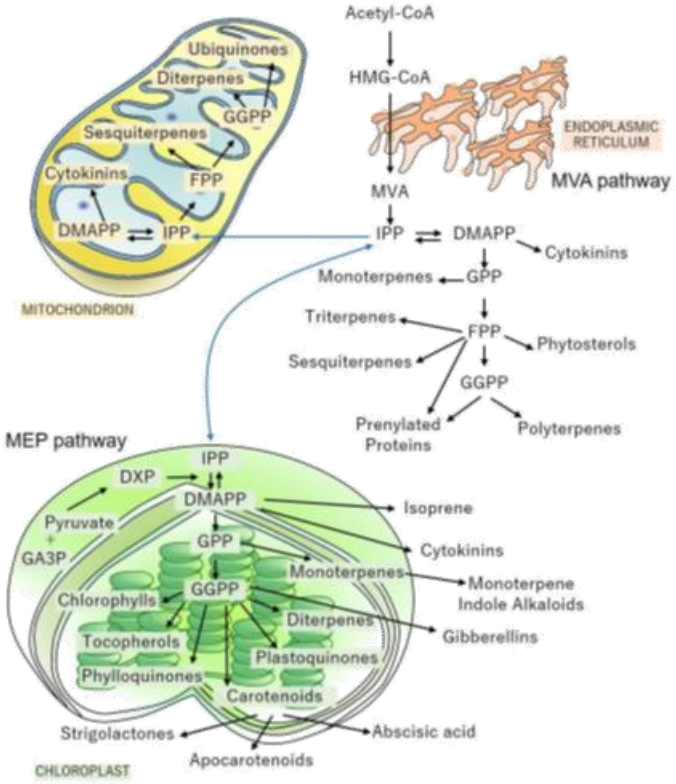

Figure 1-2. The MVA and MEP pathways including the compartmentalisation of reactions
The MVA pathway occurs within the cytoplasm, the MEP pathway occurs in the plastids. After the formation of IPP, condensation reactions occur to form longer isoprene units. HMG-CoA, 3-hydroxy-3-methylglutaryl CoA; FPP, farnesyl pyrophosphate; DXP, 1-deoxy-D-xylulose; GA3P, glyceraldehyde-3-phosphate. Adapted from (Nogueira, *et al.*, 2018).

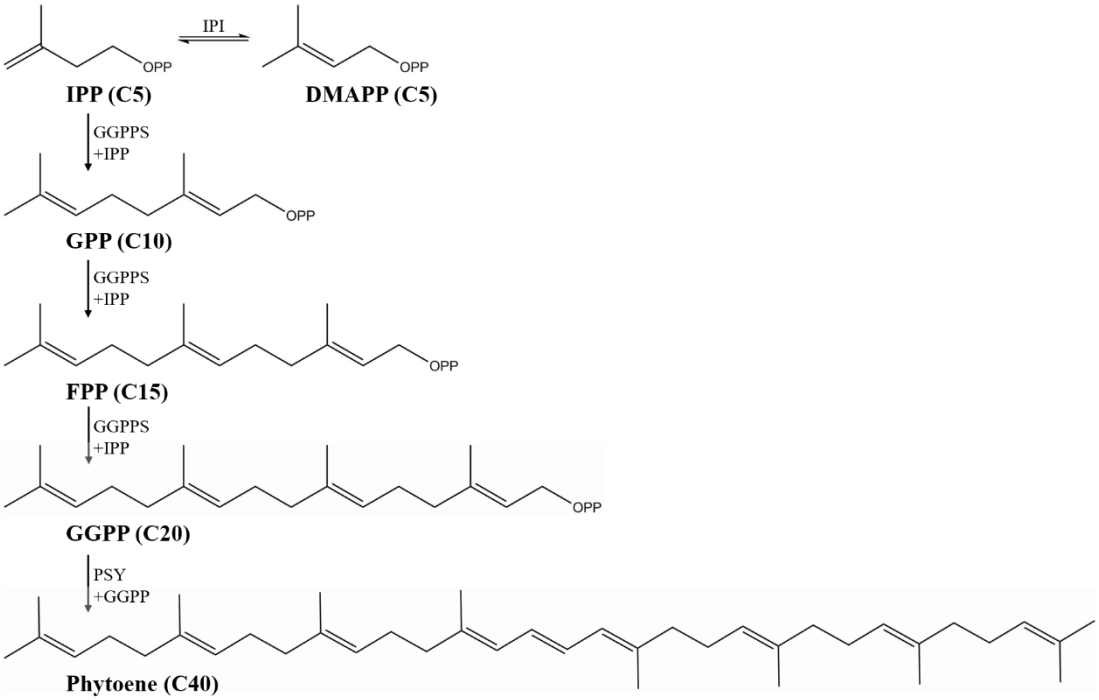

Figure 1-3. Biosynthesis of phytoene from IPP units
Carbon number shown in parentheses. IPP, isopentenyl pyrophosphate; DMAPP, dimethyl pyrophosphate; GPP, geranyl diphosphate; FPP, farnesyl diphosphate; GGPP, geranylgeranyl diphosphate; IPI, isopentenyl diphosphate isomerase; GGPPS, geranylgeranyl diphosphate synthase; PSY, phytoene synthase.

1.2.2.2 Formation of lycopene

The pathway from phytoene to lycopene, once again requires several steps (Figure 1-4). The first steps are four desaturation reactions converting phytoene to lycopene. The first two steps are performed by phytoene desaturase (PDS) to form zeta-carotene via phytofluene (Aracri, *et al.*, 1994; Mann, *et al.*, 1994). Secondly zeta-carotene desaturase (ZDS) acts to form lycopene via neurosporene (Fraser & Bramley, 2004). The extension of the conjugation extends the chromophore, and therefore, lycopene appears red.

The predominant isomer of phytoene that is observed in higher plants is the 15-*cis* form, however lycopene is most commonly seen in the all-*trans* form, therefore, to facilitate the production of all-*trans*-lycopene isomerisation reactions must occur. This is currently thought to be carried out by carotene isomerase (CRTISO) and zeta-carotene isomerase (ZISO) (Fantini, *et al.*, 2013; Isaacson, *et al.*, 2004; Isaacson, *et al.*, 2002).

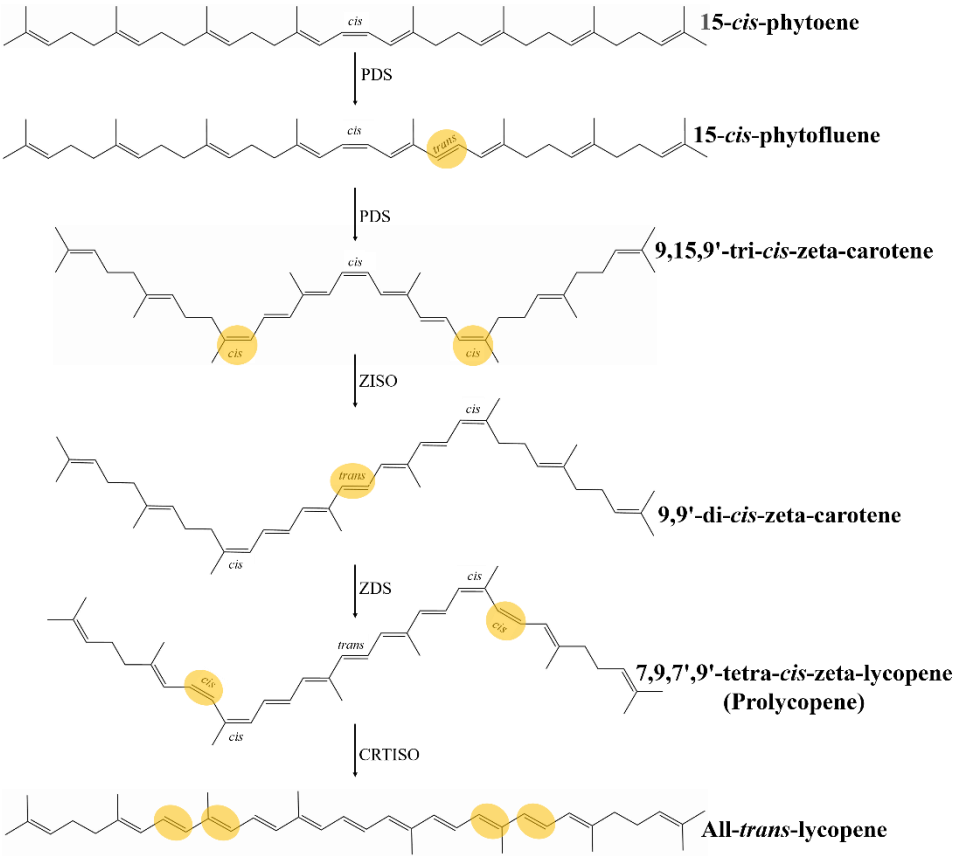

Figure 1-4. Formation of lycopene from phytoene
Orange circles highlights the double bond where isomerisation or desaturation occurs. PDS, phytoene desaturase; ZISO, zeta-carotene isomerase; ZDS, zeta-carotene desaturase; CRTISO, carotene isomerase.

1.2.2.3 Cyclisation to carotenes

The next step towards further carotenoid formation is cyclisation to form cyclohexyl rings. The enzyme epsilon-cyclase (LCY-e) forms an epsilon ring whereas beta-cyclase (LCY-b (also known as CRTL-b)) forms a beta ring (Figure 1-1) (Fraser & Bramley, 2004). The type of enzyme employed, and thus the type of ring formed creates a branching point in the pathway (Figure 1-5). The beta pathway produces gamma-carotene and beta-carotene, these have exclusively beta rings. Conversely, the alpha pathway has delta-carotene and alpha-carotene. Alpha-carotene possesses both ring types, and therefore, requires the action of both LCY-b and LCY-e (Cunningham & Gantt, 2001). In tomato, there are two beta-cyclase enzymes which act at different locales. Lycopene beta cyclase (CYC-B) acts predominately in the chromoplast whereas LCY-b acts in the chloroplasts (Ronen, *et al.*, 2000), (Bouvier, *et al.*, 2000), (Mohan, *et al.*, 2016).

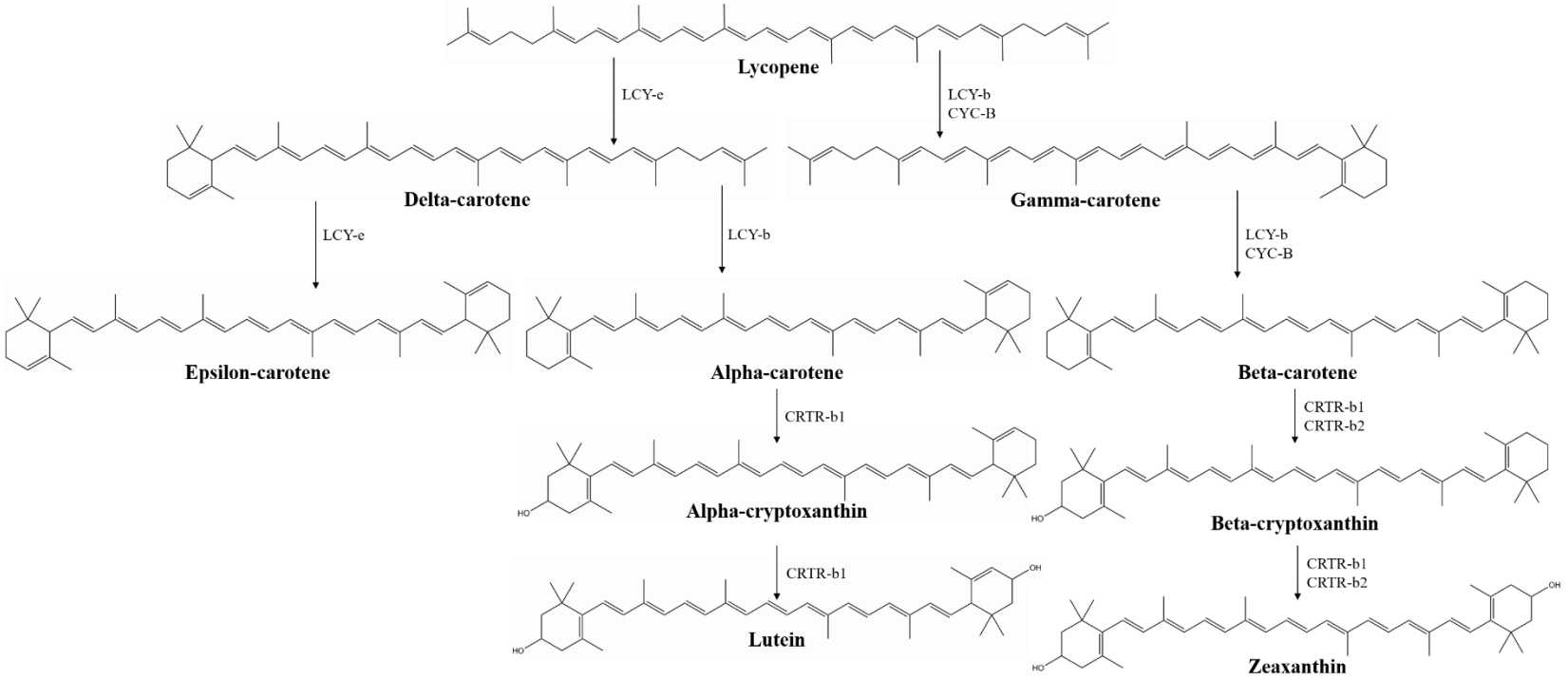

Figure 1-5. Cyclisation and hydroxylation reactions of carotenoids
LCY-b and CYC-B, lycopene beta cyclase; LCY-e, lycopene epsilon cyclase; CRTR-b1/2, beta-carotene hydroxylase.

1.2.2.4 Plant hydroxylation reactions

The defining feature of xanthophylls is the presence of an oxygen containing group (Fraser, *et al.*, 2009). This moiety increases the polarity of the compound relative to carotenes, and shifts the maximum wavelength for absorption to longer wavelengths (Harker & Hirschberg, 1998). Figure 1-5 and Figure 1-6 show the pathway for hydroxylation in tomato, which includes both hydroxylation and epoxidation steps, the latter being reversible. Hydroxylation can occur on both the branches that appear after cyclisation. Hydroxylation of alpha-carotene results in alpha-cryptoxanthin and lutein, hydroxylation of beta-carotene produces beta-cryptoxanthin and zeaxanthin. An important enzyme in this pathway is the flower specific beta-carotene hydroxylase (CRTR-b2) which belongs to the non-haem di iron family (DellaPenna & Pogson, 2006). *Crt*R-*b2* expression can only be found in the flowers and to a much lesser extent the roots, there is no expression in the leaf (Galpaz, *et al.*, 2006). The work of D'Ambrosio, *et al.* (2011) showed overexpression of hemizygous *Crt*R-*b2* results in fruit producing seven times more violaxanthin and three times more neoxanthin than control tomatoes. The active hydroxylase in the leaf is CRTR-b1 (Walter & Strack, 2011).

The xanthophyll cycle (Figure 1-6) is an important mechanism for the regulation of light in plants. Epoxidation and de-epoxidation reactions allow for the ratio of zeaxanthin to violaxanthin to be carefully controlled. This provides a mechanism to deal with changing light conditions. Under high light the synthesis of zeaxanthin is dominant, under low light, it is violaxanthin which takes over (Yamamoto, *et al.*, 1962). There is also a mono-epoxidated carotenoid intermediate; antheraxanthin. The epoxidation reactions are carried out by zeaxanthin epoxidase (ZEP) which acts on both zeaxanthin and antheraxanthin to add an epoxy group onto the 5, 6 position of the 3-hydroxyl-beta ring (Fraser & Bramley, 2004). Violaxanthin de-epoxidase (VDE) then removes this epoxide group under high light conditions to revert to zeaxanthin (Rockholm & Yamamoto, 1996).

Neoxanthin is formed from violaxanthin by neoxanthin synthase (NXS, also abbreviated NSY). In place of the epoxide group seen in violaxanthin, neoxanthin has an allene group attaching the end ring to the backbone. The epoxide group is then arranged to a 5-hydroxyl group. The biosynthesis of neoxanthin is not completely understood with the genes involved not fully elucidated. The amino acid sequence of the reported tomato NXS is similar to that of the chomoplastic lycopene beta-cyclase (CYC-B) (Bouvier, *et al.*, 2000; Fraser & Bramley,

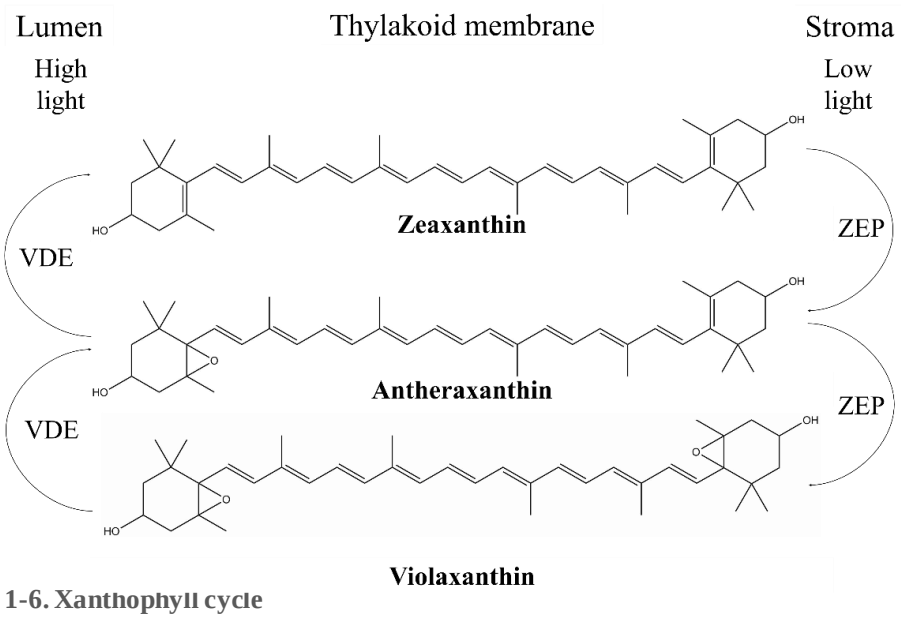

Figure 1-6. Xanthophyll cycle
High light stimulates the action of VDE, low light stimulates ZEP. VDE, violaxanthin de-epoxidase; ZEP, zeaxanthin epoxidase. Adapted from (Racsko & Schrader, 2012)

2004). However, more recent work has also identified the *nxd1* gene as necessary for neoxanthin synthesis, with knock-out mutants lacking neoxanthin (Neuman, *et al.*, 2014).

1.2.2.5 Ketocarotenoid synthesis

The biosynthesis of ketocarotenoids is rarely observed in higher plants, with only one exception reported (Seybold & Goodwin, 1959). The flowers of *Adonis aestivalis* and *Adonis annua* accumulate astaxanthin, causing a deep red colour. Most plants lack a carotenoid oxygenase, and therefore synthesis of the ketocarotenoids is impossible. However, *Adonis* does employ an oxygenase, which seems to have developed separately from those seen in bacteria (discussed below). The *Adonis* oxygenase more closely resembles the plant beta-carotene hydroxylase enzymes (Li, *et al.*, 2008) possibly suggesting an alternative route for synthesis of ketocarotenoids; rather than the addition of a keto groups to the beta-ring, the group is added indirectly through keto-enol tautomerization (Cunningham & Gantt, 2005). Here, a hydroxyl group is added with desaturation of the adjacent carbon-carbon bond. This will then tautomerize to the more stable keto group (Cunningham & Gantt, 2005). Another possible route for astaxanthin synthesis in *Adonis* is by addition of a hydroxyl group to the 4 position by a carotenoid beta-ring-4-dehydrogenase which is then converted to a keto group by a carotenoid 4-hydroxy-beta-ring-4-dehydrogenase. An additional hydroxyl group can then

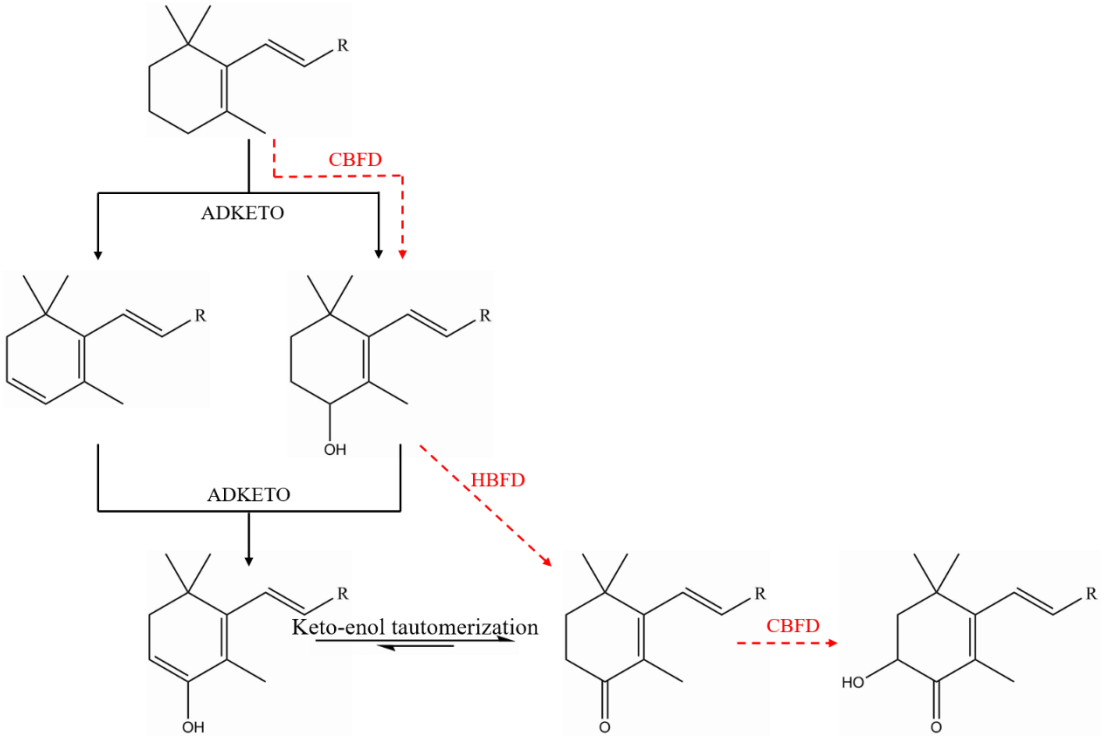

Figure 1-7. Ketocarotenoid production in *Adonis*
Black lines indicate the first pathway which was proposed, which proceeds through hydroxylation and tautomerization. Red dashed lines show the second suggested route, through hydroxylation followed by oxidation to the keto group. ADKETO, putative enzyme for ketocarotenoid formation in *Adonis*; CBFD, carotenoid beta-ring 4-dehydrogenase; HBFD, 4-hydroxy-beta-ring 4-dehydrogenase.

also be added to the 3 position by the initial enzyme (Cunningham & Gantt, 2011). Both suggested routes are shown in Figure 1-7.

More commonly seen in nature is the production of ketocarotenoids by the combined action of hydroxylase and oxygenase enzymes. While the pathways for the biosynthesis of beta-carotene differ between different species, and differ between bacteria and plants, they still produce the same precursor for ketocarotenoid production; beta-carotene. Hydroxyl and keto groups are then added onto the 3, 3' and 4, 4' positions respectively. There are three characterised bacterial hydroxylases, CRTZ (Misawa, *et al.*, 1990), CRTR (Masamoto, *et al.*, 1998), and CYP175A1 (Blasco, *et al.*, 2004). Further carotenoid hydroxylases exist in algae and yeast. The algal hydroxylase CRTR-b is similar to those seen in plants (Linden, 1999) with endogenous plant beta-carotene hydroxylases CRTR-b1 (Galpaz, *et al.*, 2006), CRTR-b2 (D'Ambrosio, *et al.*, 2011) and CYP97A29 (Stigliani, *et al.*, 2011) also having the potential to act in the ketocarotenoid pathway. There are also several members of the oxygenases, as

summarised by Zhu, *et al.* (2009). These are broken down into three types, BKT (Huang, *et al.*, 2006), CRTW (Misawa, Kajiwara, *et al.*, 1995) and CRTO (Mochimaru, *et al.*, 2005), although there is some confusion of the distinction between BKT and CRTO. Most of the oxygenases characterised belong to the CRTW class. Within this class several oxygenases share homology with the BKT oxygenases. There are also a few enzymes which can act as both a hydroxylase and oxygenase. Astaxanthin synthase (CRTS) from *Xanthophyllomyces dendrorhous* is one of these bifunctional enzymes, it acts alongside the reductase CRTR to produce astaxanthin in *X. dendrorhous* (Barredo, *et al.*, 2017).

The elucidation of the ketocarotenoid pathway (Figure 1-8) was performed by Fraser, *et al.* (1997) using the genes *Crt*Z and *Crt*W. These have since become the genes of choice to induce ketocarotenoid production in plants (Enfissi, *et al.*, 2019; Hasunuma, *et al.*, 2008; Mortimer, *et al.*, 2017; Nogueira, *et al.*, 2017; Nogueira, *et al.*, 2019). An Fe^{2+} co-factor is beneficial for maximal enzyme activity and the presence of O_2 is vital. CRTZ and CRTW enzymes are relatively promiscuous with their substrates; they can function in any order with prior hydroxylation or ketolation not impacting on the efficiency (Fraser, *et al.*, 1997). Astaxanthin is formed from beta-carotene via eight intermediary ketocarotenoids. The function of *Crt*Z and *Crt*W was characterised using *E. coli* by Misawa, Satomi, *et al.* (1995).

1.2.2.6 Carotenoid storage

The predominant site for carotenoid storage within plant cells is inside the plastids. The plastids (except proplastids) are also capable of carotenoid synthesis. Chromoplasts are so named due to the large accumulation of pigments which occurs within them. They can develop from proplastids or chloroplasts and develop structures specifically for the role of carotenoid sequestration. Figure 1-9 shows the types of plastids, and the differentiation which can occur amongst them.

Proplastids are the progenitor of all the plastid types, although they themselves lack any carotenoid synthesis (Jarvis & López-Juez, 2013). The etioplasts develop in dark grown plants as a precursor to full chloroplasts and as such, they contain carotenoids which relate to photosynthesis, although not in large amounts. The presence of the carotenoids lutein and violaxanthin are vital for the formation of etioplasts (Park, *et al.*, 2002). Upon exposure to light they then develop into chloroplasts (Sun, *et al.*, 2018).

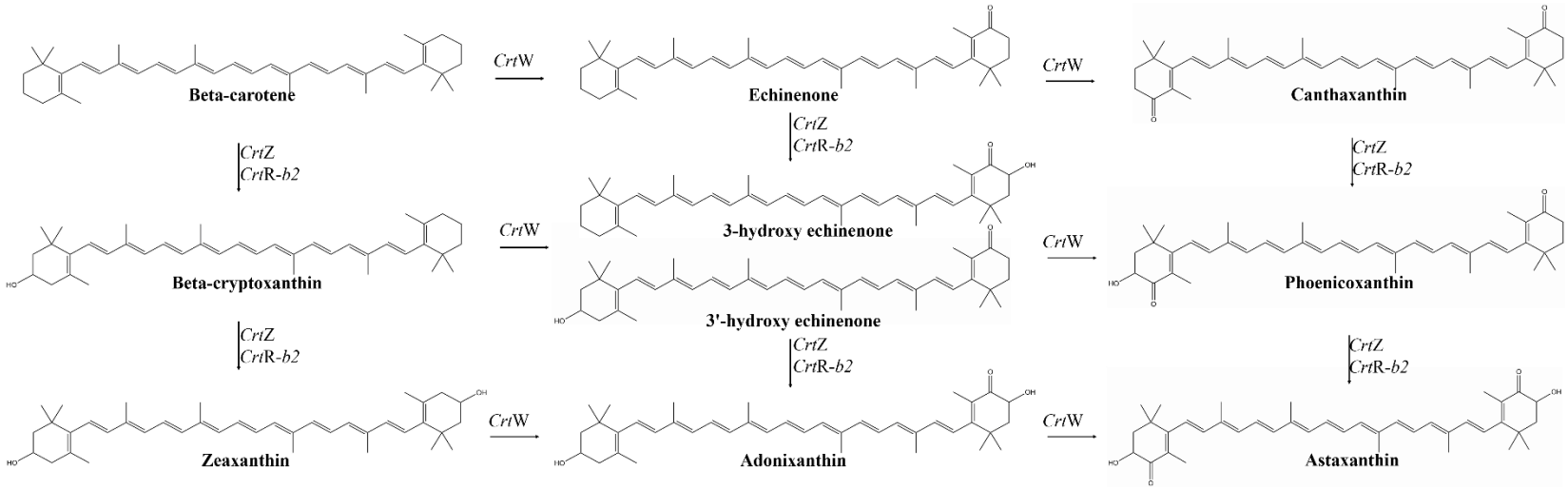

Figure 1-8. Ketocarotenoid pathway showing genes used within this work
*Crt*Z and *Crt*W are bacterial carotenoid hydroxylase and oxygenase respectively. *Crt*R-*b2* is the plant carotenoid hydroxylase. Hydroxylation and ketolation can occur in any order to produce any of the ketocarotenoids shown above.

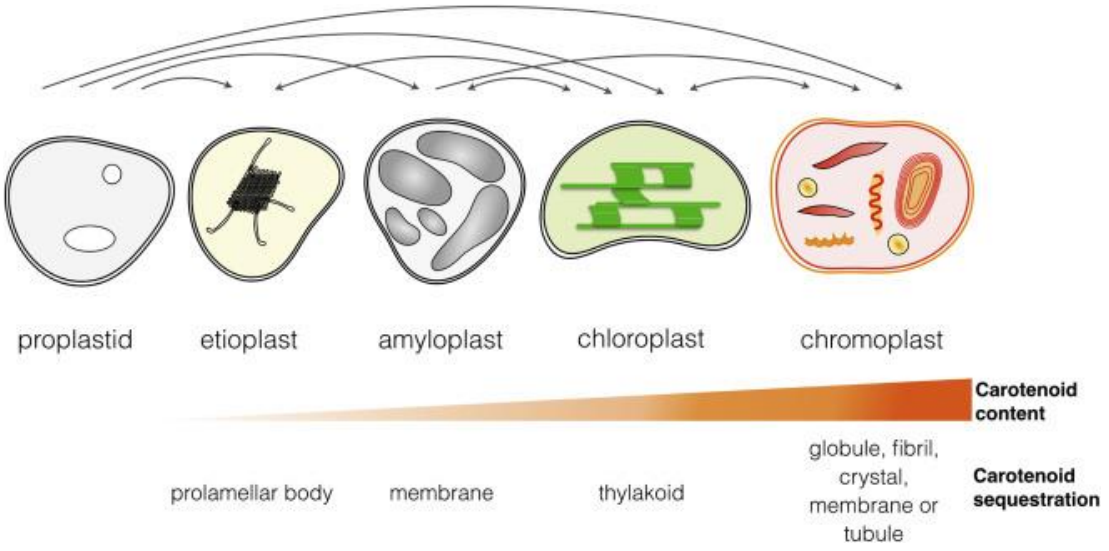

Figure 1-9. Differentiation between plastid types
Taken from (Sun, *et al*., 2018).

Chloroplasts are probably the most well-known plastid, with them being the defining feature of eukaryotic photosynthetic organisms. Chloroplasts contain thylakoid membranes in which both chlorophylls and carotenoids are accumulated. Plastoglobules are also found attached to the thylakoids. Carotenoid biosynthesis occurs primarily in the envelope membranes (Joyard, *et al.*, 2009), although it can also occur in the thylakoids, and this provides a mechanism for regulation (section 1.2.2.4). Chloroplasts are found in leaves as well as mature green fruit. The amyloplasts are located in the starchy tissues of plants such as the seeds and roots and only have a limited role in carotenoid regulation (Howitt & Pogson, 2006).

Chromoplasts are the most important organelle for the synthesis and storage of carotenoids. Upon fruit ripening the chloroplasts differentiate into chromoplasts to facilitate the accumulation of carotenoids (Figure 1-10). The thylakoid membranes are degraded, along with the chlorophylls. In the place of the thylakoid membranes, other internal structures develop to enhance carotenoid storage. These structures are the inner membranes of carotenoid rich sacs, along with an increase in the plastoglobule number and size (Egea, *et al.*, 2010). Chromoplasts have lipoprotein structures which can associate with the lipophilic carotenoids. These structures can be globular, crystalline, membranous, fibrillar or tubular, with more than one type co-existing in a cell (Camara, *et al.*, 1995). Globular chromoplasts accumulate plastoglobules. Crystalline chromoplasts have crystals of carotenoids. Fibrillar and tubular

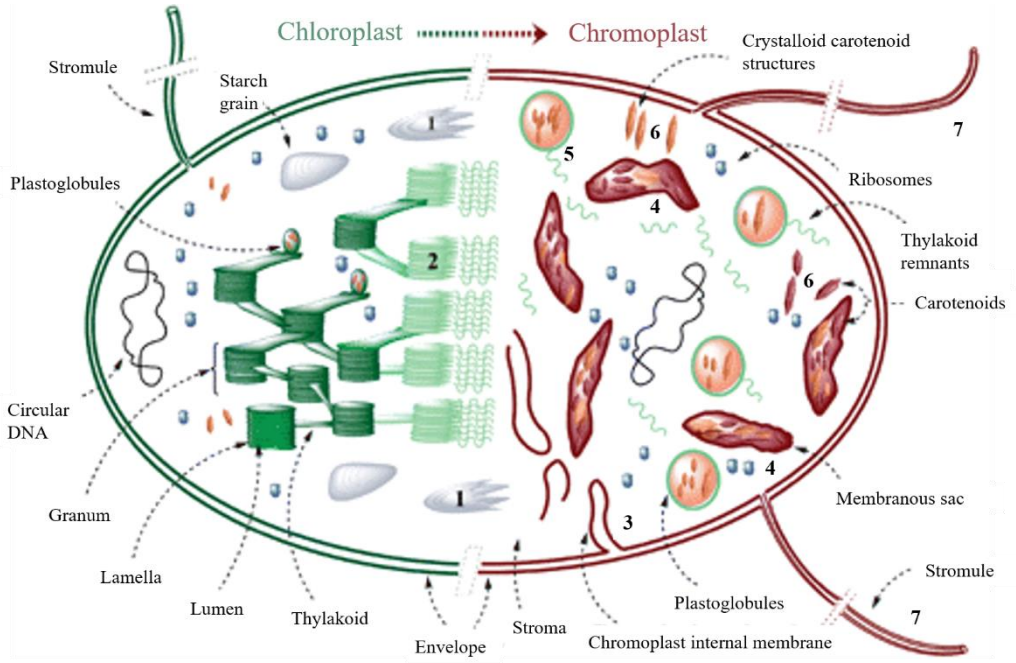

Figure 1-10. Development of chloroplasts to chromoplasts
1) breakdown of starch granules, 2) breakdown of thylakoids and grana, 3) plastid envelope inner membrane synthesis, 4) formation of carotenoid rich membranous sacs, 5) plastoglobuli increase in size and number, 6) carotenoid crystals, 7) increase in stromules. Taken from (Egea, *et al*., 2010).

chromoplasts have elongated structures for carotenoid storage. Membranous chromoplasts have a minimal number of plastoglobules, but instead store the carotenoids in membranes (Vishnevetsky, *et al.*, 1999). The chromoplasts observed in tomato fruit are mostly globular or crystalline. This is in contrast to that seen in pepper, where fibrils are formed. The polarity of the carotenoids seen in these two Solanaceae species may explain the difference in the approach to carotenoid storage. Tomato accumulates the very non-polar, and therefore lipophilic lycopene, whereas pepper accumulates a broader range of carotenoids, including the more polar xanthophylls. Esterified xanthophylls are also associated with the fibrillar chromoplasts.

1.2.2.7 Carotenoid degradation

Carotenoids can be cleaved and degraded by two main processes; non-enzymatic degradation, and enzymatic cleavage. The products from carotenoid cleavage are the apocarotenoids which have a large impact on the tomato volatile composition and taste. Non-enzymatic breakdown is the degradation of a carotenoid caused by any damaging species which is not an enzyme, such as reactive oxygen species, singlet oxygen species, heat and light (Britton, *et al.*, 2009).

Enzymatic cleavage is performed by the carotenoid cleavage dioxygenases (CCDs) and nine-*cis*-epoxycarotenoid dioxygenases (NCEDs), with at least seven CCDs being found in tomato (Wei, *et al.*, 2016). Several of the CCDs appear to have originated from a duplication event, leading to pairs of similar CCDs, in tomato these are CCD1a/b and CCD4a/b. Each CCD has its own role, and they are often localised to specific regions. Figure 1-11 shows the substrate for the CCDs, and which apocarotenoids can be produced from carotenoid degradation.

CCD1a and CCD1b cleave at the double bonds in carotenoids (Ilg, *et al.*, 2014). The preferred site for cleavage differs between CCD1a and CCD1b, with CCD1b being more promiscuous. Both produce C14 and C13 species, including pseudoionone, geranylacetone and beta-ionone (Simkin, *et al.*, 2004). CCD1b is highly expressed in ripening fruit and both CCD1a and CCD1b are located in the cytoplasm. CCD7 and CCD8 are involved in strigolactone biosynthesis (Kohlen, *et al.*, 2012; Vogel, *et al.*, 2010). CCD4 enzymes cleave beta-carotene, along with other carotenoids at the 9,10 position and act in the plastoglobules which is the site of carotenoid accumulation (Hou, *et al.*, 2016). This has been confirmed with knock-out and overexpression studies (Rottet, *et al.*, 2016).

The expression of the CCDs can be very tissue specific or widely distributed depending on the individual CCD. CCD1a is mostly expressed throughout the plant, but with only low expression in the fruit, young leaves and pistil. CCD1b is generally expressed at a much higher level that CCD1a, but expression in the root and stem are similar. CCD4a is only expressed in the flower tissues and red fruit. CCD4b is mostly expressed in leaf tissue but there is lower expression throughout the plant. CCD7 is expressed everywhere, mainly in the orange fruit. CCD8 is mostly found in the root, with expression also occurring constitutively with the exception of the calyx and immature fruit. CCD-like has a more specific expression, it is localised to the root, stem, flower, pistal and mature green fruit (Wei, *et al.*, 2016). The expression pattern highlights the high level of control and specificity which the CCD enzymes possess. Apocarotenoids are postulated to regulate carotenogenesis and also play an important role in many other plant aspects such as plant development (Hou, *et al.*, 2016).

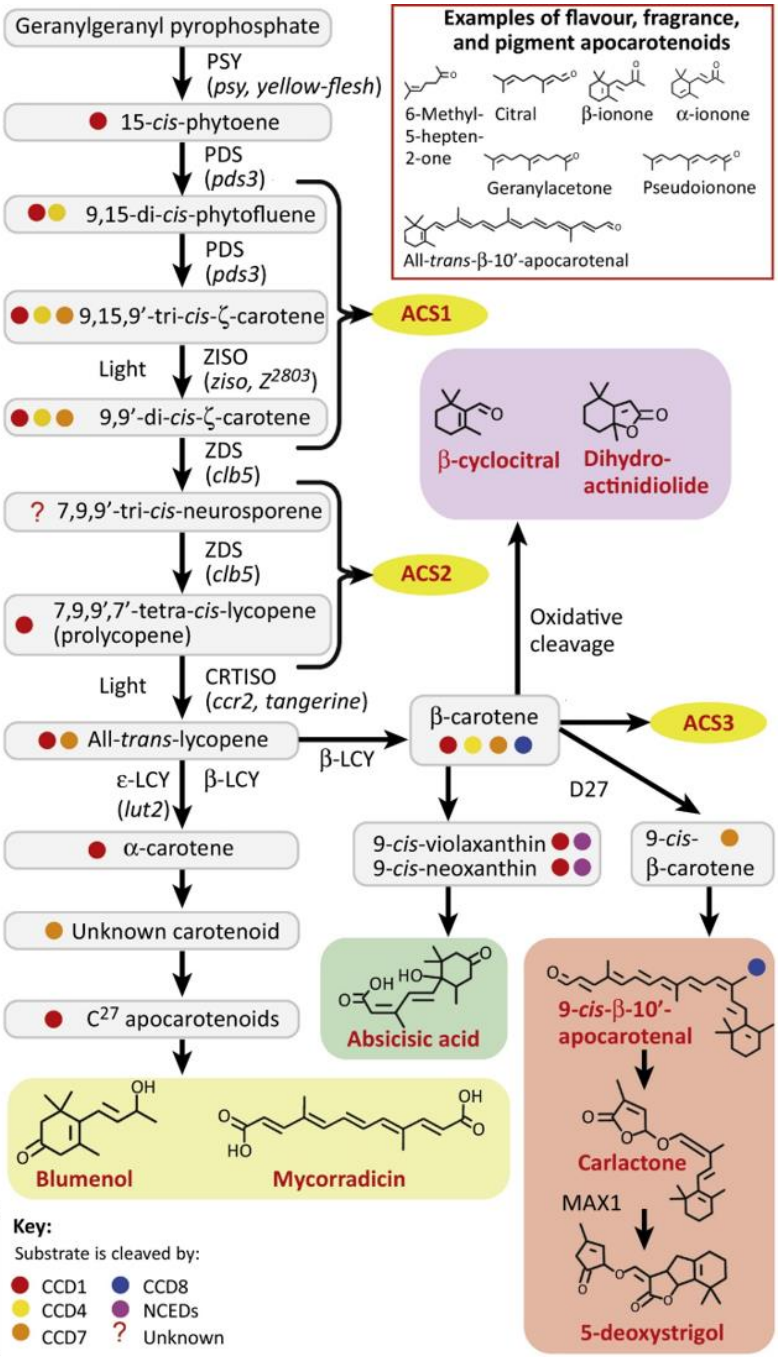

Figure 1-11. Apocarotenoid formation
Coloured dots show the substrates for each CCD enzyme. CCD1 acts throughout the pathway, whereas the others are more specific. All CCDs act on beta-carotene. NCED cleaves violaxanthin and neoxanthin to form abscisic acid. D27 isomerises beta-carotene before cleavage by CCD7 and CCD8. MAX1 modifies carlactone to other strigolactones. Apocarotenoid signalling molecules (ACS) function to regulate a range of processes. PSY, phytoene synthase; PDS, phytoene desaturase; ZISO, 15-*cis*-zeta-carotene isomerase; ZDS, 15-*cis*-zeta desaturase; CRTISO, carotene isomerase; β-LCY, beta-cyclase. *psy*, *yellow-flesh* *pds3*, *ziso*, Z^{2803}, *clb5*, *ccr2*, *tangerine* and *lut2* are Arabidopsis mutants. Adapted from (Hou, *et al.*, 2016).

1.2.3 Esterification

1.2.3.1 Esterification for carotenoid storage

In some plant species hydroxyl-carotenoids can undergo esterification with a fatty acid. If the carotenoid possesses a hydroxyl group, as seen in the xanthophyll violaxanthin or the ketocarotenoid astaxanthin, it can condense with the carboxyl group of a fatty acid to form an ester bond (Figure 1-12). This can occur on any of the hydroxyl groups present on a carotenoid. Often during ripening the free forms of carotenoids decrease whilst the esterified forms increase (Minguez-Mosquera & Hornero-Mendez, 1994). In pepper only the free forms are observed before ripening (Howitt & Pogson, 2006). The spectral properties of carotenoid esters are the same as the free carotenoids, therefore when using the spectrum it can be difficult to distinguish the esterified and free form of an individual carotenoid. To overcome this, carotenoid extracts are often saponified to remove any fatty acids, therefore, the esterified carotenoid content of plants is rarely measured (Bunea, *et al.*, 2014). Another approach to overcome the problem when analysing esterified carotenoids is to consider the polarity. Xanthophylls are more polar than the carotenes, however, upon addition of a fatty acid the compound becomes very non-polar. This provides a distinction between esterified and free carotenoids. The fatty acid also stabilises the carotenoids, probably due to the decrease in polarity allowing for the carotenoid to be stored in the lipid rich membrane (Hornero-Méndez & Mínguez-Mosquera, 2000). In chloroplasts carotenoids are associated with the thylakoid membranes, during conversion to chromoplasts these membranes are disorganised, leaving the carotenoids in the stroma. Esterification of the carotenoids then helps the carotenoid integrate into the newly formed membrane (Mercadante, *et al.*, 2017).

Not all plants have esterified carotenoids and within a species not all tissues will have esterified compounds. Mango, mandarins, goji berries, peppers and potatoes all have notable amounts of esterified carotenoids (Bunea, *et al.*, 2014). The length of the fatty acid chain also varies between species; however, they are generally the saturated C12:0 (lauric acid), C14:0 (myristic acid), C16:0 (palmitic acid) or C18:0 (stearic acid). Unsaturated fatty acids have also been found such as, C18:1 (oleic acid), C18:2 (linoleic acid) or C18:3 (linolenic acid). Tomatoes do not have any esterified carotenoids in the fruit and mainly accumulate carotenes instead.

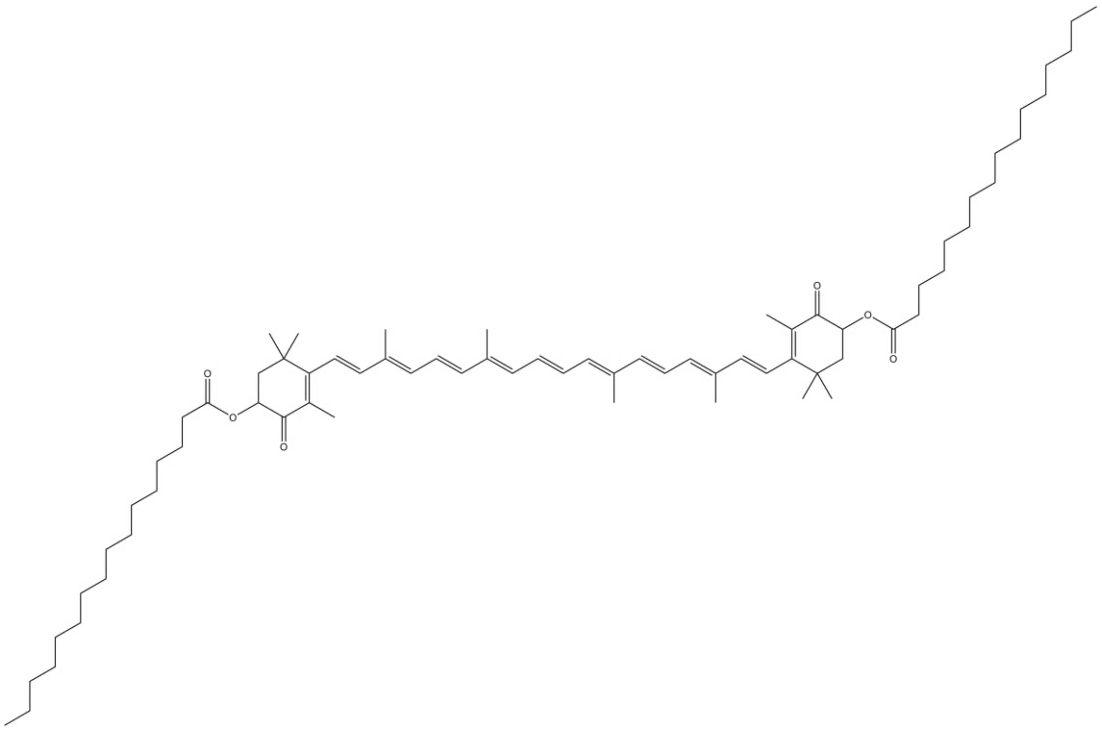

Figure 1-12. Astaxanthin esterified with two palmitic acid C16:0 fatty acids

However, there is esterification of carotenoids in the flowers. The dominant carotenoids found in tomato flowers are violaxanthin and neoxanthin, both of which are esterified (Galpaz, *et al.*, 2006). This esterification leads to an overproduction and high pigmentation of tomato flowers. Although esterified carotenoids are not endogenously found in tomato fruit, they have been observed after metabolic engineering to obtain ketocarotenoids (Enfissi, *et al.*, 2019; Huang, *et al.*, 2013; Nogueira, *et al.*, 2017). Esterified carotenoids are often associated with fibrillar chromoplasts, these are absent from tomato fruit. Instead the esterified carotenoids in metabolically engineered plants are located mainly in the plastoglobules, with sequestration also occurring in the membrane (Enfissi, *et al.*, 2019). The formation of the plastoglobuli shows plasticity; an alteration to the metabolic composition influences the number and size of the plastoglobules (Ariizumi, *et al.*, 2014). Interestingly, despite no *de novo* synthesis of carotenoids, esterified xanthophylls are also found in human skin (Wingerath, *et al.*, 1998).

1.2.3.2 Effect on bioavailability

The impact of esterification on the bioavailability of carotenoids is controversial. With carotenoids presenting as an important health food, the bioavailability of the carotenoids from food is an important consideration. There are multiple steps which comprise bioavailability. The first is the release of the carotenoid (esters) from the food matrix and then suspension into lipid droplets which are provided by the food. Within the lipid droplet they are transported to the small intestine. Carotenoid esters may be hydrolysed here to their free form or retain the fatty acid conjugate before micellarisation with bile salts. Further hydroxylation can still occur in the micelles. The micelles provide delivery to the epithelial cells of the intestines, where the carotenoids are transported across the brush border into the enterocytes. It is unclear whether esterified carotenoids can cross the brush border (Failla, 2019). Esterified beta-cryptoxanthin has previously been found in human faeces indicating that there may not be complete hydrolysis of the esterified carotenoids, and that there is limited uptake of esterified carotenoids without hydrolysis (Hernández-Alvarez, *et al.*, 2016). Once in the enterocytes the carotenoids are fused into the lipid transport globules called chylomicrons. These then enter the lymphatic and blood system where they are degraded and taken up by the liver. The liver can store and secrete carotenoids as required. Carotenoids are delivered to peripheral tissue by secretion in lipoprotein particles (Failla, 2019). This process is illustrated in Figure 1-13.

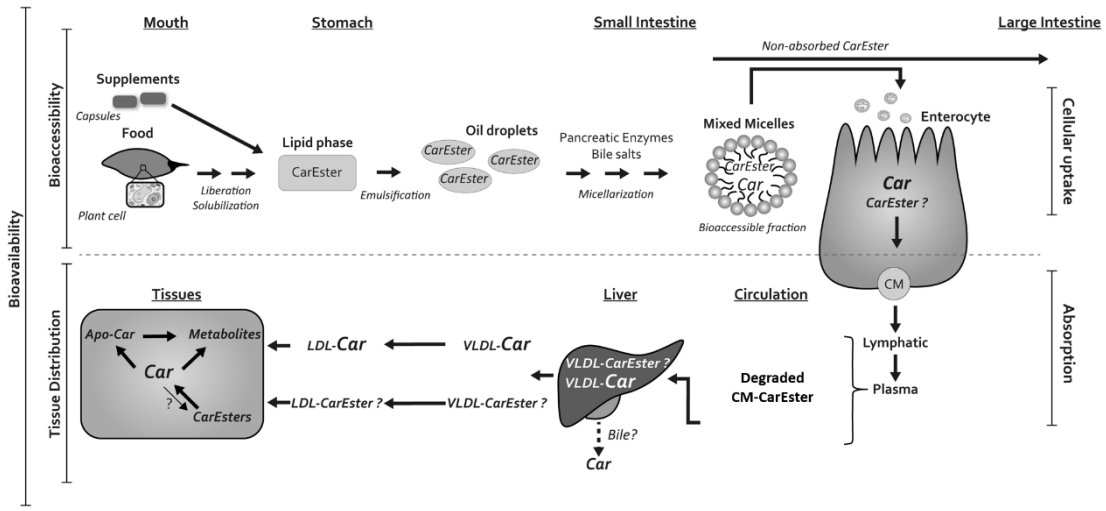

Figure 1-13. Process of digestion, absorption and distribution comprising the bioavailability of carotenoids

CarEster, carotenoid ester; Car, carotenoid; CM, chylomicron; VLDL, very low density lipoprotein; LDL, low density lipoprotein; Apo-car, apocarotenoid. Taken from (Failla, 2019).

Only free carotenoids are found within animal tissues, suggesting hydroxylation of esterified carotenoids to free carotenoids can occur within animal tissues. It could, therefore, be said that the esterified carotenoids are not as bioavailable as the free carotenoids as they require extra processing steps before accumulation, resulting in a lower uptake. However, the esterification of carotenoids stabilises them and thus provides a larger pool of carotenoids available for uptake. There is a lack of evidence regarding the bioavailability of esterified ketocarotenoids. One study showed a limited uptake of capsanthin esters when using a mix of carotenoids with 56% capsanthin, most of which was esterified (Pérez-Gálvez, *et al.*, 2007). Studies using other carotenoids generally show no change or an increase in bioavailability with carotenoid esters compared to free carotenoids (Mercadante, *et al.*, 2017). Bowen, *et al.* (2002) showed that lutein esters did not affect the uptake into serum, and there may have been a possible increase in uptake with lutein esters. However, the amount of dietary fat given alongside the supplements also varied and may have influenced uptake.

Cleavage of esters of beta-cryptoxanthin upon uptake into tissues has been reported and is comparable to free beta-cryptoxanthin uptake (Breithaupt, *et al.*, 2003). Zeaxanthin esters have also been shown to have a higher bioavailability than free zeaxanthin (Breithaupt, *et al.*, 2004). These all confirm carotenoid esters are as bioavailable or more bioavailable than free carotenoids.

1.2.3.3 Genetic process of esterification

The pathway for carotenoid esterification is one which has only recently started to be elucidated. Ariizumi, *et al.* (2014) identified two allelic tomato mutants generated from an ethyl methansulphonate (EMS) mutagenesis panel with a lack of xanthophyll esters present in the petals. The lack of esterified carotenoids causes a pale yellow petal phenotype. Thus, the gene which was found to be mutated was named the pale yellow petal (*pyp*) gene. The gene is located on chromosome 1.

Without a functional *pyp* gene no esterified carotenoids are present in the petals of tomato. Without the formation of esters, the total carotenoid content is decreased. However, the *de novo* synthesis of carotenoids is not impacted, therefore it must be the degradation of free carotenoids which causes the difference in total carotenoid content. It is likely that degradation is carried out by the carotenoid cleavage dioxygenases (CCDs) (section 1.2.2.7). The levels of free violaxanthin and neoxanthin were observed to increase with the *pyp* mutation. However,

the increase was not to the same level as the carotenoids which would normally be esterified. The changes in the carotenoid composition also affected the plastoglobuli. The plastoglobuli failed to fully develop from chloroplasts and the total plastoglobule number was decreased (Ariizumi, *et al.*, 2014). This reinforces the concept that the development of plastoglobuli is closely linked with the carotenoid content. The storage structures do not form until there is a need for carotenoid sequestration.

Segregation experiments showed that the *pyp* gene is a monogenic recessive trait, therefore a mutation in both alleles of the gene is required to have an impact on the plant. Expression of *pyp* occurs throughout the plant. Two forms of mutation were found in the pale yellow petal plants, *pyp*1-1 has a predicted loss of the last 361 amino acids caused by a nonsense mutation which generates a stop codon and *pyp*1-2 has a missense mutation which causes a non-synonymous substitution. The effect of the mutations on the protein structure has not been studied. Gene expression analysis indicates *pyp*1-1 expression is reduced compared to wildtype and *pyp*1-2 expression. Unsurprisingly, considering the impact the gene has on esterification, *pyp* is an acyltransferase. It has as alpha/beta hydrolase-hold and lysophospholipid acyltransferase like domain (LPAT) which incorporate acyl groups into acceptors. It is the LPAT domain which is most affected by both *pyp*1-1 and *pyp*1-2 mutations. There is one homologue found in tomato, this is the chloroplastic acyltransferase-like gene Solyc02g094430, however the protein only shares 51% identity with *pyp*. The role of Solyc02g094430 has not yet been elucidated. Homologues can also be found in other related species. Phytyl ester synthase (PES) 1 and 2 from Arabidopsis are involved in phytyl ester synthesis and so also have acyltransferase action (Lippold, *et al.*, 2012). PYP shares most homology with PES1 (58%). Cucumber, lotus, cantaloupe and soybean also have *pyp* homologues (Ariizumi, *et al.*, 2014). Recently a ripening-specific acyltransferase (*rsAcT*) has also been identified in pepper (Berry, *et al.*, 2019). *rsAct* is homologous to *pyp* with a query cover of 97%. It also shares homology with PES1 and PES2, although to a lesser extent (92% and 89% respectively).

The *pyp* gene has also been introduced into other plant species to try and upregulate esterification. Petunia flowers are a pale yellow colour. This is thought to be due to a lack of carotenoid esterification in the petals, especially esterification of *trans* xanthophylls. To overcome this Kishimoto, *et al.* (2020) expressed a range of acyltransferases, including *pyp* in

petunia plants. The expression of *pyp* strongly correlated with an increase in total carotenoid content, however, there was only a minimal increase in the total carotenoid ester content. Interestingly, despite *pyp* not acting on zeaxanthin in tomato it was found to increase the levels of esterified zeaxanthin in petunia. Conversely, it did not change the esterification level of violaxanthin or neoxanthin.

An acyltransferase has also recently been characterised in wheat (Watkins, *et al.*, 2019). Identified as xanthophyll acyltransferase (*xat*), it is a member of the Gly-Asp-Ser-Leu esterase/lipase (GDSL) gene family and accumulates in the apoplast. XAT has been reported to act on a broad range of xanthophylls yet functions mainly on lutein during wheat grain desiccation. Previous work had identified the locus in which *xat* sits; the *Lute* locus in on the short arm of chromosome 7D (Ahmad, *et al.*, 2015). The enzymatic motifs in XAT and PYP are different. XAT has a GDSL motif, whereas PYP has a LPAT domain. The localisation of the two enzymes also differs, XAT sits in the apoplast, separate from the carotenoids, PYP is predicted to be associated with the plastoglobules, which is the site for carotenoid storage.

1.2.4 Uses of carotenoids

1.2.4.1 Market

The market value for carotenoids reflects how important they are to multiple different industries. In 2017 the market stood at nearly $1.5 billion, with a predicted growth up to $2.0 billion by 2022. The growth in the astaxanthin market ($427 million) is expected to overtake that of capsanthin ($385 million) by 2022, with a predicted annual growth rate of 8% (McWilliams, 2018). The carotenoid market end products can be divided into food, cosmetics, pharmaceuticals, supplements and feed, with the feed segment expected to show the most growth. This illustrates the wide range of industries which rely on the production of carotenoids (Markets and Markets, 2020).

1.2.4.2 Role in animals

Carotenoids are found throughout the natural world and fulfil many different roles throughout different species. Their distinctive yellow to red colouration provides the pigmentation of many animals, plants and algae. However, many animals cannot synthesise carotenoids *de novo* and thus rely on dietary intake.

One of the most attractive properties of carotenoids is their potent antioxidant activities, which leads to a significant clinical interest. It is the structure of carotenoids that confers this characteristic antioxidant property. The extended conjugated system created by the long chain of regular double bonds (Stahl & Sies, 2007) provides a system which can donate electrons, thus quenching free radicals and reactive oxygen species (ROS) (Lobo, *et al.*, 2010). This intrinsic property helps protect against multiple ROS induced diseases, an example of which is cardiovascular disease (Siti, *et al.*, 2015). Carotenoids prevent the oxidation of low density lipoproteins, which are associated with an increased risk of atherosclerotic plaques (Britton, *et al.*, 2004). However, beta-carotene has also been seen to have negative effects in smokers, with an increase in mortality from cardiovascular disease (Omenn, *et al.*, 1996) and an increased risk of lung cancer (ATBC, 1994).

Humans also require carotenoids for protection against many cancers including, lung, breast, prostate and colorectal (Fraser & Bramley, 2004). There are several possible mechanisms by which carotenoids are anticarcinogenic including; anti-oxidant effects, anti-inflammatory effects, immune modulation, cell differentiation induction, apoptosis induction, anti-proliferation effects, and wnt/β-catenin signalling modulation (Abramczyk & Surmacki, 2016). The extent to which these different mechanisms are utilised is unknown, however the link between cancer and carotenoids is well established (Aghajanpour, *et al.*, 2017; Griffiths, *et al.*, 2016; Ziegler, 1989). The consumption of tomato products with bioavailable lycopene has been shown to reduce the risk of prostate, breast, lung, colorectal, endometrial, ovarian, cervical, pancreatic, gastric, head and neck cancers (Rowles & Erdman, 2020).

Dietary carotenoids are required for eye health. Lutein, *meso*-zeaxanthin and zeaxanthin are the macular pigments and are accumulated in the retina. Here, they filter high-intensity light and reduce oxidative stress (Arunkumar, *et al.*, 2020). Neither zeaxanthin nor lutein can be produced *de novo* by animals, therefore all the accumulated macular pigments must come from the diet. *Meso*-zeaxanthin is extremely rare in the diet and is therefore thought to come from an isomerisation reaction of lutein which occurs only in the eye (Bhosale, *et al.*, 2007).

Another important role for carotenoids in animals is for pro-vitamin A activity. Vitamin A is essential for the human body to function correctly (World Health Organisation, 1997) and in the developing world over 70% of the pro-vitamin is obtained from plants (Britton, *et al.*, 2004). Insufficient vitamin A leads to vitamin A deficiency (VAD) with symptoms of night

blindness, growth problems and a compromised immune system which can leave patients prone to infections. Any carotenoids which possess a beta ring, such as beta-carotene, zeaxanthin and beta-cryptoxanthin have provitamin A activity. While beta-carotene can be given as a dietary supplement, in the developing world this is not viable due to problems with distribution and cost. Increasing the amount of beta-carotene in a staple food overcomes all of this, leading to the rationale for Golden Rice (Ye, *et al.*, 2000) (Paine, *et al.*, 2005) (Tang, *et al.*, 2009). Beta-carotene is cleaved to retinal (vitamin A) upon absorption (Bohn, *et al.*, 2019). The enzyme responsible for this in humans is beta-carotene 15,15'-monooxygenase (BCO) (Lindqvist & Andersson, 2002).

1.2.4.3 Role in plants

Carotenoids play an important function in many aspects of plant biochemistry. Photosynthesis is probably the most important of these. There are four carotenoids bound to each light harvesting system of photosystem II (LHC-II) and are vital for folding of LHC-II (Liu, *et al.*, 2004). Carotenoids absorb light in the region of the maximal wavelength emitted from the sun, the energy is then transferred to chlorophylls for use in photosynthesis (Polivka & Frank, 2010). This also expands the range of wavelengths available for a plant to harness in photosynthesis (Hashimoto, *et al.*, 2016). Carotenoids can also act as regulators within this process; when there is excess sunlight the energy can be absorbed and then dissipated by the conjugated double bond system found in carotenoids. This is shown in Figure 1-6.

1.2.5 Ketocarotenoids

1.2.5.1 Uses of ketocarotenoids

Astaxanthin is one of the highest value carotenoids, largely due to its commercial use in multiple industries. Astaxanthin was initially found in lobster where it is largely responsible for the colouration of the animal. Continuing on from this discovery, astaxanthin was, and still is, primarily used in the aquaculture industry. It is used as a supplement in the diet to provide colouration to the flesh of fish. Similarly, it has also been used in the poultry industry to provide colouration to the yolks of eggs (Breithaupt, 2007). Other ketocarotenoids such as canthaxanthin are also frequently used for this purpose. Consumers prefer foods which have a stronger, more intense colour due to the perception that the colour relates to the health benefits. Commercially this colour is frequently given by a synthetic colourant added to the feed. However, the feasibility of using natural pigment sources high in phoenicoxanthin and

canthaxanthin has been shown to be economically viable (Nogueira, *et al.*, 2017). The addition of pigments is not only aesthetic but also plays an important role in fish vitality, reproduction, ultra-violet protection, communication and immune response (Davinelli, *et al.*, 2018; Higuera-Ciapara, *et al.*, 2006). In the natural ecosystem, fish can obtain astaxanthin from microalgae, shrimp and many other small aquatic animals.

Astaxanthin has a fully conjugated structure with delocalisation of π electrons. Alongside this the hydroxyl and keto groups present on the beta-rings allow for free radical quenching at the ring end groups, and not just in the backbone as seen in beta-carotene (Goto, *et al.*, 2001). It has also been suggested astaxanthin can provide free radical scavenging within the membranes. This is due to the polar end groups allowing penetration into the membrane. This is a unique feature of the ketocarotenoids and may play a role in membrane stability (Davinelli, *et al.*, 2018). These structural characteristics of astaxanthin make it a very potent antioxidant, and therefore it is the base of numerous health promoting products (Ambati, *et al.*, 2014; Lim, *et al.*, 2018). Astaxanthin supplements have been shown to be effective at preventing or slowing the progression of several health problems. Much like the other carotenoids, astaxanthin consumption has been linked to an inhibition of cancers, diabetes and cardiovascular diseases (Ambati, *et al.*, 2014). Comparison of the anticancer properties against two other carotenoids, beta-carotene and canthaxanthin, were performed by Chew, *et al.* (1999). This study revealed that astaxanthin appears to be more bioavailable, with higher plasma concentrations detected. However, accumulation in the tumour tissue was lower, with canthaxanthin being more prevalent. While all the carotenoids decreased the size of the tumour, it was astaxanthin which showed the most effect, in a dose-dependent manner. Astaxanthin has also be formulated into a medicinal drink for a range of autoimmune diseases including Crohn's, psoriasis, diabetes, graft versus host disease and multiple sclerosis (Lignell & Böttiger, 2001). Astaxanthin appears to help in immune diseases by increasing the number of secretory cells and increasing population of T-helper cells along with immunoglobulin (Ig) A, IgG and IgM (Higuera-Ciapara, *et al.*, 2006).

1.2.5.2 Sources of ketocarotenoids

Astaxanthin is one of the most highly sought after ketocarotenoids. It can be found throughout nature; in bacteria, algae, yeasts and marine animals. However, it is rarely seen in plants. Despite being ubiquitous, most of the commercial astaxanthin is obtained from synthetic

sources relying on petrochemicals. Furthermore, synthetic sources of astaxanthin have not been approved for human consumption due to concerns over the toxic starting materials used (Khoo, *et al.*, 2019). However, there are other sources which are commercially viable and provide an alternative source of ketocarotenoids.

Haematococcus pluvialis is an important microorganism for the production of natural astaxanthin. *H. pluvialis* has been reported to produce 80 mg/L astaxanthin (5.7% of dry weight) with optimal culture conditions (Azizi, *et al.*, 2020). Further exploitation of *H. pluvialis*, to enhance astaxanthin has been done by UV mutagenesis. This has extended possible astaxanthin production to 175 mg/L (Hong, *et al.*, 2018), which offers competition to the synthetic market, with industrially viable amounts being produced. However, there are still barriers to the use of natural astaxanthin sources such as *H. pluvialis*. The culturing and downstream processing is very energy intensive and contamination can cause loss of the product.

The yeast *Xanthophyllomyces dendrorhous* has also been used for natural astaxanthin production. *X. dendrorhous* can also produce other carotenoids including the ketocarotenoid canthaxanthin. Metabolic engineering of *X. dendrorhous* has been used to increase both the production of astaxanthin, and also the production of the intermediary carotenoids such as the rare ketocarotenoid echinenone (Visser, *et al.*, 2003). Gassel, *et al.* (2013) used random mutagenesis followed by genetically engineering to obtain 10 mg/g dry weight of astaxanthin in fermenter conditions. Other combined mutagenesis approaches, alongside different culture conditions have been used to increase astaxanthin production. For example, UV radiation and then subsequent N-methyl-N′-nitro-N-nitroso-guanidine (NTG) mutagenesis, followed by culture conditions supplemented with oak extract has recently been employed (Kothari, *et al.*, 2019). This created a 1.4 fold increase in astaxanthin production. Furthermore, the ability to perturbate the carotenoid pathway within *X. dendrorhous* to create a cell factory for the production of different ketocarotenoids is highly attractive. There are few sources for the intermediate carotenoids available.

Canthaxanthin has been produced (14 mg/g) by the algae *Asterarcys quadricellulare*, and provides a good starting point for future optimisation and carotenoid enhancement (Singh, *et al.*, 2019). Canthaxanthin is also the main carotenoid in some strains of seawater bacteria, with a total production of 1.2 mg/g (Asker, 2018). Whilst this is not industrially feasible, it does

provide us with a source of almost solely (99%) canthaxanthin. Another ketocarotenoid for which there is no commercial natural production is echinenone. However, it is made by the cyanobacteria *Synechocystis*, with 30% of the total carotenoid content being echinenone (Menin, *et al.*, 2019). *Synechocytis* has also been engineered for astaxanthin production (Menin, *et al.*, 2019). The production of adonixanthin is similar, it is made in small quantities by *Brevundimonas* and *Erythrobacter*, but not to an industrially feasible level (Asker, *et al.*, 2018).

While there are alternatives to chemical synthesis available, there is still a large gap in the market for natural ketocarotenoids. Considering the structure of astaxanthin, there are three possible stereoisomers. Two of these are commonly found in nature, 3*S*, 3*S*' and 3*R*, 3*R*'. The third, 3*R*, 3*S*' is seen in synthetic astaxanthin. The isomer of astaxanthin is dictated by the source; astaxanthin from *X. dendrorhous* produces the 3*R*, 3*R*' isomer whereas *Eupausia superba* produces the 3*S*, 3*S*' isomer (Ambati, *et al.*, 2014). It has been reported the 3*R*, 3*R*' isomer is not as bioactive as the 3*S*, 3*S*' isomer (Yang, *et al.*, 2013). Plants expressing bacterial genes for the production of ketocarotenoids have been shown to produce the more useful 3*S*, 3*S*' isomer (Nogueira, *et al.*, 2017). Plants can also produce a range of ketocarotenoids to a commercially viable level. Therefore, the use of higher plants should be able to compete with the production from microorganisms and provide a new way of sustainable ketocarotenoid production. Examples of metabolic engineering for ketocarotenoid production in plants is discussed in section 1.3.

1.3 Cloning and breeding strategies

1.3.1 Crop enhancement

The importance of carotenoids is clear, and this confers the high value nature of them. They are required for many different industries, spanning both the human and animal market. Considering their prominence in the health and beauty related industries and the ever increasing shift for consumers to demand natural and renewable sources the current, synthetic method for production is becoming undesirable. There have been many different approaches to overcome this, with metabolic engineering of plants already proving to be a feasible alternative. Plants can produce compounds which are identical to those seen in microorganisms, with the additional benefit of only producing the bioactive isomers

(Sheludko, 2010). The land use for plant growth is also comparable to that required for large scale fermentation of yeasts and bacteria, but with the ability for seasonal crop rotation to allow for food production to continue.

Modification of the carotenoid pathway is not always predictable and straightforward (Zheng, *et al.*, 2020). There are several accounts where the introduction or overexpression of a gene has caused a bottleneck to form elsewhere, or a feedback loop to change other parts of the pathway. Enfissi, *et al.* (2019) reports that the introduction of the ketocarotenoid genes actually causes an increase in lycopene levels, rather than the production of ketocarotenoids. This was speculated to be due to the flux of beta-carotene into ketocarotenoids, causing an absence of beta-carotene, and therefore, lycopene was produced to counter this. Silencing effects can also be seen with metabolic engineering, this often occurs if an endogenous gene is upregulated, especially in a constitutive manner (Zheng, *et al.*, 2020). For example, the addition of the endogenous tomato *Crt*R-*b2* gene into tomato caused silencing when the insert was homozygous resulting in a reduction in transcript levels and lower xanthophyll content in the flowers (D'Ambrosio, *et al.*, 2011). The effects of metabolic engineering on the wider metabolism, and therefore on plant health, can also be difficult to predict. Modification of the carotenoid pathway can have wide ranging effects, both positive and negative. Loss of vigour and dwarfism were observed in overexpression of PSY, probably due to the reduction in gibberellin caused by the metabolic shift into carotenogenesis (Fray, *et al.*, 1995). Overexpression of *lcy*-b in tomato enhances the beta-carotene content and also produced a higher fruit productivity (D'Ambrosio, *et al.*, 2004). The same gene expressed in the fruit also caused an increase to abscisic acid (ABA), decrease in ethylene production and an increase in cuticle thickness and shelf-life (Diretto, *et al.*, 2019). However, mutagenesis or metabolic engineering of plants for carotenoid synthesis has often been successful, with plants being used for the production of carotenes, carotenoids and ketocarotenoids, with a variety of different methods being employed to achieve this. Conventional breeding, genetic modification, targeting induced local lesions in genomes (TILLING) and clustered regularly interspaced short palindromic repeats (CRISPR) based site directed mutagenesis have allowed for the modification of pre-existing carotenoid pathways or the introduction of new pathways into many species.

1.3.2 Conventional breeding

Conventional, or selective breeding has been performed by humans since the cultivation of plants began. A very similar process to the one used thousands of years ago is still used today. Wild parents of a species are used to generate a population with segregating traits. The best performing lines, the plants which show the traits of interest with minimal adverse characteristics, are then selected to be continued onto further generations (Manshardt, 2004). This process is then repeated for many iterations and has produced many of the commercial crops that we consume today. The major disadvantage to this approach is the time required to cycle through enough generations to achieve the desired trait combinations. Furthermore, some traits correlate with each other. Therefore in removing an undesirable trait, a desirable trait may have to be sacrificed too (Breseghello & Coelho, 2013). Selective breeding also limits the genetic variation and can leave crops vulnerable to annihilation by infection, as seen in banana (Ordonez, *et al.*, 2015). Modern techniques are now being used to help identify traits of interest. Quantitative trait loci (QTL) mapping can identify regions in the genome which segregate with a trait of interest. These regions can then be traced through the breeding programme with the help of a molecular marker (Alqudah, *et al.*, 2019). More recently linkage disequilibrium (LD) mapping has also been used with genome wide association study (GWAS) to allow the genetic cause of traits to be identified (Alqudah, *et al.*, 2019). Many have already been identified in tomato (Tieman, *et al.*, 2017; G. Zhu, *et al.*, 2018).

1.3.2.1 Mutagenesis

Mutagenesis is considered to be a conventional breeding approach; however, it is very different to that discussed above. The plant metabolism can be altered using random mutagenesis. Here, the DNA is altered by a mutagen. However, the site of mutation is random, and therefore large panels of plants are required to identify one with the modification in the gene of interest. Commonly used mutagens are ethyl methansulphonate (EMS), dimethyl sulphate (DMS) or high energy radiation. EMS has been used to generate several important tomato lines with an altered carotenoid profile (Ariizumi, *et al.*, 2014; Galpaz, *et al.*, 2006; Galpaz, *et al.*, 2008). Mutagenesis is also the basis of the TILLING approach. Here the mutagen is used to introduce mutations to large panel of seeds, which are then screened by high throughput methods to identify those of interest (Kurowska, *et al.*, 2011). There is normally a specific target site within the genome which is focussed on. The TILLING

approach has been used to create genetic resources available for the scientific community (Minoia, *et al.*, 2010) as well as directly used for the modification of the carotenoid pathway. Silletti, *et al*. (2013) identified a tomato allele which was responsible for the two fold increase of lycopene in fruit. Similarly, EMS was used to generate a TILLING population in wheat to identify modifications in *lcy*-e which resulted in a 75% increase in beta-carotene levels (Richaud, *et al.*, 2018). The main disadvantage to using mutagens to reverse engineer plants, is the randomness of the process. As the mutations can occur anywhere throughout the genome, it requires large numbers of plants to identify any of interest. Furthermore, although a desirable mutation is identified in the region of interest, it is highly likely there may be other, uncharacterised mutations elsewhere in the genome. However, mutagenesis does provide us with a useful tool for identifying which genes are involved in a particular process, and thus, can lead to forward engineering of said gene.

1.3.3 Genetic modification

Genetic modification is the alteration of a genome by recombinant DNA techniques. Here, genes can be upregulated, downregulated, knocked-out, or entirely new genes introduced. This approach allows for the addition of genes from one species into another. This expands the options for genetic engineering considerably and allows genes from unrelated species to be introduced into other organisms. This opens up the possibilities for expanding the carotenoid pathway into producing non-endogenous carotenoids, for example, the production of ketocarotenoids in tomato and other higher plants. However, not all species are amenable to genetic transformation. Whilst tobacco, tomato and aubergine can all be genetically modified, pepper cannot. This limits the extent to which the carotenoid pathway in pepper can be altered. However, tomato is very amenable to genetic modification and has provided a model platform for understanding and enhancing the carotenoid pathway. For example, the downregulation using RNA interference (RNAi) of the regulatory gene for controlling light induced pathways, de-etiolated1 (*DET1),* increased both the carotenoid and flavonoid content giving the high-pigment-2 phenotype (Davuluri, *et al.*, 2005). In an overexpression approach, the bacterial phytoene synthase, *Crt*B, was expressed in tomato fruit, to enhance the total fruit carotenoids without affecting the isoprenoids or tocopherols (Fraser, *et al.*, 2002). Ketocarotenoid production in higher plants relies on genetic modification, although there have been several different approaches to achieve this over the last 15 years. Table 1-1 details all the previous

approaches to stimulate higher plants to produce ketocarotenoids. The success of these varies, with the highest reported content being 16 mg/g of astaxanthin in tomato (Huang, *et al.*, 2013), whereas the lowest reports trace amounts with unintended upregulation higher in the pathway (Enfissi, *et al.*, 2019; Huang, *et al.*, 2013).

Modern metabolic engineering strategies are precise and have many advantages over the conventional breeding strategies. The time required to make a specific modification is much less, with only one generation required to introduce a gene of interest, and then another one or two generations to ensure a stable integration. Furthermore, the modification is controlled, with the only major unknown being the site of insertion. While insertional mutagenesis can occur, it seems to be rare within plants, and therefore the off target effects of genetic modification are minimal.

1.3.3.1 CRISPR

The clustered regularly interspaced short palindromic repeats (CRISPR) and CRISPR associated protein (Cas) system can be used to knock-out or decrease expression of genes. Furthermore, CRISPR has recently also been employed to introduce new DNA. CRISPR/Cas is a relatively new approach to gene editing, but one whose use is steadily growing (Tyagi, *et al.*, 2020). It offers a powerful approach to genetic manipulation of plants (Wada, *et al.*, 2020). The CRISPR approach to gene editing has been recently used for the modification of the carotenoid pathway in tomato. Both *psy* and *Crt*R-*b2* have been targeted using CRISPR/Cas (D'Ambrosio, *et al.*, 2018). This approach had a high success rate, with 84% of plants having at least one modification and 69% having both genes edited. Lycopene content has also been increased fivefold by the knock-out of five genes using CRISPR/Cas (Li, *et al.*, 2018).

CRISPR/Cas has been adapted from the bacterial adaptive immune system, whereby the foreign DNA is degraded by introducing site specific double stranded breaks (D'Ambrosio, *et al.*, 2018). Cas9 is the most common enzyme employed in CRISPR/Cas. Cas9, alongside guide RNA is responsible for the identification and destruction of the foreign, or target DNA. The guide RNA is complementary to the target region and identifies target regions after binding as a Cas9 complex to protospacer adjacent motif (PAM) sequences (Wada, *et al.*, 2020). If a target sequence is located, then the guide RNA will form a DNA-RNA duplex and Cas9 activates as a nuclease to cleave the DNA three base pairs above the PAM. This system can be used for genetic engineering, with design of the guide RNA providing flexibility to target

any region of choice. In eukaryotic cells once a double strand break is made the cell will try to repair it, either by non-homologous end joining (NHEJ) or homologous repair (HR) (Xu, *et al.*, 2015). NHEJ is prone to imperfect repair, and therefore deletions, insertions or substitutions are common. HR requires a correct template, and this provides the opportunity to perform precise modifications, such as transgene insertion and base substitutions (D'Ambrosio, *et al.*, 2018).

The CRISPR/Cas system provides an approach for easy removal of DNA which can in turn inactivate a gene. It is a powerful and precise method for genetic modification which doesn't have either of the main disadvantages seen elsewhere. It is quick and there are minimal off target effects (Tyagi, *et al.*, 2020). CRISPR/Cas is also a method of genetic manipulation whereby no foreign DNA is introduced to the host, therefore the risks associated with other forms of genetic modification are much lower, and therefore the regulations for CRISPR/Cas could be different (Eckerstorfer, *et al.*, 2019). While CRISPR/Cas is expanding into using HR to introduce or intentionally alter DNA, this has not yet been achieved with large, multigene constructs (Hahn, *et al.*, 2018). There is, therefore, still an application of the 'classical' approach to genetic modification.

Table 1-1. Previous genetic engineering approaches for ketocarotenoid production in higher plants
PSY, phytoene synthase; BKT, beta-carotene ketolase; CaMV, cauliflower mosaic virus; IDI, isopentenyl pyrophosphate isomerase; CRTE, geranylgeranyl pyrophosphate synthase; CRTB, phytoene synthase; CRTI, phytoene desaturase; CRTY, lycopene beta-cyclase; CRTZ, beta-carotene hydroxylase; CRTW beta-carotene oxygenase; CRTO, beta-carotene oxygenase; PDS, phytoene desaturase; LMW, low molecular weight; BHY, beta-carotene hydroxylase; CYC-B, lycopene beta-cyclase; LCYB, lycopene beta-cyclase; CRTR-b2, beta-carotene hydroxylase, GBSS, granule bound starch synthase, ZEP, zeaxanthin epoxidase, LCYE, lycopene epsilon-cyclase.

Species	Enzymes	Promoters	Primary ketocarotenoid(s)	Content	Esterified carotenoids	Reference
Arabidopsis thaliana	β-carotene-oxygenase *(H. pluvialis)*	napA Seed specific	4-ketolutein, canthaxanthin, phoenicoxanthin and astaxanthin	1% total ketocarotenoid content	Astaxanthin, phoenicoxanthin and adonixanthin	(Stålberg, *et al.*, 2003)
Arabidopsis thaliana	β-carotene-oxygenase *(H. pluvialis)* and PSY *(A. thaliana)*	napA Seed specific	4-ketolutein, canthaxanthin, phoenicoxanthin and astaxanthin	23% total ketocarotenoid content	Astaxanthin, phoenicoxanthin and adonixanthin	Stålberg, *et al.*, 2003)
Arabidopsis thaliana	BKT (*C. reinhardtii, C. zofingiensis* and *H. pluvialis)*	CaMV 35S Constitutive	Astaxanthin	2 mg/g	Astaxanthin	(Zhong, *et al.*, 2011)

***Brassica napus* (canola)**	IDI (*Paracoccus*), CRTE *(P. ananatis*), CTRB (*P. ananatis*), CRTI (*P. ananatis*), CRTY (*P. ananatis*), CRTZ (*Brevundimonas*) and CRTW (*Brevundimonas*)	CaMV 35S Constitutive	Echinenone	116.9 μg/g	(Fujisawa, *et al*., 2009)
***Daucus carota* (carrot)**	BKT1 (*H. pluvialis)*	CaMV 35S Constitutive	Astaxanthin	91.6 μg/g (roots)	(Jayaraj, *et al*., 2008)
Daucus carota	BKT1 (*H. pluvialis)*	Ubquitin (Arabidopsis) Constitutive	Unreported	Unreported	Jayaraj, *et al*., 2008)
Daucus carota	BKT1 (*H. pluvialis)*	*RolD* (*A. rhizogenes*) Root specific	Astaxanthin	Approximately 91.6 μg/g (roots)	Jayaraj, *et al*., 2008)
***Glycine max* (soybean)**	CRTB (*P. ananatis*) and CRTW (*Brevundimonas*) or BKT1 (*H. pluvialis)*	Lectin (CRTB) and β-conglycinin (CRTW and BKT1) Seed specific	Canthaxanthin	52 μg/g	(Pierce, *et al*., 2015)

Lotus japonicus	CRTW (*Paracoccus*)	CaMV 35S Constitutive	Echinenone, canthaxanthin, adonixanthin and astaxanthin	89.8 µg/g total ketocarotenoid content	Used saponified samples	(Suzuki, *et al.*, 2007)
Nicotiana benthamiana	CRTZ and CRTW (*Brevundimonas)* fusion	CaMV 35S Transient expression	3'OH echinenone isomer	78.2 µg/g		(Nogueira, *et al.*, 2019)
Nicotiana glauca	CRTW (*N. punctiforme*)	CaMV 35S Constitutive	Adonixanthin	56 µg/g (flower)	Violaxanthin	(Gerjets, *et al.*, 2007)
Nicotiana glauca	CRTO (*Synechocystis*)	CaMV 35S Constitutive	3'OH echinenone and 4-ketolutein	74.9 µg/g (nectary), 65.9 µg/g (petal)		(Zhu, *et al.*, 2007)
Nicotiana glauca	CRTZ and CRTW (*Brevundimona*s)	CaMV 35S Constitutive	4-ketolutein	1.04 mg/g	Astaxanthin and adonixanthin (in senescing leaves)	(Mortimer, *et al.*, 2017)
***Nicotiana tabacum* (tobacco)**	CRTO/BKT1 (*H. pluvialis*)	PDS Ripening related	Astaxanthin	83.9 µg/g (flower)	Astaxanthin, phoenicoxanthin, adonixanthin, 3(')OH echinenone and violaxanthin	(Mann, *et al.*, 2000)

Nicotiana tabacum	CRTZ and CRTW (*Paracoccus)* fusion	CaMV 35S Constitutive	Echinenone	900 µg/g	Adonixanthin, astaxanthin, zeaxanthin and lutein	(Ralley, *et al.*, 2004)
Nicotiana tabacum	CRTO (*Synechocystis*)	CaMV 35S Constitutive	Echinenone and adonixanthin esters	49.5 µg/g and 74.6 µg/g respectively (flower)	Adonixanthin and 4-ketolutein	Gerjets, *et al.*, 2007)
Nicotiana tabacum	CRTO (*Synechocystis*) and CRTZ (*P. ananatis*)	CaMV 35S Constitutive	Adonixanthin and echinenone	108.3 µg/g and 97.3 µg/g respectively (flower)	Zeaxanthin, lutein, adonixanthin and 4-ketolutein	Gerjets, *et al.*, 2007)
Nicotiana tabacum	CRTW (synthesised based on *Brevundimonas* protein, optimised for rape*)*	P*rrn* Targeted to plastids	Astaxanthin	1.88 mg/g		(Hasunuma, *et al.*, 2008)
Nicotiana tabacum	CRTZ and CRTW fusion (synthesised based on *Brevundimonas* protein, optimised for rape*)*	P*rrn* Targeted to plastids	Astaxanthin	5.44 mg/g		Hasunuma, *et al.*, 2008)

Nicotiana tabacum	CRTW and CRTZ fusion	P*rrn* Targeted to plastids	Astaxanthin	3.29 mg/g	Hasunuma, *et al*., 2008)
Nicotiana tabacum	BKT *(C. reinhardtii)*	CaMV 35S Constitutive	Astaxanthin	1.60 mg/g	(Huang, *et al*., 2012)
***Oryza sativa* (rice)**	ZmPSY1 (maize), PaCRTI (*P. ananatis*) and CRTW (*Brevundimonas*)	Wheat LWM glutenin (ZmPSY1), barley D-hordein (PaCRTI) and maize γ-zein (CRTW)	Astaxanthin	Unreported	(Breitenbach, *et al*., 2014)
Oryza sativa	ZmPSY1 (maize), PaCRTI (*P. ananatis*), sCrBKT (*C. reinhardtii*)	Wheat LWM glutenin (ZmPSY1), barley D-hordein (PaCRTI) and maize γ-zein (sCrBKT) Endosperm specific	Canthaxanthin	3.96 μg/g	(Bai, *et al*., 2017)
Oryza sativa	sZmPSY1 (maize), sPaCRTI (*P. ananatis*), and sCrBKT (*H. pluvialis*)	Glb1 (sZMPSY1), GluB4 (sPACRTI) and GluC (sCRBKT) Endosperm specific	Canthaxanthin	25.82 μg/g	(Q. Zhu, *et al*., 2018)

Oryza sativa	sZmPSY1 (maize), sPaCRTI (*P. ananatis)*, sCrBKT (*C. reinhardtii*) and sHpBHY (*H. pluvialis*)	Glb1 (sZMPSY1), GluB4 (sPACRTI), GluC (sCRBKT) and GluB1 (sHpBHY) Endosperm specific	Astaxanthin	16.23 µg/g		(Q. Zhu, *et al.*, 2018)
***Solanum lycopersicum* (tomato)**	CRTZ and CRTW (*Paracoccus*) fusion	CaMV 35S Constitutive		Trace amounts		(Ralley, *et al.*, 2004)
Solanum lycopersicum	CrBKT (*C. reinhardtii*)	CaMV 35S Constitutive	Astaxanthin	174.8 µg/g	Astaxanthin	(Huang, *et al.*, 2013)
Solanum lycopersicum	CrBKT (*C. reinhardtii*) and HpBHY (*H. pluvialis*)	CaMV 35S Constitutive	Lycopene*	2.85 mg/g *19.9 µg/g astaxanthin	Astaxanthin	(Huang, *et al.*, 2013)
Solanum lycopersicum	CrBKT (*C. reinhardtii*) in high beta-carotene background	CaMV 35S Constitutive	Canthaxanthin	2.25 mg/g	Astaxanthin	(Huang, *et al.*, 2013)

Solanum lycopersicum	CrBKT (*C. reinhardtii*) and HpBHY (*H. pluvialis*) in high beta-carotene background	CaMV 35S Constitutive	Astaxanthin	16.10 mg/g	Astaxanthin	(Huang, *et al.*, 2013)
Solanum lycopersicum	CRTZ (*Brevundimonas*), CRTW (*Brevundimonas*) and CYC-B	CaMV 35S (ZW), *S. galapagense* promoter (CYC-B)	Phoenicoxanthin and canthaxanthin	594 µg/g and 899 µg/g respectively	Phoenicoxanthin	(Nogueira, *et al.*, 2017)
Solanum lycopersicum	CRTZ and CRTW (*Brevundimonas)*	CaMV 35S Constitutive	Lycopene*	3.4 mg/g *with 75.0 µg/g astaxanthin	Phoenicoxanthin and some astaxanthin	(Enfissi, *et al.*, 2019)
Solanum lycopersicum	CRTZ (*Brevundimonas*), CRTW (*Brevundimonas*) and LCYB	CaMV 35S Constitutive	Canthaxanthin	611.5 µg/g	Phoenicoxanthin	(Enfissi, *et al.*, 2019)

Solanum lycopersicum	CRTZ (*Brevundimonas)*, CRTW (*Brevundimonas)*, LCYB and CRTR-b2	CaMV 35S Constitutive	Astaxanthin	179.4 µg/g	Astaxanthin and some phoenicoxanthin	(Enfissi, *et al.*, 2019)
Solanum phureja	BKT1 (*H. pluvialis*)	Patatin Tuber specific	4-ketolutein and astaxanthin	9.8 µg/g and 9.5 µg/g respectively	Unidentified ketocarotenoid esters	(Morris, *et al.*, 2006)
Solanum phureja	CRTZ and CRTW (*Brevundimonas)*, and OR (cauliflower)	CaMV 35S (ZW) GBSS (OR, tuber specific)	Astaxanthin	7.1 µg/g (tuber)	Unidentified ketocarotenoid esters	(Campbell, *et al.*, 2015)
***Solanum tuberosum* (potato)**	CRTO (*Synechocystis*) into a ZEP knockout	CaMV 35S Constitutive	Adonixanthin	8.5 µg/g		(Gerjets & Sandmann, 2006)
Solanum tuberosum	BKT1 (*H. pluvialis*)	Patatin Tuber specific	Astaxanthin	0.6 µg/g	Unidentified ketocarotenoid esters	(Morris, *et al.*, 2006)
Solanum tuberosum	BKT (*H. pluvialis*), CRTB	Patatin Tuber specific	4-ketolutein and astaxanthin	0.6 µg/g and 0.5 µg/g respectively	Unidentified ketocarotenoid esters	(Morris, *et al.*, 2006)

Solanum tuberosum	CRTZ and CRTW (*Brevundimonas)*	CaMV 35S Constitutive	4-ketolutein	13.70 µg/g (tuber)	Astaxanthin and adonixanthin	(Mortimer, *et al*., 2016)
***Zea mays* (corn)**	PSY1 (maize), RNAi-LYCE (maize), sCrBKT (*C. reinhardtii*), sBrCRTZ *(Brevundimonas)* crossed into a high-oil variety	LMW glutenin (PSY1), barley D-hordein (LYCE), maize γ-zein (sCrBKT and sBrCRTZ) Endosperm specific	Astaxanthin	16.77 µg/g		(Farré, *et al*., 2016)

1.4 Aims and objectives

This study aimed to optimise the production of valuable ketocarotenoids, using tomato fruit as a sustainable cell-factory. The approach builds on previous findings and resources to assess the effective combination and temporal expression of gene products, using genetic crossing and transgenic approaches. In addition to biosynthetic capacity, concurrent sequestration and the role of esterification has been investigated.

1.4.1 Objective 1: Characterising the role of *Crt*R-*b2* in improving ketocarotenoid production in tomato fruit.

Previously published ketocarotenoid producing tomato accessions designated ZWRI (section 3.1.2) produce phoenicoxanthin and canthaxanthin (Nogueira, *et al.*, 2017) but low levels of the bihydrolated end product astaxanthin. Therefore, the overexpression of an additional hydroxylase was combined with ZWRI to further elevate astaxanthin production, the end product of the heterologous pathway introduced.

1.4.2 Objective 2: Ketocarotenoid production using a single transformation event with fruit specific promoters.

Based on the outputs from objective 1, the genes *Crt*W, *lcy* and *Crt*R-*b2* were expressed using a single construct in tomato fruit. A selection of complementary promoters for controlled expression during fruit development and ripening were chosen to avoid silencing and optimise the temporal timing of production. A single transformation event is attractive as it avoids the problems associated with multiple backgrounds, and reduces the time required to achieve a ketocarotenoid producing line.

1.4.3 Objective 3: Identifying the role of the carotenoid acyltransferase pale yellow petal (*pyp)* gene on carotenoid esterification.

The *pyp* mutant tomato variety which has an absence of carotenoid esters in the flowers was crossed into the ketocarotenoid ester producing ZWRI line. The esterification of carotenoids allows for sequestration and storage, and therefore should allow for greater amounts of carotenoids to be produced in tomato fruit, yet the molecular basis of carotenoid esterification in tomato fruit is unknown.

Chapter II:
Materials and Methods

2.1 Plant cultivation

2.1.1 Origin of tomato lines used in this study

The tomato line ZW(Ø)RI(Ø)UU/U0/00 was kindly provided as F_2 seed by Dr. Marilise Nogueira. Moneymaker seed for the generation of T_0 plants transformed with the astaxanthin construct, were purchased from Moles seed (UK). Tomato seed for the *pyp* mutant (TOMJPE5508-1) was provided by University of Tsukuba, Gene Research Centre, through the National Bio-Resource Project (NBRP) of the AMED, Japan (NBRP, 2012).

2.1.2 Seed preparation and growth conditions

Seeds were treated in 50% HCl solution for at least 20 minutes before being thoroughly washed in water. Seeds were then heat treated at 67°C for three days. Seeds were sown on F2+sand compost (Scotts Levington) then transferred into M3 growing media (Scotts Levington) once established. All tomato plants (*Solanum lycopersicum*) were grown in glasshouse conditions with day temperatures of approximately 25°C for 16 hours and night temperatures of 15°C for eight hours with regular watering.

2.1.3 Material collection

Fruit was harvested by hand, when ripe. With the exception of during the ripening series, the ripe stage was determined by colour and firmness, this ensured all genotypes were harvested at their individual point of ripening regardless of the days post breaker. During the ripening series tomatoes were tagged at breaker; when the first sign of orange, or darkening appeared on the fruit. Fruit was then collected at breaker (B), breaker plus three days (B+3), breaker plus five days (B+5), breaker plus seven days (B+7) and breaker plus 14 days (B+14). Mature green fruit was harvested at a point where the fruit was fully expanded but had not yet begun to change colour. Unless otherwise stated, at least three fruit per plant were harvested and pooled. For metabolite analysis the fruit was lyophilised, then homogenised before storage at -80°C until analysis. For molecular analysis fresh material was immediately processed.

For metabolite analysis leaf material was harvested from mature plants, before senescence began. Several leaves from each plant were harvested, and pooled before lyophilisation, homogenisation and storage. For molecular analysis single, expanding leaves were harvested for immediate analysis.

Flower material was harvested at anthesis, with ten flowers taken per plant. The petals and stamen were separated then lyophilised and stored at -80°C.

2.1.4 Photosynthetic capacity

The photosynthetic capacity ($\frac{F_v}{F_m}$) of plants was determined using Hansatech instruments Pocket PEA fluorimeter. All recordings were taken in constant weather conditions, without supplementary lighting. The dark adaptation time for the plants was established prior to recording data. This was performed by covering a small section of leaf, by using clips provided by Hansatech. The section of leaf was left in the dark for increasing amounts of time until there was no change in the $\frac{F_v}{F_m}$ value from the previous dark adaptation time. This time was then used in all subsequent recordings. The optimal intensity of light was also established in a similar manner; the light intensity was decreased until no further change was observed. After ascertaining the optimal experimental set up, three leaves spread throughout the plant were measured and treated as technical replicates. Three biological replicates per genotype were used. Clips were positioned on each leaf avoiding the veins. After dark adaptation the Pocket PEA equipment was then used to expose the leaf to a bright light, and the $\frac{F_v}{F_m}$ value recorded.

2.2 Assembly of multigene construct for temporal astaxanthin production

2.2.1 Source of components

The plasmids used in this study originate from a variety of sources. 35S (pICH51288), nos (pICH41421), ATPase (pICH71431) and RbcS3C (pICH71411) have come from the MoClo Plant Parts Kit which was a gift from Nicola Patron (Addgene kit # 1000000047). The pPAtUbq10 promoter (GB0223) was provided in the GoldenBraid 2.0 kit which was a gift from Diego Orzaez (Addgene kit # 1000000076). The plasmid for *Crt*W (AB377271) was provided by Dr. Marilise Nogueira. The *crt*R-*b2* and latter part of phosphoenolpyruvate carboxylase (PPC2) have been synthesised by Eurofins Scientific (Luxembourg). Other components have been cloned from *S. lycopersicum* moneymaker variety.

2.2.2 DNA extraction from plant material

Genomic DNA was extracted from expanding leaves using Qiagen DNeasy Plant Mini Kit (Qiagen). Fresh leaf tissue (100 mg) was flash frozen in liquid nitrogen before being placed in a TissueLyser LT (Qiagen) for two minutes at 50 Hz with a 3 mm tungsten carbide ball (Qiagen). Buffer AP1 (400 µl) and RNase A (4 µl) were added to the sample and vortexed. Tubes were incubated for ten minutes at 65°C with inversion three times during incubation. Buffer AP2 (130 µl) was added, vortexed then the sample was placed on ice for five minutes. A QIAshredder Mini spin column was inserted into a collection tube (2 ml) before the lysate was added to the column and centrifuged for two minutes at 18400 g (Eppendorf 5424). Flow through was placed in a clean, sterile microcentrifuge tube along with 1.5x volume of buffer AP3. A DNeasy Mini spin column was placed in a collection tube (2 ml), before the sample was transferred and centrifuged for one minute at 18400 g. Flow through was discarded. The column was transferred to a new collection tube (2 ml) and two portions of buffer AW (500 µl) added with centrifugation for one minute at 18400 g after each addition. Before elution the column was placed in a 1.5 ml microcentrifuge tube and two portions of buffer AE (50 µl) added with a five minute room temperature incubation and centrifugation for one minute at 18400 g.

2.2.3 RNA extraction from plant material

Total RNA was extracted from expanding leaf and ripe fruit using the RNeasy Plant Mini Kit with DNase I (Qiagen). Tissue was freshly harvested, and flash frozen in liquid nitrogen. 100 mg was weighed and the tissue ground using a Tissue Lyser II or Tissue Lyser LT (Qiagen) with the material remaining frozen throughout. Buffer RLT with beta-mercaptoethanol (450 µl) was added and vortexed, after this point the tissue was allowed to thaw. Lysate was transferred to a sterile shredder spin column in a collection tube and centrifuged for two minutes at 18400 g (Eppendorf 5424). Supernatant was transferred to a clean tube (1.5 ml), and a 0.5 volume of ethanol was added and mixed by pipetting before transfer to a spin column in a collection tube and centrifuged for 30 seconds at 8000 g with the flow through discarded. Buffer RW1 (350 µl) was added to the column and centrifuged for 30 seconds at 8000 g. DNase I was prepared by the addition of buffer RDD in a 1:7 ratio. The diluted DNase I (80 µl) was then added directly to the column and incubated at room temperature for 15 minutes. Buffer RW1 (350 µl) was then added to the column and spun for 30 seconds at 8000 g with

flow through discarded. Buffer RPE (500 µl) was then applied twice with centrifugation for two minutes at 8000 g after each addition. The spin column was then added to a fresh collection tube (1.5 ml) for a final centrifugation at 18400 g for one minute. To elute the RNA, RNase free water (30 µl ripe fruit, 50 µl leaf) was added to the column and centrifuged for one minute at 8000 g.

2.2.4 Nucleic acid quantification

All nucleic acids were quantified on a Nanodrop ND-1000 spectrophotometer (Thermo-Fisher Scientific, USA). The nanodrop was equilibrated with molecular water, before being blanked with the buffer in which the nucleic acid was eluted in. 1 µl per sample was loaded onto the nanodrop for quantification. The appropriated setting was used according the type of sample, e.g. DNA or RNA.

2.2.5 Reverse transcription PCR

RNA was converted to cDNA using Quantitect RT kit (Qiagen). 12 µl of RNA (500 ng – 1000 ng) was added to gDNA wipeout buffer (2 µl), the reaction was then incubated for two minutes at 42°C before being placed on ice. Reverse transcription was then performed by the addition of reverse transcription buffer (4 µl), reverse transcription primers (1 µl) and reverse transcriptase enzyme (1 µl) with 30 minutes at 42°C followed by three minutes at 95°C. cDNA was then stored at -20°C until use.

2.2.6 Primer design

Primers used for all cloning are detailed in section 2.5. For inserts over 1 kb long the sequence was spilt into two and cloned initially into level -1 before digestion and ligation to combine the two parts into the level 0 vector. Each primer includes an overhang with sequences for either BsaI (level -1) or BpiI (level 0) restriction sites. A four base overhang complementary to the Golden Gate vector is also included. Upon cloning the overhang is removed.

2.2.7 PCR conditions

All PCR reactions were performed using Phusion High Fidelity DNA polymerase (NEB) in a BioRad T100 thermocycler. Primers (0.5 µM), dNTPs (200 µM), Phusion HF buffer (1x concentration), plasmid DNA (50 pg) and one unit of Phusion polymerase were used per reaction. Cycling conditions were an initial denaturation at 98°C for 30 seconds, with 30 cycles

of 98°C for 10 seconds, X°C for 20 seconds and 72°C for 20 seconds followed by a final extension of 72°C for 10 minutes. X represents the annealing temperature which varied for each primer set; E8 promoter part A: 60°C, PPC2 part A: 62°C, *lcy* part A: 68°C, *Crt*W part A and *lcy* part B: 70°C, E8 promoter part B and pPAtUbq10: 65°C, *Crt*W part B, *Crt*W part C and *Crt*R-*b2*: 72°C. When the annealing temperature was equal to the extension temperature a two-step protocol was used with one 20 second annealing and extension step.

2.2.8 Agarose gel electrophoresis

Agarose gel electrophoresis was used to analyse nucleic acid products. These were made by the addition of agarose (Bioline; 1% w/v) to TAE buffer (tris 40 mM, acetic acid 20 mM, EDTA 1 mM). The solution was microwaved until all the agarose had dissolved. After the liquid gel had cooled slightly GelRedTM nucleic acid gel stain (Biotium) was added at a 1 in 10000 dilution. The gel was then cast into an appropriate gel tray and left to set.

Samples were prepared by the addition of 6x loading dye and water. Samples were then loaded into the gel and a ladder (100 bp or 1 kb step, Promega) was run alongside. Gels were visualised once the loading dye had migrated down approximately 75% of the gel. Visualisation was performed using a U:Genius3 (Syngene, UK) system with ultra-violet light.

2.2.9 PCR clean up

PCR products were purified from the PCR reaction mixture by the Wizard SV PCR clean up kit (Promega). PCR products were first run on an agarose gel, as per 2.2.8. If the PCR reaction was specific and only one band was visible on the agarose gel, the PCR product was cleaned up from the PCR reaction mixture. If the agarose gel revealed an unspecific amplification then the correct band was excised from the gel, and then cleaned.

2.2.10 Digestion and ligation

The Golden Gate cloning technique uses a 'one-pot' digestion and ligation step, whereby both the restriction enzymes and the ligase is added to the reaction mix. The temperature of the reaction then cycles between the optimal temperature for both enzymes. 100 ng of vector DNA was added with a 2:1 ratio of insert to vector accounting for the variation in size. BsaI (level -1 or level 1; NEB; 0.5 µl) or BpiI (level 0 or level 2; NEB; 0.5 µl), T4 ligase (Promega; 0.5 µl), bovine serum album (1.5 µl), T4 buffer (Promega; 1.5 µl) and molecular quality water up

to 15 µl were also added with the reaction kept on ice. The cycling conditions used were 37°C for 20 seconds, then 40 cycles of 37°C for three minutes and 16°C for four minutes, with two final 5 minute steps, one at 50°C to linearise the remaining plasmid, then one at 80°C to heat inactive the enzymes.

2.2.11 Cloning into *Escherichia coli*

DH5α cells were used for transformation with plasmids. The cells were made in house to be chemically competent and were stored at -80°C until use. Before use, cells (25 µl) were thawed slowly on ice. The ligation reaction was added to the thawed cells; 2 µl for TOPO cloning and the whole (15 µl) reaction for Golden Gate cloning. The cells were then incubated on ice for 30 minutes before heat shocking at 42°C for 45 minutes then ice for two minutes. 500 µl of super optimal broth with glucose (SOC) was added to the cells and the mixture was incubated for 45 minutes at 37°C with shaking at 200 rpm to allow for recovery

After recovery, cells were plated onto Luria broth (LB) agar plates with isopropyl beta-D-1-thiogalactopyranoside (IPTG) X-gal and the appropriate antibiotic (100 µg/ml ampicillin for TOPO vectors and golden gate level -1 and level 1 vectors, 50 µg/ml spectinomycin for level 0 golden gate vectors, 50 µg/ml kanamycin for level 2 golden gate vectors). Plates were then incubated at 37°C for 16 hours.

White colonies were selected from the plates, and a single colony placed into 5 ml of liquid LB with the appropriate antibiotic. Cultures were grown for 16 hours at 37°C with shaking at 200 rpm.

2.2.12 Extraction of plasmids from bacteria

Wizard Plus SV Miniprep DNA purification kit (Promega) was used for extraction of plasmid DNA from bacteria. Overnight cultures were centrifuged at 1500 g for 10 minutes (Eppendorf 5810R) to form a pellet. Cell resuspension solution (250 µl) was added to the pellet for resuspension before transferal to a microcentrifuge tube (2 ml). Cell lysis solution (250 µl) and alkaline protease (10 µl) solution was added, with four inversions after each addition, followed by a five-minute room temperature incubation. Neutralisation solution (350 µl) was also added and mixed by inversion. The sample was centrifuged (Eppendorf 524) for 10 minutes at 18400 g.

Cleared lysate was placed into a spin column in a collection tube (2 ml) and centrifuged again for one minute. Flow through was discarded. Wash solution (750 µl then 250 µl) was added sequentially to the column, with one, then two minutes of centrifugation each time. Flow through was discarded. The column was then placed into a microcentrifuge tube (1.5 ml) and DNA eluted with 60 µl nuclease free water and centrifugation for one minute.

2.2.13 Confirmation of constructs

To confirm the assembly of the multigene construct three complimentary approaches were used. Firstly, the plasmid was digested using an appropriate restriction enzyme which generated a clear digested banding pattern. XbaI was used for the digestion of the level 2 Golden Gate vectors. Plasmid DNA (500 ng), buffer D (Promega; 2 µl), XbaI (Promega; 1µl), bovine serum albumin (0.2 µl) and up to 20 µl molecular quality water were used per digestion. The mixture was incubated at 37°C for an hour before visualisation as per 2.2.8. A PCR was also used to confirm the presence of the desired insert within the plasmid. PCR was performed using PuReTaq Ready-to-go PCR beads (GE Healthcare, UK) in a BioRad T100 thermocycler. Specific primers for the insert (1 µl; 10 µM of both forwards and reverse), plasmid DNA (50 pg) and molecular grade water was used to obtain a final volume of 25µl. Cycling conditions were an initial denaturation at 95°C for five minutes then 30 cycles of 95°C for 30 seconds, recommend Tm for 30 seconds, 72°C for one minute, then a final extension of 72°C for five minutes. Finally, the plasmid was sequenced using multiple primers to ensure all joins were covered. Sequencing was performed by Eurofins Scientific (Luxembourg).

2.2.14 Maintenance of bacterial stocks

To preserve bacterial cultures for long term storage glycerol stocks were made. An overnight bacterial culture (500 µl) was added to 50% (v/v) glycerol (500 µl) to achieve a suspension of cells in 25% (v/v) glycerol solution. Cells were revived from the glycerol stock by streaking of the glycerol onto LB plates with the appropriate antibiotic. A single colony was then picked for culturing and plasmid extraction.

2.3 Generation of T_0 tomato lines

2.3.1 Growth media

The process of *Agrobacterium* transformation and subsequent plant transformation required several different media. B5MS10 is a half strength Murashige and Skoog (MS) medium with Gamborg's B5 vitamins (B5). It was made using MSB5 (Duchefa Biochemie, Netherlands; 2.2 g), sucrose (Sigma; 10 g) and phytoagar (Duchefa Biochemie, Netherlands; 8g) in water (up to 1 L) and pH adjusted to 5.8. KCMS medium was used for cotyledon generation and *Agrobacterium* mediated tomato transformation. KCMS was prepared using MS medium with Gamborg's B5 vitamins (4.4 g), sucrose (20g), KH_2PO_4 (200mg) and phytoagar (8g, only in agar, absent in the broth) in water (up to 1 L). Yeast extract beef (YEB) medium was required for the growth of *Agrobacterium*. YEB was prepared using beef extract (5 g), yeast extract (1 g), peptone (5 g), sucrose (5 g), MgSO4.7H2O (300 mg) and agar-agar (20 g) in water (up to 1 L), then the pH was adjusted to 7.2. Regeneration medium (2Z) was made using MSB5 (4.4 g), sucrose (30 g), phytoagar (8 g), 1x Nitsch vitamins, timentin (Duchefa; 300 mg) and kanamycin (100 µg) in water (up to 1 L). Rooting medium was made using MS (4.4 g), sucrose (30 g), phytoagar (6.0 g), 1x Nitsch vitamins, indole-3-acetic acid (IAA; 1 mg), timentin (300 mg) and kanamycin (100 µg) in water (up to 1 L).

2.3.2 Seed preparation

Seeds (moneymaker from Moles seeds, Essex, UK) were washed in 50% (v/v) HCl overnight. The acid was then removed, and the seeds rinsed thoroughly in water. 70% ethanol was then added to the seeds for five minutes. The ethanol was then removed and replaced with a washing solution of bleach (Kleen Off, Jeyes Group Ltd) and Tween 20 (two drops) for 10 minutes. Seeds were then thoroughly rinsed with water and sown on B5MS10 agar medium. Seeds were left in the dark for four days, then exposed to light for four days with a 60-100 µmol m^{-2} s^{-1} photosynthetically active radiation (PAR) 16 hour light/ 8 hour dark cycle.

2.3.3 Cotyledon generation

Explants were generated from week old seedlings. Leaves were cut in MS media to maintain vigour. Sterile scalpels and forceps were used to cut cotyledons from the stem, and to cut the tip of the leaf. 2 cm^2 leaf explants were placed, topside up on solid KCMS medium

supplemented with thiamine (0.9 mg) and acetosyringone (Sigma; 100 µM). Explants were incubated at 25°C for one day with a 20-30 µmol m^{-2} s^{-1} PAR 16 hour light/8 hour dark photoperiod.

2.3.4 Cloning into *Agrobacterium tumefaciens*

The *A. tumefacians* strain LBA4404 (Invitrogen) were used for stable plant transformation. These cells were transformed with isolated plasmids from *E. coli* by heat shock transformation. Cells were thawed slowly on ice before plasmid DNA (1 µg) was added. The cells were then incubated on ice for 30 minutes before being flash frozen in liquid nitrogen for five minutes, then placed at 37°C for five minutes. SOC (1 ml) was added, and the cell mixture transferred to a 15 ml falcon tube. Cells recovered at 28°C for two hours with shaking at 180 rpm. Cells were centrifuged for three minutes at 1500 g, with the supernatant removed. The remaining cells were resuspended in YEB medium (100 µl). After a short spin to remove cell aggregates 100 µl of cells were plated onto YEB agar plates with rifampicin (50 µg/ml), streptomycin (100 µg/ml) and kanamycin (50 µg/ml). Plates were incubated at 28°C for two days.

A single colony was then selected from the plate and placed into YEB with antibiotics (5 ml). Cultures were grown at 28°C for 24 hours with shaking at 180 rpm. The 5 ml starter culture was then added to fresh YEB (45 ml) + antibiotics and grown at 28°C with 200 rpm shaking until an optical density of >0.5 was achieved. This was then used for *Agrobacterium* mediated tomato transformation (2.3.5)

2.3.5 *Agrobacterium* mediated tomato transformation

The *Agrobacterium* culture produced in 2.3.4 was centrifuged at 2000 rpm for 10 minutes to pellet the cells. Cells were then resuspended in KCMS and diluted to an optical density of 0.05. The culture was then supplemented with 2,4-dichlorophenoxyacetic acid (Sigma; 0.2 mg/L), kinetin (Sigma; 0.1 mg/L) and acetosyringone (Sigma; 100 µM) and incubated for five minutes. Explants (2.3.3) were removed from the KCMS agar and incubated with the *Agrobacterium* culture for 30 minutes at 28°C shaking at 60 rpm in the dark. Explants were blotted dry and placed on fresh KCMS agar then incubated for two days with 20 – 30 µmol m^{-2} s^{-1} PAR, 16 hour light/8 hour dark photoperiod.

2.3.6 Regeneration and rooting

Explants were grown for callus formation on 2Z with *trans*-zeatin riboside (Sigma, Germany; 2 mg/L) regeneration medium for one week. Following this the explants were placed on 2Z with *trans*-zeatin riboside (Sigma; 1 mg/L) with sub-culturing occurring every two weeks. Once shooting had occurred explants were placed onto a rooting medium to induce root formation. Shoots were separated from the callus and placed onto the medium. Once rooting had occurred shoots were placed into soil.

2.4 Screening of plants

2.4.1 Generation of TOPO vectors

TOPO cloning was used for the generation of plasmids which were used as positive controls for screening, or in standard curves for quantitive PCR.

Amplification was performed using PuReTaq Ready-to-go PCR beads in a BioRad T100 thermocycler. Primers (10 µM; 1 µl) for both forward and reverse pairs, genomic DNA (25 ng) and molecular grade water was used to obtain a final volume of 25µl. Primers are detailed in 2.5. The PCR reaction was cleaned up as detailed in 2.2.9. The TOPO-TA cloning kit (ThermoFisher) was then used to ligate the PCR product into the pCR2.1 TOPO vector. PCR product (2 µl), vector (0.5 µl) and salt solution (1.2 M NaCl, 0.06 M $MgCl_2$; 0.5 µl) were incubated together at room temperature for 15 minutes before transformation (2.2.11).

2.4.2 PCR for detection of 35S-*Crt*R-*b2* and beta-cyclase promoters (*S. lycopersicum and S. galapagense)*

PCR reactions for screening of the ZW(Ø)RI(Ø)UU/U0/00 and $P^{MT/WT}$ZW(Ø)RI(Ø) lines were all performed using PuReTaq Ready-to-go PCR beads in a BioRad T100 thermocycler. Primers (10 µM; 1 µl) for both forward and reverse pairs, genomic DNA (25 ng) and molecular grade water was used to obtain a final volume of 25µl. Cycling conditions were an initial denaturation at 95°C for 2 minutes then 30 cycles of 95°C for 30 seconds, 55°C for 30 seconds, 72°C for 30 seconds, then a final extension of 72°C for 5 minutes.

2.4.3 Quantitive real-time PCR (qPCR) for *Crt*R-*b2* copy number.

Copy number was determined relative to the single copy gene *pds*. Standard curves were made from TOPO vectors containing the relevant insert with the concentration ranging from 10 pg/µl to 0.001 pg/µl. Primers were designed to amplify a 147 bp fragment over the 35S and *Crt*R-*b2* border and a 73 bp fragment of *pds*. 2x qPCRBIO SyGreen mix LO-ROX (PCR-biosystems; 10 µl), forward and reverse primers (0.8 µl) and water (4.4 µl) were made into a master mix, this was pipetted into individual reactions using the QIAgility (Qiagen) robot. 4 µl DNA (25 ng), plasmid DNA (standard curve) or water was subsequently added to each reaction using the Qiagility. The cycling conditions were 95°C two minutes, 40 cycles of 95°C for five seconds then 60°C for 20 seconds, then melt analysis from 55°C to 99°C in 1°C increments in a Rotor-Gene Q (Qiagen).

2.4.4 Quantitive real-time PCR (qPCR) for *Crt*R-*b2* expression

The expression of *Crt*R-*b2* was determined using standard curves (0.001 to 10 pg/µl) generated from TOPO vectors containing the relevant PCR fragment. Data was normalised to *actin*. Primers were used to amplify a 97 bp fragment of *Crt*R-*b2* and a 73 bp fragment of *actin*. RNA was extracted from leaf (2.2.3) and converted to cDNA (2.2.5), this was diluted 1 in 100 times for use in qPCR and 4 µl used per reaction. 2x qPCRBIO SyGreen mix LO-ROX (10 µl), forward and reverse primers (0.8 µl) and water (4.4 µl) were made into a master mix, this was pipetted into individual reactions using the QIAgility (Qiagen) robot. 4 µl DNA (25ng), plasmid DNA (standard curve) or water was subsequently added to each reaction using the Qiagility. Cycling parameters are as in 2.4.3.

2.4.5 Southern blot analysis for UU/U0/00 copy number

Genomic DNA (10 µg) and plasmid DNA (50 pg) were digested with HindIII HF (NEB) for 16 hours at 37°C before heat inactivation for 20 minutes at 80°C. Digested DNA was run on an agarose gel (section 2.2.8) without stain for 4 hours at 25 V. The gel was then stained in 33000x GelRed for 25 minutes with constant agitation before imaging.

The gel was placed in a denaturation solution (0.5 M NaOH, 1.5 M NaCl) for 2 x 15 minutes with shaking, before being rinsed in sterile water. Neutralisation solution (0.5 Tris-HCl, pH 7.5, 1.5 M NaCl) was used to soak the gel for 2 x 15 minutes with shaking. Before transfer, the gel was left in 20x SSC solution (3 M NaCl, 300 mM sodium citrate, pH 7.0) for 10

minutes. The blot was transferred to a positively charged nylon membrane (Roche) overnight by compressing the gel and membrane together, ensuring no air bubbles were present and the set up kept moist using 20x SSC.

After transfer, the membrane was crosslinked in a trans-illuminator (UVItec) for one minute at 120 mJ. In a hybridisation tube the membrane was rolled with a mesh for 15 minutes with 2x SSC. SSC was discarded before 20 ml pre-hybridisation buffer (DIG easy Hub, Roche) was added to the tube and rotated for an hour at 50°C

The probe used was designed to span the 35S and *Crt*R-*b2* border, created using the DIG probe synthesis kit (Roche). In a sterile PCR tube, 10 pg of DNA from a plasmid with the desired sequence, PCR buffer (5 µl), PCR DIG synthesis mix (5 µl), forward and reverse primers (5 µl), enzyme mix (0.75 µl) and up to 50 µl molecular quality water were added and briefly centrifuged. An initial denaturation of two minutes at 95°C was used before 30 cycles of 95°C for 30 seconds, 55°C for 30 seconds, 72°C for 40 seconds. A final extension of seven minutes for 72°C was used to ensure complete replication. PCR product (28 µl) and molecular water (50 µl) were boiled for five minutes, immediately iced and added to hybridisation buffer (7 ml). The prehybridization buffer was then replaced with the hybridisation buffer with probe and incubated overnight at 50°C.

The hybridisation buffer was replaced with 50 ml low stringency wash buffer (2X SSC, 0.1% SDS) and the membrane rotated for five minutes at room temperature before the low stringency wash was poured off. 50 ml pre-warmed (68°C) high stringency wash buffer (0.1X SSC, 0.1% SDS) was added to the tube and incubated for 15 minutes at 68°C, twice.

Washing was done using washing buffer (0.1 M maleic acid, 0.15 M NaCl, pH 7.5, 0.3% Tween 20; 50 ml) for two minutes with constant shaking then discarded. Blocking solution (DIG Luminescent Detection Kit; 50 ml) was incubated for 30 minutes with shaking then discarded. Antibody solution (DIG Luminescent Detection Kit, diluted 1 in 10000; 50 ml) was incubated with the membrane for 30 minutes with shaking and rinsed off with water. Two further 15 minute wash steps with washing buffer were performed. Detection buffer (20 ml) was applied for three minutes. The membrane was removed from the buffer and coated with CSPD (DIG Luminescent Detection Kit; 4 ml) and incubated for five minutes at room temperature, excess CSPD was removed before incubation for 10 minutes at 37°C.

The membrane was placed face up in a cassette and an autorad placed on top. The cassette was incubated for one hour before development. Autorads were developed using an autodeveloper from Photon Imaging systems.

2.4.6 T_0 insert detection by PCR

The presence or absence of the insert was determined using a quick DNA extraction protocol followed by PCR. DNA was extracted from approximately 10 mg of leaf tissue. The leaf tissue was placed into 200 µl of sucrose solution (Tris HCl 50 mM, NaCl 300 mM, sucrose 300 mM) and ground using a pipette tip until the solution was coloured. The solution was incubated at 100°C for 10 minutes then kept on ice until amplification. The PCR was performed using PuReTaq Ready-to-go PCR beads using the unquantified DNA from the quick extraction (1 µl), forward primer (1 µl), reverse primer (1 µl) and water (22 µl). Primers amplified a region within the *Crt*W coding region (2.5). Cycling conditions were 95°C for two minutes followed by 30 cycles of 95°C for 30 seconds, 59°C for 30 seconds, 72°C for 30 seconds then a final extension of 72°C for five minutes.

2.4.7 T_0 copy number analysis

Copy number was determined relative to the single copy gene *pds*. Standard curves were made from TOPO vectors containing the relevant insert with the concentration ranging from 10 pg/µl to 0.001 pg/µl in a five point standard curve. Primers were designed to amplify a 103 bp fragment over the 35S and *Crt*W border and a 73 bp fragment of *pds*. The Rotor-Gene SYBR green® PCR kit (Qiagen) was used to perform the assay. Genomic DNA (1 µl, 25 ng), water (1µl), or a point on the standard curve (1 µl) was added to SYBR green (12.5 µl), forward primer (2 µl), reverse primer (2 µl) and molecular water (7.5 µl). The cycling conditions were 95°C five minutes, 40 cycles of 95°C five seconds then 60°C for 10 seconds, then melt analysis from 70°C to 99°C in 1°C increments Rotor-Gene Q (Qiagen).

2.4.8 High resolution melt curve analysis for *pyp* mutation

High resolution melt (HRM) was used to determine the presence of the single base change responsible for the *pyp* mutation using the Type-it HRM PCR kit (Qiagen). HRM master mix (12.5 µl), forward and reverse primer mix (1.75 µl), water (9.75 µl) and genomic DNA (1 µl, 25 ng) were mixed and analysed using a Rotor-Gene Q (Qiagen). Cycling and melt conditions

were 95°C for five minutes, then 40 cycles of 95°C for 10 seconds, 55°C for 30 seconds, 72°C for 10 seconds followed by an HRM from 65°C to 95°C in 0.2°C increments.

2.4.9 Expression analysis of *pyp*

Fruit cDNA was isolated as described in 2.2.3 and 2.2.5 and diluted 1 in 100. Quantification was performed using a standard curve of the relevant plasmid with the amounts ranging from 0.001 pg to 10 pg across five points. Data was normalised to *actin*. Primers were used to amplify a 118bp fragment of *pyp* and a 73 bp fragment of *actin*. Genomic DNA (2.5 µl), water (2.5 µl), or a point on the standard curve (2.5 µl) was added to SYBR green (10.0 µl), forward primer (1.6 µl), reverse primer (1.6 µl) and molecular water (4.3 µl). The cycling conditions were 95°C five minutes, 40 cycles of 95°C five seconds then 60°C for 10 seconds, then melt analysis from 50°C to 99°C in 1°C increments Rotor-Gene Q (Qiagen).

2.5 Primers

Table 2-1. Primers used throughout this work
Lower case bases at the start of sequences denotes extra base pairs which are removed upon cloning. Lower case in orange are the site of a single base change to remove a restriction site. Orange shows complementary overhangs, green is the level -1 overhangs, blue is the level 0 overhangs and red is the BsaI or BpiI restriction site. PPC2 promoter part B was synthesised with the overhangs shown, this removed the need for a PCR. F, forwards; R, reverse. *Actin* primers have been taken from (Cheng, *et al.*, 2017)

Screening Primers		
Name		Sequence 5' to 3'
S. lycopersicum beta-cyclase	F	CCAACTTATTTTATCACTTGATAACTAAAC
	R	TTTTCCCAATCCCAGTCCCA
S. galapagense beta-cyclase	F	CACTTGATAACTAGAGTTTGGGTTC
	R	TGTAGTCAGTGCATGGACGG
35S-*Crt*R-*b2*	F	CCCACTATCCTTCGCAAGAC
	R	GGACTGAGAAACGGGTTATG

35S-*Crt*W	F	AACAATTACCAACAACAACAAACA
	R	TGACTGTTGTCACAGCGGAA
*Crt*W	F	ACTTCTTCAGAACTTACTTCGG
	R	GAAGGTTAGCAGGTCTA
pds	F	AAGGCGCTGTCTTATCAGGA
	R	ACTGCTGACAACCAGTGAGA
pyp HRM	F	GGATATACTTGTTTGAAGAAGTG
	R	GAA GTA TCG TAC TGT GCA GTT
Golden Gate Cloning Primers		
Name		Sequence 5' to 3'
E8 promoter part A	F	ttGAAGACaaGGAGCTAGAAGGAATTTCACGAAATCG
	R	ttGAAGACaaGaTGACAACTTGACAACTACATTTC
E8 promoter part B	F	ttGAAGACaaCAtCTTTTTTTTGGATAAAAATAGC
	R	ttGAAGACaaCATTAAAAATCTCAATATGAGGATGCC
PPC2 promoter part A	F	tttGGTCTCaACATGGAGATACATTCTACTTTGAAGTTGTTTAATG
	R	tttGGTCTCaACAATATCAAAAATGTGAATATATCGATATG
PPC2 promoter part B*	F	GAAGACaaGATA
	R	GAAGACaaCATT
pPAtUbq10 part A	F	ttGAAGACaaGGAGGGAGGTCGACGAGTCAGTAATA
	R	ttGAAGACaaCgTCGATCTAAGATTAACAGAATC

pPAtUbq10 part B	F	ttGAAGACaaGAcGACGATTTTCTGGG
	R	ttGAAGACaaCATTCTGTTAATCAGAAAAACTCAGATT
*Crt*W part A	F	ttGAAGACaaAATGGCTTCTATGATATCCTCTTCCGC
	R	ttGAAGACaaTCTACCAGGAGCAAGAGATCCGTGCATAG
*Crt*W part B	F	ttGAAGACaaTAGACCTAGACTTAACGCTGCTGTTGGAAGGC
	R	ttGAAGACaaTGCCTTCCGAAGTGGAAGCAAG
*Crt*W part C	F	ttGAAGACaaGGCACCACGAGCACCACCTTACTCCTTGGAGGC
	R	ttGAAGACaaAAGCTCAAGACTCTCCTCTCCAAAGTCTCC
*Crt*R-*b2*	F	ttGAAGACaaAATGGCTGCTGGAATTAGTGCTTCTG
	R	ttGAAGACaaAAGCTCACAGTAAGCCTTTTGAGATCTTGATTCGACG
lcy	F	ttGAAGACaaAATGGATACTTTGTTGAAAACCCCAAATAAC
	R	tttGAAGACaaTTaGTCTCAGGTACAAGCTCTAAAAGAGC
	F	ttGAAGACaaCtAAAAAGGAGAATCTTGATTTTGAGCTTCC
	R	ttGAAGACaaAAGCTCATTCTTTATCCTGTAACAAATTGTTG
Expression Primers		
Name		Sequence 5' to 3'
actin	F	GGAGATTGAAACTGCCAGGAGCA
	R	CTGCAGCTTCCATACCAATCATGG
*Crt*R-*b2*	F	ACATGTTCGTTCACGATGGA
	R	AGCTGATGTGCTGCAGCTA

pyp	F	TGGAGCTACACCTGTCACTG
	R	TACGATGTAAGGCCTCACGG
Golden Gate Sequencing Primers		
Name		Sequence 5' to 3'
Level -1/0 sequencing	F	AGCGAGGAAGCGGAAGAGCG
	R	GCCACCTGACGTCTAAGAAACC
Level 1 sequencing	F	CTGGTGGCAGGATATATTGTGGTG
	R	GAACCCTGTGGTTGGCATGCACATAC

2.6 Metabolite analysis

2.6.1 Carotenoid and chlorophylls extraction

Carotenoids and chlorophylls were extracted from 10 mg freeze dried leaf or fruit pericarp and skin. An internal standard of tocopherol acetate (10 µg) was added to fruit extractions. Methanol (250 µl) and chloroform (500 µl) were added and vortexed after each addition. Samples were incubated on ice for 20 minutes. Water (250 µl) was added and vortexed before centrifugation (Eppendorf 5424) at top speed for five minutes. The organic chloroform phase was collected in a clean microcentrifuge tube. The aqueous phase was re-extracted with chloroform (500 µl) as before and organic phases pooled. Samples were dried using a GeneVac Ex-2 Plus evaporator.

2.6.2 Extraction of polar and non-polar metabolites

When analysis of both polar and non-polar metabolites was required (GC/MS) the following protocol was used. Dried homogenised fruit tissue (10 mg) was added to a microcentrifuge tube (2 ml). Methanol (400 µl) and water (400 µl) were added and vortexed. The samples were inverted on a rotator (Stuart rotator SB3) for one hour in the dark. Chloroform (800 µl) was

added and vortexed before centrifugation at maximum speed for five minutes (Eppendorf 5424). Both polar and non-polar phases were collected separately.

2.6.3 Thin layer chromatography for carotenoids

Carotenoids were extracted from freeze dried leaf as described in section 2.6.1. Dried extracts were resuspended in ethyl acetate (50 µl). 6 µl was dotted onto silica gel, F254 60 plates (Merck). A mobile phase of 40:60 (v/v) ethyl acetate:hexane was used. Authentic standards were run alongside samples for identification and retention factors (Rf) calculated.

2.6.4 Ultra-high pressure liquid chromatography system

Carotenoids were run on an Ultra High-Performance Liquid chromatography (UPLC) for identification and quantification. Plant tissue was extracted as per 2.6.1. Fruit and flower tissue extracts were resuspended in 50 µl of 1:4 ethyl acetate: acetonitrile, leaf tissue extracts were resuspended in 150 µl of the solvent mix for carotenoid analysis or 600 µl for chlorophyll analysis. The column used was a BEH C18 2.1 mm x 100 mm, 1.7 µm with a BEH C18 VanGuard re-colunm 2.1 mm x 50 mm, 1.7 µm on an Acquity UPLC Waters with photo diode array detection (PDA). The mobile phase consisted of 50:50 (v/v) methanol:water (A) and 75:25 (v/v) acetonitrile:ethyl acetate (B). The column was maintained at 30°C throughout analysis. The gradient of solvents was 50% A / 50% B for 30 seconds, then 30% A / 70% B for four minutes 30 seconds, then 0% A / 100% B for two minutes, then 30% A / 70% B for one minute before finishing on 50% A / 50% B for two minutes. The PDA scanned the UV/Vis spectra at 250 nm to 600 nm.

2.6.5 High pressure liquid chromatography system

Plant tissue was extracted as per section 2.6.1. Fruit and flower tissue extracts were resuspended in ethyl acetate (50 µl). A C30 reverse phase 5 µm column (250 mm x 4.6 mm) coupled to a C30 5 µm guard column (YMC Inc, USA) was used on a Waters high pressure liquid chromatography (HPLC) system, with a 610 pump, 996 PDA, 717 plus autosampler and 600S controller. The column was maintained at 25°C (Jones Chromatography 7955). The mobile phase solvents were methanol (A), 50:50 (v/v) methanol:water with 0.2% ammonium acetate (B), *tert*-methyl butyl ether (C). The flow rate was 1 ml/minute of 95% A / 5% B for six minutes, then changed to 80% A / 5% B / 15% C over one minute, then a linear gradient

to 30% A / 5% B / 65% C over 42 minutes. The PDA scanned the UV/Vis spectra at 220 nm to 600 nm.

2.6.6 Gas chromatography mass spectroscopy (GC/MS)

Samples were extracted as per 2.6.2. Approximately all of the non-polar extract (750 µl) was transferred to a glass vial, 20 µl of the polar extract was transferred to an insert within a glass vial. The extracts were spiked with internal standards, 10 µg D4 succinic acid for the polar extract and 10 µg D27 myristic acid for the non-polar extract. All extracts were then dried.

Derivatisation of the samples occurred before analysis. Methoxyamine hydrochloride (MeOX) was dissolved in pyridine to achieve a concentration of 20 mg/ml. MeOX (30 µl) was then added to samples and incubated at 40°C for one hour. N-Methyl-N-(trimethylsilyl) trifluoroacetamide (MSTFA) (70 µl) was added and incubated at 40°C for 2 hours. Samples were then transferred into a glass insert if they were not previously in one.

An Agilent 7890A gas chromatography system using Agilent G1701ES enhanced mass selective detector (MSD) productivity ChemStation software was used for GC/MS analysis. An Agilent 7683 series autosampler, Agilent 7683B injector and Agilent 5975C inert MSD were coupled to the GC system. Samples were randomised, and 1 µl injected into the injector which was held at 280°C, a splitless mode was used. Samples were separated using a DB-5ms GC column (Agilent technologies; 30 m, 0.25 mm, 0.25 µm) and a temperature gradient of 70°C for three minutes before increasing 4°C per minute up to 325°C which was maintained for one minute. The carrier gas (helium) flow rate was 1.3 ml/minute. After separation of the metabolites through the GC they entered the MS via a 250°C transfer line. The MS source was maintained at 230°C, the MS quadrupole was held at 150°C. Full scan mode was used ranging from 50 m/z to 1000 m/z using 70 eV positive electron impact ionisation (EI+). Retention times were locked to the internal standards.

2.6.7 Semi-volatile analysis and sample preparation

Fresh whole fruit for semi volatile analysis was homogenised in a blender and the juice kept frozen until analysis. Freeze-thaw cycles were minimised. Prior to analysis samples were left to thaw at 4°C and samples were not kept at room temperature for more than 12 hours. For ZW(Ø)RI(Ø)UU/U0/00 samples, 1.5 ml of juice was pipetted into brown glass screw cap vials (Anatune Ltd, UK) alongside these was a blank of air and an external standard of 20 ppb

acetophenone-β, β, β-D3 (Sigma-Aldrich, USA; 2 ml). For $P^{MT/WT}$ZW(Ø)RI(Ø) samples, 2 g ± 0.2 g was weighed into the glass vials and an internal standard of 10 ppm acetophenone-β, β, β-D3 (Sigma-Aldrich, USA; 10 µl) was added. A blank of air was also included.

Samples were analysed using an Agilent 7890B gas chromatography system using MassHunter GC/MS acquisition software. The GC was coupled with an Agilent 5977B MSD and Gerstel multipurpose sampler (MPS) (Gerstel, Germany). Samples were incubated in the MPS which was heated to 60°C. Samples were shaken at 300 rpm for 30 minutes, after 10 minutes the fibre was introduced to a depth of 25 mm. Headspace sampling used a StableFlex solid-phase microextraction (SPME) fibre assembly (Supelco, USA). The assembly is comprised of a divinylbenzene, carboxen, polydimethylsiloxane (DVB/CAR/PDMS) 50/30 µm fibre with 23 gauge needle. The fibre was conditioned for 30 minutes at 270°C prior to first use, then for five minutes for subsequent uses. The oven was heated to 320°C for five minutes with a 200:1 split to remove contaminants. After head space sampling the fibre was introduced 54 mm into the injection port lined with a 0.75 mm straight/SPME inlet liner (Restek Corp, USA). The injection port was maintained at 250°C and the fibre was kept here for five minutes for complete desorption. A splitless mode was used with a solvent delay of 3.8 minutes and septum purge flow of 3 ml/minute. Volatiles were separated using a J&W HP-5ms GC Column, 30 m, 0.25 mm, 0.25 µm (Agilent) with helium as the carrier gas at 1.0 ml/min linear velocity. The oven gradient was 40°C for two minutes, then increased by 5°C per minute to 120°C which was maintained for two minutes, then increased 5°C per minute to 250°C which was maintained for two minutes, then increased 6°C per minute to 300°C which was held for five minutes. After separation of the metabolites through the GC they entered the MS via a 250°C transfer line. The MS source was maintained at 230°C, the MS quadrupole was held at 150°C. Normal scan mode was used ranging from 30 m/z to 550 m/z using 70 eV positive electron impact ionisation (EI+).

2.6.8 GC/MS data processing

Raw data was processed through automated mass spectral deconvolution and identification system (AMDIS). Compounds were identified using an in-house library which was constructed from standards and the NIST08 library. Relative quantification to the internal standard, where present, was performed.

2.6.9 Liquid chromatography mass spectrometry (LC/MS)

For identification of esters and to confirm the identity of adonixanthin epoxide in ZWRIU0 liquid chromatography/mass spectrometry (LC/MS) was used. Carotenoids were extracted as per 2.6.1. HPLC was then used to separate the metabolites and obtain an absorption spectrum using a diode array detector (Dionex). A C30 reverse phase column (3 µm, 150 mm x 2.1 mm) with guard column was used. The mobile phase consisted of methanol with 0.1% formic acid (A) and tert-methyl butyl ether with 0.1% formic acid (B). The gradient ran from 100% A / 0% B for five minutes, 95% A / 5% B for four minutes, then a linear gradient to 25% A / 75% B over 30 minutes, then 10% A / 90% B for 10 minutes. A flow rate of 0.2 ml/minute was used. Ionisation was provided by an atmospheric pressure chemical ionisation (APCI) in positive mode on a maXis (Bruker). Capillary temperature was 200°C and vaporisation temperature was 400°C. The mass was scanned from 100 – 1600 m/z.

Identification of esters present in P^{WT}ZWRI was performed using an Agilent infinity II (1290) LC/MS quantitive time of flight (Q-TOF) ion mobility 6560 (Agilent). Metabolites were separated on a C30 reverse phase column (3 µm, 150 mm x 2.1 mm). The mobile phase consisted of methanol with 0.1% formic acid (A) and tert-methyl butyl ether with 0.1% formic acid (B). The gradient ran from 100% A / 0% B for two minutes, then changing to 80% A / 20% B over one minute, holding at this ratio for three minutes, then a linear gradient to 30% A / 70% B over four minutes, holding at this ratio for 10 minutes, then a linear gradient to 100% A / 0% B for two minutes with a final hold for five minutes. A flow rate of 0.2 ml/minute was used. Ionisation was provided by APCI in positive mode. Capillary temperature was 250 °C and vaporisation temperature was 450°C. The mass was scanned from 100 – 1700 m/z with MS/MS between 700 and 1700 m/z.

2.6.10 Thin layer chromatography for lipid separation

HPTLC silica 60 F_{254} (Merck, Germany) thin layer chromatography (TLC) plates were used with a mobile phase of 91:30:7 acetone:toluene:water solvent mix. A TLC tank was left to saturate with the mobile phase before the TLC plate was added. Lipids were applied onto the TLC plate after extraction as described in 2.6.1, and resuspended in methanol (5 µl) and chloroform (5 µl). The whole extract was applied. A standard mix of 20 µg of each standard was applied to the left most lane. The standards used were mono, di and tri acylglycerol mix, monogalactosyldiacylglycerol, digalactosyldiacylglycerol, phosphotidylethanolamine and

phosphatidylcholine. After application of the samples to the plate, the plate was placed into the tank. Once the solvent front had migrated to approximately and inch from the top of the plate, the plate was transferred to a tank with vaporised iodine.

2.6.11 Sub-chromoplast fractionation

The method for sub-chromoplast fractionation is based on the method reported by M. Nogueira, *et al.* (2016). 120 g of fruit, between breaker +3 and breaker +5, per genotype were harvested, deseeded and chopped. The fruit was stored overnight, in darkness at 4°C to reduce the starch content. Keeping everything at 4°C, extraction buffer (0.4 M sucrose, 50 mM trizma base, 1 mM dithiothreitol (DTT), 1 mM ethylenediaminetetraacetic acid (EDTA)) was added to cover the fruit, left for five minutes then the fruit was blended (Waring blender 8010ES) twice for three seconds. The slurry was filtered through muslin by gentle pressure. The extracted juice was then divided by two to create two technical replicates per genotype. The juice was added to 500 ml centrifuge pots (Nalgene™) and topped up with extraction buffer to 2/3 of the bottle was full. After balancing the pots were loaded onto a Sorvall RC-5C centrifuge (Thermo Scientific) using a F12 6 x 500 LEX (Thermofisher Scientific) rotor and centrifuged for 10 minutes at 5000 x g at 4°C. The supernatant was discarded leaving the pellet in the bottle along with 5 ml of supernatant. The pellet was then resuspended in the remaining supernatant and the mixture placed in a 50 ml centrifuge tube (thick-wall ultratubes, Nalgene™) along with extraction buffer to ¾ of the tube. After balancing the tubes, they were centrifuged (RC-5C) in a F21 8 x 50 (Thermofisher Scientific) rotor for 10 minutes at 9000 x g at 4°C. The supernatant was then completely removed.

The pellet was resuspended in 3 ml of 45% sucrose gradient buffer (sucrose 45% w/v, tricine 50 mM, EDTA 2 mM, DTT 2 mM, sodium bisulphite 5 mM; pH 7.9) and placed into a potter-Elvehjem tissue grinder on ice, the centrifuge tubes were then rinsed with 45% sucrose buffer and the buffer added to the potter. Chromoplasts were broken using the potter-Elvehjem 10 times. The mixture was then placed in a chilled 50 ml falcon tube, and the potter was rinsed with 10 ml of 45% sucrose buffer. This was kept on ice.

The sucrose gradient was made in a 38.5 Ultra-Clear™ centrifuge tube (Beckman Coulter). 8 ml of the 45% sucrose solution with sub-chromoplast juice was added to the bottom of the tube. 6 ml of 38% sucrose buffer (sucrose 38% w/v, tricine 50 mM, EDTA 2 mM, DTT 2 mM, sodium bisulphite 5 mM; pH 7.9) was added carefully on top in a circular motion. In the same

fashion, 6 ml of 20% sucrose buffer (sucrose 20% w/v, tricine 50 mM, EDTA 2 mM, DTT 2 mM, sodium bisulphite 5 mM; pH 7.9), 4 ml of 15% sucrose buffer (sucrose 15% w/v, tricine 50 mM, EDTA 2 mM, DTT 2 mM, sodium bisulphite 5 mM; pH 7.9) and finally 8 ml of 5% sucrose buffer (sucrose 5% w/v, tricine 50 mM, EDTA 2 mM, DTT 2 mM, sodium bisulphite 5 mM; pH 7.9) were added. After balancing with 5% sucrose buffer, tubes were centrifuged (XPN-90 Ultracentifuge, Beckman Coulter) in a SW28 (Beckman Coulter) rotor for 20 hours at 100000 x g at 4°C with vacuum on.

After centrifugation photographs of the gradient were taken. Fractions were then collected using the 203B fraction collector (Gilson) and pump (MINIPULS® 3 Peristaltic Pump). The gradient was fractioned into 1 ml per 1.5 ml microcentrifuge tube, 31 fractions in total. The pellet was not collected.

For extraction of carotenoids and proteins, fractions were transferred to a microcentrifuge tube (2 ml). Methanol (250 µl) was added and vortexed, then chloroform (750 µl) and an internal standard of tocopherol acetate (10 µg). The extraction was incubated on ice for 20 minutes. Phases were then separated by centrifugation (Eppendorf 5424) at maximum speed for five minutes. The bottom layer was removed at collected in a separate tube. Chloroform (750 µl) was added to the original tube, vortexed and centrifuged as before. The bottom layer was removed and pooled with the previous organic phase. This was the carotenoid extract. Cold methanol (750 µl) was added to the original tube, vortexed and centrifuged at maximum speed for 10 minutes. The supernatant was discarded, and the pellet stored at -20°C. Carotenoids were then analysed as described in section 2.6.4.

2.6.12 Data analysis

Raw data was processed by taking the mean of the technical replicates for each biological sample. The mean of the technical replicates was then used for the statistical analysis and the calculation of the standard deviation. Data has been presented as the mean of the biological replicates ± standard deviation. Statistical analysis was performed using XLSTAT premium 2019.4.2 (Addinsoft). Analysis of variance (ANOVA) or T-test were used as stated. Graphs were produced using Graphpad Prism 8.

Chapter III:

Improvement of astaxanthin production in tomato fruit

3.1 Introduction

3.1.1 General background

To date several iterative rounds of gene combinations have been used to produce the non-endogenous ketocarotenoids in tomato fruit (Enfissi, *et al.*, 2019; Mortimer, 2010; Nogueira, *et al.*, 2017). In this work the combination of the biosynthetic ketocarotenoid genes *Crt*Z and *Crt*W in combination with a high beta-carotene background and the overexpression of the plant hydroxylase *Crt*R-*b2* has generated astaxanthin producing fruit. Ketocarotenoid esters were also produced, as found previously in other ketocarotenoid producing lines (Nogueira, *et al.*, 2017). However, the level and composition of the ketocarotenoids esters are different to those previously seen.

3.1.2 Generation and nomenclature of ketocarotenoid producing lines

The line used in this work is comprised of several different backgrounds. Table 3-1 and Figure 3-1 summarise the pedigree of each trait.

The first approach used to try and produce ketocarotenoids in tomato used two bacterial genes; both of these are from the bacteria *Brevundimonas.* A carotenoid hydroxylase (*Crt*Z abbreviated Z); which hydroxylates the 3 and 3' position of the beta ring and a carotenoid oxygenase (*Crt*W abbreviated W); which adds a keto group to the 4 and 4' position of the beta ring were transformed into *S. lycopersicum* moneymaker (LA2706) background. This should have provided all the required genes for production of ketocarotenoids. However, the resulting ketocarotenoid content was minimal (160 µg/g); instead it was lycopene that accumulated. The accumulation of lycopene was believed to be due to the absence of beta-carotene, and therefore an absence of a negative feedback signal to inhibit lycopene synthesis (Enfissi, *et al.*, 2019). Throughout this work, *Crt*Z and *Crt*W genes have been called ZW. If the two genes were not present and the material was azygous for the genes, the symbol phi (Ø) is used to show this, i.e. ZWØ. If present, ZW was in the hemizygous state, as silencing and loss of vigour was observed when present in the homozygous state.

In order to overcome the depletion of beta-carotene in the ZW line it was crossed with a recombinant introgression line which was high in beta-carotene (Enfissi, *et al.*, unpublished). The high beta-carotene line had the lycopene cyclase (*cyc*-b, also called the B-gene) allele

from *Solanum galapagense* (LA0483), this including the *S. galapagense cyc*-b promoter which is more active than the *S. lycopersicum* equivalent. The background for the introgression was UC204B which was backcrossed seven times to achieve the desired promoter without any other traits from *S. galapagense*. Throughout both this work and previously published work (Nogueira, *et al.*, 2017) this high beta-carotene line has been denoted as RI. Like ZW, the Ø symbol represents an azygous state. Since homozygous RI is optimal for carotenoid production and prevents separating progeny all RI presented was homozygous.

A combination of the ZW and RI lines, gives the ZWRI line (Nogueira, *et al.*, 2017). This produced more ketocarotenoids (3 mg/g) than the previous approach but stopped short of astaxanthin and instead accumulated phoenicoxanthin and canthaxanthin. The biosynthetic step from phoenicoxanthin or canthaxanthin to astaxanthin is by further hydroxylation. The ZWRI line interestingly produced ketocarotenoid esters as well as free ketocarotenoids in the tomato fruit, a process which does not naturally occur in tomato.

To increase the production of fully hydroxylated ketocarotenoids, the stable ZWRI variety from the publication by Nogueira, *et al.* (2017) was crossed with a third tomato line. Originally designed to increase non-ketolated xanthophylls, this third line had been transformed with the plant beta-carotene hydroxylase (*Crt*R-*b2)* under a 35S promoter (D'Ambrosio, *et al.*, 2011). The background for this transformation was redsetter, with a single, hemizygous event being given the symbol U. Therefore, homozygous is denoted as UU, hemizygous as U0 and azygous as 00. The optimal zygosity of this gene was unknown, and therefore all three possibilities were analysed.

The resulting line from the crossing of ZW(Ø)RI(Ø) and UU/U0/00 is the ZW(Ø)RI(Ø)UU/U0/00 line. The characterisation of this line forms the basis of this chapter. This line has two hydroxylases, one oxygenase and an upregulated cyclase, therefore there was a strong push towards ketocarotenoid production. Interesting phenotypic effects were also observed in this line, some from the constitutive expression of genes throughout the plant, and others through genetic silencing due to overexpression.

Table 3-1. Summary of all the genetic components of ZW(Ø)RI(Ø)UU/U0/00
The abbreviations are used throughout this work to refer to the respective genes.

Genetic feature(s)	Abbreviation	Features	Background	Reference
Transformation of carotenoid hydroxylase (*Crt*Z) and carotenoid oxygenase (*Crt*W)	**ZW**	• Transformation of *Brevundimonus* genes to stimulate ketocarotenoid production • Depleted in beta-carotene • Accumulates lycopene	Moneymaker cultivar	(Enfissi, *et al.*, 2019)
Upregulation of lycopene cyclase (c*yc*-b) by introgression of the *S. galapagense* promoter	**RI**	• Introgression line incorporating the strong c*yc-b* promoter from *S. galapagense* into *S. lycopersicum* • Accumulates beta-carotene	*Solanum galapagense* backcrossed seven times into *Solanum lycopersicum* (UC204B)	Unpublished
*Crt*Z, *Crt*W and upregulation of c*yc-b*	**ZWRI**	• Ketocarotenoid producing line • Accumulates phoenicoxanthin and canthaxanthin • Produces ketocarotenoid esters in fruit	Moneymaker and UC204B cultivars	(Nogueira, *et al.*, 2017)
Transformation of *Crt*R-*b2* under a 35S promoter	**UU/U0/00**	• Overexpresses the endogenous beta-hydroxylase *CrtR-b2* • Accumulates violaxanthin and neoxanthin • Analysed as homozygous (UU), hemizygous (U0) or azygous (00)	Redsetter cultivar	(D'Ambrosio, *et al.*, 2011)
*Crt*Z, *Crt*W, upregulation of c*yc-b* and overexpression of *Crt*R-*b2*	**ZW(Ø)RI(Ø)UU/U0/00**	• ZW: azygous (Ø) in control plants or hemizygous in test plants • RI: azygous (Ø) in control plants or homozygous in test plants • Analysed as homozygous (UU), hemizygous (U0) or azygous (00) for *Crt*R-*b2* • Increased astaxanthin production	Moneymaker, UC204B and Redsetter.	Current work

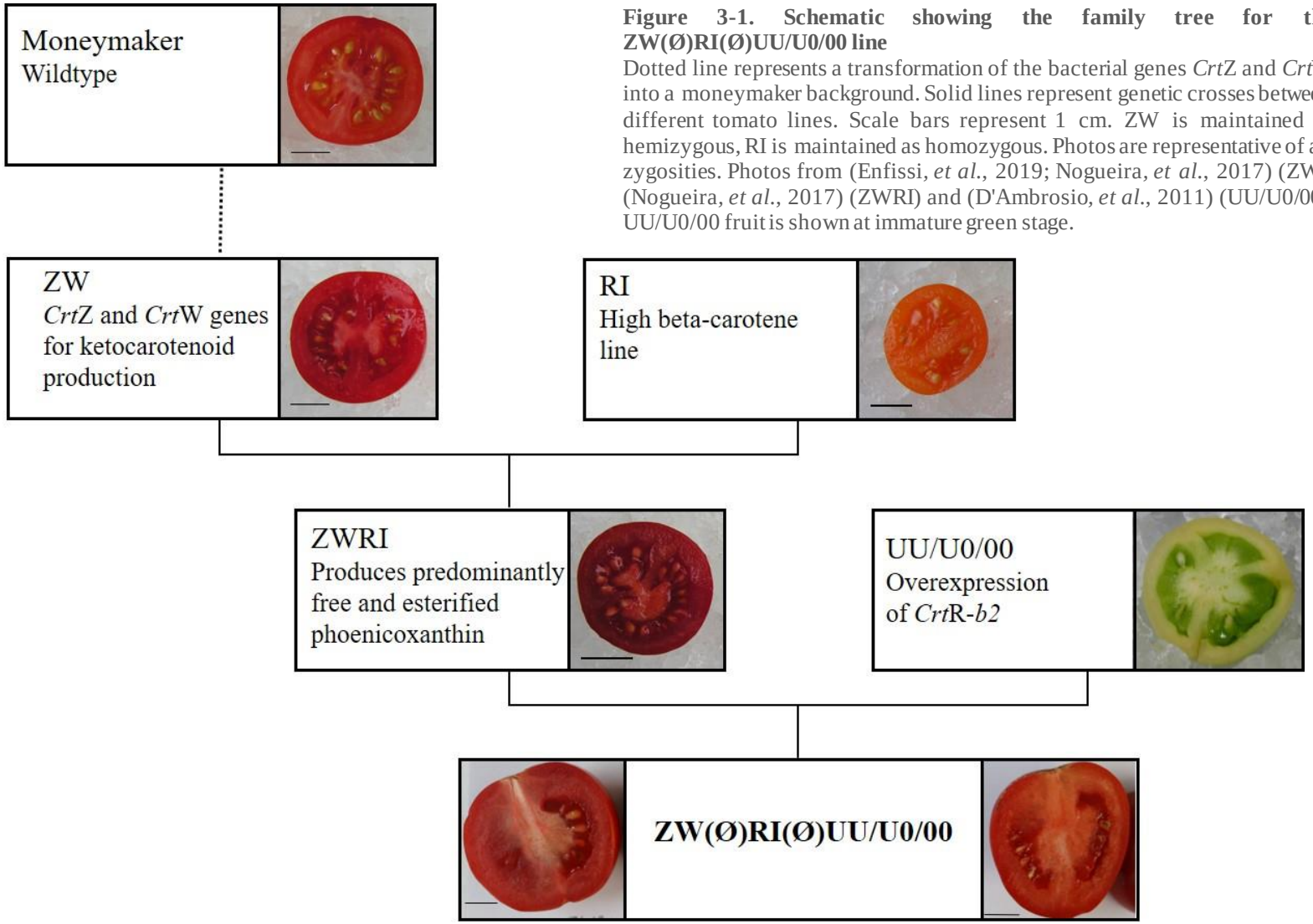

Figure 3-1. Schematic showing the family tree for the ZW(Ø)RI(Ø)UU/U0/00 line

Dotted line represents a transformation of the bacterial genes *Crt*Z and *Crt*W into a moneymaker background. Solid lines represent genetic crosses between different tomato lines. Scale bars represent 1 cm. ZW is maintained as hemizygous, RI is maintained as homozygous. Photos are representative of all zygosities. Photos from (Enfissi, *et al.*, 2019; Nogueira, *et al.*, 2017) (ZW), (Nogueira, *et al.*, 2017) (ZWRI) and (D'Ambrosio, *et al.*, 2011) (UU/U0/00). UU/U0/00 fruit is shown at immature green stage.

3.2 Results

3.2.1 Identification and molecular characterisation of plants overexpressing *Crt*Z, *Crt*W, *cyc*-b and *Crt*R-*b2*

The characterisation of plants from the ZW(Ø)RI(Ø)UU/U0/00 line required multiple approaches. F_2 plants were created by self-pollination of hemizygous/heterozygous F_1 plants. Therefore, F_2 were segregating on all three of the genetic components; for any given genotype, one in 64 plants was expected to carry the desired combination. Whilst the optimal zygosity has already been achieved in the parental line and is known for two of the three events, the *Crt*R-*b2* component was yet to be optimised. The impact of the zygosity had a marked effect on the resulting carotenoid profile.

Screening for ZW was by observation; ZW produced ketocarotenoids in the leaf material, this provided a brown colouration visible throughout the plant from the cotyledon stage onwards (Figure 3-3). ZW was known to silence when homozygous and produced a crippled phenotype with severe loss of vigour in seedlings (Figure 3-3). Given this discernible difference in appearance, selection of plants was visual providing it was carried out at seedling stage.

RI is an introgression event, both the presence and zygosity of the promoter could be detected by PCR. An azygous plant would have both alleles from the *S. lycopersicum* promoter, a homozygous plant would have both alleles from the *S. galapagense* promoter, and a heterozygous plant would have one of each. Specific primers (section 2.5) could be used to distinguish between the two alleles, therefore amplification by PCR could confirm zygosity (Figure 3-2). RI functions optimally when homozygous.

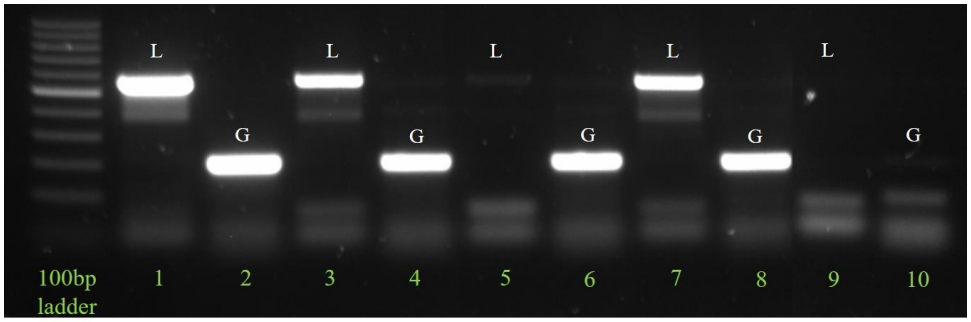

Figure 3-2. Image of agarose gel of PCR amplified fragments used for screening of RI
Lanes with L refer to the *S. lycopersicum* allele, lanes with G refer to the *S. galapagense* allele. Fragment size verified with a commercial ladder. Lanes 1 + 2 are a positive plasmid control. Lanes 3 + 4, 7 + 8 show a heterozygous plant, lanes 5 + 6 show a homozygous plant. Lanes 9 + 10 are a no template control.

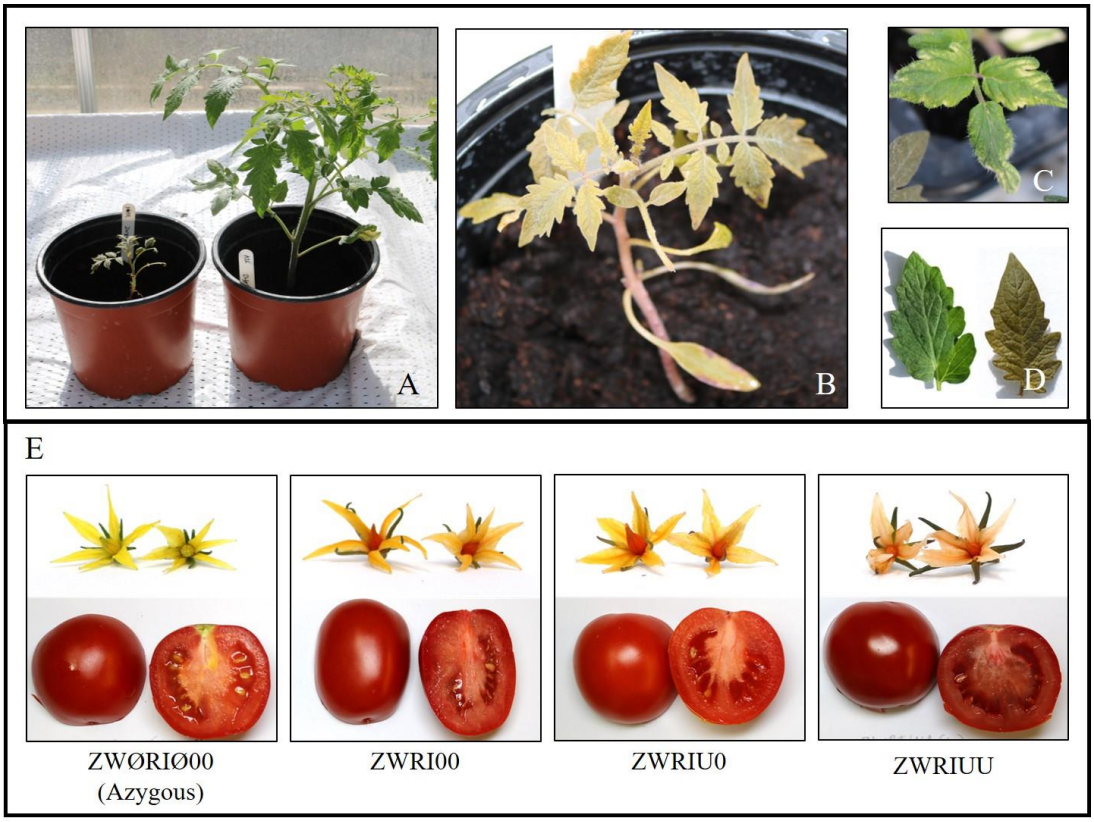

Figure 3-3. Phenotypes of the ZW(Ø)RI(Ø)UU/U0/00 line
A) Comparison of the stunted homozygous ZW phenotype (left) and an ZWØ phenotype (right). B) Closer image of the stunted phenotype of a homozygous ZW plant. Plants develop slower, causing stunted growth, smaller leaves and mottling of the brown colouration. C) Variegated leaves caused by the homozygous UU transgene. D) Comparison of a green azygous leaf (left) and a brown ZW leaf. E) Changes in fruit and flower caused by the zygosity of UU/U0/00. The orange colouration to the flowers is produced by ZW forming ketocarotenoids. ZWRIUU has paler petals than ZWRIU0 or ZWRI00. Fruit morphology changes according to the backgrounds present, the redsetter background elongates the fruit, however this is reduced in ZWRIU0 and ZWRIUU. The colour of fruit correlates with the carotenoid profile (section 3.2.2). Each tissue is shown at scale within a tissue type.

Screening for UU/U0/00 required several different approaches. Initially a PCR was used to detect the presence and absence of the transgene, however the zygosity could not be established using this approach. Specific primers were designed which span the 35S-*Crt*R-*b2* border to selectively amplify only the extra, overexpressed transgene. Similar to ZW, UU/U0/00 also has a phenotypic effect. Although the optimal zygosity for UU/U0/00 was unknown, it had previously been reported to have some silencing effects when homozygous (D'Ambrosio, *et al.*, 2011). This silencing manifested itself to give paler petals, and variegation of the leaves (Figure 3-3). These phenotypic changes were not as obvious as those seen in ZW however, and so the physical appearance could only be used alongside other approaches.

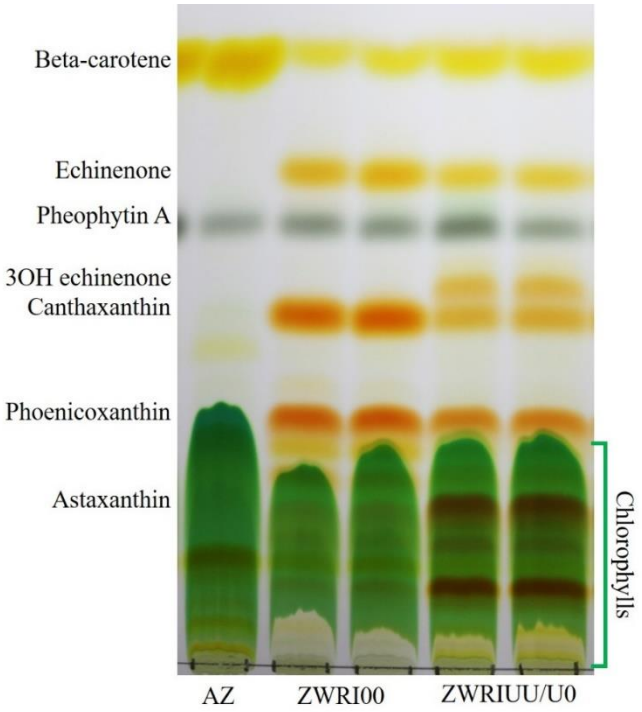

Figure 3-4. TLC plate of leaf material from ZW(Ø)RI(Ø)UU/U0/00
Carotenoid enriched extracts were obtained from fresh leaf material. Carotenoid identification is based on the Rf values from authentic standards. AZ is the azygous (ZWØRIØ00) control.

Thin layer chromatography (TLC) was a useful technique for quick, qualitative analysis of carotenoids. TLC was used to help screen for the UU zygosity. The zygosity impacted the carotenoid profile, and therefore the use of a TLC provided a visual way of distinguishing between classification of plants. Figure 3-4 shows a typical TLC of leaf material from seedlings, it appeared to show clear differences between plants. However, after further analysis on older plants it seemed that the carotenoid profile of plants at seedling stage was not representative of the zygosity, and therefore other techniques needed to be used.

A Southern blot was used to help identify the zygosity of selected plants. Southern blot analysis allowed for the zygosity to be identified using the intensity of fluorescence given by each band; a homozygous band would be twice as intense as a hemizygous band, as there was double the amount of the specific DNA region in which the probe can bind. Using the results from the selected plants, the phenotypic characteristics could be matched to a zygosity, and therefore not all plants required a Southern blot. The probe used to identify the transgene was created from the same primers as those used for the PCR of UU/U0/00; they span the 35S-*Crt*R-*b2* border. The copy number could also be obtained by the number of bands present.

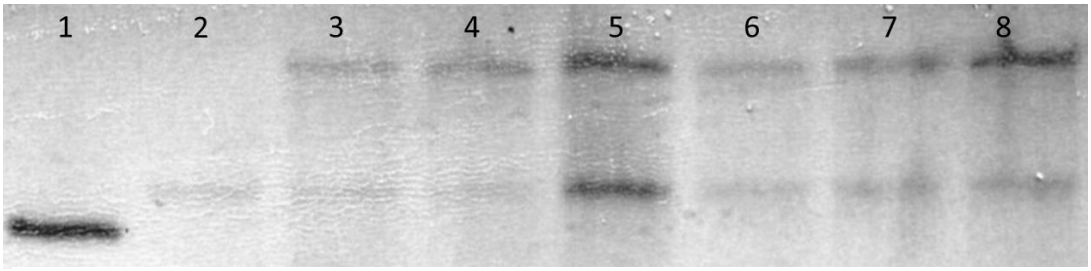

Figure 3-5. Southern blot to determine zygosity of UU/U0/00
1. Plasmid control. 2. moneymaker control. 3. U0 parent. 4-8. Selection of ZW(Ø)RI(Ø)UU/U0/00 plants. Band 5 is noticeably darker on both the blot and the post digestion agarose gel; therefore, it is omitted from analysis. 4,6 and 7 are hemizygous, 8 is homozygous

Figure 3-5 shows two bands, only one of which is specific to transgenic plants, and therefore the UU/U0/00 insert is a single copy. Looking at the intensity of the specific band (topmost band) and taking into account the intensity of DNA after digestion, a visual comparison between samples was made. This confirmed that the UU/U0/00 parent plant is hemizygous (U0) and that the presumed phenotypes matched the zygosities. Plants with variegated leaves and paler petals were homozygous.

Quantitive, real-time PCR (qPCR) was another technique used to confirm the zygosity of UU/U0/00. Two approaches were used; the first was to identify the copy number of unknown samples by comparison to samples with a known zygosity. After confirmation of a single insertion by Southern blot, the qPCR analysis using the same primers would identify a hemizygous event as a single copy, and a homozygous event as a double copy. Normalisation to the known single copy gene *pds* was carried out and quantification made by standard curve. Samples were also compared to previously identified zygosities, provided by E. Rapacz. This technique presented a clear difference in hemizygous and homozygous plants, homozygous plants had nearly twice (×1.8) the calculated DNA concentration as hemizygous plants (Figure 3-6).

The other approach which used qPCR was by analysing the expression profiles of both endogenous and transgenic *Crt*R-*b2* in hemizygous and homozygous leaf. As homozygous plants experienced silencing the expression levels were expected to be lower, despite more copies of the gene. Normalisation to the housekeeping gene *actin* was performed and quantification made to a standard curve. The results from duplicated samples, performed in individual reactions (Figure 3-7) were as predicted; expression of *Crt*R-*b2* was lower in homozygous plants.

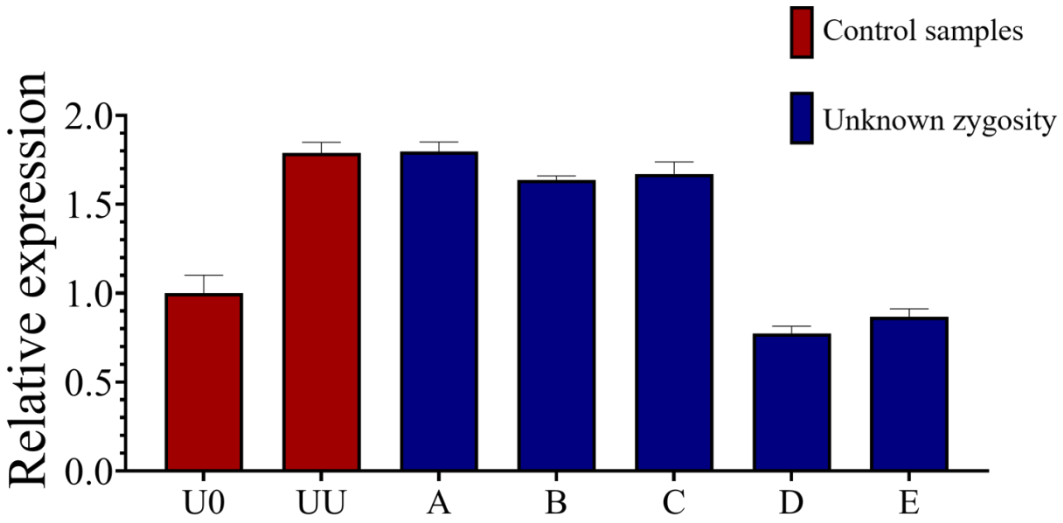

Figure 3-6. Copy number analysis using genomic DNA of 35S-*Crt*R-*b2* relative to *pds*
Relative concentration of 35S-*Crt*R-*b2* normalised to *pds*. Scaled to the hemizygous control. Control samples of known zygosity were provided by E. Rapacz. A, B and C are homozygous, D and E are hemizygous. Error bars show the standard deviation as calculated by $\sqrt{\left(\frac{SD}{mean}\right)^2_{CrtR\text{-}b2} + \left(\frac{SD}{mean}\right)^2_{actin}}$

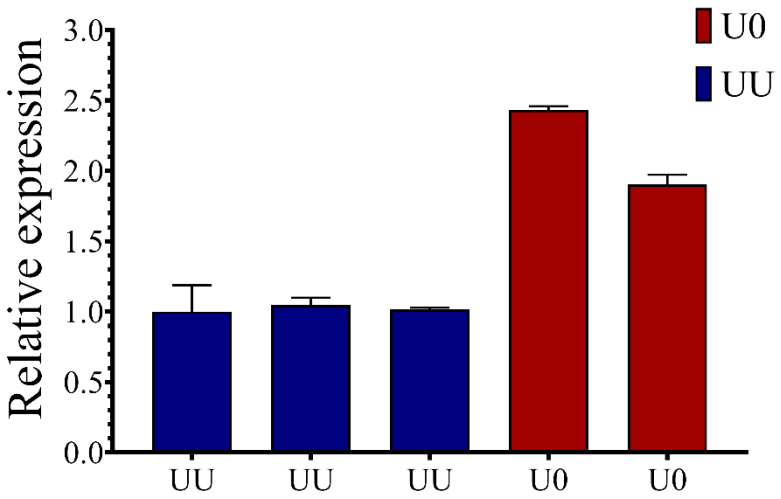

Figure 3-7. Expression analysis of *Crt*R-*b2* in hemizygous and homozygous leaf
Relative expression from calculated concentration, normalised to actin. Scaled to first homozygous sample. Error bars show the standard deviation as calculated by $\sqrt{\left(\frac{SD}{mean}\right)^2_{CrtR\text{-}b2} + \left(\frac{SD}{mean}\right)^2_{actin}}$

3.2.2 Analyses of carotenoid content in fruit of the F_2 generation

To analyse the changes in carotenoid content, plants from azygous, ZWRI00, ZWRIU0 and ZWRIUU were assessed using UPLC (section 2.6.4), this provided a quick way of analysing all free carotenoids and mono-esters. Example chromatograms are shown in Figure 3-8. Quantities of carotenoids have been obtained by analysis of a minimum of two biological replicates and three technical replicates for each group of plants. Absorbance values were corrected to an internal standard of tocopherol acetate before conversion to amount in μg/g dry weight (DW) using calibration curves. Where the exact carotenoid calibration curve was not available a curve for a similar carotenoid was used.

One of the unknowns in this piece of work was the impact of zygosity of UU/U0/00, which zygosity would give the most optimal carotenoid profile, and whether the possible silencing of homozygous UU would be detrimental to vigour and carotenoid production. Comparison of ZWRIUU to ZWRIU0 shows that the zygosity of UU/U0/00, did have a large impact on the carotenoids which were accumulated. ZWRIU0 had more violaxanthin (infinite increase (20 μg/g)), adonixanthin epoxide (×9), astaxanthin (×2) and adonixanthin (×8) than ZWRIUU. These were all compounds which were fully hydroxylated, therefore suggesting the *Crt*R-*b2* gene is active. More striking was the difference in the carotenoids which were reduced in ZWRIU0 compared to ZWRIUU. These were phoenicoxanthin (×0.05), canthaxanthin (×0.01), 3'OH echinenone (×0.006), echinenone (×0.09) and beta-carotene (×0.01). There was also a non-significant reduction in 3OH echinenone (×0.33) and esterified carotenoids (×0.25). The di-esters of ZWRIU0 were not analysed on this system. The predominant free carotenoid in ZWRIU0 was adonixanthin epoxide (260 μg/g). The identification and possible synthesis for this is discussed in 3.2.4. The main target for this work was astaxanthin, which was increased to higher levels (142 μg/g) than seen before. These changes are shown in Figure 3-9, with full amounts detailed in Table 3-2.

Comparison of ZWRIUU and ZWRI00 clearly reveals that silencing was occurring. These two genotypes have similar carotenoid profiles despite the addition of an extra copy of the hydroxylase gene. The only significant differences between ZWRI00 and ZWRIUU are in canthaxanthin (×2) and 3'OH echinenone (×2) which are higher in ZWRIUU.

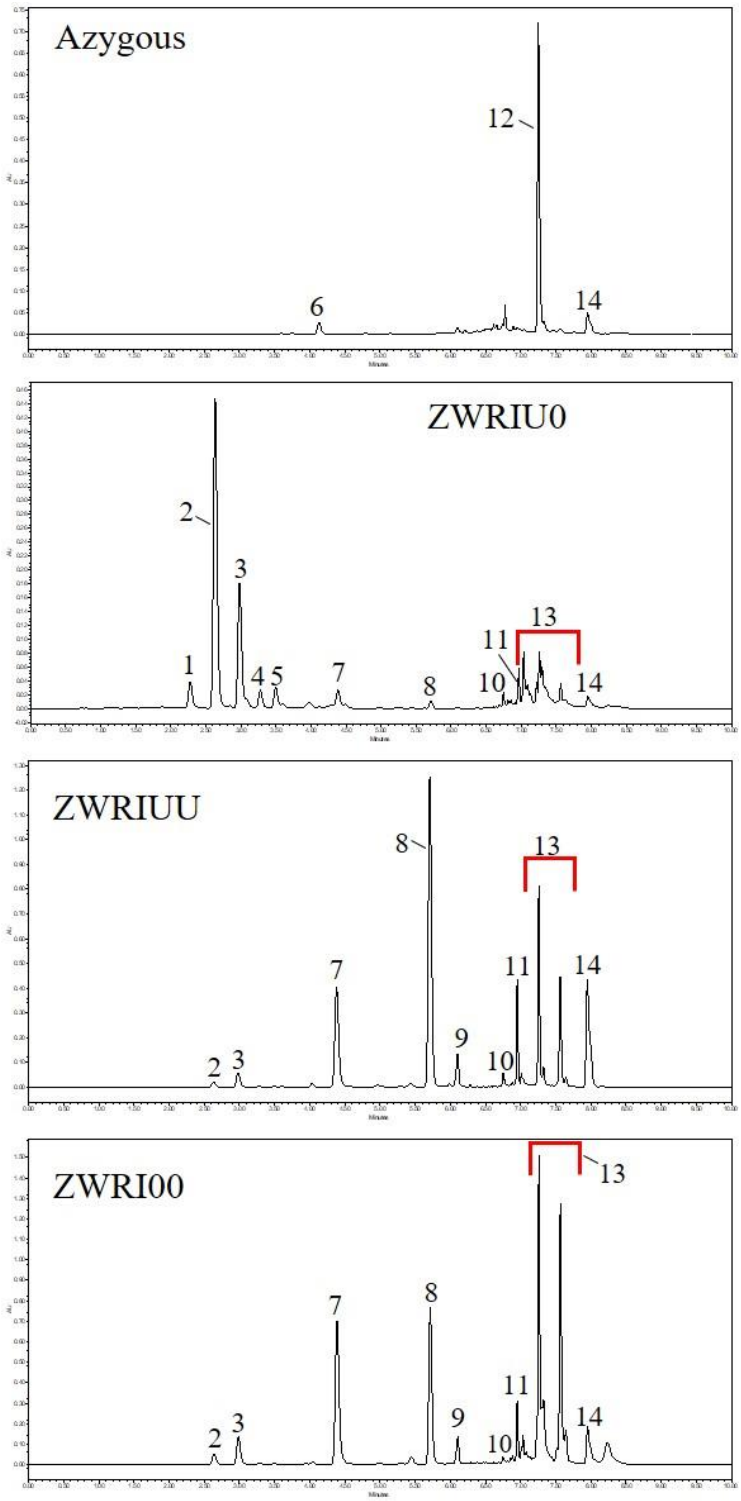

Figure 3-8. Example chromatograms from the F_2 generation of ZWRIUU/U0/00
1) Violaxanthin, 2) Adonixanthin epoxide, 3) Astaxanthin, 4) Unknown, 5) Adonixanthin, 6) Lutein, 7) Phoenicoxanthin, 8) Canthaxanthin, 9) 3'OH echinenone, 10) 3OH echinenone, 11) Echinenone, 12) Lycopene, 13) Esterified carotenoids, 14) Beta-carotene

Comparison of the chromatograms in Figure 3-8 give a visual way of showing the similarities between ZWRI00 and ZWRIUU, this is in juxtaposition to the contrasting chromatograms of ZWRIU0 and ZWRIUU.

The azygous control was very different to the plants with ketocarotenoid genes regardless of zygosity. As observed before in traditional tomatoes the azygous control accumulated predominantly lycopene, but also contained lutein and beta-carotene. In ZWRIUU and ZWRI00 lycopene and lutein were severely decreased (×0.02), beta-carotene was increased (×5), and there was accumulation of ketocarotenoids. The increase in beta-carotene was likely to be due to the overall increase in carotenoids, and therefore the precursor was also upregulated. ZWRIU0 maintained the azygous level of beta-carotene. A summary of the predominant carotenoids across all genotypes is shown in Table 3-3.

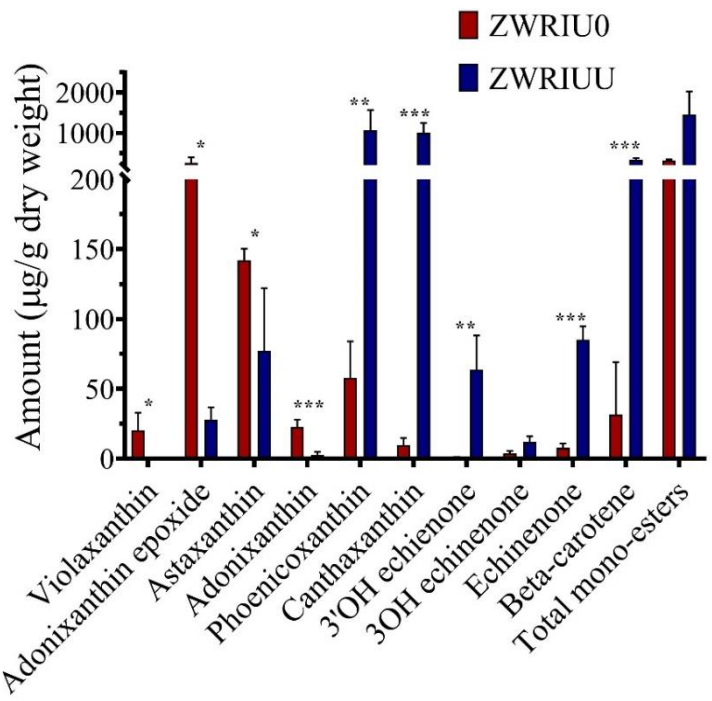

Figure 3-9. Carotenoid profile of ZWRIU0 and ZWRIUU fruit
Amounts calculated from a minimum of three biological and three technical replicates, with four fruits per plant pooled. Error bars represent the standard deviation. Statistical significances are generated from an ANOVA with Tukey post hoc test, *0.05≥p≤0.01, ** 0.01>p≤0.001, ***<0.001.

Table 3-2. Carotenoid content of fruit from the F_2 generation of ZW(Ø)RI(Ø)UU/U0/00
Amounts in µg/g dry weight with ± standard deviation. All values are calculated from at least two biological replicates, of four pooled fruit per plant. Each biological replicate is an average of three technical replicates. Lycopene was not quantified (NQ) in fruit with esters due to co-elution.

Carotenoid	Azygous	ZWRI00	ZWRIU0	ZWRIUU
Violaxanthin	0.00 ±0.00	0.00 ±0.00	20.42 ±12.39	0.00 ±0.00
Adonixanthin epoxide	0.00 ±0.00	49.82 ±5.96	261.27 ±133.10	27.69 ±8.98
Astaxanthin	0.00 ±0.00	130.80 ±18.44	141.93 ±8.30	77.23 ±44.81
Unknown A	0.00 ±0.00	5.06 ±1.18	20.24 ±8.19	0.00 ±0.00
Adonixanthin	0.00 ±0.00	6.81 ±1.08	22.64 ±5.13	2.56 ±2.25
Lutein	18.60 ±9.04	0.00 ±0.00	0.37 ±0.13	0.00 ±0.00
Phoenicoxanthin	0.00 ±0.00	1193.91 ±217.94	57.81 ±26.11	1063.66 ±499.81
Canthaxanthin	0.00 ±0.00	462.28 ±76.57	9.64 ±5.10	997.22 ±245.96
3'OH echinenone	0.00 ±0.00	27.47 ±12.26	0.38 ±0.76	63.59 ±24.55
3OH echinenone	0.00 ±0.00	24.82 ±16.28	3.87 ±1.57	11.92 ±4.01
Echinenone	0.00 ±0.00	68.12 ±15.57	7.72 ±3.03	84.94 ±9.76
Lycopene	686.09 ±195.90	NQ	NQ	NQ
Beta-carotene	56.11 ±31.17	224.38 ±87.49	31.53 ±37.65	331.58 ±45.90
Phytofluene	324.11 ±42.83	0.00 ±0.00	0.00 ±0.00	0.00 ±0.00
Phytoene	138.56 ±29.30	10.83 ±3.63	3.65 ±3.00	13.10 ±2.85
Carotenoid mono-esters	0.00 ±0.00	2400.76 ±722.23	322.65 ±25.28	1450.71 ±575.53

Table 3-3. Summary of free carotenoid profiles in ZW(Ø)RI(Ø)UU/U0/00
Amounts in µg/g DW. Percentages calculated from total of known, identified carotenoid only. Information for ZWRIØ comes from (Nogueira, *et al*., 2017).

Modifications	Predominant groups	Specific carotenoids	Total free carotenoids
Azygous	Carotenoids only	56% lycopene	1223
ZWRIØ	Carotenoids	77% lycopene, 2% ketocarotenoids	3287
ZWRI00	Ketocarotenoids (89%)	54% phoenicoxanthin, 21% canthaxanthin	2209
ZWRIUU	Ketocarotenoids (87%)	40% phoenicoxanthin, 37% canthaxanthin	2683
ZWRIU0	Ketocarotenoids (86%)	44% adonixanthin epoxide, 24% astaxanthin,	588

3.2.3 Identification of esters; ketocarotenoids and fatty acids

In order to identify the unknown esters present in ZWRIU0, samples were run on liquid chromatography mass spectrometry/mass spectrometry (LC/MS/MS). Using the spectra and retention time the base carotenoid could be identified. This could then be subtracted from the mass, with the remainder belonging to the attached fatty acid(s). The retention time suggests that in ZWRIUU and ZWRI00 all the esters are mono-esters, with no di-esters present. However, in ZWRIU0 there are also di-esters of astaxanthin and adonixanthin epoxide produced. The identification of the mono-esters was aided by the work done on ZWRI by (Nogueira, *et al.*, 2017). Esters in this line were identified as phoenicoxanthin and adonixanthin C14:0 and C16:0. The esters present in ZWRIUU and ZWRI00 are presumed to be the same as those in ZWRI.

3.2.4 Identification and confirmation of the rare carotenoid adonixanthin epoxide

The predominant carotenoid in the F_2 generation of ZWRIU0 has been identified as adonixanthin epoxide (Figure 3-10). It had previously been found in the previous ketocarotenoid work but was but not previously identified in tomato fruit. The retention time for this carotenoid was at 2.6 minutes (UPLC method section 2.6.4). This is early in the run, between violaxanthin and astaxanthin. This retention time suggested the carotenoid was relatively polar, indicating the presence of multiple oxygens. The spectrum had two maxima, one at 455 nm and one at 473 nm. The shape was between that of the bell shape from a ketocarotenoid and the triple wave shape of an epoxide (Figure 3-11). LC/MS analysis provided a mass of 599 m/z, and also revealed mono and di esters of this carotenoid. Combination of this evidence identified this carotenoid as adonixanthin epoxide, also called 4-ketoantheraxanthin, the structure is shown in Figure 3-10. The polarity matched the presence of two hydroxy, one keto and one epoxy groups. This also provides two possible sites at which esterification can occur.

Adonixanthin epoxide had been previously reported as 4-ketoantheraxanthin in ZW tobacco (Hasunuma, 2008; Huang, *et al.*, 2013; Shindo, *et al.*, 2008). Shindo, *et al.* (2008) provides full structural identification, including by nuclear magnetic resonance (NMR) imaging. Their findings match the characterisation performed on the predominant carotenoid of F_2 ZWRIU0. This further strengthens the identification of this carotenoid as adonixanthin epoxide.

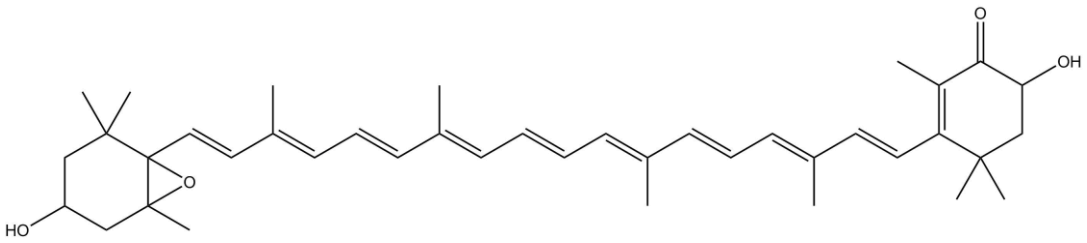

Figure 3-10. The proposed structure of adonixanthin epoxide

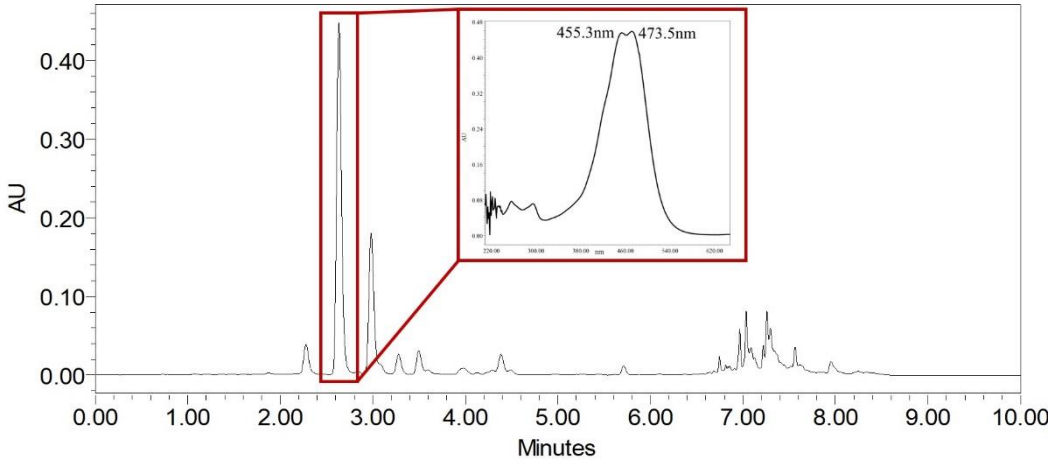

Figure 3-11. Chromatogram of ZWRIU0 from UPLC analysis with spectrum of adonixanthin epoxide
The red box highlights the peak representing adonixanthin epoxide, which is the predominant carotenoid of F_2 ZWRIU0. The inserted spectrum is from adonixanthin epoxide and has maxima at 455 nm and 474 nm.

3.2.5 Semi-volatile analysis of ketocarotenoid producing fruit

Many of the volatiles produced from tomato fruit are from the cleavage and degradation of carotenoids. If the carotenoid profile is altered, it follows that the volatile profile is also altered. Analysis of the volatiles allows for an insight into the degradation of specific metabolites, such as carotenoids. The addition of ketocarotenoids resulted in novel volatiles which were not seen in the azygous controls. These volatiles gave an indication of where the ketocarotenoids were cleaved. Cleavage products are often involved in downstream signalling; therefore, the volatile profile can give an important understanding of how a change in carotenoid profile has the potential to affect other biological pathways.

Figure 3-12 displays a heatmap of all 26 volatile compounds that showed a significant difference within azygous, ZWRI00, ZWRIU0 and ZWRIUU. There was clear grouping of different volatiles to different genotypes, with most differences occurring between the azygous control and any of the ketocarotenoid producing genotypes. The carotenoid derived volatiles farnesyl acetone, 2,3,5,8-tetramethyl-1,5,9-decatriene, sulcatol, sulatone, 1,3,4-trimethyl-3-cyclohexanene-1-carboxaldehyde, perillene, 2,6,6-trimethyl-cyclohexanone, 2-methyl-1-hepten-6-one, 2,6-dimethyl-2,6-octdiene, 2,3-epoxygerianial, 2,7-dimethyl-3,5-octadiene, 3,7-dimethyl-3,5-octadienal, beta-citral and pseudoionone were all observed with a higher

abundance in the azygous control than the ZW containing genotypes. Accordingly, the ketocarotenoid derived volatiles beta-isophorone and oxo-cyclocitral were only present in fruit with ketocarotenoids. There were also other, non-significant ketocarotenoid derived volatiles which were only observed in ZWRI00, ZWRIU0 or ZWRIUU. These were also completely absent in the control but present in the ketocarotenoid profiles.

There were volatiles which are not directly related to carotenoids which showed a significant change. Some of these related to fatty acids or esters; *n*-octane, formic acid and isopropyl acetate. Interestingly, these were all only altered in ZWRIU0; with a significant increase from that present in ZWRI00 or ZWRIUU. The other seven significant volatiles were from other parts of the plant metabolism, such as amino acids or phenolics. These volatiles show no trend in which genotype they were altered in.

The prevalent feature from comparison of the volatile data is the number of compounds which differ between azygous and ZWRIUU/U0/00. Out of the 26 significantly different compounds, 17 of these were from comparison of the control background to any of the ketocarotenoid genotypes with the majority derived from carotenoids. ZWRIUU/U0/00 had a significant reduction in the carotenoid derived volatiles compared to Az. The effect of the UU component was less marked; there were four significant compounds identified when comparing ZWRIUU and ZWRIU0. Three of these related to fatty acids, and one from phenylalanine. The remaining five significant volatiles differed in ZWRI00 when compared to the other backgrounds. The relative amounts of all the significant volatiles are display in Table 3-4.

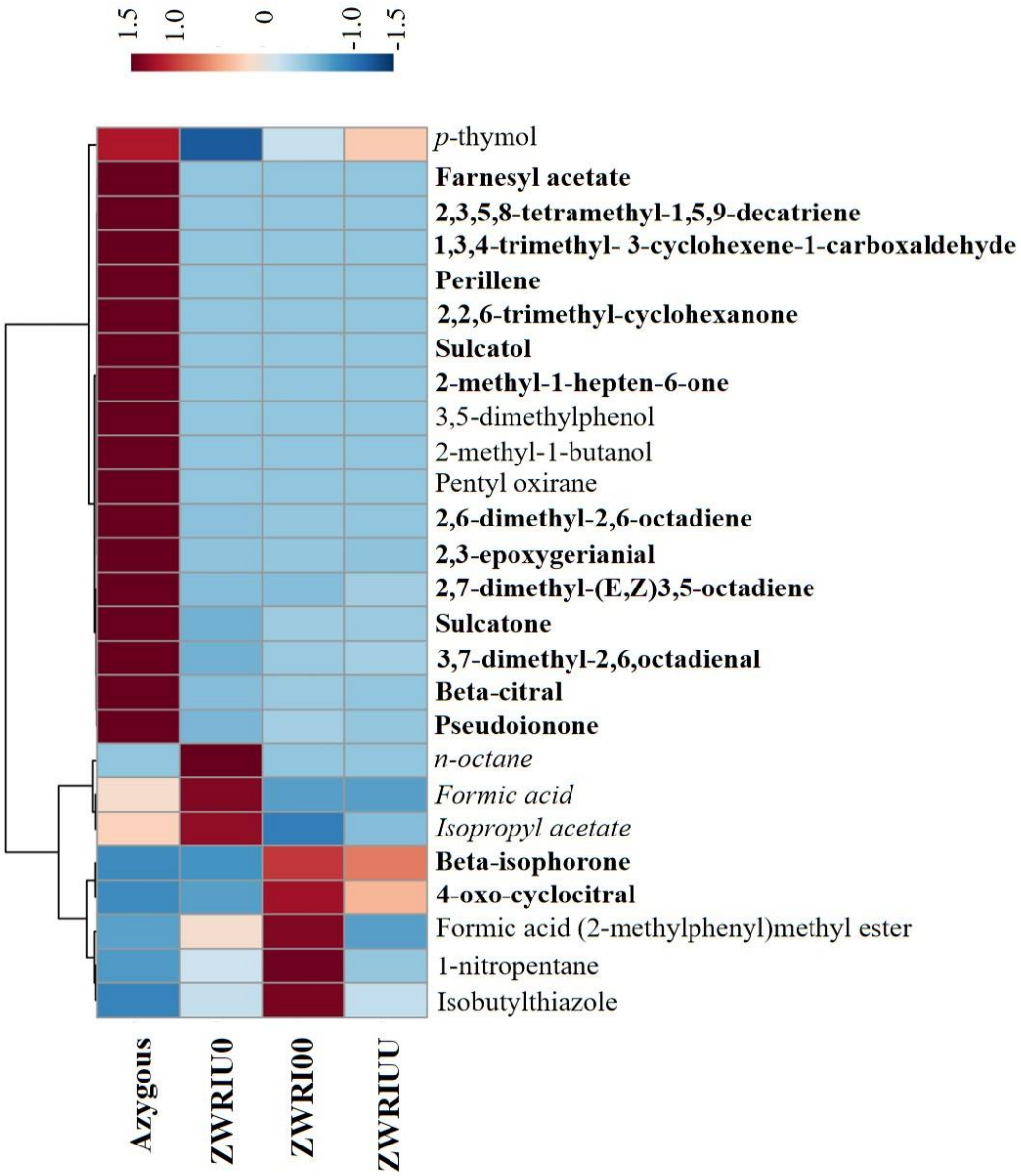

Figure 3-12. Heat map of volatiles from ZW(Ø)RI(Ø)UU/U0/00
Relative changes of all significantly different volatile detected by SPME analysis. Red indicates an increase and blue a decrease in relative abundance. Data scaled using autoscaling as described in (Van den Berg, *et al.*, 2006). Compounds in bold are derived from carotenoids. Compounds in italics are associated with fatty acids or esters. Plain font indicates an alternative or unknown pathway. Five fruit per plant were pooled with at least two biological and three technical replicates analysed per genotype. Identification of compounds was largely based on the NIST database, this along with full compound names are detailed in section 7.1.3.

Table 3-4. Relative amounts of significant volatiles produced by all genotypes of ZW(Ø)RI(Ø)UU/U0/00
All values have been scaled, with the smallest value set at 1 and shown ± the standard deviation. Five fruit per plant were p ooled with at least two biological and three technical replicates analysed per genotype.

Volatile	Azygous	ZWRI00	ZWRIU0	ZWRIUU
Formic acid	3.60 ±5.09	0.00 ±0.00	8.64 ±1.79	0.00 ±0.00
Isopropyl acetate	2.47 ±1.21	0.00 ±0.00	4.40 ±1.43	1.00 ±1.19
2-methyl-1-butanol	11.27 ±1.88	0.00 ±0.00	0.00 ±0.00	0.00 ±0.00
n-Octane	0.00 ±0.00	0.00 ±0.00	65.61 ±18.25	0.00 ±0.00
1-Nitropentane	44.81 ±63.38	1451.20 ±222.71	426.20 ±116.53	229.51 ±150.11
Pentyl-oxirane	60.47 ±20.15	0.00 ±0.00	0.00 ±0.00	0.00 ±0.00
3,5-dimethylphenol	47.87 ±22.83	0.00 ±0.00	0.00 ±0.00	0.00 ±0.00
2-methyl-1-hepten-6-one	5184.12 ±2846.44	0.00 ±0.00	0.00 ±0.00	0.00 ±0.00
Sulcatone	7785.75 ±832.81	719.72 ±128.86	0.00 ±0.00	650.64 ±473.46
Sulcatol	215.80 ±88.34	0.00 ±0.00	0.00 ±0.00	0.00 ±0.00
2-Isobutylthiazole	494.84 ±189.21	2627.19 ±475.18	1134.53 ±609.96	1129.82 ±251.80
2,2,6-trimethyl-cyclohexanone	33.59 ±10.97	0.00 ±0.00	0.00 ±0.00	0.00 ±0.00
2,6-dimethyl-2,6-octadiene	408.02 ±196.79	9.98 ±9.07	2.41 ±2.09	6.64 ±7.81
3,7-dimethyl-2,6,octadienal	103.16 ±72.26	8.54 ±9.90	0.00 ±0.00	10.81 ±18.72
Beta-isophorone	0.00 ±0.00	74.58 ±9.15	2.50 ±4.33	62.29 ±41.28
p-Thymol	27.02 ±6.47	11.48 ±10.14	0.00 ±0.00	16.95 ±3.18
Perillene	225.75 ±57.29	0.00 ±0.00	0.00 ±0.00	0.00 ±0.00
2,7-dimethyl-(E,Z)3,5-octadiene	146.39 ±76.62	0.00 ±0.00	0.00 ±0.00	8.96 ±13.97

Volatile	Azygous	ZWRI00	ZWRIU0	ZWRIUU
1,3,4-trimethyl-3-cyclohexene-1-carboxaldehyde	37.50 ±19.04	0.00 ±0.00	0.00 ±0.00	0.00 ±0.00
2,3-epoxygerianial	199.93 ±83.66	1.62 ±2.81	0.00 ±0.00	0.00 ±0.00
Beta-citral/ Neral	978.96 ±322.22	54.39 ±25.18	9.01 ±15.60	29.36 ±36.62
Formic acid (2-methylphenyl) methyl ester	92.50 ±19.22	673.99 ±148.49	320.87 ±161.72	88.34 ±30.63
Oxo-cyclocitral	0.00 ±0.00	480.02 ±143.81	30.93 ±40.08	289.41 ±265.26
Pseudoionone	4909.17 ±470.67	572.89 ±146.15	136.78 ±28.97	378.75 ±258.30
2,3,5,8-tetramethyl-1,5,9-decatriene	17.42 ±13.09	0.00 ±0.00	0.00 ±0.00	0.00 ±0.00
Farnesyl acetone	344.62 ±239.54	0.00 ±0.00	0.00 ±0.00	0.00 ±0.00

3.2.6 Carotenoid analysis of leaf material in the F_2 generation

While it is the tomato fruit that is of commercial value, the rest of the plant biomass can be rendered for by-products. If valuable products are synthesised in the leaf, they could be useful. The same ketocarotenoids were observed in leaf as in fruit, although the amounts and ratios differed.

Contrary to what is observed in the fruit, there was no significant difference found between hemizygous and homozygous *Crt*R-*b2*. Both profiles were very similar, suggesting the effect of the silencing phenomenon only occurred in fruit. Comparison of ZWRIU0 and ZWRI00 did reveal differences. ZWRIU0 had an increase in neoxanthin, adonixanthin epoxide, astaxanthin, and adonixanthin. This reflected the role of the additional hydroxylase. Similarly to the fruit, phoenicoxanthin, canthaxanthin and echinenone were reduced. Figure 3-13 shows a graphical representation of the differences of carotenoids in leaf between genotypes.

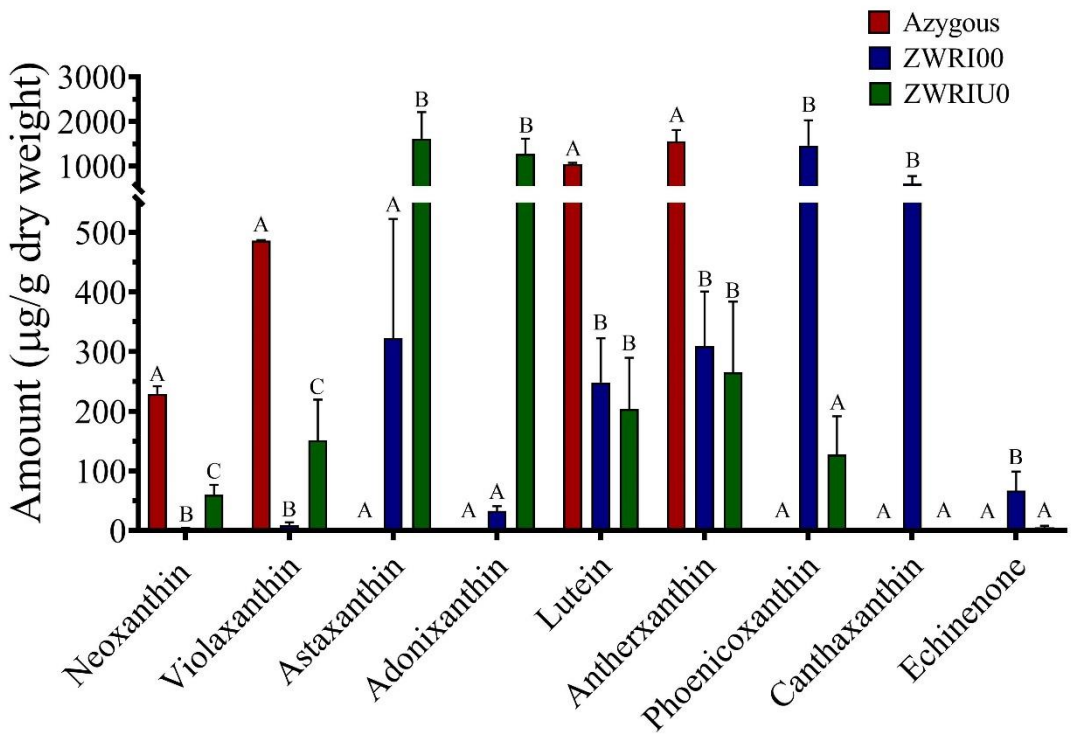

Figure 3-13. Significant carotenoids of ZW(Ø)RI(Ø)U0/00 in leaf material
Average of three technical and at least three biological replicates. Error bars show the standard deviation. Letters represent the statistical grouping from an ANOVA for each individual carotenoid.

The profile of all ketocarotenoid producing plants was very different to that of the azygous control. The azygous leaf only contained neoxanthin, violaxanthin, lutein, antheraxanthin and beta-carotene. These were all at a higher level than observed with the presence of ketocarotenoids. The ZWRIUU, ZWRIU0 and ZWRI00 all produced an unknown compound, to high levels in the leaf. This compound has been designated unknown A. This unknown was also observed in the fruit, but at lower levels. It eluted after astaxanthin with a maximal wavelength of 454 nm. The quantitive amounts present in leaf tissue are shown in section 7.1.5.

3.2.7 Change in carotenoid profile during ripening

Chloroplasts develop into chromoplasts as fruit ripens. The green fruit contain chloroplasts, while the red fruit have chromoplasts. Carotenoid accumulation with the concurrent reduction in chloroplasts is a feature of ripening. The ketocarotenoid producing plants formed fruit which was never fully green in appearance but an orange-brown colouration (Figure 3-14), reflecting the presence of the red ketocarotenoids alongside green chlorophylls.

The addition of ketocarotenoids to immature and mature fruit created a very different profile to that seen in azygous fruit. Endogenous carotenoids such as lutein, phytoene and lycopene were lower in ketocarotenoid containing fruit, however the chlorophylls and the derivatives remained unchanged. All of the ketocarotenoids increased throughout ripening. The prevalent carotenoid present within the fruit tissue varied with genotype; ZWRI00 predominantly accumulated phoenicoxanthin, ZWRIU0 predominantly accumulated astaxanthin and ZWRIUU predominantly accumulated canthaxanthin. The amount of each individual carotenoid was low or absent at the mature green (MG) stage, then by breaker (B) the carotenoids began to appear in fruit. ZWRI00 and ZWRIUU had a similar profile to each other, with some variations in the amounts or ratios of carotenoids. ZWRIU0 accumulated the fully hydroxylated carotenoids, astaxanthin and adonixanthin epoxide. Within the analysis there was often a large standard deviation of the data. This is especially true for ZWRIUU at breaker +14 days (B14). This large region of error reflected the instability within the ZW(Ø)RI(Ø)UU/U0/00 line, which appeared to be vulnerable to environmental conditions.

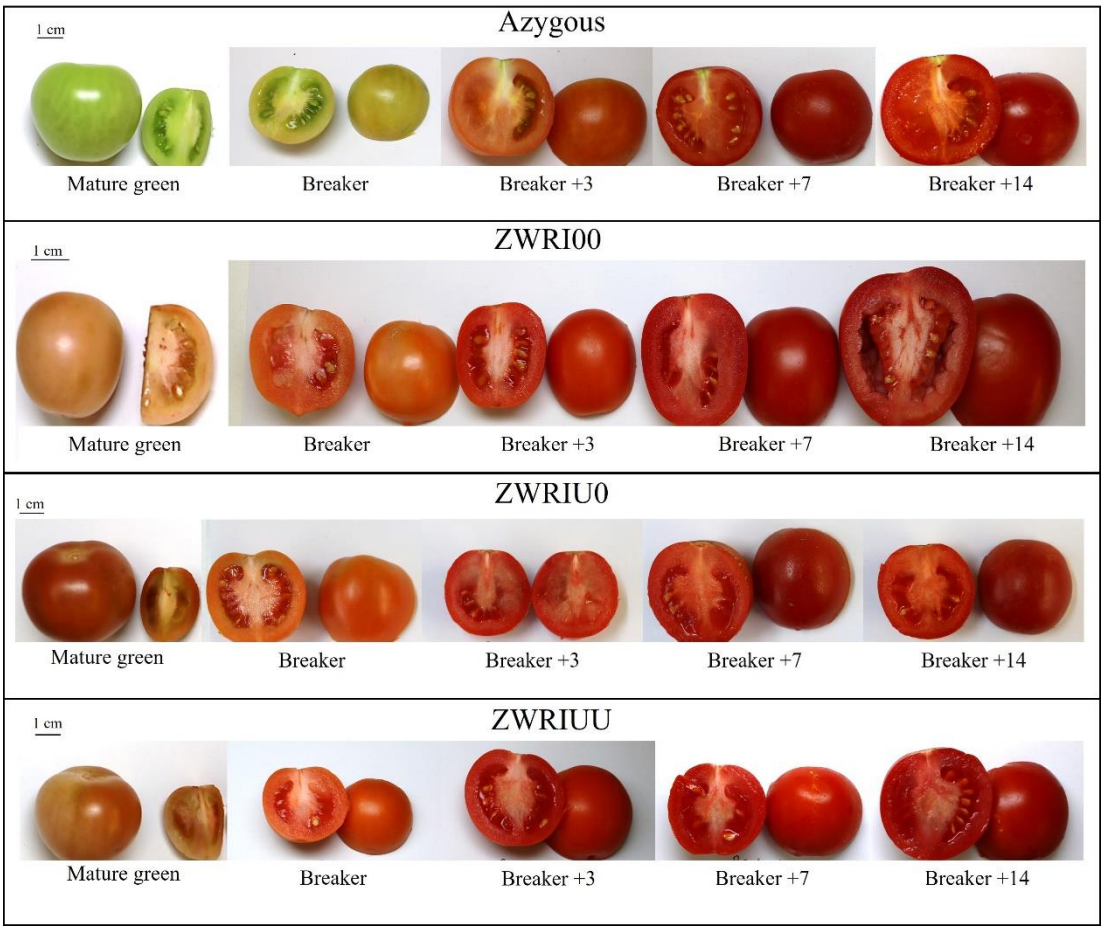

Figure 3-14. Fruit phenotypes observed throughout ripening of ZW(Ø)RI(Ø)UU/U0/00
Scale bars all represent 1 cm.

Adonixanthin epoxide was predominantly seen in ZWRIU0 (68 µg/g) with only a small (21 µg/g) amount being found in ZWRIUU. The change to this carotenoid through ripening was unusual; from MG to B3 there was a decrease in the content, then from B3 to B14 the levels increased again to a similar level as was present in MG. Astaxanthin slightly increased over time in ZWRIUU and ZWRI00, however, the increase in ZWRIU0 was more pronounced (e.g. 53 µg/g to 208 µg/g). Phoenicoxanthin increased through ripening in all ketocarotenoid genotypes but was found in much higher amounts in ZWRIUU (883 µg/g) and ZWRI00 (1554 µg/g) than ZWRIU0 (100 µg/g). Canthaxanthin was very similar, with the exception of a reversal between ZWRIUU (1075 µg/g) and ZWRI00 (795 µg/g), although ZWRIU0 (45 µg/g) still accumulated least. 3'OH echinenone and 3OH echinenone were different despite being structural isomers and biosynthetically related. In the case of 3'OH echinenone, there was a

gradual increase over time, which reached between 3 μg/g and 80 μg/g. Conversely 3OH echinenone increased sharply at B3 in ZWRIUU and ZWRI00 to 10 μg/g and 17 μg/g respectively. In ZWRIU0 the pattern was more similar to 3'OH with a gradual increase up to 5 μg/g. The change in echinenone levels through ripening was noticeably different between genotypes. ZWRIUU and ZWRI00 had almost identical levels, with a maximal amount of 51 μg/g. On the other hand, ZWRIU0 produced very little echinenone (3 μg/g), and this did not change through ripening.

Pheophytin and chlorophyll B were only observed at MG and B for all genotypes. Lutein was mostly seen in azygous fruit with lower levels found in ketocarotenoid producing fruit. Lutein gradually decreased over ripening. Lycopene was also only detected in azygous fruit, although this may be to do with co-elution with ketocarotenoid esters. Lycopene sharply increased from MG to B7, but then plateaued from B7 to B14. Phytoene started to accumulate from B3, but only in azygous fruit. The accumulation of beta-carotene was interesting (Figure 3-15). The azygous plants maintained a reasonable constant level of beta-carotene throughout ripening. On the other hand, ZWRI00 and ZWRIUU continued to accumulate, and by B14 these genotypes had achieved levels approximately five times higher than azygous plants. ZWRIU0 plants were slower to accumulate beta-carotene, but the levels did gradually increase, with the resulting amounts being equal to the azygous control.

There were also two unknowns which were found at different stages of development. The first, denoted as unknown A ran at 3.2 minutes with a maximum at 454 nm, which is likely to be the same as that found in the leaf. The second, unknown B ran at 3.4 minutes with a maximum at 450 nm and looked similar to a carotene.

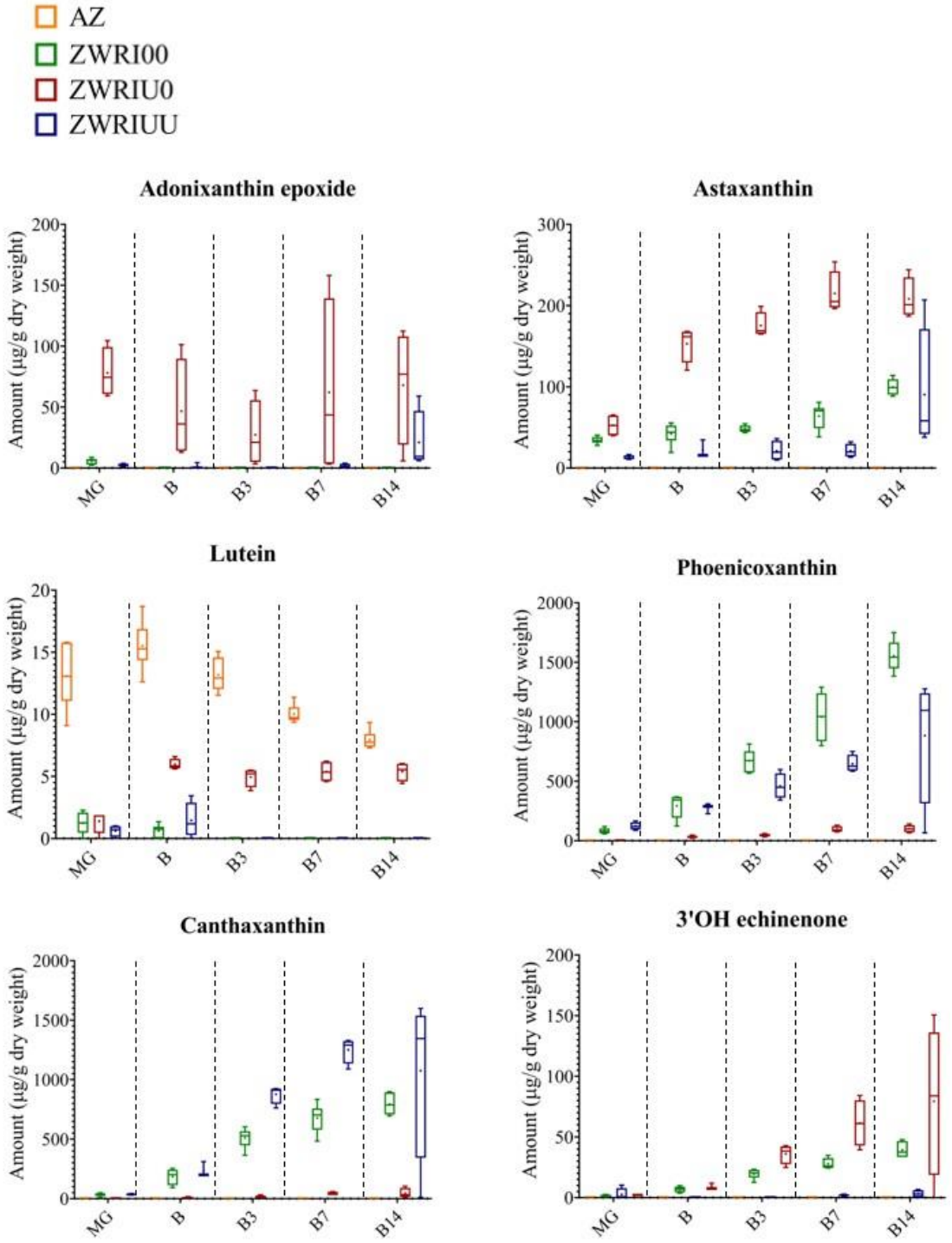
AZ
ZWRI00
ZWRIU0
ZWRIUU
Adonixanthin epoxide
Astaxanthin
Lutein
Phoenicoxanthin
Canthaxanthin
3'OH echinenone
Amount (µg/g dry weight)
MG
B
B3
B7
B14

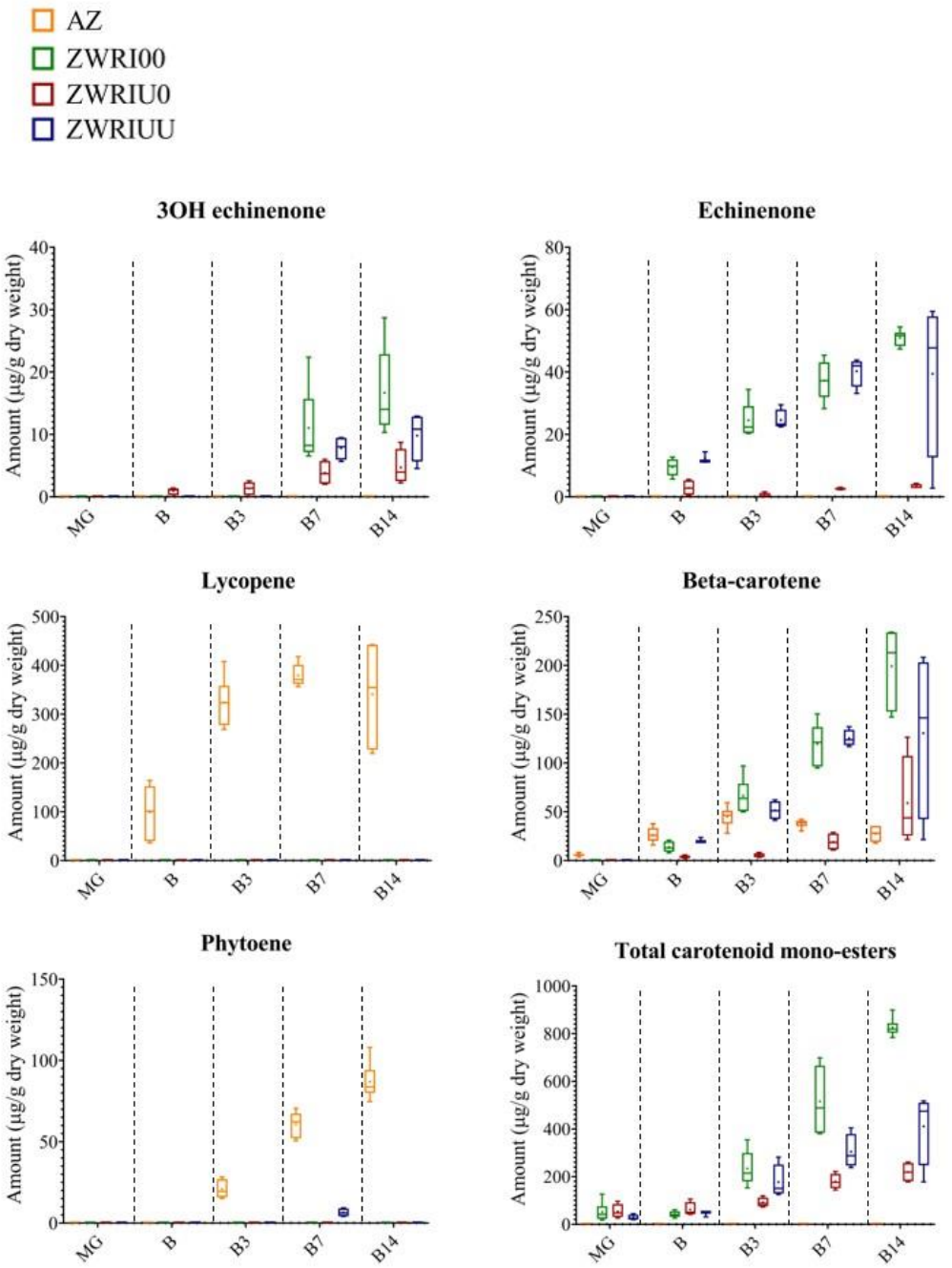

Figure 3-15. Carotenoid changes throughout ripening
The size of each box represents the first and third quartiles, with the line representing the median. The length of the whiskers is from the minimum and maximum values within the biological replicates. The mean is shown by a dot within each box. Data was created from three technical replicates and between three and six biological replicates. Azygous – orange, ZWR00 – green, ZWRIU0 – red, ZWRIUU – blue. MG – mature green, B – breaker, B3 – breaker +3 days, B7 – breaker +7 days, B14 – breaker +14 days.

3.2.8 Effect on the wider metabolism due to an altered carotenoid metabolism.

In order to assess the effects of altering the carotenoid metabolism has on the wider metabolism, compounds from the primary and intermediary metabolism were analysed. GC/MS allowed for semi-quantitive analysis of several different classes of metabolites, which could be used to judge the wider metabolic changes. Considering the similarities seen so far between ZWRI00 and ZWRIUU, only ZWRI00 was taken forwards for broader metabolic analysis.

Principal component analysis (PCA) (Figure 3-16) was used to visually identify the extent of metabolic perturbations. The three genotypes did not form distinct clusters, and therefore it was expected that there would not be any major changes in the broader metabolism. The PCA showed that ZWRI00 has the most biological variation within it. All the other groups clustered more tightly. In order to force a separation, a second PCA (Figure 3-17) was created with only the significant compounds included. This showed more clustering; however the groups were still not distinct from each other. The PCA did show that ZWRI00 was much more similar to azygous than ZWRIU0. ZWRIU0 did begin to group away from the azygous, but not to the extent where it could be considered as separate. More detailed analysis of the individual significant compounds was also performed (Table 3-5).

The detected tocopherols, which were significantly impacted, were alpha-tocopherol and gamma-tocopherol. There was no consensus in how these were altered, with alpha having had an increase but gamma having had a decrease in the ketocarotenoid plants. There were no changes between ZWRI00 and ZWRIU0. Similarly, the sterols did not show an overall trend between genotypes, except that the two ketocarotenoid producing genotypes were once again, the same. Products from the tricarboxylic acid (TCA) cycle also did not show a clear pattern of change.

Amino acids and their derivatives did however show a general trend, all of the amino acids were decreased to a considerable extent in ZWRI00 and ZWRIU0. Aspartic acid ((×0.3), GABA ((×0.2), glycine ((×0.2), isoleucine ((×0.1), leucine ((×0.1), pyroglutamic acid ((×0.2) and valine ((×0.1) were all decreased compared to the azygous control. Once again there were no significant differences between ZWRI00 and ZWRIU0. The only confirmed

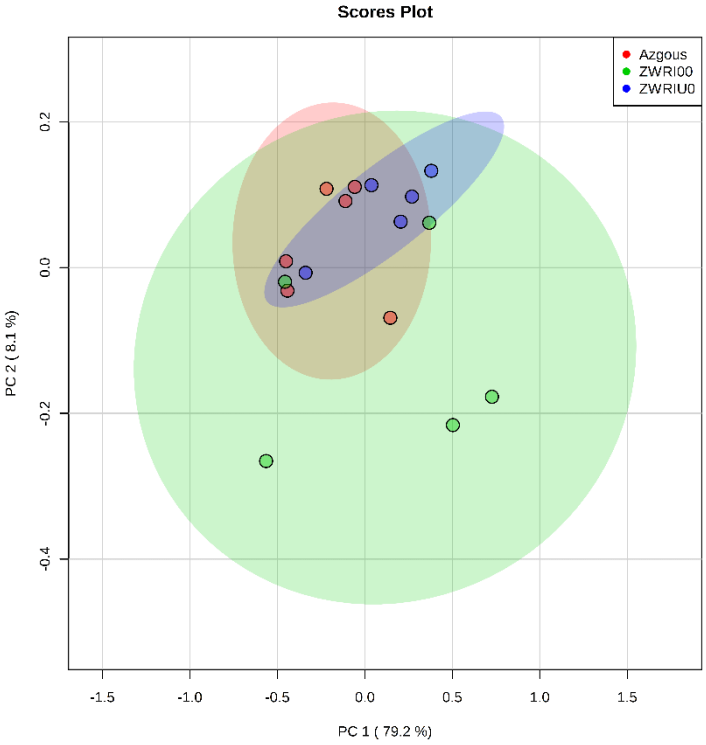

Figure 3-16. Principal component analysis of all compounds detected from GC/MS analysis Azygous shown in red, ZWRI00 in green and ZWRIU0 in blue. Each point represents a biological replicate with the ellipse representing the 95% confidence region.

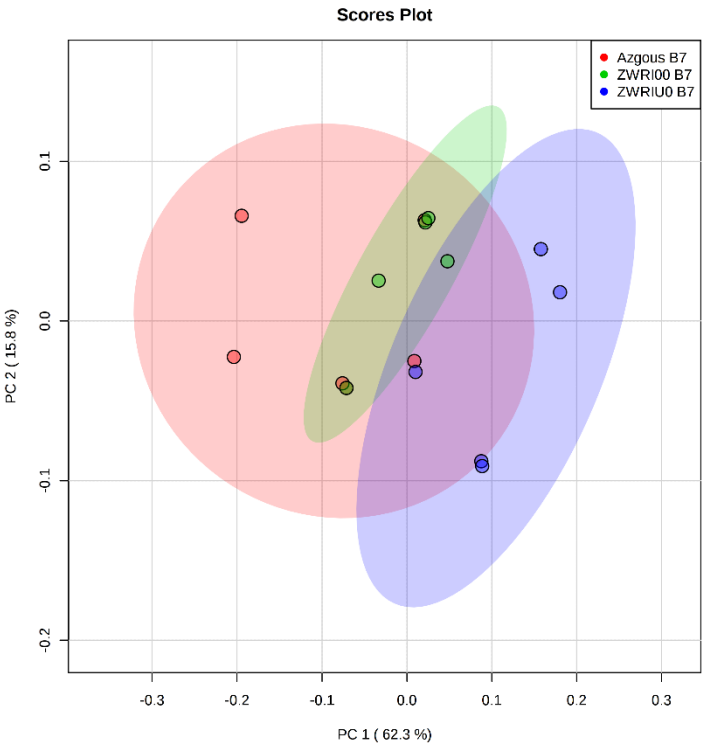

Figure 3-17. Principal component analysis of significant compounds detected from GC/MS analysis Azygous shown in red, ZWRI00 in green and ZWRIU0 in blue. Each point represents a biological replicate with the ellipse representing the 95% confidence region.

Table 3-5. Relative amounts of significant metabolites from the broader metabolism
Each value is an average of six biological replicates ± the standard deviation. Metabolites starting with 'Unknown' are only putatively identified as shown in section 7.1.2.

Metabolite	Azygous		ZWRI00		ZWRIU0	
Isoprenoids						
Alpha-tocopherol	6158.76	±554.88	10650.62	±782.31	11557.47	±1454.75
Gamma-tocopherol	848.56	±511.70	108.38	±35.18	301.88	±246.30
Amino Acids						
Aspartic acid	341.03	±209.67	134.62	±80.59	105.91	±68.24
GABA	1296.91	±748.30	673.91	±778.37	254.13	±210.46
Glycine	17.71	±12.70	4.74	±4.81	3.39	±5.70
Isoleucine	57.97	±29.12	1.00	±2.24	5.83	±6.88
Leucine	57.97	±29.12	7.24	±5.52	8.30	±5.33
Pyroglutamic acid	1674.84	±726.50	178.28	±207.04	326.32	±158.15
Valine	15.50	±13.85	1.04	±2.32	1.86	±2.56
Unknown – leucine	34.27	±12.15	6.19	±6.42	5.71	±5.64
Sterols						
Beta-amyrin	6401.60	±931.62	3980.77	±1484.69	4134.41	±957.62
Sitosterol	371.75	±657.01	2517.39	±986.86	2624.32	±1753.86
Stigmasterol	3972.13	±712.42	6849.10	±1274.83	6340.70	±1238.40
Unknown beta-amyrin	3184.41	±758.47	1947.87	±738.19	2328.55	±611.20
Fatty acids						
C18:0	5919.49	±785.47	7592.97	±1339.38	4603.57	±781.36
Unknown - C14:0	616.14	±522.94	1701.93	±208.81	3509.78	±1774.11
TCA derivatives						
Citric acid	8903.00	±2224.57	12676.06	±1960.87	10684.17	±1604.66
Isocitric acid	73.49	±63.97	17.31	±38.71	154.30	±27.62
Itaconic acid	310.55	±104.84	99.33	±68.15	96.89	±26.64
Malic acid	281.93	±135.77	850.19	±182.58	458.75	±217.05
Sugars						
Fructose	33477.63	±2288.49	35656.61	±1998.74	42796.16	±2728.96
Galactaric/Galacturonic acid	29.00	±16.77	10.76	±6.11	59.57	±40.16
Glyceric acid	3.70	±2.11	ND		ND	
Mannose/Glucose	36586.08	±4956.97	40668.07	±3619.62	44721.20	±3142.38
Unknown - fructose	287.94	±91.08	99.32	±37.53	116.38	±37.85
Unknown - turanose	132.99	±37.14	189.47	±37.83	229.82	±90.99

Metabolite	Azygous		ZWRI00		ZWRIU0	
Other						
Methylphosphate	43.43	±50.90	49.44	±33.81	341.56	±133.82
Naringenin	3700.37	±6285.53	20404.11	±15379.59	7666.53	±3833.03
Unknown - ethanolamine	1.49	±2.42	8.34	±1.47	3.56	±5.23
Unknown - naringenin	359.19	±623.78	1822.29	±745.54	1078.37	±312.16
Unknown - thiobarbituric acid	150.98	±27.03	219.61	±43.19	163.66	±23.57
Unknown	60.14	±11.36	122.00	±27.14	140.82	±20.20

fatty acid which was significantly different between the groups was C18:0. This was increased in ZWRI00 (×1.2) and decreased in ZWRIU0 (×0.8).

The impact on the sugar profile was important as these are largely responsible for the taste. Within the sugars detected there were a variety of changes, with the overall sugar profile. having been altered by the addition of ketocarotenoids. Fructose (×1.3), galactaric/galacturonic acid (×2.0) and mannose/glucose (×1.2) were increased in ZWRIU0, as was the unconfirmed turanose (×1.7). However, glyceric acid was decreased to below a detectable level in both ZWRI00 and ZWRIU0.

There were also several unknown or unclassified metabolic changes which were observed. The flavonoid naringenin was increased (×5.5) in ZWRI00, which is a similar trend to the unconfirmed naringenin. Naringenin is the dominant flavonoid, as shown by the prevalence in the azygous control. A table of all the detected metabolites and the level of identification are in sections 7.1.6 and 7.1.2 respectively.

In order to compare the development of fruit through ripening, ZWRIU0 was analysed at both B7 and B14. It was previously known that ZWRI00 isn't fully ripe until after B7, and that azygous is ripe at B7. However, for ZWRIU0 the ripening was unknown. The ripening series performed previously (3.2.7) indicated that there was little change in carotenoid levels between B7 and B14. The wider profile showed the same effect. There are seven significantly different compounds, most of which are unknowns. B14 has higher amounts of alanine (×2.0), unknown C16:0 propylester (×7.0), unknown glycerol-1-C18:0 (×3.3) and unknown 41.0 min (×1.4) it also has lower amounts of fructose (×0.8), mannose/glucose (×0.9) and unknown 22.1 min (×0.4).

3.2.9 Detailed analysis of free and esterified carotenoid content in fruit of the F_4 generation

Whilst the UPLC has provided a quick and reliable method for determination of the free and mono-esterified carotenoids, it is not optimal for the analysis of di-esterified carotenoids. For the F_4 generation of ZW(Ø)RI(Ø)UU/U0/00 the free and mono-esterified carotenoids have been determined on the UPLC system. This was then followed by quantification of the di-esterified carotenoids by using the HPLC system.

For each generation the line with the highest astaxanthin content and best vigour was used to generate the next generation. Seed from ZWRIUU was used for ZWRIUU. Seed from ZWRIU0 was used for ZWRIU0 and so on. Each generation was segregating on ZW and additionally on UU/U0/00 for ZWRIU0. The amounts of each carotenoid found in the F_4 generation differed from the amounts determined in the F_2 generation. However, the trends between the genotypes were similar as indicated in Table 3-6 where the amounts of carotenoids in the F_4 fruit are detailed. ZWRIU0 still produced the higher amounts of adonixanthin epoxide than ZWRIUU or ZWRI00. However, the amount was lower than previously seen. Likewise, in both F_2 and F_4 astaxanthin remained highest in ZWRIU0, along with adonixanthin and unknown A. ZWRI00 and ZWRIUU had similar carotenoid profiles, both accumulated phoenicoxanthin and canthaxanthin with minimal synthesis of other carotenoids. Beta-carotene is increased in both ZWRI00 and ZWRIUU. The total free carotenoid content was significantly higher in ZWRI00 and ZWRIUU, although ZWRIU0 has a reduced free carotenoid content.

ZWRI00 and ZWRIUU had the highest levels of mono-esterified carotenoids, with ZWRIU0 having approximately 50% less. Conversely, the di-esters were accumulated in ZWRIU0, and only found at low levels in ZWRI00 and ZWRIUU. This differing preference for mono or di esters can only be seen through HPLC analysis. Therefore, with the previous generations the total ester content for ZWRIU0 has been underestimated. Considering both mono-esters and di-esters, the total carotenoid ester content is similar across all ketocarotenoid genotypes. ZWRIUU did accumulate significantly more total esters than ZWRIU0.

The spectra suggest that the parent carotenoid for all the di-esterified carotenoids is astaxanthin. Therefore, total astaxanthin content is much higher in ZWRIU0 than the other genotypes. Combining the free astaxanthin and the di-esterified astaxanthin can be used to

estimate the total astaxanthin content, but this does exclude any astaxanthin which may be a mono-ester. ZWRIU0 has a considerably higher astaxanthin content (569.2 μg/g) than ZWRI00 (122.8 μg/g) or ZWRIUU (220.9 μg/g). This emphasises the trend seen with the free astaxanthin.

3.2.10 Sub-plastid location for storage of ketocarotenoids and carotenoid esters

In order to understand the sequestration of carotenoids and their esters, a sub-plastid fractionation was performed (Figure 3-18). The outputs from this approach are in Figure 3-18. Three genotypes were analysed; azygous, ZWRI00 and ZWRIU0. The visual differences between all three were striking, the azygous sample contained a less intense colouration throughout the gradient. The only accumulation of colour was a small section within the membranes and crystals section. Contrary to this the ketocarotenoid genotypes displayed colour throughout a much wider range of the gradient. The plastoglobule section was especially different, with ZWRI00 and ZWRIU0 having had a much thicker and more intense band. Similarly, the membrane area is much more widely dispersed, with potential layering having occurred within this section. ZWRI00 and ZWRIU0 had a similar pigment distribution, however ZWRI00 was red, whereas ZWRIU0 was orange.

For a quantitive comparison, 31 fractions were collected and analysed on the UPLC system. This revealed that there were minimal changes to the location of endogenous carotenoids. Violaxanthin accumulated in fraction 17 of the azygous and 19 in ZWRIU0. Lycopene and lutein were only seen in azygous; these provided the colouration of the membrane band visible in Figure 3-18. Beta-carotene was also unaffected, with storage between fraction 17 and 24, this was the membrane and crystal region in all genotypes. However, ZWRIU0 had a more specific region in which beta-carotene was found. Azygous and ZWRI00 had multiple peaks for beta-carotene, indicating there may have been several discrete storage locations. ZWRIU0 also had a higher percentage stored within the early fractions, the plastoglobules fractions. ZWRI00 also had the most beta-carotene (3.2.9).

All the ketocarotenoids were stored in the plastid membrane. This was true for both ZWRI00 and ZWRIU0. Each detected ketocarotenoid behaved in a very similar manner, producing the overall trend. ZWRIU0 once again had a less broad site for storage than ZWRI00. The carotenoid mono-esters were also found associated to the membranes, but they were also sequestered in the plastoglobules to a lesser extent.

Table 3-6. Carotenoid content of fruit from the F_4 generation of ZW(Ø)RI(Ø)UU/U0/00
Amounts in µg/g dry weight with ± standard deviation. All values are calculated from at least three biological replicates, of four pooled fruit per plant. Each biological replicate is an average of three technical replicates. Lycopene was not quantified (NQ) in fruit with esters due to co-elution.

Carotenoid	Azygous	ZWRI00	ZWRIU0	ZWRIUU
Adonixanthin epoxide	0.00 ±0.00	2.50 ±1.11	36.15 ±28.80	17.94 ±17.28
Astaxanthin	0.00 ±0.00	59.51 ±7.91	119.94 ±31.60	76.91 ±12.94
Unknown A	0.00 ±0.00	0.00 ±0.00	25.77 ±12.08	0.00 ±0.00
Adonixanthin	0.00 ±0.00	0.00 ±0.00	7.95 ±1.90	0.00 ±0.00
Lutein	11.67 ±1.06	0.00 0.00	0.00 ±0.00	0.00 ±0.00
Phoenicoxanthin	0.00 ±0.00	734.41 ±244.81	154.01 ±115.56	686.39 ±114.90
Canthaxanthin	0.00 ±0.00	450.07 ±124.66	65.97 ±73.58	630.75 ±140.37
3OH' echinenone	0.00 ±0.00	15.59 ±6.91	1.70 ±1.81	26.28 ±10.21
3OH echinenone	0.00 ±0.00	11.12 ±3.70	4.31 ±2.88	9.20 ±2.38
Echinenone	0.00 ±0.00	27.63 ±8.63	9.56 ±8.65	30.01 ±5.40
Lycopene	369.41 ±62.01	NQ	NQ	NQ
Beta-carotene	37.71 ±9.39	85.77 ±39.13	39.56 ±36.20	109.09 ±28.75
Phytofluene	202.32 ±7.32	0.00 ±0.00	0.00 ±0.00	0.00 ±0.00
Phytoene	36.57 ±7.23	23.24 ±9.90	0.00 ±0.00	0.00 ±0.00
Total free	657.68 ±63.54	1413.58 ±421.74	478.45 ±185.25	1595.41 ±265.07
Total mono-esters	0.00 ±0.00	1309.49 ±622.36	593.84 ±220.47	1707.05 ±231.02
Total di-esters	0.00 ±0.00	63.24 ±19.90	449.30 ±109.17	143.99 ±70.42
Total esters	0.00 ±0.00	1168.27 ±881.73	1043.14 ±349.78	1851.04 ±221.74

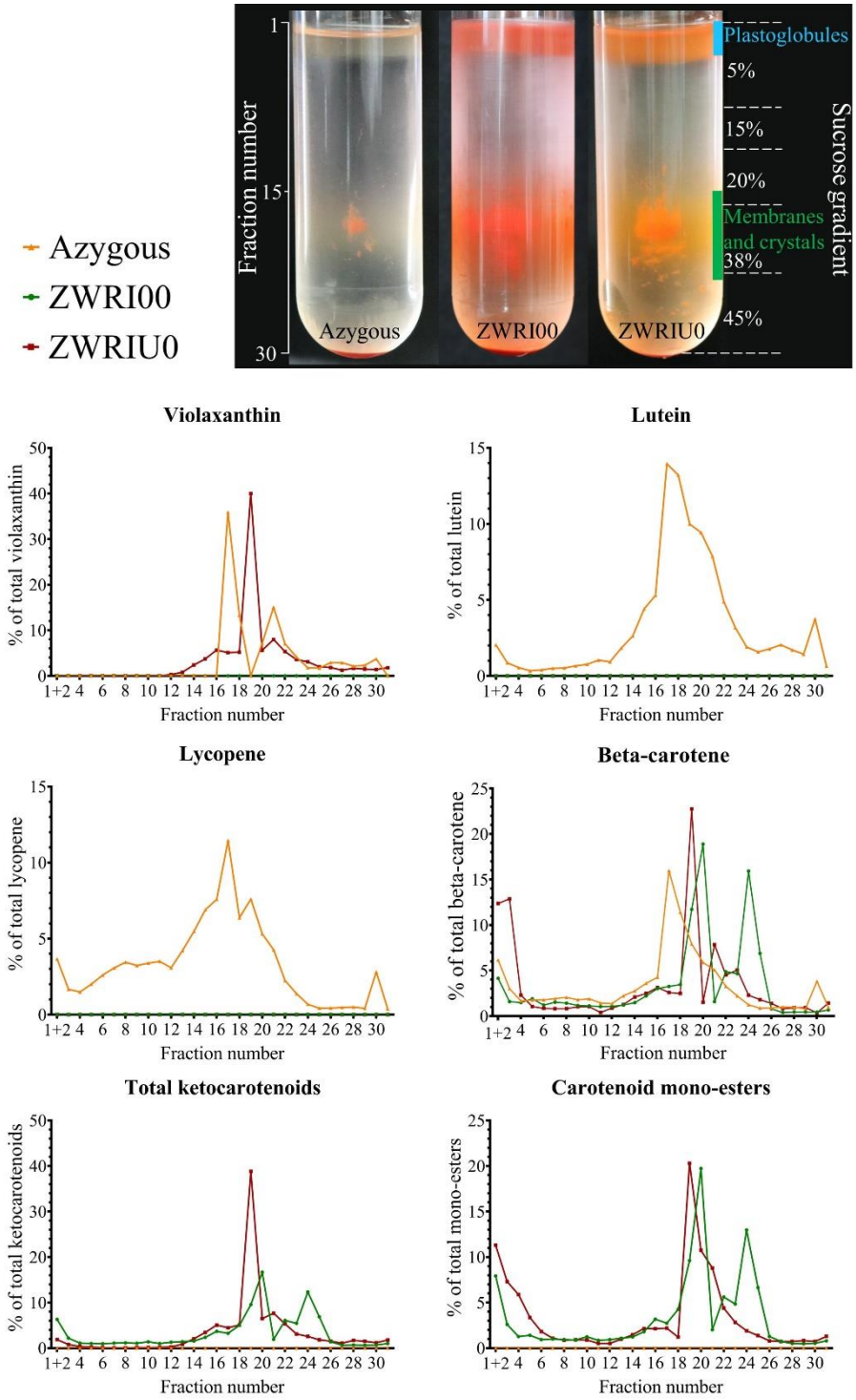

Figure 3-18. Sub-plastid fractionation of azygous, ZWRI00 and ZWRIU0
Top image shows the banding of colour within the sucrose gradient, with sub-plastid locations shown. Graphs represent the storage location of specific carotenoids by comparison of the fraction number to the sub-plastid location. Orange represents azygous, green represents ZWRI00 and red ZWRIU0. Data are from two technical replicates from pooled samples.

3.2.11 Carotenoid analysis of leaf material of the F_4 generation

The leaf content from the F_4 generation is very similar to that already seen in F_2. Leaf material from the F_4 was analysed for both carotenoid and chlorophyll content. Interestingly, despite the change in colour across all genotypes there was no change in the chlorophyll levels (Figure 3-19). Chlorophyll A, chlorophyll B and the degradation product pheophytin were measured. In order to look for environmental and generational changes carotenoid analysis was also performed again (Table 3-7). As seen before, the ketocarotenoid genotypes had less neoxanthin, violaxanthin, lutein and beta-carotene, but they did accumulate ketocarotenoids instead. ZWRI00 was highest in phoenicoxanthin, canthaxanthin and 3'OH echinenone. ZWRIU0 and ZWRUU had very similar carotenoid profiles, with both having adonixanthin epoxide and astaxanthin as the predominant carotenoids. The similarity of ZWRIUU and ZWRIU0, and the difference in ZWRIUU and ZWRI00 suggested that silencing is a phenomenon that only produces a metabolic effect in the fruit. The only difference seen between F_2 and F_4 is in echinenone. In F_2 echinenone was highest in ZWRI00, in F_4 it is highest in ZWRIU0 and ZWRIUU.

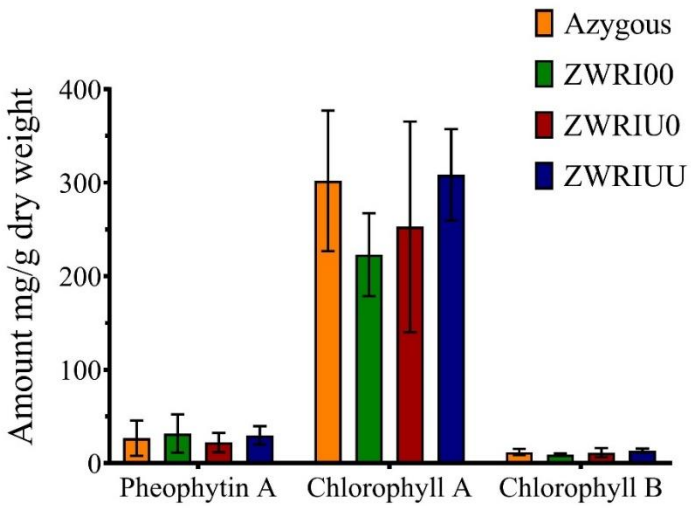

Figure 3-19. Quantification of chlorophylls in leaves of F_4 ZW(Ø)RI(Ø)UU/U0/00 plants
Values obtained from at least three biological replicates and three technical replicates. Quantification is relative providing an initial screen to detect differences across genotypes. Error bars show the standard deviation.

Table 3-7. Amounts of carotenoid in leaf material of F_4
Amounts in µg/g dry weight with ± the standard deviation.

Carotenoid	Azygous	ZWRI00	ZWRIU0	ZWRIUU
Neoxanthin	389.92 ±56.23	0.00 ±0.00	80.94 ±39.63	91.71 ±4.68
Violaxanthin	593.16 ±73.83	0.00 ±0.00	143.75 ±72.27	122.92 ±2.54
Unknown A	0.00 ±0.00	82.78 ±20.83	417.83 ±284.98	433.47 ±48.30
Unknown C	0.00 ±0.00	102.49 ±47.11	198.80 ±136.95	203.20 ±17.40
Lutein	1486.42 ±261.41	380.72 ±233.25	190.40 ±113.65	239.57 ±25.07
Beta-carotene	1245.99 ±250.58	53.09 ±29.88	130.69 ±62.04	116.61 ±7.08
Adonixanthin epoxide	0.00 ±0.00	130.13 ±40.53	2392.66 ±788.34	2140.34 ±144.57
Astaxanthin	0.00 ±0.00	175.16 ±42.06	515.60 ±381.15	852.41 ±117.32
Phoenicoxanthin	0.00 ±0.00	2114.78 ±594.24	244.71 ±164.83	922.91 ±161.09
Canthaxanthin	0.00 ±0.00	1123.66 ±389.90	0.00 ±0.00	174.21 ±74.62
3'OH echinenone	0.00 ±0.00	73.89 ±23.50	0.00 ±0.00	11.06 ±4.82
3OH echinenone	0.00 ±0.00	0.00 ±0.00	31.65 ±22.47	17.33 ±2.28
Echinenone	0.00 ±0.00	104.48 ±33.32	19.11 ±18.91	90.58 ±9.92

3.2.12 Photosynthetic capacity of brown and green plants

Analysis of the leaf data has already revealed that the chlorophylls are not affected by the change to the carotenoid profile. The brown colouration of the leaves is therefore most likely be due to the presence of ketocarotenoids in the leaf. Carotenoids are vital accessory pigments for photosynthesis; therefore it could be that an alteration to carotenoids in the leaf affects photosynthesis. When plants are exposed to light chlorophylls are bombarded with photons which transitions them to an excited state. The energy from this excitation is dissipated through several pathways; one of these pathways being photosynthesis. Changes in photosynthesis can be measured by altered chlorophyll fluorescence.

In order to investigate this impact on photosynthesis, the efficiency of photosystem II (PSII) was measured. This is done by using the $\frac{F_v}{F_m}$ ratio, as shown below:

$$\frac{F_v}{F_m} = \frac{F_m - F_0}{F_m}$$

F_m is the maximal fluorescence, F_0 is the initial, or minimal fluorescence and F_v is the variable fluorescence. This gave the maximum potential efficiency for PSII. A value of 0.85 is optimal for a healthy plant, with lower values indicating stress or an inhibition of photosynthesis. Before taking the measurement, the leaf is dark adapted, so all the photosystems become fully oxidised and ready to accept new photons into the reaction centres to initiate photochemistry. The leaf is then exposed to an intense light which quickly reduces all the reaction centres, allowing for measurement of F_v, F_m, and other parameters.

Figure 3-20 shows the $\frac{F_v}{F_m}$ measurements from both F_2 and F_4. Both generations revealed the same trend, with the azygous plants nearing the optimal ratio of 0.85, and the other genotypes being significantly lower. F_4 also reveals a significant reduction on ZWRIU0 and ZWRIUU compared to ZWRI00.

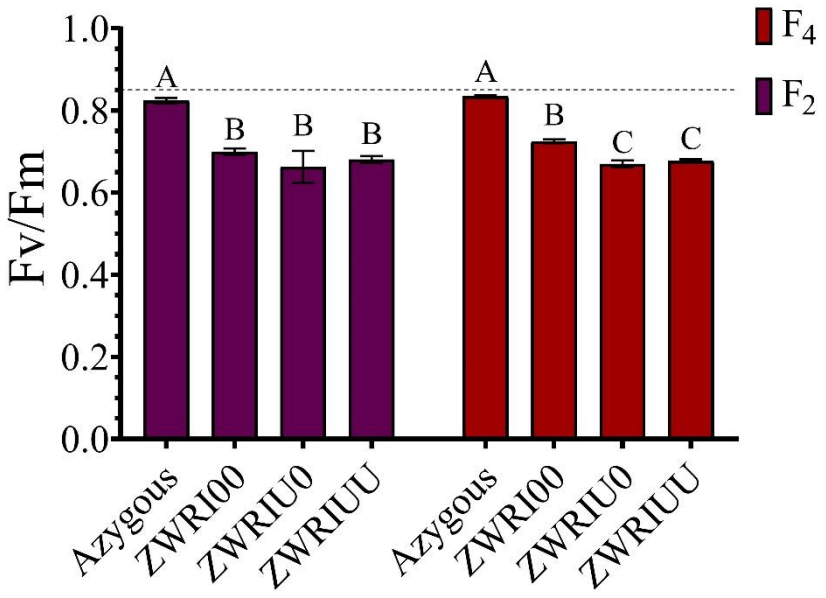

Figure 3-20. Photosynthetic capacity of leaves from ZW(Ø)RI(Ø)UU/U0/00
Results from three technical and three biological replicates. Optimal dark adaptation time and light intensity were established prior to data collection. Statistical analysis is an ANOVA performed within a single generation. Error bars show standard deviation.

3.3 Discussion

3.3.1 Complexity of screening the ZW(Ø)RI(Ø)UU/U0/00 line

The ZW(Ø)RI(Ø)UU/U0/00 line is very complicated. It has multiple genes, each with their own optimal zygosity, and conflicting, silencing promoters. The combination of so many genes not in a single construct creates problems with segregation. Empirically, for each generation, over 200 plants had to be individually screened to identify those with a desired genotype. This is laborious, time consuming, and therefore not commercially viable. The resulting background from the amalgamation of three different *S. lycopersicum* cultivars, and two different tomato species creates a unique cultivar. This provides an extra layer of complexity, with gene expression and metabolomics varying cultivar to cultivar. The addition of multiple constitutive promoters has also resulted in silencing, this is discussed further in 3.3.2, but silencing also provides yet another challenge for the screening of the ZW(Ø)RI(Ø)UU/U0/00 line.

The initial approach to screening was by using the phenotypes and is the most effective. This provided the quickest and simplest method for rapid selection. While having a constitutive promoter can cause complications, the 35S promoter used for ZW is beneficial. The constitutive expression provides colouration to the entire plant and while this may impact the photosynthesis and vigour, it does allow for quick genotype selection. The silencing that occurs also provides a clear phenotypic signal, so once again, the strong promoter is of benefit here.

The screening approach for RI is also simple and relatively quick. The benefit of this trait having come from an introgression is that there are two alternatives of an allele rather than multiple copies of a single allele. The alternative alleles at one locus allow for the detection of one, to rule out the presence of the other in a homozygous state. A simple and crude DNA extraction followed by a straightforward PCR can provide a rapid screening method. Once candidates have been selected these can then be confirmed with a more rigorous, but time consuming, DNA extraction-PCR procedure. The main advantage to the RI trait is that the zygosity does not impact the efficiency of the promoter, and therefore it can be maintained as homozygous. This removes the need for future screening.

It is the UU component which adds most complexity to the screening of ZW(Ø)RI(Ø)UU/U0/00. While presence/absence is easy to detect by a simple PCR, the zygosity has proven more difficult to determine, and has also proven to be important. A UU plant, with no other genetic modifications or background effects gives a relatively clear phenotypic difference between hemizygous and homozygous plants. This is masked by the other genes in ZW(Ø)RI(Ø)UU/U0/00. The flowers still maintain a difference, but flowers only appear at a mature stage, and thus do not prove useful for screening, only for confirmation. While the use of a TLC to determine genotype seemed to be promising, the immature leaves do not reflect the whole plant. This has been confirmed by the analysis of leaf carotenoids; the leaf does not behave in the same way as the fruit, different genotypes cluster dependent on the tissue type. While a TLC of the fruit may show the clear separation of zygosities the fruit stage is once again too late to screen. The carotenoid profile of ZWRI00 an ZWRIUU are also similar. Consequently, these may be hard to distinguish on a TLC. The Southern blot did provide an accurate way of screening; however, a Southern blot is not high throughput, requiring three consecutive days per blot and thus, not feasible for screening 200 plants. The qPCR methods present the most reliable and quick way of screening. Both the qPCR for copy number and the qPCR for expression provide a quick and clear way of separating zygosities. Having established both copy number and expression analysis works, and that both techniques agree, it is probably the copy number approach which should be carried forward. In this analysis the genomic DNA rather than RNA is the substrate for the reaction. DNA is both more stable, and more readily obtainable. The copy number approach is also selective for only the additional *Crt*R-*b2* and does not detect the endogenous gene. The expression analysis is not selective. Any future screening for *Crt*R-*b2* should predominantly rely on qPCR and then be confirmed with phenotype.

Another factor which adds complexity to the ZWØRIØUU/U0/00 line, is the range of carotenoids which are found within it. Among the carotenoids the ketocarotenoids are relatively polar, especially those most oxygenated like astaxanthin. The addition of the fatty acids lowers the polarity of the ketocarotenoids making them more hydrophobic and thus they elute with a greater retention time. In the present case the retention time is close to beta-carotene. This wide range of polarity makes the analysis of the ZW(Ø)RI(Ø)UU/U0/00 line on a single system very difficult. While the UPLC system used provides a much quicker way of determining the carotenoid content than the HPLC, the di-esters do not elute off the column

with the current method. Therefore, these cannot be analysed from the UPLC platform. The HPLC method does reveal the di-esters however the more polar ketocarotenoids do not resolve well. Astaxanthin elutes over a long period of time (two minutes) and canthaxanthin and phoenicoxanthin co-elute. This means that HPLC data cannot be used to accurately determine the free ketocarotenoids. Throughout this work, it has been the UPLC that has been used to determine the carotenoid content, with the knowledge that di-esters will not have been quantified. It is only ZWRIU0 which produces di-esters. After the initial screening of the earlier generations using the UPLC, the HPLC has then been used to accurately quantify the di-esters in the final, F_4 generation.

3.3.2 Silencing of *Crt*R-*b2* in fruit

As previously mentioned, *Crt*R-*b2* appears to silence when homozygous. This is as published by D'Ambrosio, *et al.* (2011). The silencing is most likely due to the overexpression of *Crt*R-*b2* by the 35S promoter on top of the endogenous expression of *CrtR-b2*. Silencing is clearly observed in the fruit, with ZWRI00 and ZWRIUU having very similar carotenoid profiles. The effect of a homozygous *Crt*R-*b2* is similar to having no *Crt*R-*b2*. Silencing can be caused by multiple constitutive promoters (35S) or overexpression of endogenous genes.

Silencing in leaf is less clear. Looking at the carotenoid profile (Figure 3-13 and Table 3-7) there is little difference between ZWRIU0 and ZWIUU. This is contrary to what is found in the fruit. The carotenoid profile appears to show no silencing occurs, and instead *Crt*R-*b2* is equally efficient as hemizygous or homozygous. However, the expression analysis shown in Figure 3-7 reveals that there is silencing of *Crt*R-*b2* when homozygous. The expression is reduced by approximately 50%. In leaf tissue it appears that although silencing occurs, the effects of it are minimal. This would suggest that the expression of the *Crt*R-*b2* is not the bottle neck. Expression at 50% still has the same metabolomic effect, and therefore it is not the expression that is the limiting factor. There are several possible reasons for the discrepancy between the transcriptome and metabolome. It is not uncommon for the expression of a gene to not correlate with the downstream effects. The leaf may provide a more stable environment for the protein than the fruit, and therefore the protein is available for a greater duration of time. Furthermore, as *Crt*R-*b2* is not endogenously expressed in the leaf the effect of the additional *Crt*R-*b2* could be stronger. Given that although silencing occurs and no effect is seen, it would suggest that the optimal zygosity for *Crt*R-*b2* within the leaf is homozygous.

This would remove the problems associated with screening while still maintaining the expression of *Crt*R-*b2*. However, this is different for expression in the fruit.

The effects of silencing in other tissues is much more pronounced. The phenotypes of the flowers show this well (Figure 3-3). The petals of the flowers from ZWRIUU are much paler than their counterparts. This is strong evidence for silencing. The fruit also displays this when looking at the carotenoid profile. It is ZWRIU0 which contains the highest proportion of fully hydroxylated carotenoids. Violaxanthin, astaxanthin, adonixanthin and adonixanthin epoxide are all fully hydroxylated and are all increased in ZWRIU0. However, ZWRIUU accumulates beta-carotene, canthaxanthin and echinenone which all lack a hydroxyl group. The silencing of *Crt*R-*b2* in the fruit seems to be so severe, that all activity of the non-endogenous *Crt*R-*b2* is abolished. Therefore, for the fruit hemizygous is optimal.

3.3.3 Metabolite composition of ZWRIU0

The aim of the work in this chapter was to further develop and improve the production of ketocarotenoids in tomato, with a special attention towards astaxanthin. Previous work had achieved the production of the less hydroxylated carotenoids canthaxanthin and phoenicoxanthin but had stopped short of astaxanthin production. The addition of the extra hydroxylase *Crt*R-*b2* has added complexity but has also allowed for the production of astaxanthin to be dominant over the other carotenoids.

The F_3 generation clearly demonstrates how the levels of canthaxanthin and phoenicoxanthin are reduced in ZWRIU0 and replaced with astaxanthin. The accumulation of the echinenones gives an indication as to which biosynthetic route the ketocarotenoids proceed through. ZWRI00 and ZWRIUU accumulate echinenone to a much higher level than ZWRIU0. Echinenone is higher than either 3OH echinenone or 3'OH echinenone in ZWRI00 and ZWRIUU. On the other hand, ZWRIU0 accumulates 3'OH echinenone. This suggests that ZWRI00 and ZWRIUU probably synthesise the ketocarotenoids with the oxygenation from *Crt*W occurring before the hydroxylation by *Crt*Z. On Figure 3-21 this is shown as a dominant drive from left to right. ZWRIU0 however, also accumulates other hydroxylated carotenoids such as violaxanthin and adonixanthin, therefore the hydroxylation is probably stronger than the oxygenation. On Figure 3-21 this is a downwards push, before a push to the right. The addition of *Crt*R-*b2*, which is a hydroxylase rationalises this. If *Crt*R-*b2* is not silenced then,

in combination with *Crt*Z it provides the dominance of hydroxylation over oxygenation. Figure 3-21 shows the changes in carotenoid profile of ZWRIU0 compared to ZWRI00.

One of the most valuable ketocarotenoids is astaxanthin. The ZWRIU0 line predominantly synthesised this in the esterified form and is also a predominant free carotenoid. The presence of other carotenoids, both ketolated and not, shows that there is room for further astaxanthin synthesis. Currently while astaxanthin is the dominant carotenoid, there is also production of its precursors. These precursors could be converted to astaxanthin if the enzymes could process them more efficiently. It is unknown which enzyme is the limiting factor. The presence of the other ketocarotenoids suggest it may be *Crt*W which limits astaxanthin formation. Another possibility is a limitation in the sequestration, the enzyme responsible for the esterification of astaxanthin may work slower than those which synthesise astaxanthin. The presence of ketocarotenoid derived volatiles supports this. Another viable route to further increase the production of astaxanthin could be by ensuring there are more early carotenoids. While the RI component ensures that cyclisation to beta-carotene occurs, there is no downstream upregulation of phytoene or lycopene. The detection and quantification of lycopene is difficult as it co-elutes with the esters, however there is a clear decrease in lycopene in the ketocarotenoid producing plants. To overcome this, the line may need to be crossed with a variety engineered to enhance early carotenoids. This would provide a reservoir of early carotenoids which could be converted to ketocarotenoids.

The production of adonixanthin epoxide is unusual. It has been reported in tobacco (Hasunuma, 2008) and tomato (Enfissi, *et al.*, 2019) before, however this carotenoid is rarely identified. The previously reported amount in tomato fruit is much lower than produced in this study. However, comparing the amount seen in leaf shows the antithesis, with the published amounts being over twice as high. What is common amongst all the studies which have found adonixanthin epoxide is that it is much more prevalent in the leaf material than the in fruit. This follows the same trend as the other epoxide carotenoids found in tomato; antheraxanthin, violaxanthin and neoxanthin all accumulate to the highest levels in green tissue. The pathway for the production of adonixanthin epoxide is unknown. It has previously been suggested that it is produced by the action of *Crt*W on antheraxanthin. However, antheraxanthin is only detected at low levels in the ZWRIU0 lines, therefore it seems that there is a limited amount of precursor for adonixanthin epoxide if the synthesis occurs through this route. ZWRI00 also

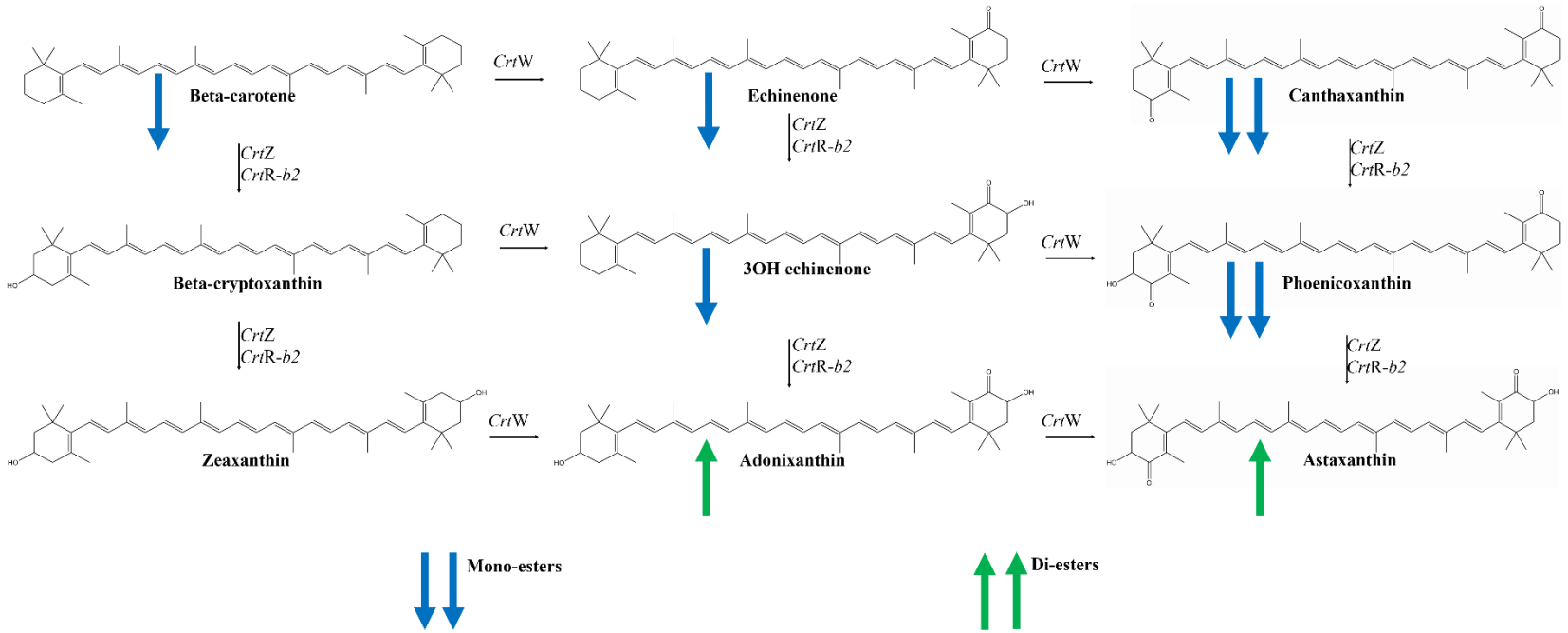

Figure 3-21. Carotenoid changes in ZWRIU0 compared to ZWRI00.
For simplicity 3'OH echinenone is excluded but follows the same trend as 3OH echinenone. Blue arrows represent a decrease of the carotenoid in ZWRIU0, green arrows represent an increase.

has little antheraxanthin or adonixanthin epoxide, however with the addition of the UU/U0 component there is a greater push towards the fully hydroxylated carotenoids, such as zeaxanthin, violaxanthin and antheraxanthin. Therefore, it seems reasonable that with the action of *Crt*R-*b2* the pool of antheraxanthin is temporarily increased, before *Crt*W then oxygenates it into adonixanthin epoxide. Another possible route for synthesis of adonixanthin epoxide, and the stimulus for the name, is through epoxidation of adonixanthin. Adonixanthin is found in higher amount in ZWRIU0 fruit than in any of the other genotypes. Therefore, it could be that the increase in adonixanthin has stimulated an epoxidation reaction. The enzyme which may be responsible for this is unknown, with the only carotenoid epoxidase in tomato being ZEP. It has previously been suggested that ZEP or a paralog can act on other substrates (Khan, *et al.*, 2016). Therefore, it is feasible that ZEP could be acting on adonixanthin to produce adonixanthin epoxide. The true biosynthetic pathway is also potentially a mixture of these two routes, as shown in Figure 3-22, although without flux analysis this cannot be elucidated.

Changes in carotenoids occur throughout ripening. As the fruit matures from breaker to fully ripe the carotenoid content increases. Meanwhile the chlorophylls decrease. All of the ketocarotenoids follow this trend except adonixanthin epoxide. Adonixanthin epoxide remains at a constant level throughout ripening. This correlates with it being most prevalent in green tissue. The esters also accumulate throughout ripening. This implies that once carotenoids are esterified, they are stored rather than degraded. The presence of the ketocarotenoids, or of the ketocarotenoid genes slows ripening down. While an azygous fruit is soft and fully ripe at B7, a ketocarotenoid fruit does not reach this stage until B14. The variation in ripening can make comparison of different genotypes challenging, with the fully ripe stage being most easy to distinguish by feel rather than by days post breaker. This delayed ripening presents an opportunity for an extended shelf life.

Carotenoids are stored in various locations throughout the plastid. The endogenous carotenoids lutein and lycopene are mostly found in the membranes and when in excess, lycopene crystallises with only a small amount being present in the plastoglobuli. Beta-carotene is similar, but with a higher percentage stored in the plastoglobuli than is seen in lycopene or lutein. Interestingly, ZWRIU0 has the highest concentration of beta-carotene stored in the plastoglobuli. The reason for this is unclear, as the total beta-carotene content is highest in

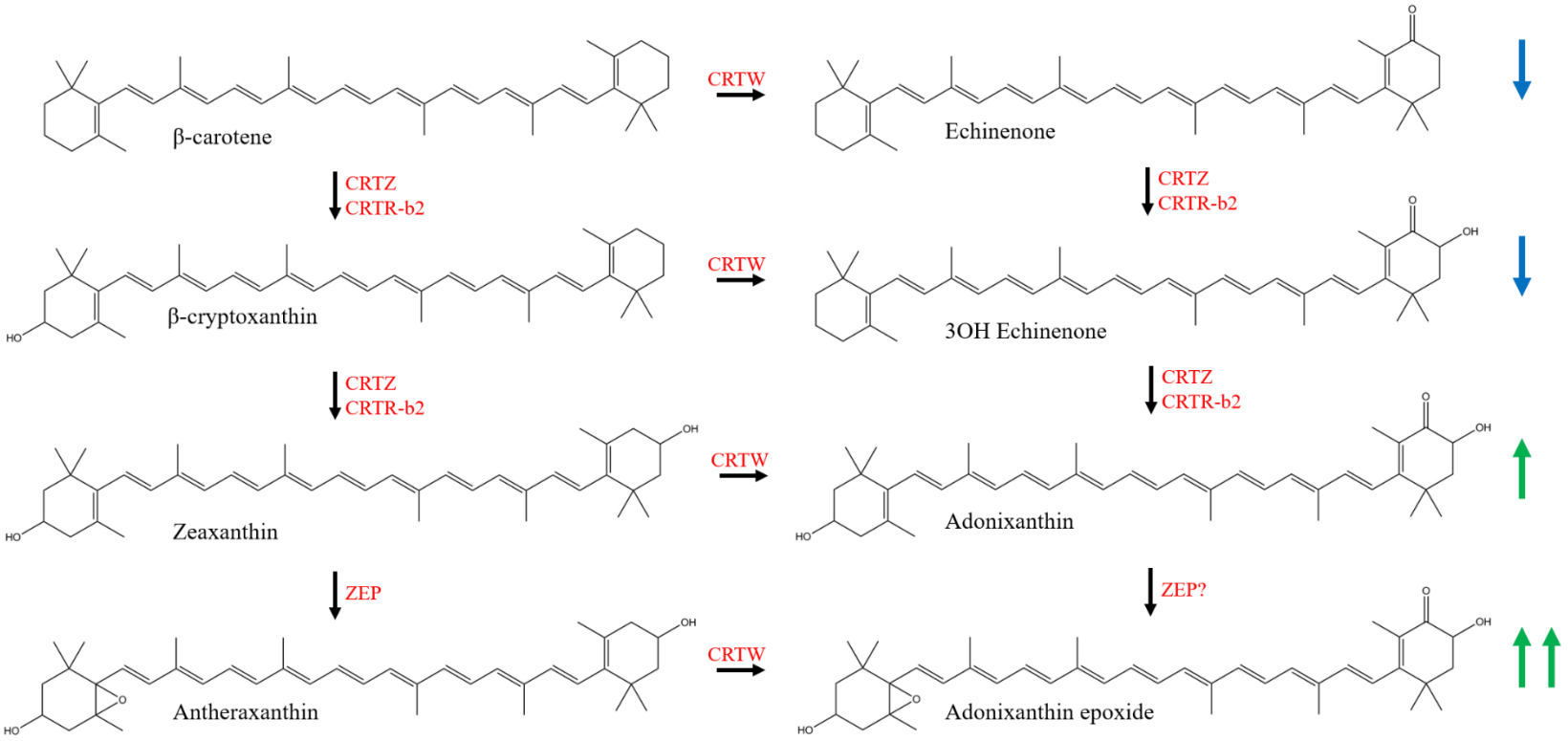

Figure 3-22. Possible putative pathways for the biosynthesis of adonixanthin epoxide
For simplicity 3'OH echinenone is excluded but follows the same trend as 3OH echinenone. Blue arrows represent a decrease of the carotenoid in ZWRIU0, green arrows represent an increase.

ZWRIUU and ZWRI00. It is possible that there are more plastoglobuli in ZWRIU0, and therefore more can be stored here. However, this is something that has not been investigated. The storage of beta-carotene in plastoglobules in ZWRIU0 could also be due to conversion of the membrane bound beta-carotene into ketocarotenoids, thus raising the relative percentage of that remaining in the plastoglobuli. ZWRI00 has more total beta-carotene, so the depletion of the membrane associated beta-carotene may not have impacted the relative amount in the plastoglobuli. The esters and ketocarotenoids are also found in both the membrane and the plastoglobuli. Despite their differing polarities they are still stored in the same locations. As the membrane is lipid rich, the expectation is for the most non-polar compounds, i.e., the esters to accumulate here, whereas the more polar compounds would become enveloped into the plastoglobuli. However, this does not seem to be the case. The relatively polar ketocarotenoids are found in the membrane, this is due to their ability to incorporate into the membrane, with the more polar end groups aligning with the lipophobic head group of the membrane and the carotenoid backbone to align with the lipophilic tail of the membrane. The only carotenoid which is found purely within the membrane is violaxanthin. This could explain why no violaxanthin esters are observed.

The metabolism of an organism is a complicated and interlinked mechanism. Perturbation of one part frequently has an effect on other parts. While all the modifications were focussed on altering the carotenoid pathway, analysis of the broader metabolism has shown small effects elsewhere. The PCA plots shown in Figure 3-16 and Figure 3-17 reveal that there are minimal changes to the overall metabolism. However, while the overall trend is that of no change, there are small, but significant changes to individual metabolites.

The changes in the tocopherols reveal a curious trend. Gamma-tocopherol is reduced in the ketocarotenoid producers, yet the methylated alpha-tocopherol is increased. This is the same as observed by Enfissi, *et al.* (2019). This would suggest that either the presence of ketocarotenoids or the metabolic alterations made have resulted in an altered tocopherol pathway. The more methylated a tocopherol is, the more potent vitamin E activity it has (Seppanen, *et al.*, 2010), therefore, as the ketocarotenoid producing fruit are higher in the most potent tocopherol, it suggests they may have a higher vitamin E content. The overall tocopherol content is also higher in ZWRI00 (×1.5) and ZWRIU0 (×1.7) than azygous, this further supports the hypothesis that the ketocarotenoid producers have a higher vitamin E

activity. Although the chlorophyll content in ZWRI00 and ZWRIU0 is decreased, they both have more pheophytin. This suggests there is more chlorophyll degradation, and as the tocopherols are produced from the chlorophyll derivative phytol, the increase in tocopherol can be rationalised.

The free amino acids show a very clear correlation, they are all reduced in ZWRI00 and ZWRIU0 compared to the azygous. Once again, this reflects the same trend as shown in the previous ketocarotenoid work by Enfissi, *et al.* (2019). The reduction may indicate that a shift of resources from the primary metabolism of amino acids towards the secondary metabolism of carotenoids occurs. On the other hand, it could instead be the result of ZWRI00 and ZWRIU0 making more proteins, both those directly engineered and those indirectly upregulated as a consequence. With an increase in protein synthesis it may be expected that there is a decrease in the protein building blocks; the amino acids.

The sterols show no clear trend. Beta-amyrin is reduced in the ketocarotenoid tomatoes. This helps to explain the difference in fruit phenotype. Both ZWRI00 and ZWRIU0 have peel that is less waxy than azygous. This may be, in part, to the changes in the phytosterols. Sitosterol and stigmasterol are both increased in ZWRI00 and ZWRIU0, this may suggest there are structural changes to the membranes, possibly caused by the presence of ketocarotenoid esters. The fatty acid C18:0 is reduced in ZWRIU0, however no other significant changes were observed. Considering the generation of esterified carotenoids, this is surprising.

The changes to the profile of the sugars will have a large impact on the overall taste profile (Quinet, *et al.*, 2019; Tandon, *et al.*, 2003). There is no overall trend in the sugar composition, but some large changes to individual sugars. Fructose, galactaric/galacturonic acid and mannose/glucose are all increased in ZWRIU0. One issue with the analysis of sugars is distinguishing between them. This is why some of the sugars are not definitely identified but instead broadly classified.

Analysis of semi-volatile data also gives an insight into the compounds which are perturbated by the molecular engineering. Most of the significantly different compounds are carotenoid derived, this shows the extent to which the carotenoid profile was altered. It also indicates the importance of carotenoids on the volatile profile of tomato fruit. 14 carotenoid derived volatiles were reduced in the ketocarotenoid backgrounds, these are either from the carotenoid backbone or the beta-rings. The presence of hydroxy and keto groups changes the beta-ring,

and therefore changes the volatiles produced. Some of those produced can only be found in the ketocarotenoid producers such as 4-oxo-cyclocitral. ZWRI00 has the highest proportion of 4-oxo-cyclocitral. This can be explained by the accumulation of canthaxanthin in this line. 4-oxo-cyclocitral is a direct cleavage of the beta ring of any non-hydroxylated ketocarotenoid such as canthaxanthin. Figure 3-23 shows the cleavage point of the carotenoids and the subsequent volatiles produced. This clearly shows where the novel volatiles arise from.

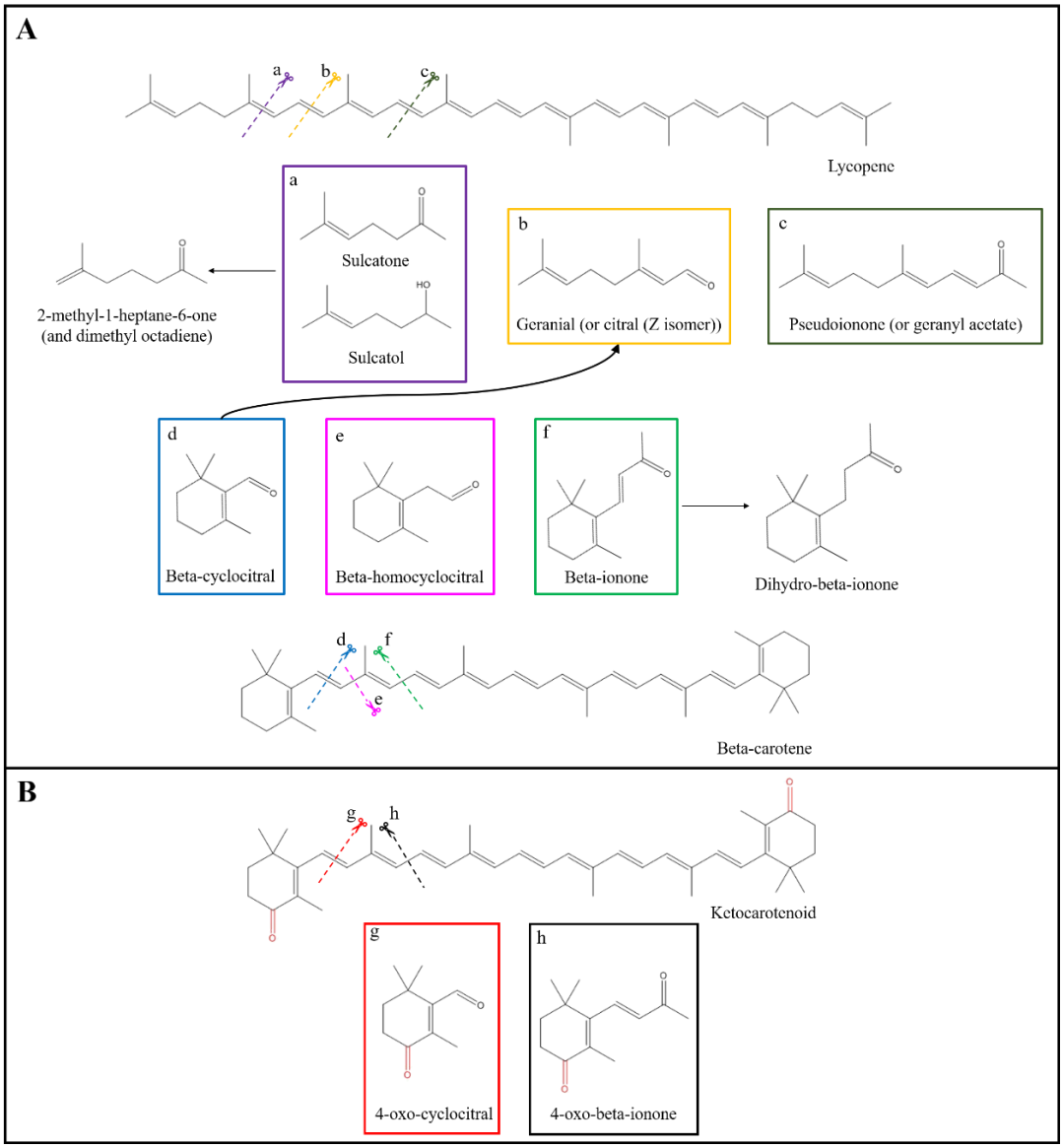

Figure 3-23. The cleavage pathway of carotenoid derived volatiles, including those specific to ketocarotenoids

The colour of the box matches the coloured scissors, which show the cleavage site. Arrows reflect reactions which may occur with the reaction preceding down the arrow.

ZWRIU0 has an increase in the fatty acid derived volatiles, this may be due to ZWRIU0 having di-esters, and therefore, the largest pool of fatty acids to breakdown into volatile compounds.

The analysis of chlorophyll content in the leaf has revealed that despite the brown colouration there is no difference in chlorophyll content. The brown colouration is instead provided purely by the addition of ketocarotenoids. However, the photosynthetic capacity is reduced in ZWRIUU/U0/00 therefore there must be some change to the photosynthetic process. The brown leaf will block some of the absorption of red light into the photosystem, only letting the blue light pass through. This could have an impact on photosynthesis. Carotenoids also play a vital role in photosynthesis as accessory pigments; a change to the carotenoid content could affect this. Previous work by Mortimer (2010) has shown that the ketocarotenoids can also act as accessory pigments, and that it is not solely beta-carotene which can fulfil this role. ZWRIUU/U0/00 all have a reduction in the beta-carotene level within the leaf, therefore it is possible that the ketocarotenoids are acting as accessory pigments within these genotypes, how this affects the photosynthetic capacity in unknown.

3.3.4 ZWRIU0 is susceptible to environmental conditions

Comparison across the generations of ZWRIUU/U0/00 clearly shows that there are large changes between each generation. The predominant carotenoid has changed between each generation of ZWRIU0, with large changes also seen in the mono-ester content. Figure 3-24 shows a summary of the major carotenoids in all three of the generations analysed. The predominant free carotenoid changes from adonixanthin epoxide (F_2), to astaxanthin (F_3) and then to phoenicoxanthin (F_4). However, considering the standard deviation, astaxanthin is also very prominent in F_4. The shift in carotenoid content is interesting, with several possible reasons to explain it. The number of generations a plant has been through since the original cross(es) were made can impact the stability of the expressed genes. The F_2 generation may still be segregating, or the activity of the genes may still be unsettled, or not optimised. This effect would diminish through the generations. Environmental factors could also play a large role. Carotenoids are involved in free radical quenching, and in photosynthesis. Thus, if the environment is not optimal and the plants are stressed the carotenoid profile could change to reflect this. By the same logic, seasonal variations can affect plants too. The F_2 generation was grown in the winter of early 2017, F_3 was grown in an unusually hot and sunny spring of 2018 and F_4 was grown in an average spring in 2019. While all plants were grown under

supplementary lighting and heating to try and remove this seasonal fluctuation, the outside conditions could help to explain the variation. The F_3 generation had the most sunlight, and also the most natural heat, although cooling systems were in place to mitigate some of this. F_3 was the most visually healthily crop with the largest yield (not recorded) and quickest growth time. F_2 and F_4 were more similar in their yield. However, F_4 was grown closer to the middle of the year than F_2 and it was grown in a different glasshouse, with a wider range of accepted conditions. Considering the growth conditions of each generation, it is perhaps not surprising that it was the F_3 generation, which had most light and warmth, that produced the highest levels of the free form of the end ketocarotenoid astaxanthin. With optimal conditions the expression of secondary metabolism genes, such as the carotenoid genes, can be expressed maximally. If the environment is not optimal the plant would push to ensure there is enough of the vital metabolites before pushing into the secondary metabolism. Interestingly, alongside the highest astaxanthin production, F_3 also has the lowest proportion of free mono-esters. There are two possible explanations for this. One explanation is that with the favourable environmental conditions the need for esterification is reduced, the stress on the plant is less, therefore the carotenoids do not need to be stabilised through esterification. Another explanation is that with the accumulation of astaxanthin there is an increase in di-esters rather than mono-esters. Unfortunately, these were not measured in F_3 so cannot be confirmed. The total content of free carotenoids remains consistent through the generations.

Throughout this work the biological variation has been reasonably high. The closeness of technical replication suggests that this variation is due to genuine biological variation as opposed to technical or human error. Furthermore, the standard deviation of azygous plants is often smaller than that in ZWRIUU/U0/00. The ripening series in Figure 3-15 shows the extent of the biological variation well. Interestingly, the variation increases through ripening. This could suggest that it is a variation in the ripening profile that is partially responsible for the region of error.

The variation which occurs both through generations and within a generation, makes the ZWØRIØUU/U0/00 line difficult to predict. The multiple genes introduced through multiple crossing events make ZW(Ø)RI(Ø)UU/U0/00 challenging to work with. While ZWRIU0 does yield high astaxanthin, the ZW(Ø)RI(Ø)UU/U0/00 line is not feasible to be used in a commercial environment. This is because the screening is laborious and requires specialised

equipment. Growers would not be able to be certain of, or even predict the possible yield as the environmental susceptibility seems to play a large role in the resulting carotenoid content. Valuable lessons have been learnt through analysis of ZW(Ø)RI(Ø)UU/U0/00; The importance of silencing caused by multiple copies of the same promoter, the effect of multiple backgrounds, and the need to have genes which function optimally when homozygous. Considering these lessons, it seems as though the way to overcome the problems is by the biosynthesis of astaxanthin in tomato modified by a single, multigene construct.

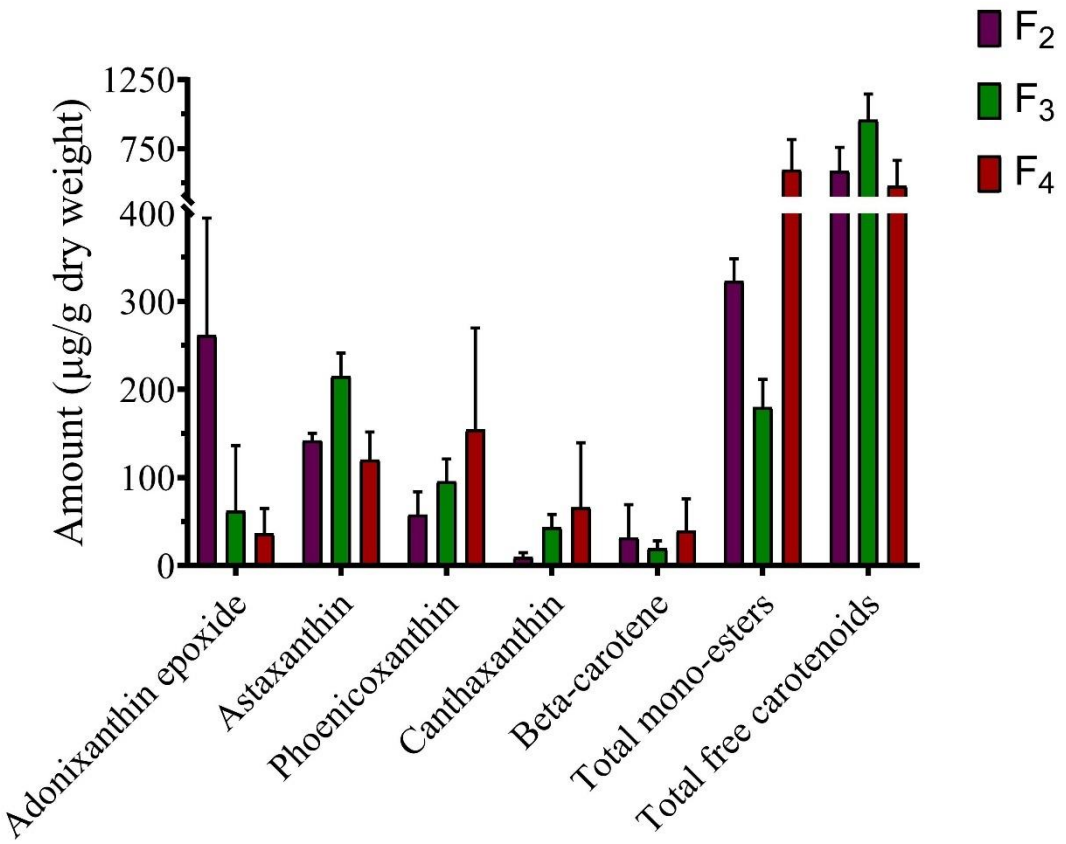

Figure 3-24. Comparison of major carotenoid amounts found in all generations of ZWRIU0 analysed
Error bars represent the standard derivation.

Chapter IV:
Single transformation of a multigene construct for improved ketocarotenoid production

4.1 Introduction

4.1.1 Golden gate cloning

The idea of a single transformation procedure removes the problems associated with background effects and also reduces the time required due to crossing plants. The Golden Gate cloning strategy (Engler, *et al.*, 2014) allows for the compilation of several genes into one vector. This allows for a more controlled and simplified way of transformation and molecular engineering than used in chapter III. The Golden Gate strategy utilises type IIS restriction sites to cleave the DNA one or two base pairs away from the restriction enzyme recognition site. This allows for scar-less annealing of modules, whereby no extra nucleotides are added to the sequence as a result of the cloning protocol used, which can be observed in some other cloning strategies. Accompanying Golden Gate is the Modular Cloning toolkit (MoClo) (Weber, *et al.*, 2011) which is provided by several laboratories and can be added to by anyone using the system. The standardisation of modular parts allows for set parts of a gene, i.e., promoter, coding region (cds) and terminator, to be created in predefined plasmids, with a standard restriction site and set overhangs. Each part has a specific overhang, and therefore when the modules are combined the overhangs are complementary and will ligate together automatically. For example, promoter fragments are designed to have a 3' overhang which is complementary to the 5' end of the cds. MoClo therefore creates a system in which modules can be easily combined to produce a larger construct. Each module is created in a 'level 0' vector and these can then be combined to form the 'level 1' gene. Level 1 genes can then be further combined to form a 'level 2' multigene construct.

4.1.2 Construct design

An important feature for the design of this construct was to overcome the problems seen in chapter III. Therefore, to include all the required coding regions whilst minimising the potential for silencing was a priority. With the overall aim being the production of ketocarotenoids, with an emphasis towards astaxanthin, the choice of genes to execute this was an iteration of those previously used.

Carotenoid oxygenase genes are absent from the tomato genome, and therefore, an oxygenase was required. While there are multiple oxygenases that have been utilised for ketocarotenoid production (Choi, *et al.*, 2007; Jayaraj, *et al.*, 2008), it was *Crt*W that was selected for this

construct. *Crt*W is a well characterised oxygenase, and was already available in a plasmid, thus minimising the cloning work that was required. The work from chapter III, along with the previous work using *Crt*Z (Nogueira, *et al.*, 2017) has shown that *Crt*Z is not sufficient to stimulate the production of large amounts of hydroxylated carotenoids. However, over expression of the endogenous carotenoid *Crt*R-*b2* can provide the necessary hydroxylation (D'Ambrosio, *et al.*, 2011). Therefore, it is *Crt*R-*b2* that was selected for use in this construct. The work done by Enfissi, *et al.* (2019) revealed the importance of considering the production of the early carotenoids when trying to upregulate the later carotenoids. Therefore, a lycopene beta-cyclase enzyme was included to ensure there was an adequate pool of beta-carotene to synthesis into ketocarotenoids. Previously used was the naturally occurring *S. galapagense* beta-cyclase allele with the powerful *S. galapagense cyc*-b promoter which provides a strong regulation for the cyclase. However, *S. galapagense* is hard to germinate, and therefore potentially difficult to transform. While the RI introgression line could have been used, this would have started to introduce potential background effects. Lycopene beta-cyclase (*lcy*) was selected as the alternative approach to increase beta-carotene synthesis. This enzyme is endogenously expressed in the leaf material, therefore overexpression with a fruit promoter should avoid silencing effects.

As previously mentioned, a priority for the design of this construct was to avoid silencing. Silencing can occur when there is too much of a transcript, and therefore, to compensate the transcription is switched off. Considering this, the use of constitutive promoters was kept to a minimum. However, the constitutive expression of *Crt*W provides a useful and early colour screen, and therefore, *Crt*W was placed under the control of 35S. With the expression of *Crt*W being continuous, the expected effect of this would be a decrease in the beta-carotene levels as the ketocarotenoid synthesis begins. However, the ketocarotenoid content would be low in immature fruit and other tissues as the pool of precursors would be low, and there would be no additional hydroxylation. The hydroxylase *Crt*R-*b2* is a chromoplastic gene. The E8 promoter (Zhao, *et al.*, 2009) is an ethylene responsive promoter, and thus is active during fruit ripening. Using E8 to regulate *Crt*R-*b2* ensures that only minimal hydroxylated carotenoids and ketocarotenoids form until the fruit is ripening, this should allow for the available beta-carotene to build before the flux is shifted towards later carotenoids. The lycopene beta-cyclase *lcy* is a chloroplastic gene, and therefore would require a fruit promoter for activity in the fruit. In order to increase the beta-carotene content for production of

ketocarotenoids, the promoter needed to be active early in fruit development. Originally the chosen promoter was the tomato pro-rich promoter (TPRP), however, due to problems cloning (section 4.2.2) this was replaced with the phosphoenolpyruvate carboxylase promoter (PPC2). These promoters are active in early fruit development. Figure 4-1 shows the predicted timing of all the genes within the ketocarotenoid construct.

The terminators were chosen from those readily available in the MoClo plants part kit.

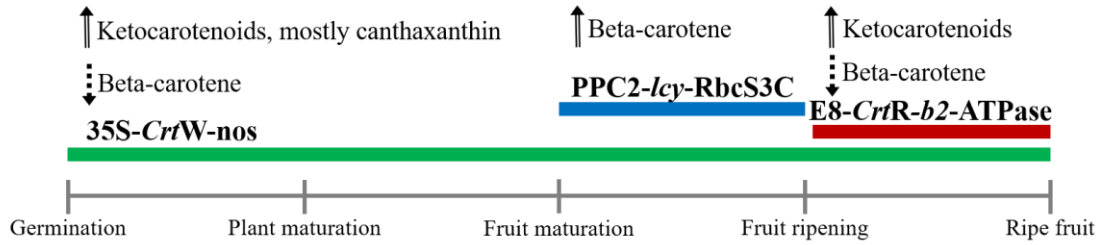

Figure 4-1. Timeline of plant development with the predicted expression window of each gene in the ketocarotenoid construct
Dotted arrows represent predicted decreases in carotenoids, striped arrows represent a predicted increase in carotenoids.

4.2 Results

4.2.1 Creation of 35S-*Crt*W-nos module

The synthesis of the 35S-*Crt*W-nos level 1 vector only required the conversion of a pre-existing *Crt*W plasmid into that suitable for Golden Gate cloning. Both the promoter, 35S, and the terminator, nos, came directly from the MoClo plants part toolkit in level 0 vectors.

The sequence for the *Crt*W signal peptide (SP) and cds contained three BpiI and one BsaI sites. All of these needed to be removed before *Crt*W could be used in Golden Gate cloning. The unwanted restriction sites were removed by splitting the sequence into three parts. PCR was used to amplify each part, with the primers designed to cover the region in which a single nucleotide polymorphism (SNP) needed to occur. If possible, the SNP region would be covered by both a forward and reverse primer, this overlapping approach also allowed for multiple SNPs to occur in one PCR reaction. The substitute bases were selected from those which would remove the restriction recognition site but not change the amino acid produced, if there were multiple options, the one with the highest natural prevalence was chosen. Figure 4-2 shows the changes and primer locations in *Crt*W. Although the SP and cds were split into three parts, after PCR amplification, all three parts were ligated simultaneously into a level 0 vector.

4.2.1 Creation of E8-*Crt*R-*b2*-ATPase module

The E8 promoter was cloned from genomic DNA obtained from moneymaker tomato plants. The full length of the E8 promoter varies from 2101 bp to 2256 bp depending on the accession and the species of tomato (Zhao, *et al.*, 2009). This was deemed too long for use in the construct. To overcome this, the previously published (Sun, *et al.*, 2012) truncated version was used, with a 5' untranslated region (5'UTR) region added. The E8 sequence includes a BpiI site, this was removed by converting the base at 559 bp from T to A. The conversion was performed by PCR which amplified the promoter in two parts. The SNP was covered by both forwards and reverse primers. The 5'UTR was as annotated in GenBank DG317599.1. Appropriate overhangs to allow for cloning into a level 0 Golden Gate vector were included in the primer sequences.

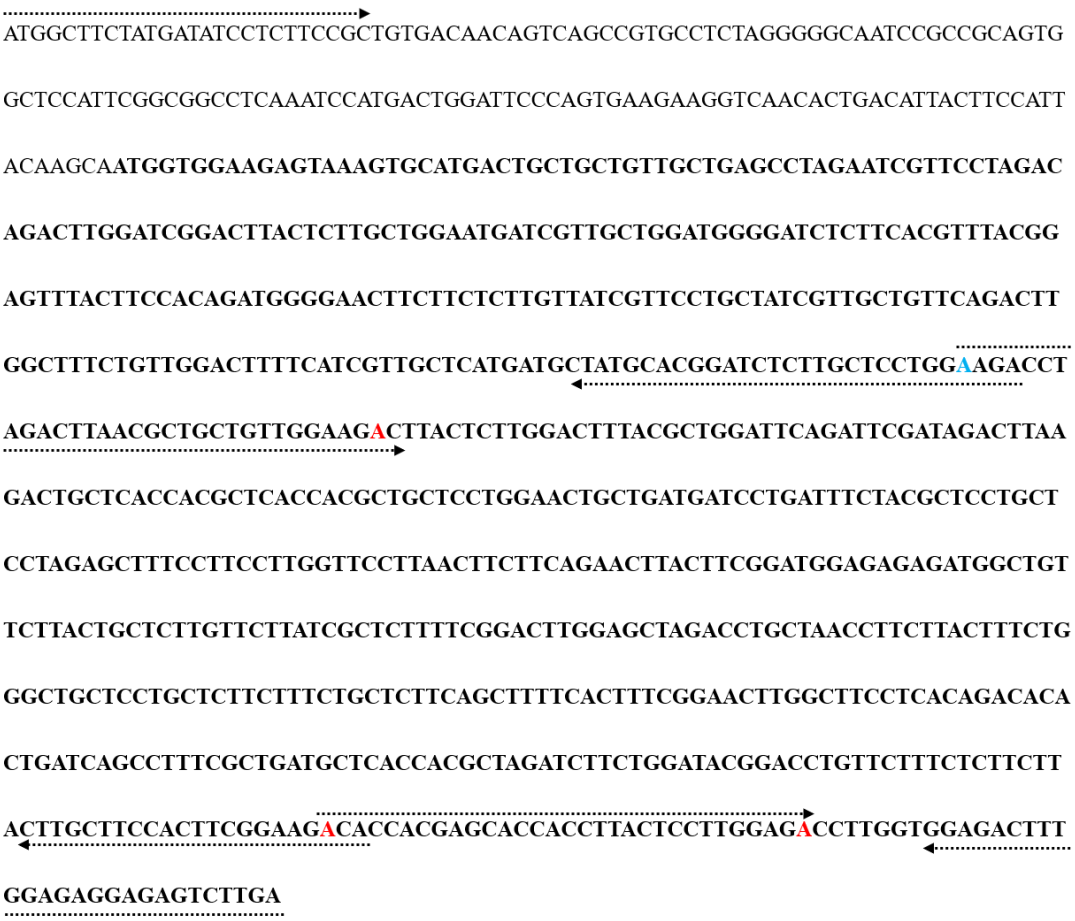

Figure 4-2. Sequence of the unaltered signalling peptide and coding region of *Crt*W
Coding region is shown in bold. To remove restriction recognition sites bases were changed, blue letters indicate the base pair was changed from an A to a T, red letters indicated an A was changed to a G. Dashed arrows show the position of primers, reverse primers are shown underneath the sequence and were the reverse complement.

In order to mitigate potential silencing, the cds for *Crt*R-*b2* was altered whilst maintaining the amino acid sequence. Where possible each three letter codon was changed to another, alternative codon which still codes for the same amino acid. The alternative codon was chosen for optimisation in plants. Eurofins Scientific analysed the sequence and created the resulting, alternative sequence. This was then synthesised by Eurofins, with the required overhangs added to the end of the sequence (Figure 4-3). This created a mock level 0 vector which was then used directly when making the level 1 construct.

The terminator ATPase was used directly from the MoClo plants part tool kit (section 2.2.1).

```
tt GAA GAC aaA ATG GCT GCT GGA ATT AGT GCT TCT GCA TCT TCA AGA ACA ATA AGA CTG AGA CAC AAT CCA TTC CTT TCA CCA AAA TCT GCA TCT ACA GC  < 100
               M   A   A   G   I   S   A   S   A   S   S   R   T   I   R   L   R   H   N   P   F   L   S   P   K   S   A   S   T   A
             10          20          30          40          50          60          70          80          90

T CCA CCG GTT TTG TTC TTT TCA CCA CTC ACT AGG AAC TTT GGA GCA ATT TTG TTG TCT AGA AGA AAA CCC AGA TTA GCA GTT TGC TTT GTG TTG GAA AAC  < 200
   P   P   V   L   F   F   S   P   L   T   R   N   F   G   A   I   L   L   S   R   R   K   P   R   L   A   V   C   F   V   L   E   N
             110         120         130         140         150         160         170         180         190

GAG AAG TTG AAT TCC ACG ATT GAG TCA GAA AGC GAG GTC ATT GAG GAT CGA ATT CAA GTC GAA ATC AAC GAA GAG AAA AGT CTT GCA GCC TCT TGG TTA G  < 300
 E   K   L   N   S   T   I   E   S   E   S   E   V   I   E   D   R   I   Q   V   E   I   N   E   E   K   S   L   A   A   S   W   L
           210         220         230         240         250         260         270         280         290

CT GAG AAA CTA GCT AGG AAG AAG AGT GAA AGG TTT ACC TAT CTC GTT GCA GCT GTG ATG TCA AGC CTT GGC ATA ACT TCC ATG GCA ATT CTT GCC GTG TA  < 400
A   E   K   L   A   R   K   K   S   E   R   F   T   Y   L   V   A   A   V   M   S   S   L   G   I   T   S   M   A   I   L   A   V   Y
           310         320         330         340         350         360         370         380         390

T TAC CGT TTC AGT TGG CAA ATG GAA GGT GGA GAA GTT CCG TTT AGC GAA ATG CTT GCA ACT TTT ACT CTC TCC TTT GGT GCA GCT GTG GGT ATG GAG TAT  < 500
   Y   R   F   S   W   Q   M   E   G   G   E   V   P   F   S   E   M   L   A   T   F   T   L   S   F   G   A   A   V   G   M   E   Y
           410         420         430         440         450         460         470         480         490

TGG GCT AGA TGG GCA CAT AGA GCT CTT TGG CAT GCT TCA TTG TGG CAT ATG CAT GAG TCT CAT CAT AGG CCT AGA GAA GGT CCT TTC GAA ATG AAT GAT G  < 600
 W   A   R   W   A   H   R   A   L   W   H   A   S   L   W   H   M   H   E   S   H   H   R   P   R   E   G   P   F   E   M   N   D
           510         520         530         540         550         560         570         580         590

TG TTT GCC ATA ACC AAT GCT GTT CCT GCT ATA GCA CTC TTG AGT TAT GGT TTC TTC CAC AAA GGG ATT GTA CCA GGG CTG TGT TTT GGA GCT GGG TTA GG  < 700
V   F   A   I   T   N   A   V   P   A   I   A   L   L   S   Y   G   F   F   H   K   G   I   V   P   G   L   C   F   G   A   G   L   G
           610         620         630         640         650         660         670         680         690

T ATC ACA GTC TTT GGA ATG GCC TAC ATG TTT GTA CAT GAT GGA CTT GTT CAC AAG AGG TTT CCT GTT GGA CCT ATT GCC AAT GTA CCC TAC TTC CGT AGA  < 800
   I   T   V   F   G   M   A   Y   M   F   V   H   D   G   L   V   H   K   R   F   P   V   G   P   I   A   N   V   P   Y   F   R   R
           710         720         730         740         750         760         770         780         790

GTT GCT GCT GCT CAT CAG TTA CAC CAT TCT GAC AAG TTC GAT GGT GTA CCT TAT GGC CTG TTT CTT GGT CCA AAA GAG CTA GAA GAG GTT GGA GGG CTA G  < 900
 V   A   A   A   H   Q   L   H   H   S   D   K   F   D   G   V   P   Y   G   L   F   L   G   P   K   E   L   E   E   V   G   G   L
           810         820         830         840         850         860         870         880         890

AA GAG TTG GAA AAG GAA GTT AAT CGT CGA ATC AAG ATC TCA AAA GGC TTA CTG TGA GCT Ttt GTC TTC aa  < 970
E   E   L   E   K   E   V   N   R   R   I   K   I   S   K   G   L   L   *
           910         920         930         940         950         960
```

Figure 4-3. Coding region of *Crt*R-*b2* as produced and synthesised by Eurofins genomic
The translation remains identical to the endogenous *Crt*R-*b2*. Overhangs are shown at the start and end of the sequence and include the restriction recognition site of BpiI and the required complementary overhangs for future cloning. Lower case letters denote filler bases which will be removed during cloning.

4.2.2 Creation of PPC2-*lcy*-RbcSC3 module

In the original design for the construct, the promoter chosen to regulate *lcy* was the TPRP promoter. This is a fruit specific promoter which is active during fruit development and reduced during ripening. A plasmid containing TPRP was kindly provided by Dr. Ana I. Fernandez who had also reported the sequence of TPRP (Fernandez, *et al.*, 2009). The TPRP promoter was large, 2.6 kb. The sequence was also very repetitive, with several long reads of a single base and the GC content was low, 28%. Considering the complexity and length, the TPRP promoter was to be split in half and cloned into two preparatory level -1 vectors before being combined in a level 0 vector. This allowed for shorter regions to undergo PCR rather than trying to successfully amplify the entire sequence in one reaction. Bases from 1190 until the end (2646) were successfully inserted into a level -1 vector. However, the earlier bases (1 to 1194) could not be amplified successfully. There were also a few discrepancies between the published sequence of TPRP and the sequence of the plasmid received. Considering the difficulties experienced an alternative promoter was found.

Fernandez, *et al.* (2009) also reported another early fruit specific promoter; the PPC2 promoter. PPC2 was also a long promoter, 1968bp, and also had long repetitive sections with a low GC content (25%). Due to the length of the promoter, once again it was split into two sections and cloned into level -1, before combination into level 0. Part A (1 to1037) was successfully cloned into a level -1 vector from an entry vector (pEN-L4-PPC2-R1) containing the full PPC2 promoter (Karimi, 2010). However, similar to TPRP, the other half (part B) could not be amplified. To overcome this part B (bases 1033 to 1968) was synthesised from Eurofins scientific. The required overhangs were also added during synthesis to create a mock level -1 vector which could be directly combined with part A to create the full PPC2 promoter in a level 0 vector.

The *lcy* coding region was amplified directly out of tomato RNA. The sequence includes a BsaI site which was removed by site directed mutagenesis to change the C to a T at base 192. The coding region was amplified using two pairs of primers, both spanning the SNP site. Both amplicons were then combined into a level 0 vector.

RbcSC3 was used directly from the MoClo plants part tool kit.

A genetic map of all the components used is shown in section 7.1.7.

4.2.3 Screening of T_0 plants

The transformation procedure produced 63 plants with an unknown genotype (transformation efficiency of approximately 21%). The use of the 35S promoter to regulate *Crt*W provided a way of screening by colour which would identify positive plants, however, plants with multiple copies sometimes appeared green despite the presence of the transgene. The presence of the transgene was tested by PCR amplification of a small part of *Crt*W. There were 12 plants with a brown phenotype which indicated a presence of the transgene, but with an unknown number of copies. There were also three green plants, which despite their appearance were also positive. The PCR also identified four azygous plants, plants which have survived the tissue culture process without any modification having occurred.

To confirm the number of copies of the transgene each plant had, a qPCR from genomic DNA was used. This compared the concentration of the known single copy gene *pds* to that of the unknown construct. Primers were designed which spanned the 35S-*Crt*W and therefore would only amplify the construct. A copy number ratio was then calculated by dividing the concentration of 35S-*Crt*W by that of *pds*. An output of 0.5 reflected a single copy plant, an output of 1.0 reflected a two copy plant, and higher ratios reflected multiple inserts. Performing this qPCR on the 15 plants that required it identified four single copy (35S-*Crt*W:*pds* ratio 0.46±0.18), three double copy (35S-*Crt*W:*pds* ratio 0.87±0.16) and some multiple copy plants (35S-*Crt*W:*pds* ratio 2.27±1.43). Plants with multiple inserts have not been analysed.

4.2.4 Phenotypes

The brown colouration, similar to that seen in the other two chapters was the most notable feature of ketocarotenoid production. This brown colouration also affected the mature green fruit, with it appearing beige rather than green. The ripe fruit was visibly darker, especially in the jelly. Flowers were also orange, as seen before in other ketocarotenoid producing tomatoes. Some plants displayed mottling of the brown colouration, especially along the veins. The size of the plant seemed unchanged and azygous plants had no phenotypic changes. Phenotypes are shown in Figure 4-4.

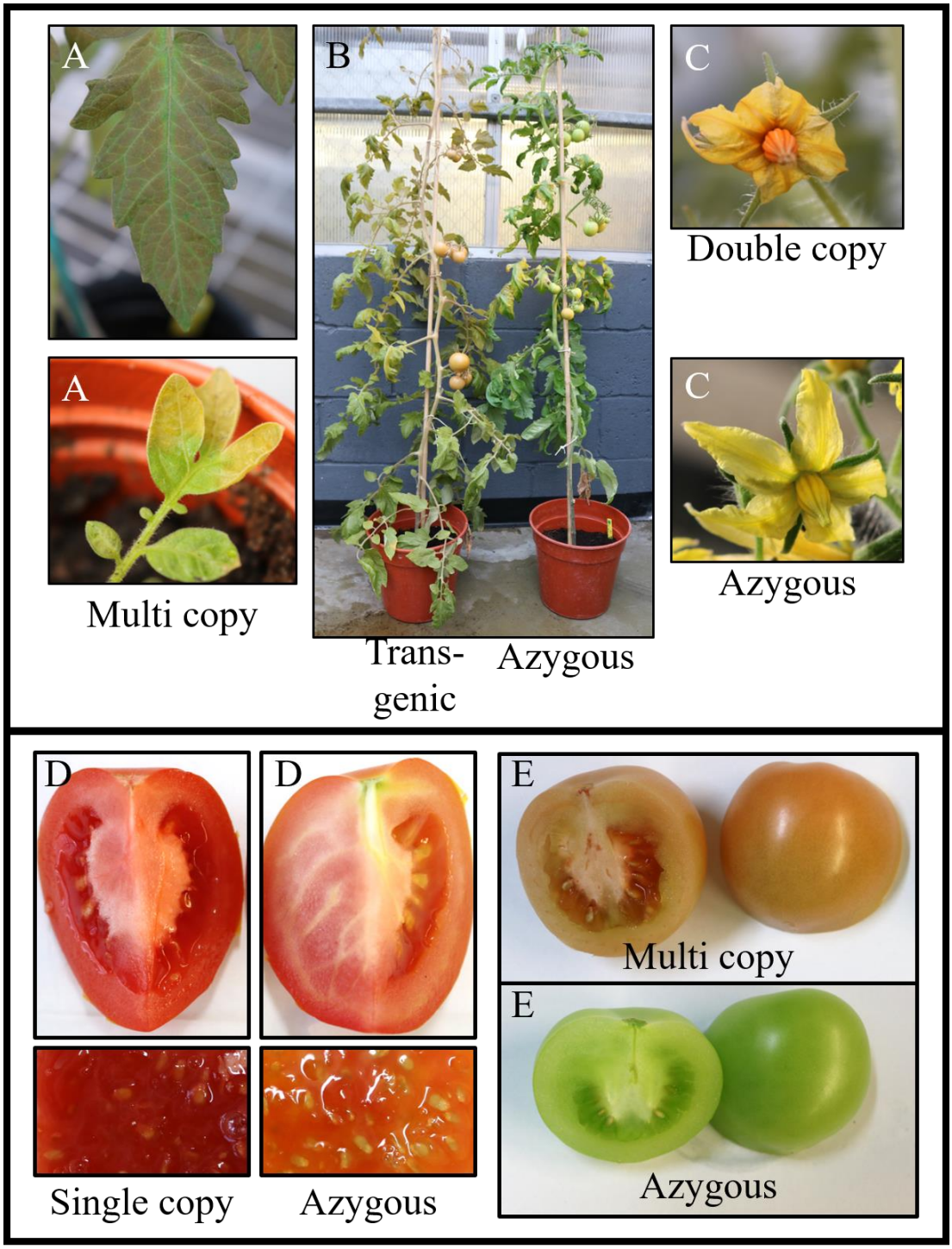

Figure 4-4. Phenotypes of the primary transformants of the multigene ketocarotenoid construct

A) Mottled phenotype created by multiple copies of the transgene. B) Comparison of a transgenic plant with azygous plant. C) Flower phenotypes. Those with the ketocarotenoid construct are coloured orange. D) Ripe fruit and the jelly and seeds. E) Mature green fruit.

4.2.5 Carotenoid content of leaf material

Although the ketocarotenoid construct was designed for production in the fruit, the colouration of the leaf caused by *Crt*W was also investigated. Leaf material was harvested from mature plants, before senescence had begun. The material was then analysed on the UPLC system (section 2.6.4) with carotenoids and chlorophylls analysed separately to ensure the correct conditions for both concentration ranges. For each plant three technical replicates were averaged. Where possible carotenoids and chlorophylls were identified by the retention time based on the comparison with authentic standards and their characteristic spectra. Amounts were estimated by reference to the response from authentic standards.

Comparison of the four azygous plants shows there was little difference between them, therefore, these were averaged for comparison with other genotypes. The standard deviation reflects the level of variation seen within the biological azygous replicates. All other plants were treated as individual genotypes, and whilst the copy number is known, where the transgene has inserted is not, and probably varies between plants. The single copy plants are identifiable by an S before the number, and double copy plant begins with a D. Amounts of chlorophylls and carotenoids are shown in Table 4-1.

The level of beta-carotene seems to be affected by the presence of the ketocarotenoid construct. Azygous contains the highest amount (333.5 μg/g), this is as seen before in other ketocarotenoids producers (section 3.2.9). Interestingly, whilst single insert plants have lowered (43.6 μg/g – 226.4 μg/g) beta-carotene all the double insert plants have no quantifiable amounts of beta-carotene in the leaf. Lutein is also higher in azygous plants, indicating a shift towards ketocarotenoid production.

Due to timing of the fruit promoters, the ketocarotenoid predicted to be most prevalent was canthaxanthin. With only *Crt*W being expressed, the hydroxylation of carotenoids was expected to be minimal, and only produced by the endogenous hydroxylase activity. Within the transgenic plants it was often phoenicoxanthin or adonixanthin epoxide which were found in the largest quantities. Both of these carotenoids have at least one hydroxyl group on them. The level of canthaxanthin, the predicted dominant ketocarotenoid, was highest in the double copy plants, although there was also large variation plant to plant. The ratio of echinenone to 3'OH echinenone did follow the expected trend, with echinenone being constantly higher than

Table 4-1. Carotenoid and chlorophyll content of leaf material in T_0 plants with the ketocarotenoid construct
Azygous amounts are from an average of four biological replicates, ± standard deviation. S refers to single copy plants, D refers to double copy plants.

Carotenoid	Azygous	S11	S34	S67	S72	D24	D27	D55
Pheophytin	32.74 mg/g ±24.91	11.90 mg/g	7.22 mg/g	10.87 mg/g	12.25 mg/g	9.60 mg/g	7.64 mg/g	16.86 mg/g
Chlorophyll A	386.14 mg/g ±68.64	381.22 mg/g	269.63 mg/g	326.52 mg/g	365.11 mg/g	238.87 mg/g	146.54 mg/g	270.70 mg/g
Chlorophyll B	16.63 mg/g ±4.23	15.17 mg/g	9.92 mg/g	13.49 mg/g	14.89 mg/g	9.37 mg/g	6.51 mg/g	10.91 mg/g
Neoxanthin	150.57 µg/g ±31.68	0.00 µg/g	0.00 µg/g	34.41 µg/g	22.08 µg/g	0.00 µg/g	0.00 µg/g	0.00 µg/g
Violaxanthin	205.59 µg/g ±33.38	0.00 µg/g	0.00 µg/g	30.98 µg/g	38.44 µg/g	0.00 µg/g	0.00 µg/g	0.00 µg/g
Adonixanthin epoxide	0.00 µg/g ±0.00	338.50 µg/g	513.18 µg/g	883.37 µg/g	823.39 µg/g	85.96 µg/g	58.74 µg/g	39.31 µg/g
Astaxanthin	0.00 µg/g ±0.00	103.16 µg/g	116.88 µg/g	59.91 µg/g	52.17 µg/g	58.98 µg/g	32.74 µg/g	25.93 µg/g
Lutein	645.66 µg/g ±118.42	214.04 µg/g	127.63 µg/g	265.41 µg/g	335.16 µg/g	107.13 µg/g	66.60 µg/g	148.87 µg/g
Phoenicoxanthin	0.00 µg/g ±0.00	718.53 µg/g	368.26 µg/g	116.34 µg/g	91.69 µg/g	504.10 µg/g	280.22 µg/g	436.07 µg/g
Unknown C	0.00 µg/g ±0.00	109.02 µg/g	81.82 µg/g	37.10 µg/g	32.28 µg/g	65.82 µg/g	30.52 µg/g	117.80 µg/g
Canthaxanthin	0.00 µg/g ±0.00	201.96 µg/g	70.99 µg/g	4.30 µg/g	0.00 µg/g	237.11 µg/g	155.28 µg/g	231.47 µg/g
3'OH echinenone	0.00 µg/g ±0.00	10.36 µg/g	4.27 µg/g	0.00 µg/g	0.00 µg/g	12.88 µg/g	8.37 µg/g	13.28 µg/g
Echinenone	0.00 µg/g ±0.00	53.59 µg/g	45.00 µg/g	38.22 µg/g	36.31 µg/g	27.56 µg/g	12.11 µg/g	34.68 µg/g
Beta-carotene	333.47 µg/g ±39.48	37.52 µg/g	43.53 µg/g	189.31 µg/g	226.41 µg/g	0.00 µg/g	0.00 µg/g	0.00 µg/g

3'OH echinenone. The hydroxylated carotenoids neoxanthin and violaxanthin were also present in two of the transgenic plant. These were also seen in the azygous plants, and as they are both hydroxylated this must have been due to endogenous hydroxylase activity.

The levels of individual carotenoids found in each plant varied. For example, the amount of canthaxanthin in S11 was 202.0 µg/g, whereas in S67 it was only 4.3 µg/g and it wasn't detected in S72. Adonixanthin epoxide was seen in notably higher quantities in all of the single copy plants. The average for a single copy plant is 639.6 µg/g, whereas in the double copy plants it was only 61.3 µg/g. Astaxanthin also followed the same trend, although to a smaller extent, and may not be due to copy number.

There was an unknown carotenoid detected in the leaf tissue. Unknown C had a maximum at 463 nm and a retention time of 4.8 minutes, therefore eluted after phoenicoxanthin. The shape of the spectrum indicated a ketocarotenoid.

The chlorophylls were seen in much higher amounts than the carotenoids. Pheophytin was observed to be highest in the azygous plants compared to the transgenic plants. The content of the other chlorophylls wasn't affected by the ketocarotenoid construct.

4.2.6 Carotenoid content of mature green fruit

The cyclase *lcy* was under the control of a fruit specific promoter which was active during fruit development, therefore, by the mature green stage the fruit should have had an increase in beta-carotene production. With an increase in beta-carotene a subsequent increase in ketocarotenoids was expected. Fruit was harvested once fully mature, but before ripening had initiated. Where possible three fruit were harvested per plant, unfortunately due to poor growth conditions only two fruits were harvested for S11 and only one fruit for S72. Three technical replicates were performed on all genotypes. Four azygous plants were analysed, and the average of the biological replicates taken. Full amounts are shown in Table 4-2.

The level of pheophytin was reduced in all of the transgenic plants compared to the azygous control, however the extent of the reduction was not consistent across all genotypes. The level of chlorophyll A varied across all genotypes, regardless of copy number. This is also true across the azygous plants; this is reflected by the large standard deviation shown in Table 4-2. The chlorophyll B content was reasonably consistent across all genotypes.

Table 4-2. Carotenoid and chlorophyll content of mature green fruit from T_0 plants with the ketocarotenoid construct
Amounts are in µg/g dry weight. Azygous amounts are from an average of four biological replicates, ± standard deviation. S refers to single copy plants, D refers to double copy plants.

Metabolite	Azygous		S11	S34	S72	D24	D27	D55
Pheophytin	3870.63	±1186.65	940.99	551.82	1780.63	237.52	227.20	1907.43
Chlorophyll A	1104.40	±1579.33	1521.38	1483.70	615.55	2114.85	2491.46	1660.87
Chlorophyll B	117.55	±64.52	89.71	72.11	84.62	90.59	115.27	127.01
Neoxanthin	1.43	±0.56	0.71	0.69	1.27	0.00	0.45	0.73
Violaxanthin	7.40	±3.51	5.61	2.23	9.75	0.00	2.04	2.49
Adonixanthin epoxide	0.00	±0.00	27.11	34.51	7.25	38.32	43.41	42.94
Astaxanthin	0.00	±0.00	11.44	11.90	5.51	24.97	27.22	16.48
Lutein	12.16	±3.96	2.30	0.87	4.86	0.87	1.00	2.23
Unknown D	0.00	±0.00	9.72	13.87	6.09	11.51	10.27	13.06
Phoenicoxanthin	0.00	±0.00	11.41	6.94	4.34	25.63	37.96	8.75
Canthaxanthin	0.00	±0.00	1.17	0.37	0.77	2.54	6.05	0.74
3'OH echinenone	0.00	±0.00	0.00	0.00	0.00	0.17	0.38	0.00
Beta-carotene	7.91	±2.66	4.91	3.42	6.14	1.73	2.79	3.57
Total esters	0.00	±0.00	49.71	28.44	39.66	44.41	70.39	44.77
Total carotenoids	28.90	±10.43	124.08	103.23	85.64	150.15	201.96	135.77

The neoxanthin and violaxanthin content was similar throughout all of the genotypes. There was one (D24) which had unquantifiable levels of both the neoxanthin and violaxanthin, but the levels of these xanthophylls were low in all genotypes.

The level of lutein was reduced, to varying extents in the transgenic plants. This suggests a shift towards the beta-carotene pathway. Beta-carotene was expected to be increased with the expression of the *lcy* gene through fruit maturation. Whilst beta-carotene was decreased compared to the azygous genotype, the total carotenoids increased. This implies an increased pool of beta-carotene which has then gone into further ketocarotenoid synthesis.

Unknown D was also detected in the fruit. Unknown D eluted after astaxanthin, at 3.7 minutes the absorption maximum was at 466 nm. The shape of the spectrum resembles 3OH echinenone, however distinguishing between ketocarotenoids is difficult based purely on the spectra. Ketocarotenoids were completely absent from azygous fruits, this was as expected. With *Crt*R-*b2* from the ketocarotenoid construct not being expressed until ripe fruit, the ketocarotenoids expected to mostly accumulate are still the non-hydroxylated echinenone and canthaxanthin.

However, echinenone wasn't detected at all in the mature green fruit. Instead, the partially hydroxylate 3'OH echinenone was, but only in very small amounts (~0.3 µg/g). Canthaxanthin was found in larger quantities in some of the plants, however, this was not consistent across all genotypes. Phoenicoxanthin and astaxanthin were both found in larger than expected amounts, considering the level of hydroxylation of these ketocarotenoids. Double copy plants had higher amounts (14.6 µg/g to 27.2 µg/g) of astaxanthin than single copy plants (5.5 µg/g to 11.9 µg/g), however, the total carotenoid content was unaffected. The levels of adonixanthin epoxide varied largely across all of the transgenic plants, with most being approximately 30 µg/g. However, S72 was only 7.3 µg/g. The total content for S72 was also the lowest, 85.6 µg/g, so this lower content is reflected across all carotenoids.

The mature green fruit was also found to have carotenoids which appear to be esterified. While these have not been identified, they eluted after the ketocarotenoids but before beta-carotene, this is the region in which previously identified esters have also eluted (section 3.2.3). The total ester content was reasonably high, between 28% and 46% of the total carotenoid content. The production of esters was somewhat unexpected due to the requirement of a hydroxyl group

for esterification, however, considering the presence of free hydroxylated carotenoids perhaps not surprising.

4.2.7 Carotenoid content of ripe fruit

The expression of the additional *Crt*R-*b2* was programmed to occur during the ripening of the fruit. Therefore, by the ripe stage the fruit will have expressed all three of the genes included in the ketocarotenoid construct. It was expected that it is the ripe fruit that will contain the highest levels of ketocarotenoids, including those with hydroxyl groups. Lycopene was the most prevalent carotenoid in the azygous controls, and reasonably similar amounts are seen throughout the genotypes. Thus, the content of this early carotenoid has not been affected by the ketocarotenoid construct. Full amounts are shown in Table 4-3.

The levels of beta-carotene should have been increased through maturation by *lcy*. However, as beta-carotene is converted to other downstream carotenoids, the level may have decreased upon ripening. All of the transgenic plants demonstrated a slight decrease in beta-carotene; however, this effect was only minimal in most of the plants. S72 had the lowest beta-carotene content (17.7 μg/g) but also contained least lycopene, phoenicoxanthin and astaxanthin. The levels of lutein were decreased amongst all of the transgenic plants suggesting that the *lcy* gene was cyclising lycopene to beta-carotene and removing the lycopene available for cyclisation to delta-carotene and beyond. The reduction in lutein therefore suggested there was an increased push towards beta-carotene and its products. Similarly, phytoene was slightly decreased in the double copy plants, although in the single copy plants it was consistent with azygous. Phytofluene was also decreased, although for this carotenoid the decrease was consistent across all of the transgenic plants. Alpha-tocopherol appeared to be unchanged by the change to the carotenoid profile.

The total carotenoid content was generally increased due to the ketocarotenoid construct. However, there was one transgenic plant (S72) which had a decrease, and one (D27) with a very similar total carotenoid content.

Canthaxanthin was observed in all transgenic plants, with no distinction between single and double copies. Similar to the carotenoid content of mature green fruit, canthaxanthin was one of the minor carotenoids, in terms of quantity seen in these plants. It was phoenicoxanthin and

Table 4-3. Carotenoid content of ripe fruit from T_0 plants with the ketocarotenoid construct
Amounts are in µg/g dry weight. Azygous amounts are from an average of four biological replicates, ± standard deviation. S refers to single copy plants, D refers to double copy plants.

Metabolite	Azygous	S11	S34	S72	D24	D27	D55
Adonixanthin epoxide	0.00 ±0.00	0.00	0.00	1.53	0.00	0.00	33.97
Astaxanthin	0.00 ±0.00	130.48	159.48	48.32	153.64	140.25	225.11
Unknown A	0.00 ±0.00	12.33	20.90	5.58	25.86	23.48	31.93
Lutein	9.80 ±0.73	0.85	1.34	0.00	1.36	2.16	2.41
Phoenicoxanthin	0.00 ±0.00	213.41	161.81	89.09	172.40	138.79	285.56
Canthaxanthin	0.00 ±0.00	34.52	16.41	15.86	14.38	19.33	28.96
3'OH echinenone	0.00 ±0.00	1.84	0.78	1.34	0.72	1.13	1.18
Alpha-tocopherol	308.42 ±22.23	274.57	171.29	243.21	205.95	331.39	167.98
Echinenone	0.00 ±0.00	8.76	9.15	4.86	10.92	7.54	18.00
Lycopene	491.98 ±49.22	417.45	481.36	353.79	394.75	383.34	551.75
Phytoene	28.76 ±10.97	27.74	26.18	23.72	16.85	14.43	17.06
Gamma-carotene	10.93 ±1.70	7.24	3.98	3.94	3.63	1.64	2.21
Beta-carotene	78.56 ±5.69	41.62	55.36	17.71	55.18	23.73	74.79

Metabolite	Azygous	S11	S34	S72	D24	D27	D55
Phytofluene	200.63 ±71.99	132.84	93.81	116.32	100.57	57.49	77.29
Total esters	0.00 ±0.00	44.31	62.27	47.05	51.19	76.30	113.39
Total carotenoid	820.66 ±110.01	1073.39	1092.82	729.09	1001.47	889.60	1463.60

astaxanthin which were the main ketocarotenoids observed. Phoenicoxanthin was seen in amounts ranging from 89.1 µg/g to 213.4 µg/g, with astaxanthin ranging from 48.3 µg/g to 225.1 µg/g. While both of these had a large variation, they were consistently the dominant carotenoid within a plant. The prevalence of phoenicoxanthin and astaxanthin compared to other ketocarotenoids mirrors what has been observed before in chapter III. Adonixanthin epoxide, which was predominant in the mature green fruit was observed in much lower quantities in the ripe fruit and was only detected in one of the six transgenic plants. The levels of echinenone were similar throughout all transgenic plants analysed. The hydroxylated form 3'OH echinenone was also consistent, although seen at lower levels. While 3OH echinenone was also detected it co-eluted with another non-carotenoid compound, and therefore was excluded from analysis. The ripe fruit also seem to contain carotenoid esters, although to a smaller extent than the mature green fruit (4.1% to 8.6%). The best performing plant from this chapter for astaxanthin synthesis was the double copy plant D55 (225.1 µg/g). This is the higher than the free astaxanthin content seen in chapter III.

4.2.1 An alternative construct with constitutive expression of *lcy*

With the difficulties experienced when trying to clone the PPC2 promoter, an alternative promoter was also chosen and cloned using Golden Gate to be included in the place of PPC2. The ubiquitin 10 promoter from Arabidopsis (pPAtUbq10) was chosen, as it was readily available from the Golden Braid kit (GB0223). pPAtUbq10 was not however fruit specific, therefore this construct design was not expected to be as optimal as the one with PPC2. pPAtUbq10 is expressed throughout the plant, as a constitutive promoter.

The pPAtUbq10 promoter was needed to be converted from a Golden Braid cloning part into one suitable for Golden Gate. For this, the appropriate overhangs, which contained the complementary sequence for the level 0 vector and the restriction recognition site for BpiI were required and were added through PCR. The Golden Braid sequence also contained an internal BpiI site which was removed during the conversion from Golden Braid to Golden Gate. Primers were designed to span this restriction site in both the forward and reverse direction. The base 442 bp from the start of the pPAtUbq10 insert was changed from an A to a C. After the addition of overhangs and the removal of the BpiI site by PCR the fragments were cloned into a level 0 Golden Gate vector. The level 1 vector with pPAtUbq10-*lcy*-

RbcSC3 was then assembled before combination with the other, unaltered level 1 vectors into the final construct.

Only one plant with the alternative construct survived the tissue culture process (approximately 0.3% transformation efficiency). Copy number analysis of the plant was performed the same as in 4.2.3. The single pPAtUbq10 plant (U5) had a single copy of the transgene.

Ripe fruit was analysed for the carotenoid content, with three fruit harvested and pooled for analysis. Comparison of the carotenoid content (Figure 4-5) between the best performing single copy PPC2 plant (S11) and U5 revealed some important differences. While the levels of lycopene were not that different between S11, U5 and azygous the levels of beta-carotene were. The U5 fruit had 16.7 times more beta-carotene than S11, and 8.8 times more than azygous. The large increase in beta-carotene indicated the pPAtUbq10 promoter was more strongly expressing *lcy* than PPC2. U5 also had no detectable lutein levels indicating a complete shift to beta-carotene production. Phytoene and phytofluene were similar between S11 and U5.

The effect of more beta-carotene also effected the ketocarotenoid production. The phoenicoxanthin content was increased from 213.4 μg/g to 592.6 μg/g which is 2.8 times increase. Canthaxanthin was increase from 34.5 μg/g to 160.0 μg/g (×4.6). Echinenone showed the largest increase from 8.8 μg/g to 87.6 μg/g (×10.0). Astaxanthin was not affected. The esters were also increased (×2.9) although as these haven't been identified it is unknown which carotenoid these derive from.

The effect of the pPAtUbq10 promoter increased the total carotenoid content from 820.7 μg/g (azygous) and 1073.4 μg/g (S11) to 2356.1 μg/g (U5). A total carotenoid content of 2.4 mg/g competes with that seen in chapter III. The full carotenoid content of U5 is shown in section 7.1.8.

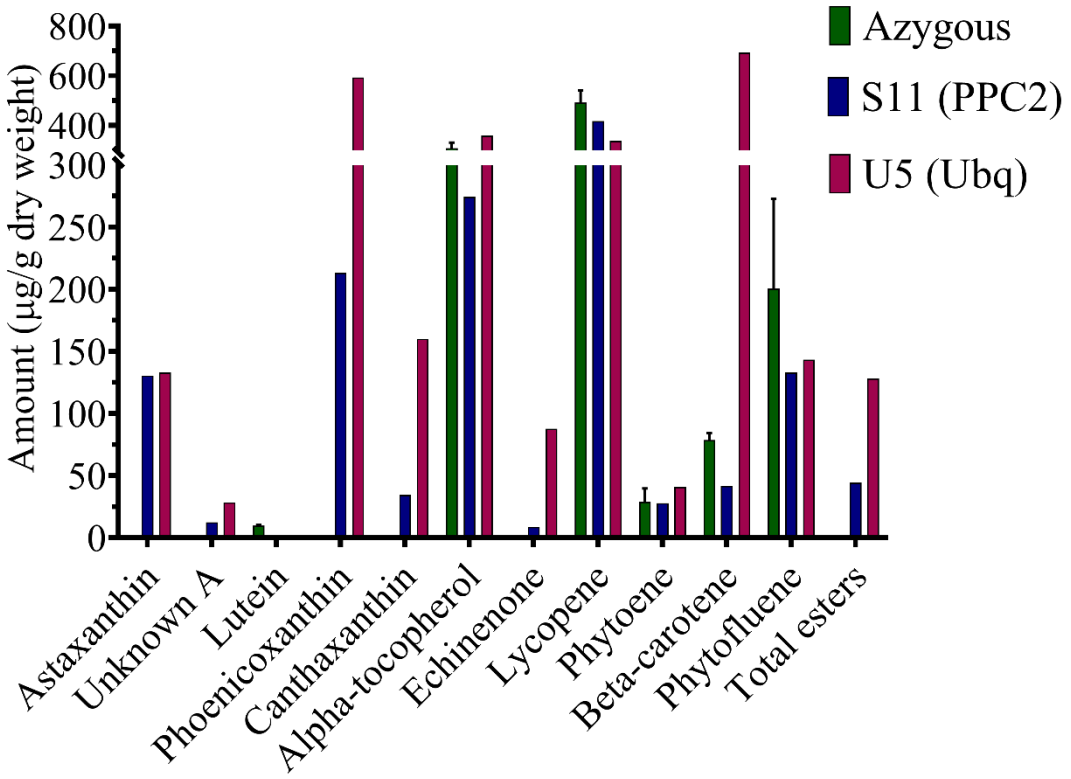

Figure 4-5. Comparison of azygous, S11 and U5 carotenoid content in ripe fruit
Both S11 and U5 have a single copy of their respective transgene. Azygous is an average of four biological replicates with error bars showing the standard deviation. S11 and U5 are single plants. Three fruit was harvested for each genotype.

4.3 Discussion

4.3.1 Golden Gate cloning

Extension of the carotenoid pathway in tomato has often depended on genetic crossing to combine several separate transformation events. The idea of a multigene construct which requires only one transformation event is something that until the advent of multi-gene engineering could not be easily achieved. Systems such as the Golden Gate approach have considerably increased the speed at which multiple genes can be added to plants. The modular system which Golden Gate is based on also allows for the easy substitution of parts. A disadvantage to strict cloning strategies such as Golden Gate is that they can be restrictive in their use. The use of specified restriction enzymes can limit flexibility when cloning. If a gene has multiple restriction recognition sites that need to be removed, using Golden Gate may not be feasible. Similarly, the pre-set overhangs can make primer design difficult. Without the ability to alter the position of primers there is limited manoeuvre room during design. The long overhangs also restrict the primer design and increase the cost of cloning.

It is the modular approach which has allowed the used of two different promoters here. This allows for subtle modifications to large constructs without the need for a new cloning programme. The idea of exchangeable level 0 parts should increase the rapidity of cloning and help to prevent the same part being made multiple times across different research groups. Thus, this work has contributed to community resources through the delivery of new molecular parts.

4.3.2 Screening and phenotypic changes

All transformation events require screening. The inclusion of a constitutive *Crt*W to provide an early colour screen was useful in rapidly identifying positive plants. However, with some multi-copy plants having the same appearance as azygous plants the phenotypic classification was not absolute. In future generations, once the possibility of multi-copy plants is removed the phenotype will be more accurate. Screening by determining the copy number relative to *pds* provides a relatively quick and easy approach to determine the plants of interest. Hopefully, the ketocarotenoid construct is optimal when homozygous, as then for generations beyond T_1 screening will not be required.

The colouration to the leaves is similar to that seen before in chapter III. The effect on the plant vigour of the brown leaves seems to be minimal, with an equal growth rate and growth size. Comparison of the colour of control plants and those with the ketocarotenoid construct reveals that the ketocarotenoid accumulation does darken the flesh. However, it is the jelly which visually shows the largest change. Unfortunately, the jelly was not analysed separately in this work. As seen before, the presence of the ketocarotenoids slows down the ripening process, possibly due to a change in other parts of metabolism.

4.3.3 Effect of the ketocarotenoid construct of carotenoid content in leaf material

The aim for this construct was to improve the synthesis of the ketocarotenoids, especially astaxanthin, beyond that already achieved in chapter III. The simplicity of a single transformation combined with the specially chosen fruit promoters should have provided an optimised method for ketocarotenoid production. It is the ripe fruit that is the end target for this work, with the timings of promoters aimed to achieve the maximal ketocarotenoid content here. However, despite aiming for the ripe fruit, other material was also analysed to assess the carotenoid alterations that were occurring. Both the leaf tissue and the mature green fruit show visible changes, and therefore, these were also analysed. The nature of analysing a T_0 generation means that each plant must be classified as a separate event, with the site of insertion being unknown. Thus, with the lack of biological replicates, there is a lack of statistical analysis that can be performed on a T_0 generation. All the comparisons made are therefore not derived from statistics but from a crude, visual evaluation.

The leaf material is, unsurprisingly dominated by the chlorophylls and derivatives. Both chlorophyll A and B were unchanged, despite the brown colouration to the plants. There is however, less pheophytin in the ketocarotenoid plants. The difference between chlorophyll A and pheophytin is the presence of an Mg^{2+} ion; chlorophyll A has one, whereas pheophytin does not. The role of pheophytin is as the first electron carrier intermediate in photosystem II (Klimov, 2002). A reduction in pheophytin may, therefore have an effect on the plants ability to complete photosynthesis. This would most likely manifest itself as a loss of vigour. Seeing as this is not observed, even the reduced level of pheophytin is probably enough to maintain sufficient photosynthesis.

The change in the profile of the hydroxylated carotenoids is pronounced. Azygous leaves accumulate only hydroxylated carotenoids and beta-carotene. Lutein is the dominant

carotenoid in the controls, whereas in the ketocarotenoid plants it is reduced by at least half. Similarly, violaxanthin and neoxanthin are decreased to small amounts, or below the limit of detection. This reduction in endogenous hydroxy carotenoids is accompanied by an increase in non-endogenous carotenoids. Adonixanthin epoxide is present in variable amounts throughout the ketocarotenoid plants. While there is no adonixanthin or antheraxanthin detected in either controls or ketocarotenoid plants, it appears *Crt*W or an unknown epoxidase is synthesising this from the endogenous hydroxy carotenoids. Similarly, phoenicoxanthin, astaxanthin and 3'OH echinenone are also observed. The expression of the additional hydroxylase gene should not be active in the leaf, therefore the presence of these must only be due to the activity of the endogenous hydroxylase. Considering the base levels of xanthophylls normally observed, the amount of hydroxylated ketocarotenoids is surprising. Endogenous *Crt*R-*b1* is able to hydroxylate ketocarotenoids. The presence of astaxanthin, which is a di-hydroxyl molecule may mean that the enzyme has acted on the non-endogenous phoenicoxanthin to form astaxanthin.

The absence of beta-carotene in the double copy plants is interesting. While the single copy plants have a reduced amount of beta-carotene, the doubles are lower than the detectable limit. A possible reason for the difference in beta-carotene levels in that the expression of the construct in the double copy plants is possibly higher, and therefore more of the initial substrate (beta-carotene) in converted into other carotenoids. However, the total carotenoid content is lower in the double copy (930.5 µg/g) than single copy (1618.9 µg/g) and azygous (1335.3 µg/g). The cost of expressing two copies of the construct may have impacted the expression or activity of other carotenoid genes. Therefore, having two copies has reduced the total carotenoid content. The complete removal of beta-carotene is then due to the push into other carotenoids, until beta-carotene is depleted. While beta-carotene is generally considered as vital for photosynthesis, it has been previously shown that other carotenoids can also fill this role (Mortimer, 2010).

4.3.4 Effect of the ketocarotenoid construct of carotenoid content in fruit.

The colour of the fruit at the mature green stage gives a clear indication that the carotenoid profile is altered. Rather than unripe fruit being green, they are a beige/brown colour. This is due to the presence of ketocarotenoids. Mature green fruit should have seen *Crt*W and *lcy* expression, with the expression of *Crt*R-*b2* just starting to initiate. Considering the genetic

profile, it is expected that beta-carotene will be accumulating alongside synthesis of the non-hydroxylated ketocarotenoids canthaxanthin and echinenone. However, considering the prevalence of hydroxy carotenoids present in the leaf, the presence of other ketocarotenoids is also expected. Mature green fruit still processes chlorophylls. There is no change in the level of chlorophyll B across the plants. However, the trend in chlorophyll A and pheophytin varies. Most of the ketocarotenoid plants have similar or increased chlorophyll A, with decreased pheophytin. This is similar to that already discussed in leaf material. Despite the programmed expression of *lcy* throughout fruit development the level of beta-carotene is lower in ketocarotenoid plants compared to the azygous control. The total carotenoid content has been increased, suggesting flux through the pathway has been elevated. One plant (D24) possess carotenoid content in the leaf that is predominant in ketocarotenoids, with a notable absence in violaxanthin and neoxanthin, and therefore a comparable total carotenoid content to the other plants in the line. This plant (D24) also has fruit which is absent for neoxanthin and violaxanthin. Despite this absence there doesn't appear to have been a push towards other carotenoids, the total carotenoid content is similar to the other ketocarotenoid plants. D24 does accumulate phoenicoxanthin and astaxanthin to reasonable high levels compared to other plants. This may suggest that in D24 the action of *Crt*W is stronger than the endogenous hydroxylase *Crt*R-*b2*, and therefore rather than forming endogenous xanthophylls, the ketocarotenoids are formed instead. Adonixanthin epoxide, canthaxanthin, phoenicoxanthin, 3'OH echinenone and astaxanthin are seen in the mature green fruit and are all seen in the largest amounts in the double copy plants. As previously discussed, the addition of the cyclase *lcy* will increase the available pool of beta-carotene. This could then be converted into ketocarotenoids. The expression of two copies of *lcy* seems to be more optimal, and therefore the levels of ketocarotenoids is higher in double copy plants. However, in the leaf adonixanthin epoxide and astaxanthin are increased in single copy plants compared to double copy plants. No expression of *lcy*, as seen in the leaf negates the action of two copies of the construct, which may explain the discrepancies between the amounts seen in single compared to double copies. While the identification of the compounds denoted as esters has not been confirmed, they are most likely to be esterified carotenoids. They elute after the known carotenoids, and therefore must be reasonably non-polar. They share the same bell shaped curve as the ketocarotenoids, however the ketocarotenoids are more polar, and therefore would not elute from the column as late as the esters do. Combining the retention time evidence with the shape

of the spectra and using the work in chapter III and V as a guide, the compounds have been classified as esters. The presence of esters in mature green fruit was unexpected, as the accumulation of ketocarotenoids doesn't occur till the ripe stage, and esters are associate with increased carotenoid content. Furthermore, the ester bond occurs through the hydroxyl group, and with no expression of an additional hydroxylase the carotenoids suitable for esterification should have been minimal. However, there is much stronger hydroxylation than expected, the endogenous hydroxylase is providing enough hydroxylation for the formation of esters.

It is in the ripe fruit where the highest amounts of ketocarotenoids were seen. This is as expected, due to the fruit specific promoters along with the structural and metabolomic changes that occur during ripening. The ultimate goal for this work was astaxanthin production, and this has been achieved. The double copy plant D55 contains the highest concentration (225.1 μg/g) of free astaxanthin seen in this work, greater than the levels achieved in chapter III. While the other plants were not as high (48.3 μg/g to 159.5 μg/g), astaxanthin is still one of the dominant carotenoids. Phoenicoxanthin also accumulates in the ripe fruit with no difference between single and double copy plants. The accumulation of phoenicoxanthin suggests that, once again, it is the hydroxylase which is inefficient. The ketocarotenoid pathway therefore halts at phoenicoxanthin and does not proceed through to astaxanthin. However, canthaxanthin is seen in much smaller quantities than astaxanthin or phoenicoxanthin. The hydroxylase *Crt*R-*b2* must therefore be functional. Levels of echinenone and 3'OH echinenone are also increased, following the general trend of increased ketocarotenoid production. One ketocarotenoid that is decreased is adonixanthin epoxide, which is often not detected at all. Adonixanthin epoxide is structurally similar to violaxanthin and antheraxanthin, therefore it may be expected that the synthesis and storage of adonixanthin epoxide is similar to the other xanthophylls. Neither violaxanthin nor antheraxanthin are detected in ripe fruit.

The total ester content has increased from mature green to ripe, however the free carotenoid to esterified carotenoid ratio has decreased, with more of the carotenoids being esterified in mature green fruit. The reason for the increase in the amount of esters may be due to the change in the plastid structure. Esters are partially stored in the plastoglobuli, and therefore, as the chloroplasts develop into chromoplasts the number of plastoglobuli increase. More plastoglobuli, means a high storage capacity, and therefore more esters can be formed. The

decrease in the ratio of the carotenoids esterified may result from the large increase in the total ketocarotenoids formed. The esterification enzyme or enzyme accessories may be a bottleneck in the esterification process. While there is the storage capacity, the sudden increase in hydroxylated ketocarotenoids produced by *Crt*R-*b2* expression may not have been processed into esters. This would therefore change the free to esterified carotenoid ratio. There is a reduction in alpha-tocopherol, this is probably due to the precursors that are shared between tocopherols and carotenoids being diverted into the carotenoid pathway. With all the additional genes now having been expressed in the ketocarotenoid construct, the level of early carotenoids such as beta-carotene are expected to be decreased, as it is synthesised into further carotenoids. Beta-carotene, gamma-carotene and phytofluene show this expected decrease. Interestingly, the level of lycopene is still high, unaltered from the control. Phytoene is also unaltered. This shows that despite the expression of *lcy* through maturation, the lycopene levels have not been changed. Considering that the total carotenoid content is increased, but the lycopene content has not changed there must be an increase earlier in the pathway than lycopene to maintain the levels of lycopene seen. This also suggests that the *lcy* gene is not functioning as well as hoped, either the promoter or the coding region is not functioning to convert all available lycopene to beta-carotene. The large pool of lycopene gives this ketocarotenoid line room for development. The availability of lycopene would allow for the production of more ketocarotenoids with future work.

4.3.5 Role of fruit specific promoters

The use of fruit specific promoters to control and direct the synthesis of ketocarotenoids in tomato is novel, with the previous approaches using constitutive promoters (Zhu, *et al.*, 2009). Whilst some previous attempts have targeted other tissues, such as seeds, the fruit has not been targeted before. One of the concerns over the use of fruit specific promoters is the longevity of expression. The fruit is only produced briefly during the life span of a tomato plant, and therefore the expression is also brief. This could stop large amounts of the desired product from being able to be synthesised. There are also many other metabolic changes which occur during the ripening process, so the alteration of the metabolic process during this time point could potentially have unintended consequences.

Comparing the results of the fruit specific PPC2 promoter and the constitutive pPAtUbq10 promoter allows an insight into how the fruit specific promoters fare. Both of these promoters

were used to regulate the *lcy* gene, therefore it is beta-carotene which should reveal most information. Comparisons have been made between the single plant with pPAtUbq10 and a single copy PPC2 plant (S11) which showed no observable perturbation to development. The ketocarotenoid construct with PAtUbq10 promoter has a very low transformation efficiency (0.3%). The possible reasons for only one pPAtUbq10 plant surviving tissue culture, are due to the constitutive expression of the lycopene beta cyclase causing a detrimental accumulation of beta-carotene early in plant development or the additional cost of expressing an extra gene during tissue culture having a negative effect to the plants.

The amount of beta-carotene produced by the pPAtUbq10 is 17 times higher than in PPC2. This immediately indicates that expression of *lcy* from pPAtUbq10 is much greater than from PPC2. The lack of lutein in U5 also supports this. Despite this large increase in beta-carotene, the lycopene, phytoene and phytofluene levels are reasonably similar, this implies that pPAtUbq10-*lcy* is still a bottleneck in converting from lycopene to beta-carotene.

The increase in beta-carotene levels has then had a positive impact on the ketocarotenoids, with all showing an increase. This suggests that in the plants with PPC2, it is the reduction in beta-carotene which prevents further synthesis of ketocarotenoids. This emphasises the importance of promoter choice, for optimal metabolomic engineering.

*Crt*R-*b2* was also under the control of a fruit specific promoter. In both mature green fruit and leaf tissue, the amount of hydroxylated carotenoids was surprising. This suggests that the endogenous hydroxylase is stronger than expected. Considering this, it is hard to pick out the activity that is from the additional *Crt*R-*b2*. Ripe fruit did see an increase in the hydroxylated ketocarotenoids; however this may also be due to the general increase in carotenoids that occurs during ripening. If the expression of *Crt*R-*b2* was strong, the expectation would be for an absence of non or partially hydroxylated intermediates. Phoenicoxanthin is seen as the dominant carotenoid in several plants, therefore it would appear that the *Crt*R-*b2* is not strongly expressed or is not efficient. If *Crt*R-*b2* were placed under a constitutive promoter it is possible the levels of astaxanthin would have been increased at the cost of phoenicoxanthin, canthaxanthin, echinenone, 3 and 3'OH echinenone.

This work shows, that despite some problems with using constitutive promoters, they may often be better. The limited time for expression when using a fruit maturation or ripening specific promoter limits the amount of transcript that is able to be produced. Time is also

required for the intricate feedback loops which occur. The formation of carotenoids and ketocarotenoids can alter the plastid number and size (Enfissi, *et al.*, 2019). The response from the plastid is vital for the storage of the increased amount of carotenoids. Therefore, to have a change in plastids, a perturbation to the carotenoid content is required, and to allow for storage of carotenoids you need altered plastids. Loops such as these need time, as structural changes have to occur. With the expression of genes being limited to a specified point in development, the plant may not have the chance to make the necessary alterations. The activity of non-specific promoters doesn't have to have negative outcomes. While silencing can occur, if the use of non-endogenous genes or genes with a low homology to the endogenous genes are used, silencing may be avoided. Similarly, if multiple different constitutive promoters are used, rather than multiple 35S promoters, silencing may be prevented. Expression of genes and production of metabolites in tissue other than the fruit can also be positive, as shown in the *Crt*W colour screen seen here. However, it goes beyond a colour screen, with the desired product being synthesised throughout the plant there is more biomass available for commercial use.

The fruit specific promoters available for research are generally poorly characterised. While there are some review papers, such as the one by Fernandez, *et al.* (2009) on the use of different promoters, it is the constitutive promoters which have been used most extensively in research, and therefore we have a better understanding of these. More tissue specific promoters need to be fully characterised to fully exploit the potential of such temporal and spatial expression.

Chapter V:

The pale yellow petal acyltransferase (Solyc01g098110) is involved in the esterification of non-endogenous ketocarotenoids

5.1 Introduction

The presence of ketocarotenoids in tomato fruit can stimulate the production of esters, with the gene responsible for this being unknown. Although ketocarotenoids are non-endogenous pigments to tomato fruit they are esterified. Esterification of carotenoids increases their stability and prevents degradation (Berry, *et al.*, 2019). Esterification is also an important mechanism for sequestration and storage (Kishimoto, *et al.*, 2020; Minguez-Mosquera & Hornero-Mendez, 1994). Esterification of carotenoids has been reported to increase their stability, prevent their degradation, while also aiding their sequestration. The pale yellow petal (*pyp*) gene has previously been identified as an important acyltransferase in tomato flower, with loss of function mutants displaying a paler petal phenotype and a lack of carotenoid esters (Ariizumi, *et al.*, 2014).

In order to identify the gene controlling the esterification of ketocarotenoids in tomato fruit, the mutated *pyp* allele was crossed into a tomato line containing ketocarotenoid esters (ZWRI) (Nogueira, *et al.*, 2017). In this way we can ascertain if the acyltransferase encoded by *pyp* is either, in part, or completely responsible for esterification of the ketocarotenoids engineered in tomato fruit.

5.2 Results

5.2.1 Generation and genotyping the lines generated from genetic crossing of *pyp* mutants and ZWRI

The maternal background *Solanum lycopersicum* variety used for this work was the ZWRI line (section 3.1.2). In order to produce ketocarotenoids in this line, it was previously transformed with the carotenoid hydroxylase (*Crt*Z) and oxygenase (*Crt*W) genes from the bacteria *Brevundimonas,* then crossed with the high beta-carotene introgression line. The resulting line from this cross is referred to by the acronym ZWRI and is a moneymaker and UC204B cross. The paternal line was that of an ethyl methansulphonate (EMS) mutagenised microtom cultivar with the strain ID TOMJPE5508-1. The mutation was found to be in the acyltransferase gene Solyc01g098110.2. This generates a pale yellow petal phenotype, and therefore this line is denoted at *pyp*.

The two parental lines were crossed to generate a heterozygous F_1 generation. However, as the *pyp* mutation is recessive no phenotype was observed. Self-fertilisation of the F_1 generation produced the F_2 generation, which segregated on the zygosities of all components. A schematic to show the production of the resulting line is shown in Figure 5-1. The nomenclature used throughout to describe the F_2 line is $P^{MT/WT}$ZW(Ø)RI(Ø). MT refers to the mutant, non-functional version of *pyp*, whereas WT is the wildtype, functional version. The absence of the ZW and RI components is denoted by a Ø following the abbreviations. When present ZW is always hemizygous and RI is always homozygous.

In order to determine the genotype of each plant at an early stage of development, a variety of techniques were used. The process of genotyping for the ZW and RI components is the same as that used in section 3.2.1. At the DNA level the *pyp* mutation is a single base change, High Resolution Melt (HRM) analysis was employed to both detect the presence/absence of the mutation and also the zygosity (Figure 5-2). Heterozygous plants were discarded, and metabolic analysis was only performed on homozygous (wildtype or mutation) plants. For analysis 200 F_2 plants were sown. After screening for ZW being hemizygous or azygous, and screening for RI being homozygous or azygous for the beta-carotene trait ~60 plants went forwards into HRM analysis. Of these, three P^{WT}ZWRI, five P^{MT}ZWRI and one P^{MT}ZWØRIØ plants were identified. In order to increase biological replication, at least for environmental

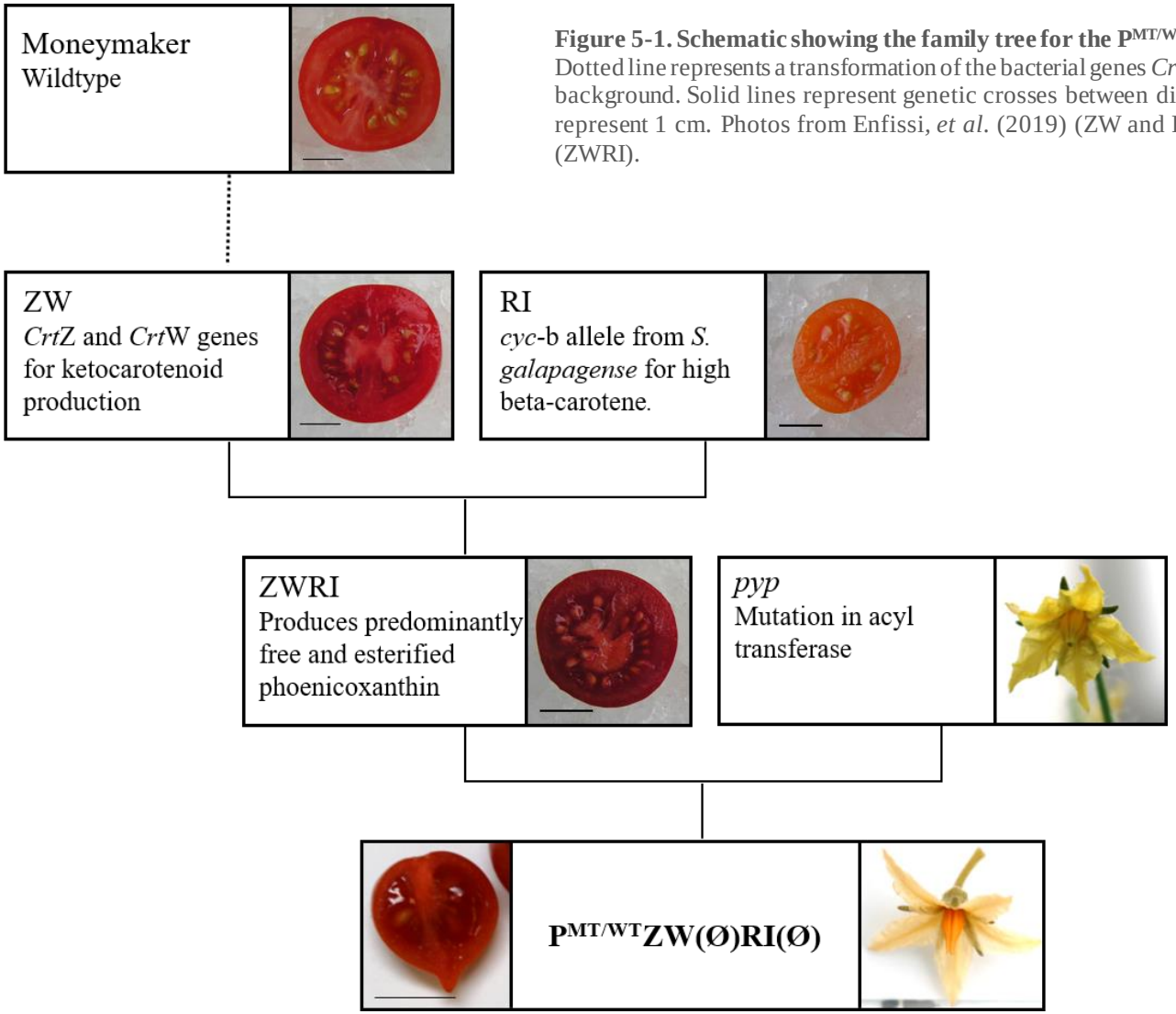

Figure 5-1. Schematic showing the family tree for the P$^{MT/WT}$ZW(Ø)RI(Ø) line
Dotted line represents a transformation of the bacterial genes *Crt*Z and *Crt*W into a moneymaker background. Solid lines represent genetic crosses between different tomato lines. Scale bars represent 1 cm. Photos from Enfissi, *et al.* (2019) (ZW and RI) and Nogueira, *et al.* (2017) (ZWRI).

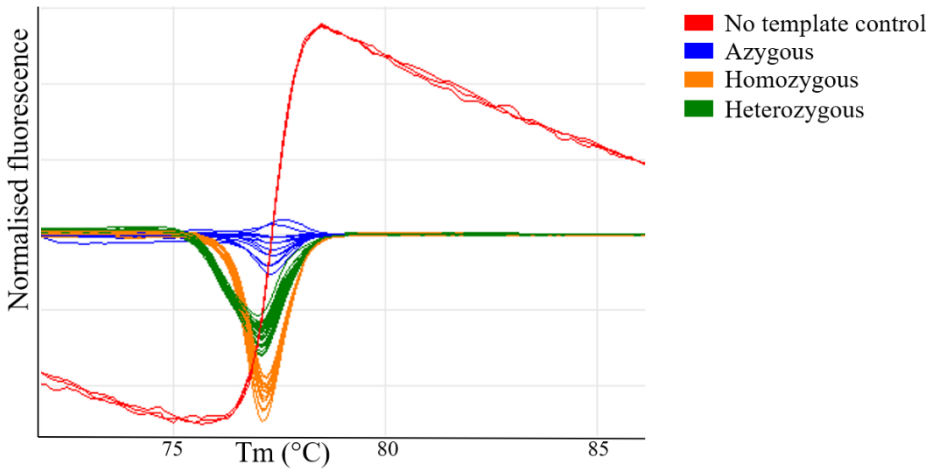

Figure 5-2. Typical high resolution melt curve
A 129 base pair fragment containing the mutated region was amplified by PCR then melted and the change in fluorescence monitored. Homozygous events are shown in orange, azygous in blue and heterozygous in green. The red line is created by the no-template control. The *x* axis represents the melting temperature in °C, the *y* axis is the normalised fluorescence.

conditions, two cuttings were made from the single P^{MT}ZWØRIØ plant. No triple azygous (P^{WT}ZWØRIØ) plants were identified, instead F_1 plants from a genetic cross of microtom and ZWØRIØ plants were used.

5.2.2 Phenotypic characteristics of lines with the *pyp* mutation

As suggested by the name of the mutation, *pyp* plants displayed a paler petal phenotype. This was exaggerated when the mutation was present in ketocarotenoid producing flowers. Petals from plants with ZWRI which were normally orange, became observably paler. The fused stamen however maintained the brighter orange colouration.

The effect of the mutation in the fruit was much more subtle. P^{MT}ZWRI was paler than its equivalent P^{WT}ZWRI, however, as expected there were no observable changes when comparing P^{MT}ZWØRIØ to P^{WT}ZWØRIØ. In order to allow for a more accurate determination of colour difference, extracts enriched in carotenoids were compared. This revealed a considerably more distinct difference between P^{MT}ZWRI and P^{WT}ZWRI. Figure 5-3 shows the phenotypes present in $P^{MT/WT}$ZW(Ø)RI(Ø). The size and shape of fruits and whole plants was wide ranging, both within the population and within each genotype. Some plants appeared more closely related to the microtom variety, whereas others were more indeterminant and moneymaker-like. However, their overall phenotype had no bearing on the colour of fruit or flower.

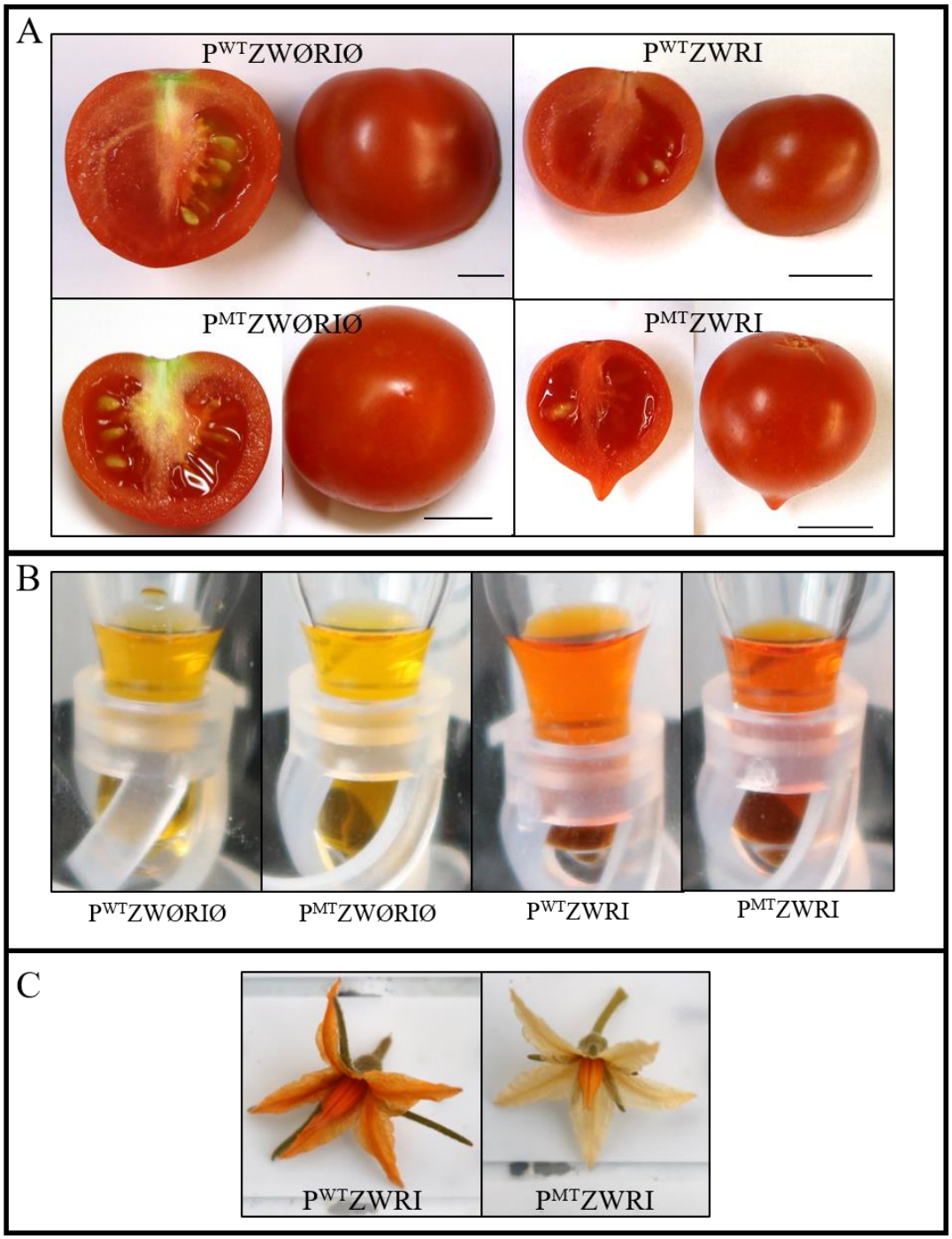

Figure 5-3. Phenotypes of different genotypes of $P^{MT/WT}$ZW(Ø)RI(Ø) plants
A) Changes in fruit appearance and morphology. ZWRI provides considerable pigmentation with and without the *pyp* mutation. Size variation is present throughout all genotypes, scale bar represents 1 cm. B) Carotenoid extract of fruit. There are minimal changes within P^{WT}ZWØRIØ and P^{MT}ZWØRIØ. The *pyp* mutation causes subtle differences between P^{MT}ZWRI and P^{WT}ZWRI. C) Flowers from ketocarotenoid producing ZWRI lines. The effect of the mutation is stark in the petals but much more subtle in the stamen.

5.2.3 Analysis of free and esterified carotenoids in fruit of $P^{MT/WT}ZW(Ø)RI(Ø)$

To analyse the changes in carotenoids beyond those visible from the phenotype, extracts from fruit and flower tissue were quantified by liquid chromatography as described in sections 2.6.4 and 2.6.5 Carotenoids were identified by the retention time based on the comparison with authentic standards and their characteristic spectra. Example chromatograms are shown in Figure 5-4. The amount of each carotenoid was estimated by reference to the response from authentic standards. Fruit material was obtained from eight fruits per plant. Fruit pericarp and skin were analysed by UPLC using a reverse phase C18 column.

The impact of *pyp* in fruit from plants with an azygous (ZWØRIØ) background was minimal. Phytofluene (×0.7) and zeta-carotene (×0.6) showed a decrease when then *pyp* mutation was present. As expected, the levels of other carotenoids remained consistent.

Comparison of free carotenoids in P^{MT}ZWRI and P^{WT}ZWRI fruit material revealed four significant differences. Only ketocarotenoids which contained a hydroxyl group, and therefore had the potential to be esterified, were significantly increased in P^{MT}ZWRI. Free astaxanthin (×3.5) and phoenicoxanthin (×2.1) were increased in plants with the *pyp* mutation. 3'OH echinenone (×0.7) was the only significant reduction, but canthaxanthin also showed a large reduction but accompanied biological variation. Table 5-1 shows the quantification of free and mono-esterified carotenoids in fruit tissue. Analysis of esters present in the fruit showed a substantial change. Only plants with ZWRI have esters due to the presence of ketocarotenoids in the fruit. In P^{MT}ZWRI plants, where the *pyp* gene is mutated, the esters were completely absent. Correspondingly the amount of free carotenoids containing hydroxyl groups increased, however the increase did not account for the absence of the esterified carotenoids, so the overall carotenoid content was reduced.

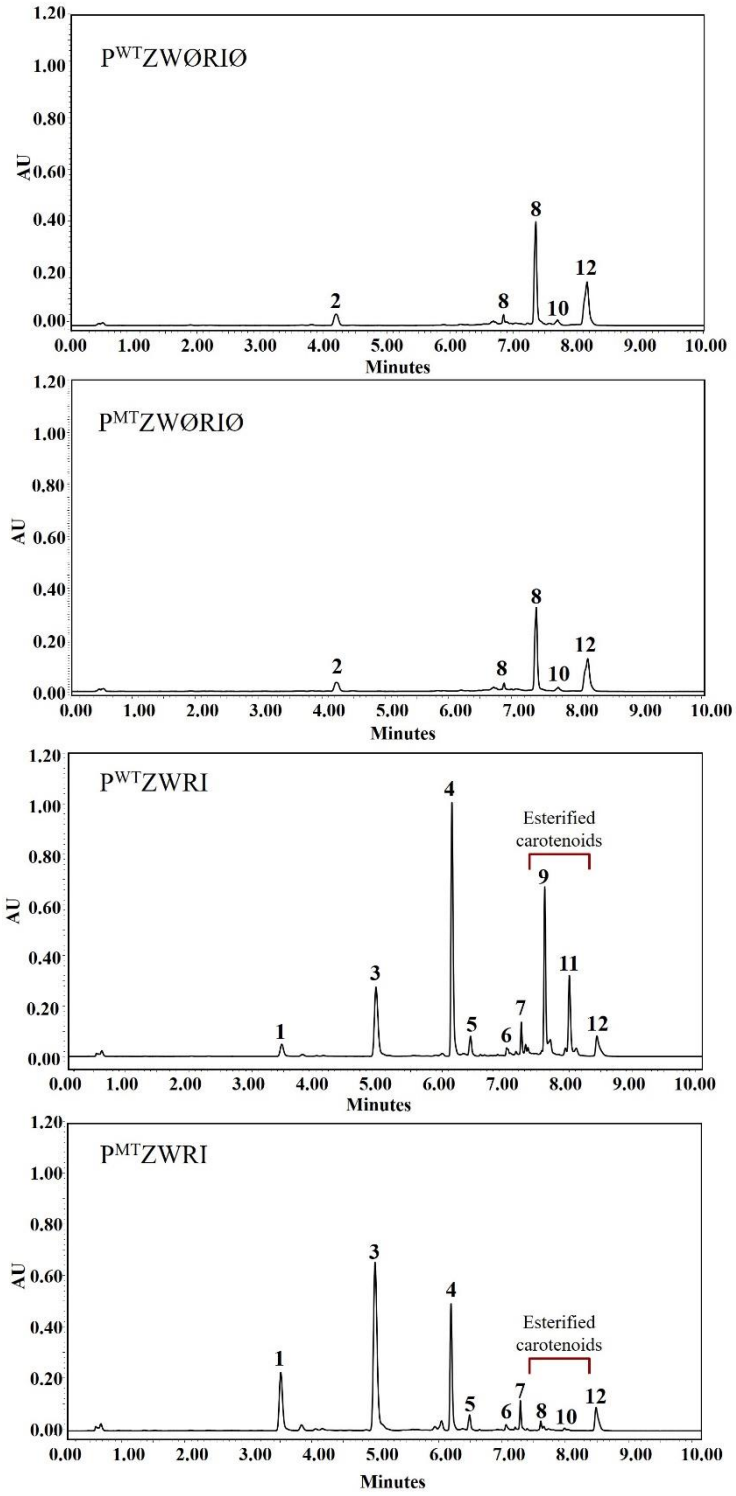

Figure 5-4. Example chromatograms from $P^{MT/WT}$ZW(Ø)RI(Ø) fruit
1) Astaxanthin, 2) Lutein, 3) Phoenicoxanthin, 4) Canthaxanthin, 5) 3'OH echinenone, 6) 3OH echinenone, 7) Echinenone, 8) Lycopene, 9) Ester 1, 10) Gamma-carotene, 11) Ester 2, 12) Beta-carotene.

Table 5-1. Carotenoid content of fruit from $P^{MT/WT}ZW(Ø)RI(Ø)$ lines
Amounts in µg/g dry weight with ± standard deviation. All values are calculated from at least three biological replicates, of eight pooled fruit per plant. Each biological replicate is an average of three technical replicates. Amounts calculated using a standard curve of each individual carotenoid or similar carotenoid. Gamma-carotene and lycopene were not quantified (NQ) in fruit with esters due to co-elution. Significant values ($p<0.05$) from a Student's T test are in bold, * $0.05>p\geq0.01$, ** $0.01>p\geq0.001$, *** $0.001>p$

Carotenoid	$P^{WT}ZWØRIØ$	$P^{MT}ZWØRIØ$	Sig.	$P^{WT}ZWRI$	$P^{MT}ZWRI$	Sig.
Astaxanthin	0.00 ±0.00	0.00 ±0.00		59.09 ±46.87	206.57 ±68.61	**
Lutein	21.48 ±6.44	23.84 ±1.67		0.00 ±0.00	0.00 ±0.00	
Phoenicoxanthin	0.00 ±0.00	0.00 ±0.00		750.12 ±387.10	1590.76 ±495.91	*
Canthaxanthin	0.00 ±0.00	0.00 ±0.00		575.56 ±112.98	439.65 ±208.04	
3'OH echinenone	0.00 ±0.00	0.00 ±0.00		27.29 ±2.90	19.13 ±3.48	**
Lycopene	15.68 ±3.06	12.27 ±1.41		0.00 ±0.00	0.00 ±0.00	
3OH echinenone	0.00 ±0.00	0.00 ±0.00		6.46 ±4.65	11.29 ±6.52	
Echinenone	0.00 ±0.00	0.00 ±0.00		24.48 ±11.62	50.24 ±38.74	
Lycopene	301.81 ±31.28	322.73 ±25.31		NQ	107.45 ±120.49	
Phytoene	98.00 ±20.48	58.77 ±17.54		14.24 ±12.66	19.17 ±12.88	
Gamma-carotene	13.34 ±4.76	10.97 ±3.55		NQ	27.69 ±20.65	
Zeta-carotene	12.07 ±2.03	7.93 ±1.48	*	0.00 ±0.00	0.00 ±0.00	
Pheophytin A	635.69 ±479.58	306.66 ±71.40		254.46 ±114.80	247.68 ±185.49	
Beta-carotene	101.78 ±45.56	110.99 ±14.54		68.85 ±52.93	220.94 ±243.87	
Phytofluene	350.55 ±34.15	256.69 ±9.17	**	0.00 ±0.00	0.00 ±0.00	
Total ester	0.00 ±0.00	0.00 ±0.00		1554.36 ±402.80	0.00 ±0.00	***

5.2.4 Analysis of free and esterified carotenoids in flowers of $P^{MT/WT}$ZW(Ø)RI(Ø)

Carotenoids were also measured in the flowers of all genotypes. Due to the visible difference between the petals and stamen, these two parts were isolated from each other and analysed separately. Both tissues displayed the same overall trend, however in general the stamen has a considerably lower carotenoid content. Flower material was analysed on two independent systems UPLC and HPLC, with a C18 and C30 column respectively. This allowed for quantification of both ketocarotenoids and carotenoid esters.

The effect of the *pyp* mutation in the petal was stark. Without a functioning PYP enzyme there were no esterified carotenoids in the flower, free carotenoids were increased, but overall carotenoid content was decreased. The non-esterified (free) versions of violaxanthin, astaxanthin, phoenicoxanthin and adonixanthin epoxide were all significantly increased, suggesting these were the carotenoids esterified in the P^{WT} plants. Quantification of the carotenoids is provided in Table 5-2, Table 5-3, Table 5-4 and Table 5-5. Comparison of P^{WT}ZWØRIØ and P^{MT}ZWØRIØ revealed that, as previously published, there were changes in free violaxanthin, free neoxanthin and xanthophyll esters. Overall the petals and stamen showed that with an absence of esters there was an increase in free carotenoids. However, this increase did not counter the large decrease from the esters, and therefore total carotenoid content was reduced, this is summarised in Table 5-6.

Flowers from plants with ZWRI backgrounds also displayed the same pattern, but with the addition of ketocarotenoid esters. In the petal, all free ketocarotenoids were altered with the exception of echinenone. Those which possessed a hydroxyl group, and are capable of esterification (adonixanthin epoxide, astaxanthin and phoenicoxanthin) were increased. Those with only a keto group (canthaxanthin) were decreased. This is in line with the overall non-significant reduction in total carotenoid content observed in the flowers as these carotenoids cannot be esterified. 3'OH echinenone has both a keto group and a hydroxyl group, however despite the presence of the hydroxyl group, and therefore the ability to be esterified, it was also reduced. As with the violaxanthin and neoxanthin esters, the ketocarotenoid esters were also completely absent in plants with the *pyp* mutation. The petals also displayed a significant decrease in the amount of chlorophyll B.

Table 5-2. Free carotenoid content of petals from the $P^{MT/WT}ZW(Ø)RI(Ø)$ line

Amounts in µg/g dry weight with ± standard deviation. All values are calculated from three biological replicates, of 15 flowers per plant. Each biological replicate is an average of two technical replicates. Free carotenoids are obtained from UPLC, esters are obtained from HPLC. Significant values ($p<0.05$) from a Student's T test; * $0.05>p\geq0.01$, ** $0.01>p\geq0.001$, *** $0.001>p$

Carotenoid	$P^{WT}ZWØRIØ$	$P^{MT}ZWØRIØ$	Sig.	$P^{WT}ZWRI$	$P^{MT}ZWRI$	Sig.
Violaxanthin	421.13 ±70.37	1551.37 ±209.45	*	99.68 ±48.96	665.92 ±179.32	**
Neoxanthin	84.71 ±17.74	268.14 ±64.69	**	11.86 ±6.69	50.90 ±48.60	
Lutein	53.36 ±28.31	46.77 ±5.36		0.00 ±0.00	0.00 ±0.00	
Chlorophyll B	284.58 ±119.63	101.46 ±35.66		156.98 ±25.82	85.34 ±29.25	*
Beta-carotene	31.22 ±10.75	18.25 ±3.05		0.00 ±0.00	0.00 ±0.00	
Adonixanthin epoxide	0.00 ±0.00	0.00 ±0.00		213.48 ±47.20	1446.46 ±245.05	**
Astaxanthin	0.00 ±0.00	0.00 ±0.00		77.59 ±50.45	403.79 ±51.07	**
Unknown D	0.00 ±0.00	0.00 ±0.00		12.48 3.92	43.94 ±9.53	**
Phoenicoxanthin	0.00 ±0.00	0.00 ±0.00		55.10 ±8.33	218.74 ±28.05	**
Canthaxanthin	0.00 ±0.00	0.00 ±0.00		31.88 ±5.07	15.46 ±2.46	**
3'OH echinenone	0.00 ±0.00	0.00 ±0.00		3.37 ±0.67	1.47 ±0.26	**
Echinenone	0.00 ±0.00	0.00 ±0.00		10.82 ±6.40	1.42 ±0.41	

Table 5-3. Esterified carotenoid content of petals from the $P^{MT/WT}$ZW(Ø)RI(Ø) line

Amounts in µg/g dry weight with ± standard deviation. All values are calculated from three biological replicates, of 15 flowers per plant. Each biological replicate is an average of two technical replicates. Free carotenoids are obtained from UPLC, esters are obtained from HPLC. Significant values ($p<0.05$) from a Student's T test; * $0.05>p\geq0.01$, ** $0.01>p\geq0.001$, *** $0.001>p$

Carotenoid	P^{WT}ZWØRIØ	P^{MT}ZWØRIØ	Sig.	P^{WT}ZWRI	P^{MT}ZWRI	Sig.
Violaxanthin mono-ester	3753.80 ±413.11	0.00 ±0.00	***	1181.87 ±1668.06	0.00 ±0.00	
Neoxanthin mono-ester	1312.60 ±202.49	0.00 ±0.00	***	296.02 ±512.72	0.00 ±0.00	
Ketocarotenoid mono-ester	0.00 ±0.00	0.00 ±0.00		475.81 ±130.90	0.00 ±0.00	**
Violaxanthin di-ester	9886.49 ±276.18	0.00 ±0.00	***	1803.49 ±1547.25	0.00 ±0.00	
Neoxanthin di-ester	485.69 ±63.79	0.00 ±0.00	***	0.00 ±0.00	0.00 ±0.00	
Ketocarotenoid di-esters	0.00 ±0.00	0.00 ±0.00		2257.28 ±480.37	0.00 ±0.00	**
Other di-esters	56.03 ±12.77	0.00 ±0.00	**	211.59 ±155.17	0.00 ±0.00	

Table 5-4. Free carotenoid content of stamen from the $P^{MT/WT}$ZW(Ø)RI(Ø) line

Amounts in µg/g dry weight with ± standard deviation. All values are calculated from three biological replicates, of 15 flowers per plant. Each biological replicate is an average of two technical replicates. Free carotenoids are obtained from UPLC, esters are obtained from HPLC. Significant values from a Student's T test; * 0.05>p≥0.01, ** 0.01>p≥0.001, *** 0.001>p

Carotenoid	P^{WT}ZWØRIØ	P^{MT}ZWØRIØ	Sig.	P^{WT}ZWRI	P^{MT}ZWRI	Sig.
Violaxanthin	193.40 ±9.93	568.51 ±54.28	***	15.86 ±7.60	27.97 ±12.51	
Neoxanthin	40.05 ±4.65	96.07 ±13.38	**	2.21 ±1.59	2.93 ±1.02	
Lutein	22.27 ±5.68	23.01 ±5.96		0.00 ±0.00	0.00 ±0.00	
Chlorophyll B	126.68 ±43.00	60.29 ±25.93		54.46 ±23.57	30.52 ±10.34	
Beta-carotene	23.37 ±6.31	13.46 ±1.71		0.00 ±0.00	0.00 ±0.00	
Adonixanthin epoxide	0.00 ±0.00	0.00 ±0.00		142.33 ±28.70	1016.43 ±411.91	*
Astaxanthin	0.00 ±0.00	0.00 ±0.00		44.87 ±20.80	214.13 ±66.52	*
Unknown D	0.00 ±0.00	0.00 ±0.00		7.25 ±1.17	14.20 ±5.25	
Phoenicoxanthin	0.00 ±0.00	0.00 ±0.00		44.98 ±16.63	135.28 ±54.95	
Canthaxanthin	0.00 ±0.00	0.00 ±0.00		16.47 ±2.83	11.10 ±5.26	
3'OH echinenone	0.00 ±0.00	0.00 ±0.00		1.23 ±0.08	0.78 ±0.38	
Echinenone	0.00 ±0.00	0.00 ±0.00		1.61 ±0.34	1.15 ±0.66	

Table 5-5. Esterified carotenoid content of stamen from the $P^{MT/WT}$ZW(Ø)RI(Ø) line

Amounts in µg/g dry weight with ± standard deviation. All values are calculated from three biological replicates, of 15 flowers per plant. Each biological replicate is an average of two technical replicates. Free carotenoids are obtained from UPLC, esters are obtained from HPLC. Significant values from a Student's T test; * 0.05>p≥0.01, ** 0.01>p≥0.001, *** 0.001>p

Carotenoid	P^{WT}ZWØRIØ		P^{MT}ZWØRIØ		Sig.	P^{WT}ZWRI		P^{MT}ZWRI		Sig.
Violaxanthin mono-ester	499.69	±75.40	0.00	±0.00	***	59.67	±26.57	0.00	±0.00	*
Neoxanthin mono-ester	215.11	±50.35	0.00	±0.00	**	0.00	±0.00	0.00	±0.00	
Ketocarotenoid mono-ester	0.00	±0.00	0.00	±0.00		172.66	±22.90	0.00	±0.00	***
Violaxanthin di-ester	871.42	±180.68	0.00	±0.00	**	0.00	±0.00	0.00	±0.00	
Neoxanthin di-ester	215.04	±67.06	0.00	±0.00	**	0.00	±0.00	0.00	±0.00	
Ketocarotenoid di-esters	0.00	±0.00	0.00	±0.00		667.12	±195.45	0.00	±0.00	***
Other di-esters	11.61	±2.39	0.00	±0.00	**	24.85	±8.73	0.00	±0.00	

Table 5-6. Summary tables of carotenoid content in $P^{MT/WT}ZW(Ø)RI(Ø)$
Amounts in mg/g dry weight with ± standard deviation. Significant values from a Student's T test; * 0.05>p≥0.01, ** 0.01>p≥0.001, *** 0.001>p.

Fruit						
Carotenoids	**$P^{WT}ZWØRIØ$**	**$P^{MT}ZWØRIØ$**	**Sig.**	**$P^{WT}ZWRI$**	**$P^{MT}ZWRI$**	**Sig.**
Total free	1.55 ±0.55	1.11 ±0.03		1.78 ±0.56	2.94 ±0.81	
Total esterified	0.00 ±0.00	0.00 ±0.00		1.55 ±0.27	0.00 ±0.00	***
Total	1.55 ±0.55	1.11 ±0.03		3.33 ±0.82	2.94 ±0.81	
Stamen						
Carotenoids	**$P^{WT}ZWØRIØ$**	**$P^{MT}ZWØRIØ$**	**Sig.**	**$P^{WT}ZWRI$**	**$P^{MT}ZWRI$**	**Sig.**
Total free	0.41 ±0.07	0.76 ±0.09	**	0.33 ±0.05	1.45 ±0.55	*
Total esterified	1.81 ±0.36	0.00 ±0.00	**	0.92 ±0.25	0.00 ±0.00	**
Total	2.22 ±0.31	0.76 ±0.09	**	1.26 ±0.21	1.45 ±0.55	
Petal						
Carotenoids	**$P^{WT}ZWØRIØ$**	**$P^{MT}ZWØRIØ$**	**Sig.**	**$P^{WT}ZWRI$**	**$P^{MT}ZWRI$**	**Sig.**
Total free	0.88 ±0.25	1.99 ±0.27	**	0.67 ±0.13	2.93 ±0.57	**
Total esterified	15.49 ±0.81	0.00 ±0.00	***	6.23 ±3.11	0.00 ±0.00	*
Total	16.37 ±1.05	1.99 ±0.27	***	6.90 ±3.06	2.93 ±0.57	

5.2.5 Ester identification in fruit

LC/MS analysis was used for the identification of the carotenoid esters observed in the fruit. Previously published carotenoid ester analysis on the ZWRI line identified the esterified carotenoids as phoenicoxanthin and adonixanthin, with C14:0 and C16:0 fatty acids conjugated to them (Nogueira, *et al.*, 2017). The esterified carotenoids detected in P^{WT}ZWRI were different to those previously reported. The inclusion of the microtom background led to the production of astaxanthin esters, with C16:0 and C18:0 fatty acids.

5.2.6 Changes in the volatile composition due to the presence of free or esterified ketocarotenoids

Analysis of the volatiles produced from fruit allows for an insight into the degradation pathways of metabolites. Volatile compounds are often produced upon enzymatic catabolism or non-enzymatic degradation of biosynthetic intermediates or end products. Apo-carotenoids are derived from carotenoids and other apo-carotenoids and are often volatile. Thus, by analysing the content of carotenoid derived volatiles, a measure of enzymatic and non-enzymatic catabolism of carotenoids can be determined. In the case of $P^{MT/WT}$ZW(Ø)RI(Ø) the role of esterification can be assessed. The characteristic volatile profile of tomato fruit with ketocarotenoids has already been discussed in section 3.2.5 therefore the work here will compare the difference caused by esterification, and not focus on the azygous background compared to ZWRI.

Collectively the $P^{MT/WT}$ZW(Ø)RI(Ø) genotypes displayed the presence of 82 volatiles, these are detailed in section 7.1.9 and graphically illustrated in Figure 5-5. As expected, comparison of all groups highlighted changes due to the presence of ketocarotenoids (i.e. between ZWRI and ZWØRIØ). However, P^{MT}ZWRI, with the lack of esters, more closely resembles the volatile composition of P^{WT}ZWØRIØ than P^{WT}ZWRI.

Despite there being no change in the esterification of carotenoids between P^{MT}ZWØRIØ and P^{WT}ZWØRIØ there are changes in the volatiles, although only two are significant. There is a generally reduction in volatiles in the mutant, with most being classified as fatty acid derived or other/unknown. The significant changes are in acetic acid (p=0.021) and *trans, trans*-2,6-nonadienal (p=0.001), both of these are fatty acid derived and are decreased in the mutant, possibly suggesting a wider role for *pyp*, either directly or indirectly.

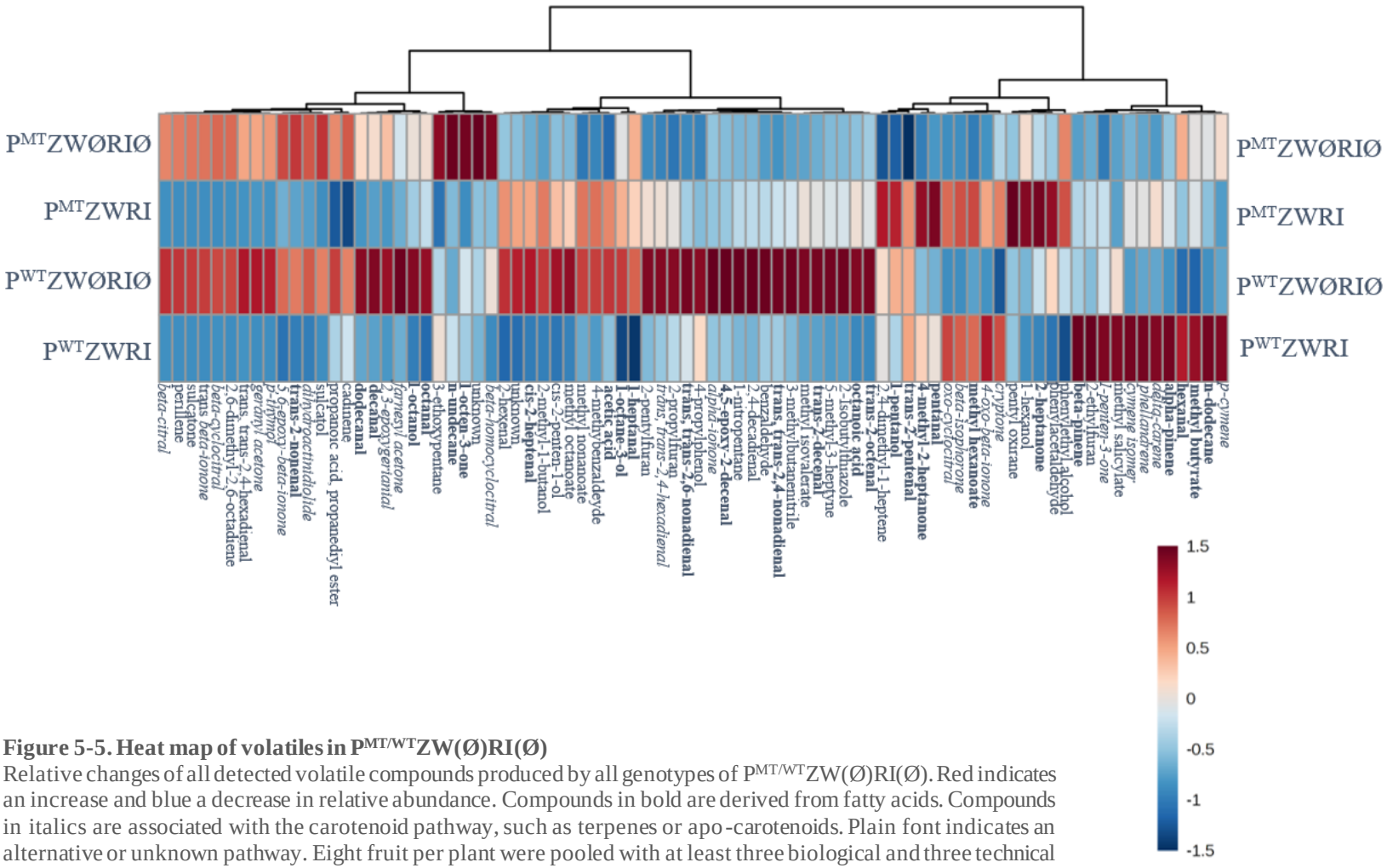

Figure 5-5. Heat map of volatiles in P$^{MT/WT}$ZW(Ø)RI(Ø)
Relative changes of all detected volatile compounds produced by all genotypes of P$^{MT/WT}$ZW(Ø)RI(Ø). Red indicates an increase and blue a decrease in relative abundance. Compounds in bold are derived from fatty acids. Compounds in italics are associated with the carotenoid pathway, such as terpenes or apo-carotenoids. Plain font indicates an alternative or unknown pathway. Eight fruit per plant were pooled with at least three biological and three technical replicates analysed per genotype. Identification of compounds was largely based on the NIST database, this along with full compound names are detailed in section 7.1.3.

There are more significant changes between P^{MT}ZWRI and P^{WT}ZWRI and these are discussed below in more detail. Generally, volatiles with an alternative or unknown role are increased in the mutant. On the other hand, compounds relating to fatty acids or carotenoids are generally decreased in the mutant, echoing the overall reduction in carotenoids.

To allow for a more focused approach to identify changes resulting from esterification, statistical analysis was only performed on P^{WT}ZWRI and P^{MT}ZWRI. This identified eight compounds with a significant change (Figure 5-6), most of which are clearly associated with carotenoid pathways. Delta-carene, phellandrene, cymene and beta-pinene were all decreased when the mutated *pyp* allele was present. These are all terpenes, and therefore derive from the same biosynthetic precursors as carotenoids. The change in fatty acid derived molecules were more individual, *n*-dodecane is decreased; whereas acetic acid is increased. However fatty acids are utilised for more than esterification of carotenoids in plants, so a general trend may not be expected.

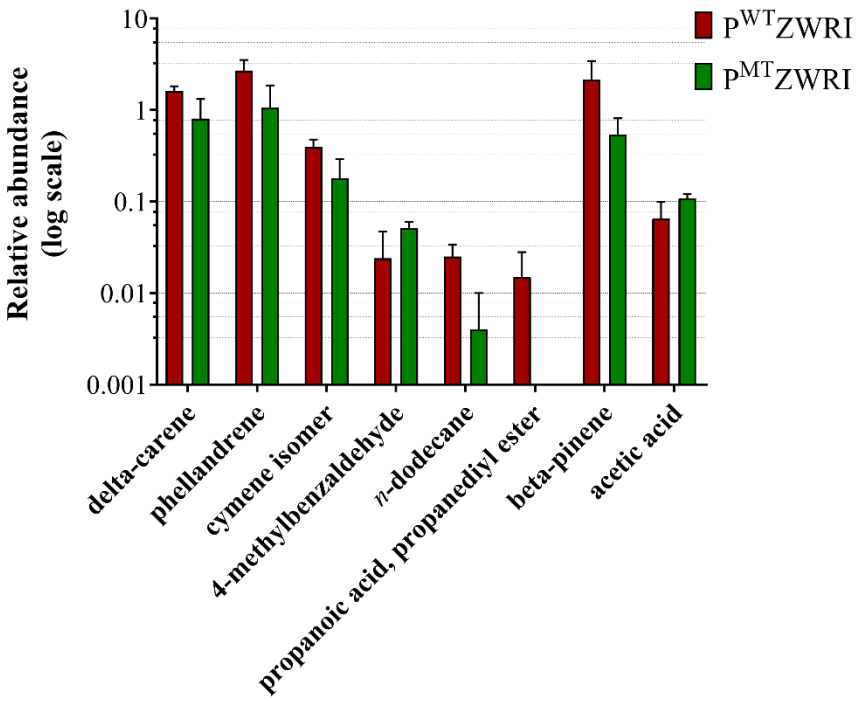

Figure 5-6. Significant volatile compounds from comparison of P^{WT}ZWRI and P^{MT}ZWRI
A Student's T test was used for identification of compounds with a significance threshold of $p \leq 0.05$. Delta-carene ($p=0.044$), phellandrene ($p=0.031$), cymene ($p=0.028$), 4-methylbenzaldehyde ($p=0.05$), *n*-dodecane ($p=0.007$), propanoic acid, propanediyl ester ($p=0.04$), beta-pinene ($p=0.029$) and acetic acid ($p=0.034$) were all significant. Eight fruit per plant were pooled with at least three biological and three technical replicates analysed per genotype. Abundance has been quantified on the basis of relative abundance to the internal standard.

5.2.7 Qualitative analysis of the lipid profile in fruit of $P^{MT/WT}ZW(Ø)RI(Ø)$

The *pyp* gene is an acyltransferase, and therefore may have a role other than that of carotenoid esterification. The lipid profile of the $P^{MT/WT}ZW(Ø)RI(Ø)$ genotypes were qualitatively analysed by TLC. This provided a comparative approach to identify changes in the lipids present, but not the quantitive changes. The TLC results shown in Figure 5-7 indicate that there may be some qualitative changes between all the genotypes, with $P^{MT}ZWRI$ and $P^{MT}ZWØRIØ$ possibly having more intense bands than their comparators as seen in DGDG. Therefore, the *pyp* gene may be involved in other lipid processes. Quantitive analysis would reveal the extent of any changes and should be included in any future work.

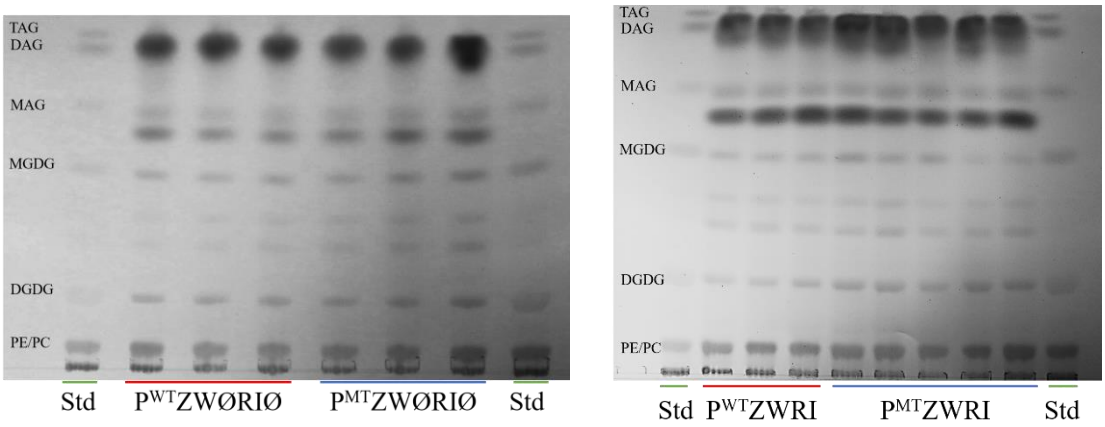

Figure 5-7. Thin layer chromatography separation of lipid classes from $P^{MT/WT}ZW(Ø)RI(Ø)$ fruit providing a qualitative analysis of lipid groups in fruit
Authentic standard mix on edges of plates, top to bottom: TAG - triacylglycerol, DAG - diacylglycerol, MAG - monoacylglycerol, MGDG - monogalactosyldiacylglycerol, DGDG - digalactosyldiacylglycerol, PE - phosphotidylethanolamine, PC - phosphatidylcholine. Lipid extract from 10 mg dried tomato fruit applied per lane, one biological replicate per lane. Darkest bands are due to carotenoids.

5.2.8 Expression of *pyp* in tomato fruit

The mutation in *pyp* is a single base change in the coding region. This is predicted to result in a truncated protein (Ariizumi, *et al.*, 2014), and may also cause a change in RNA expression. Quantitive PCR (qPCR) was performed on fruit to assess the expression of the *pyp* RNA. As shown in Figure 5-8 there were significant differences between the genotypes of $P^{MT/WT}$ZW(Ø)RI(Ø). The expression of P^{WT}ZWRI is around 10 times higher than that of P^{MT}ZWRI and P^{MT}ZWØRIØ. However, the azygous (P^{WT}ZWØRIØ) control is not significantly different from any of the other genotypes.

The level of expression of *pyp* is unaffected by the ketocarotenoid background. Interestingly there is expression of *pyp* in the ZWØRIØ backgrounds despite no ketocarotenoids for esterification.

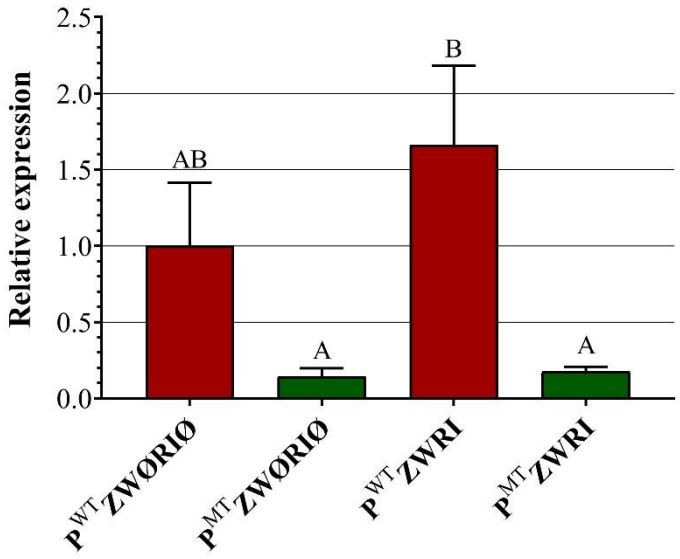

Figure 5-8. Relative expression of *pyp* in fruit
Actual concentration is adjusted to the housekeeping gene *actin*, then the relative expression is scaled, with the expression of P^{WT}ZWØRIØ set at 1. Three biological replicates per genotype. Error bars represent the standard deviation. Significant differences reported from an ANOVA.

5.3 Discussion

5.3.1 The role of *pyp* in esterification of carotenoids in different plant tissues

The *pyp* gene has been revealed to encode a vital enzyme involved in esterification of carotenoids. It has been shown to act in flower tissue (Ariizumi, *et al.*, 2014) and in fruit. It is also evident that the gene product can act on a broad range of xanthophylls, both endogenous and novel. The complete absence of esters in plants with the *pyp* mutation strongly suggests that there is no redundancy for *pyp*, and therefore it is crucial for carotenoid esterification, which is surprising considering the presence of other acyltransferases in the tomato genome.

Screening of $P^{MT/WT}$ZW(Ø)RI(Ø) still has some of the problems previously discussed. However, with ZW providing a useful colour screen and RI functioning optimally when homozygous, future generations will require significantly less labour to select for the desired trait. The *pyp* mutation is recessive, and therefore must be homozygous for an effect to be achieved. Now a homozygous line has been achieved, the mutation is stable. This prevents any problems with segregation in future generations. The recessive nature of the gene may also hint at its importance, there must be no other functioning allele in the plant before expression of a faulty version of *pyp* will occur.

Unfortunately, as the *pyp* mutation was created in a microtom cultivar there may be background effects resulting from the unusual microtom x moneymaker cross. Ideally this should have been treated as an introgression line, always crossing back into moneymaker, and therefore removing the microtom traits. The background could explain the wide range in phenotypes observed. Some plants were determinant until a side shoot formed, while others were indeterminant. Some had very small fruit, approximately 1 cm in diameter, whilst others were more in line with standard moneymaker sized fruit, approximately 3 cm. Some had very thin and fragile stems, others were normal. The height also varied between 50 cm and 2 m. Despite this large range in phenotypes the carotenoid content was reasonably consistent within genotypes.

The colouration of the petals is the most noticeable feature of the pale yellow petal plants, although it is more subtle in ZWØRIØ than in the strikingly different ZWRI. The dramatic orange colouration provided by the presence of the ketocarotenoids is remarkably softened with the absence of esters. The petals show this phenomenon with more clarity than the stamen.

In all genotypes the stamen is visibly much more intense than the petal. However, carotenoid analysis of the stamen contains a lot less carotenoids (six times less in P^{WT}). It is likely that in the stamen the pigmentation is provided by flavonoids (Bovy, *et al.*, 2007) rather than carotenoids. The low levels of carotenoids present in the stamen also explains the lack of phenotype in the stamen of *pyp* mutants. The pigments in the flowers match the previously published work by Ariizumi, *et al.* (2014). The *pyp* mutation removes all esters throughout the flower. In the azygous background, it is clear the esters are comprised of neoxanthin and violaxanthin. This is as expected, and upon removal of the esters the free forms of the aforementioned carotenoids increase in content. The xanthophyll esters are replaced with ketocarotenoid esters in plants with ZWRI, and the violaxanthin and neoxanthin di-esters are affected. The only detected ketocarotenoid that is capable of becoming a di-ester is astaxanthin, therefore it is reasonable to assume that it is this carotenoid that comprises all of the di-ester proportion in ZWRI. Although adonixanthin is also chemically able to become a di-ester there is no evidence of this as a free carotenoid in this line.

The general trend for the petals is that the carotenoids which should be esterified are increased in mutant plants; while other carotenoids are decreased. The overall carotenoid content is reduced. There is also a reduction in chlorophyll B in mutated flowers. This could possibly indicate that *pyp* has a role in other processes, such as phytol esterification during stress (Lippold, *et al.*, 2012).

An unknown compound is found in ZWRI, which appears to form an ester. This unknown, denoted Unknown D has maxima at 455 nm and 471 nm, eluting between astaxanthin and phoenicoxanthin. It is possible this is an isomer of an identified carotenoid; the spectrum would suggest an epoxide. This unknown is only found in the flower of ZWRI plants, thus may be a product from the ketocarotenoid pathway.

The pigments in the fruit also follow a similar trend to the petal pigments whereby *pyp* mutants have an increase in most hydroxy-carotenoids, the exception being 3'OH echinenone. However, unlike the flowers, the non-hydroxy carotenoids do not show a clear reduction. Canthaxanthin content is reduced in the fruit. However, beta-carotene and echinenone show an increase, although not significant. The overall carotenoid content remains the same. The total free carotenoids are not affected by the *pyp* mutation, and although all the esters are removed, the total is not significantly impacted. The proportion of ketocarotenoid esters in the

fruit is lower than in the flowers, thus, the removal of esters doesn't have the same impact on total carotenoid levels as seen in petals. The chromatograms shown in Figure 5-4, very clearly display the dramatic effect of the *pyp* mutation on esters. Peaks which correspond to esters are completely absent and reveal small peaks of lycopene and gamma-carotene which were previously masked by the esters. The increase of adonixanthin epoxide, astaxanthin and phoenicoxanthin in *pyp* mutants suggest these are esterified, which has been confirmed by LC/MS for astaxanthin and phoenicoxanthin. As previously published by Nogueira, *et al.* (2017) the ZWRI line doesn't contain significant levels of di-esters. Why there are di-esters in flower but not in fruit is unclear. The astaxanthin content is moderate in the fruit, it is not the predominant carotenoid, and as this is the only carotenoid with two OH groups detected, this is perhaps an explanation to the lack of di-esters. Mono-esters of astaxanthin are also present in the flowers, so it is possible that up to a threshold value, esterification with a single fatty acid is enough for stability of the carotenoid levels or adequate sequestration.

Phytofluene and zeta-carotene are both significantly lower in P^{MT}ZWØRIØ, these are the only two changes detected. Phytofluene is associated with the plastoglobules (Berry, *et al.*, 2019; N. Nogueira, *et al.*, 2016) and as reported by Ariizumi *et al.* (2014) the *pyp* mutants have an altered plastoglobule development in the flower. Assuming the same changes are observed in the fruit as the flower, the plastoglobules develop slower. Whilst the wildtype has fully developed chromoplasts and plastoglobules, *pyp* mutants have much flatter chromoplasts. The plastoglobules are smaller and are not fully developed. If the plastoglobule is structurally impacted in the *pyp* mutant then this could explain the decrease observed in phytofluene, and possibly in zeta-carotene.

The reduction of total carotenoid content in petals of *pyp* mutants is due to the role esterification plays in stability and storage. It is clear that with an absence of esters, the carotenoids cannot accumulate to the same levels as seen with esters. The addition of fatty acids to carotenoids changes their chemical properties. They become much more non-polar and this encourages stability within a cell and within intracellular components and membranes (Hornero-Méndez & Mínguez-Mosquera, 2000). The addition of fatty acids may also trigger a storage mechanism which prevents access or provides resistance to carotenoid cleavage dioxygenases (CCDs) and therefore catabolism is reduced. The pattern seen in the fruit is not as prominent, there is a slight, non-significant reduction in the total carotenoids but at a smaller

level than observed in the petals. Esters are completely absent, so it is still the product of *pyp* that is responsible for the esterification in flowers. However, in the fruit, the esters only contribute 47% of the total carotenoid content, in the petals this is 90% (ZWRI) or 95% (ZWØRIØ). As esters are a much smaller component of the fruit their absence has a smaller impact, and therefore the total content is unaffected. It is possible that if the total carotenoid content were increased, esterification may be more important, and the phenomenon seen in petals would occur in the fruit. If, as in the petals, esterification is vital for sequestration then the *pyp* gene has an important role for high ketocarotenoid accumulation in tomato fruit.

The volatile composition shows that in P^{MT}ZWRI there is decrease in carotenoid related molecules. The terpenes are synthesised from the same initial biosynthetic precursors as the carotenoids. Therefore it is logical that a reduction in synthesis of carotenoids also reduces the availability of the starting materials from the MVA and MEP pathways, and thus the terpenes are also reduced. The changes in products from fatty acids do not appear to follow a simple trend, they are increased or decrease in both ZWØRIØ and ZWRI. The fatty acids also play other, non-carotenoid associated roles such as membrane stability. Therefore, the changes in lipid derived volatiles may be indirect of carotenoid changes.

Overall there isn't a dramatic change in volatiles between wildtype and mutated plants. The esters don't seem to contribute to the profile of derived volatiles. This would suggest that in the *pyp* mutants, rather than an increase in degradation, either enzymatic or non-enzymatic, there is perhaps a decrease in the synthesis of carotenoids. With no change in the degradation, there would be minimal change in volatiles and therefore a decrease in synthesis must be occurring to account for the overall change in carotenoid content. However, Ariizumi, *et al.* (2014) found that the carotenoid synthesis was unaffected in *pyp* mutants. Another possibility is that the lack of esterification means the carotenoids cannot be sequestered and thus within the plastid environment cause a feedback inhibition of synthesis. This supports the hypothesis of regulation via sub-organellular compartmentalisation proposed by Nogueira (2013).

5.3.2 Specificity of substrates for esterification by *pyp*

PYP will act on a wide range of carotenoids, both xanthophylls and ketocarotenoids. In flowers the endogenous xanthophylls, violaxanthin and neoxanthin are esterified. In both fruit and flower the novel OH containing ketocarotenoids are esterified. However, there is one carotenoid of which esterified forms are never seen in tomato; zeaxanthin. Zeaxanthin is an

endogenous xanthophyll, much like neoxanthin and violaxanthin. It is also structurally similar to astaxanthin with the absence of the two keto groups. Yet, despite chemically being able to be esterified this has never been observed, even upon high accumulation of zeaxanthin (Karniel, *et al.*, 2020; Rapacz, 2019). Zeaxanthin is stored in the plastids (Galpaz, *et al.*, 2007), most likely within the membrane. The site for accumulation of the PYP protein is unknown, but based on the related phytyl ester synthases (PES) found in Arabidopsis (Lippold, *et al.*, 2012) and on unpublished work by Dr. J. Almeida it is probable that it is stored in the plastoglobules. These two different storage sites could explain why PYP does not act on zeaxanthin. However, violaxanthin and neoxanthin are also found in the membrane, yet these ae still esterified. It is possible that there is a secondary factor or enzyme which facilitates the transport of the epoxy-carotenoids violaxanthin and neoxanthin but does not act on the purely hydroxy-carotenoid, zeaxanthin. Ketocarotenoids are found in both the membrane and the plastoglobules (Enfissi, *et al.*, 2019), so it is unclear from which site the free carotenoids are esterified. Chili pepper (*Capsicum annuum*) does esterify zeaxanthin in fruit. In pepper the zeaxanthin is stored within the structural compartments of fibrils (Berry, *et al.*, 2019). Therefore, the difference in esterification of zeaxanthin between tomato and pepper could be based on the storage site of the enzyme and the substrate.

5.3.3 Possible alternative role for *pyp* in tomato fruit

The expression of *pyp* is not significantly different between any of the genotypes and the azygous control. This raised the interesting question of why an azygous tomato fruit expresses a gene that it has no need for. Quantitive analysis of the lipid profile should indicate if the *pyp* gene is involved in other lipid processes. A more sensitive and quantitive technique such as GC would be able to explore this further. It could also detect any other changes in the primary metabolism that could indicate if *pyp* has another role. The changes in chlorophyll content also suggest there could be a secondary role for *pyp*, potentially associated with phytol.

Chapter IV:
General discussion

6.1 How has the present study advanced our current understanding?

The global market for astaxanthin and the other ketocarotenoids is constantly growing. Currently at $427 million per year, the astaxanthin market has a predicted annual growth of 8% (McWilliams, 2018). This is largely due to the use of astaxanthin, alongside other ketocarotenoids, increasing in the aquaculture industry. The chemically synthesised version of astaxanthin lacks consumer preference and has poor environmental credentials. There is an increasing rejection of products which come from chemical synthesis, this is at least in part due to their reliance on petrochemical derived by-products and rare metals (Ernst, 1995). As society moves towards choosing products from renewable sources, the market opens up for plant based bio-factories. Previously, the main problem associated with plant factories was the achievable yields, yet the current study shows that tomato can produce industrially feasible levels of astaxanthin and therefore contribute to a bioeconomy as a renewable source. The production of carotenoid esters is intrinsically linked with the ability to store carotenoids. As shown with the *pyp* mutant tomatoes (Ariizumi, *et al.*, 2014), if esterification is inhibited, the total carotenoid content is affected. In order to improve the yields of ketocarotenoids from plant hosts, the process of esterification needs to be fully understood. If esterification can be enhanced, it seems reasonable to expect that the carotenoid content can be increased beyond that which has already been achieved.

One aim of this study was to show that we could advance our ability to produce ketocarotenoids in a sustainable manner, for this the tomato was chosen as the cell factory. Two different strategies were employed in this work to achieve this aim, and both resulted in similar maximal free astaxanthin concentrations (215 µg/g and 225 µg/g). While these are not as high as those published by Huang, *et al.* (2013), the data presented in this paper was from the T_0 generation, and therefore stability of the phenotype across generations is not demonstrated. In addition, the determinations have not been subjected to inter-laboratory ring tests. Both of the approaches used represent a substantial increase compared to the ZWRI parent line (Nogueira, *et al.*, 2017). Another aim of the project was to investigate the esterification process of ketocarotenoids in tomato fruit, a process which very little was known about until recently. Combination of the *pyp* mutant gene into the ketocarotenoid ZWRI line, produced tomato fruit and flowers with a complete absence of esters. This shows *pyp* is

responsible for esterification in tomato fruit. All of the objectives and the outcomes from these objectives are detailed in Table 6-1.

Objective 1 was to characterise the role of *Crt*R-*b2* in combination with *Crt*Z, *Crt*W and a high beta-carotene background for ketocarotenoid production. This was achieved by the work shown in chapter III. The optimal zygosity for *Crt*R-*b2* is hemizygous, in this state the amount of astaxanthin produced is higher, however canthaxanthin and phoenicoxanthin are lower. This shows the importance of an additional hydroxylase for ketocarotenoid production in tomato. The impact silencing can have on gene expression is also illustrated here. The work performed to achieve objective 1 has revealed the importance of understanding both the flux through the carotenoid pathway and the design of metabolic engineering to avoid silencing. The groundwork for this part of the study achieved high levels phoenicoxanthin and canthaxanthin, however, it failed to produce high levels of astaxanthin (Nogueira, *et al.*, 2017). This was surprising considering the inclusion of both the necessary genes and enhancement of the precursor pool. Despite thorough knowledge of the ketocarotenoid biosynthetic pathway there was a block in the final hydroxylation steps. The flux of carotenoids through the pathway is tightly regulated, and the full extent of this regulation isn't understood (Cazzonelli & Pogson, 2010; Sun & Li, 2020). Furthermore, after perturbation of the carotenoid pathway it is hard to predict where the next bottleneck may form. In this case it is in the hydroxylation steps. The addition of the plant hydroxylase as seen in ZWRIUU and ZWRIU0 overcame this. However, the inclusion of multiple constitutive promoters generated silencing effects, cancelling out the addition of the extra hydroxylase. The occurrence of silencing when multiple copies of the same promoter are used has been known about for over 20 years (Elmayan & Vaucheret, 1996; Stam, *et al.*, 1997; Vaucheret, *et al.*, 1998), however it is still common practice to include these in genetic engineering designs, as illustrated in Table 1-1. Similarly if endogenous genes, or genes with a high level of homology to the endogenous gene are overexpressed silencing can occur (Finn, *et al.*, 2011), this explains why the expression of *Crt*R-*b2* is lower when homozygous. The success of ZWRIU0 for the production of astaxanthin illustrates how an iterative approach to metabolic engineering can work. However, the phenomenon of silencing and blocks within metabolic pathways should always be considered when using plants for the synthesis of valuable metabolites.

Objective 2 was to use a single transformation event, with a multi gene construct that employed fruit specific promoters to produce ketocarotenoids in tomato in a temporal manner. This was achieved by the work shown in chapter IV. The construct was designed to avoid silencing, and has appeared to work, with the single and double copy plants being very similar. A single transformation event can produce free astaxanthin to a similar level as crossing multiple tomato lines with different traits. However, fruit specific promoters do not perform as well as constitutive promoters; plants which expressed *lcy* in a tissue and temporal specific manner did not produce as much of the ketocarotenoids as the plant with *lcy* under a constitutive promoter. This is the first time fruit specific promoters have been used for ketocarotenoid synthesis in tomato. Tissue specific promoters have been used in other crops, such as seed specific in Arabidopsis (Stålberg, *et al.*, 2003) and soybean (Pierce, *et al.*, 2015) and root specific in carrot (Jayaraj, *et al.*, 2008). Different tissue types can be very different entities, for example, fruit has a complex ripening process, which neither seed nor roots have. Factors like this may explain why although tissue specific promoters work in other crops, fruit specific promoters are not optimal in tomato. There is some knowledge of promoters which act during fruit ripening, however, there is much less information on promoters for fruit development (Hiwasa-Tanase, *et al.*, 2012). There are some resources available to guide promoter choice (Fernandez, *et al.*, 2009), however there is a need for more research in this area.

Objective 3 was to identify the role of *pyp* in esterification of carotenoid esters in the fruit. The work in chapter V shows that *pyp* is responsible for the esterification of carotenoids in tomato fruit. The use of a mutated *pyp* gene in a ketocarotenoid ester background prevents any esterification from occurring, furthermore, in the flowers there is a change to the total carotenoid content. Chapter V shows the importance of esterification for the accumulation of pigments, and therefore to improve the astaxanthin content in tomato, promoting esterification will need to be considered. The work on *pyp* mutant tomatoes has also revealed more information on the link between chromoplast development and carotenoid content. It appears that with lower carotenoid levels, the chromoplasts do not develop normally. The interesting specificity of PYP remains to be understood; why esterification of zeaxanthin does not occur, even when over accumulated is not known.

Table 6-1. Table of objectives and outcomes

Objective	Outcome
To characterise the role of *Crt*R-*b2* in combination with *Crt*Z, *Crt*W and a high beta-carotene background for ketocarotenoid production	Data in chapter III *Crt*R-*b2* functions optimally when hemizygous Screening of a line as complex as ZW(Ø)RI(Ø)UU/U0/00 is not feasible on an industrial scale Post-transcriptional silencing is powerful and should be considered in future strategies
Characterisation of the ZWRIU0 line	Data in chapter III Accumulation of mostly astaxanthin di-esters Storage of esters is mostly in the plastoglobuli, then in the membrane Identification of the rare carotenoid adonixanthin epoxide Identification of key changes in the volatile profile caused by the presence of ketocarotenoids
Single transformation event, with a multi gene construct to produce ketocarotenoids in tomato	Data in chapter IV Production of ketocarotenoids in tomato No phenotypic post-transcriptional silencing
Comparison of a fruit specific promoter to a constitutive promoter for *lcy*	Data in chapter IV Bottleneck at beta-carotene production when using a fruit specific promoter for *lcy* Preliminary data showing a constitutive promoter for *lcy* produces more beta-carotene and therefore more ketocarotenoids
Identify the role of *pyp* in esterification of carotenoid esters in the fruit	Data in chapter V Identified *pyp* as the gene responsible for ketocarotenoid esterification in tomato fruit and flowers Change in the lipid profile caused by the mutated *pyp* gene Identification of volatiles linked to the esterification of carotenoids

6.2 Broader perspectives

6.2.1 Can plants provide a cell factory for valuable chemicals like astaxanthin?

While astaxanthin is not vital for human health, it has multiple health promoting benefits, largely based on its potent antioxidant capacity. There are numerous cosmetic and nutraceutical astaxanthin products for promoting healthy skin (Davinelli, *et al.*, 2018), as well as claims astaxanthin can help prevent chronic diseases. The recommended daily dose for astaxanthin is 4 mg to 8 mg (Holland and Barrett Retail Limited, 2020; Vitagene, 2018). Therefore, to achieve this, 6 g of dried ZWRIU0 tomatoes would need to be consumed, assuming complete bioavailability. This represents approximately 60 g of fresh tomato, which is one large moneymaker tomato. This represents a manageable and sustainable way of achieving the recommended astaxanthin dose.

Previous work has reported a wide range in the level of astaxanthin production in higher plants. Within tomato, the amounts vary from trace amounts (Ralley, *et al.*, 2004), to tens of μg/g (Enfissi, *et al.*, 2019; Huang, *et al.*, 2013; Nogueira, *et al.*, 2017) right up to mg/g concentrations shown in one publication (Huang, *et al.*, 2013). With the exception of the work by Huang, *et al.* (2013), the amounts produced in this work, from ZWRIU0, are larger than previously seen. With the assumption that all the di-esters are astaxanthin esters, the total astaxanthin content is approximately 650 μg/g. The production of free astaxanthin is however lower. As discussed in section 1.2.3.2 the esterification of carotenoids does not affect the bioavailability. In this work the amount of free astaxanthin produced is 215 μg/g (ZWRIU0) and 225 μg/g (ketocarotenoid construct).

Astaxanthin content has been achieved in high concentrations in other species. Tobacco has been frequently used, and has achieved 5.4 mg/g astaxanthin (Hasunuma, *et al.*, 2008), however, this is still lower than the amounts seen by Huang, *et al.* (2013) in tomato. It appears that while leafy crops can provide a cell factory for production of ketocarotenoids, tomato can compete. Tomato also has the major advantage of having fewer alkaloids than tobacco, and therefore pigment extraction or direct consumption is more favourable in tomato than tobacco. Furthermore, tomato has sink tissue which allows for metabolic changes to be contained within it. This minimises the impact on vegetative tissue and therefore plant vigour.

6.2.1.1 Production of other ketocarotenoids

The amount of other ketocarotenoids produced, such as phoenicoxanthin and canthaxanthin are lower in this work than previously seen. The decrease in intermediary ketocarotenoids seen in ZWRIU0 demonstrates how the flux of carotenoids is now pushed into astaxanthin, rather than halting earlier in the pathway. While the other ketocarotenoids are also high value pigments, and have important industrial roles, the creation of a line which produces predominantly astaxanthin adds to the arsenal of plant factories we have. ZWRI00 provides a sustainable production method for phoenicoxanthin, ZWRIUU provides canthaxanthin and ZWRIU0 provides astaxanthin.

Despite having only been found in a few of the published ketocarotenoid papers, adonixanthin epoxide has been identified in all three results chapters shown in this work. While all three chapters are related in terms of the genes used, it is surprising to see this rare carotenoid in all the different lines analysed. As previously discussed, the addition of the hydroxylase *Crt*R-*b2* (UU/U0) to the ZWRI line stimulated production of adonixanthin epoxide. This is most likely to be due to an increase in hydroxylated endogenous carotenoids such as antheraxanthin, and therefore the production of the ketolated form of this, adonixanthin epoxide (or 4-ketoantherxanthin). The ketocarotenoid construct also initiated production of adonixanthin epoxide in the fruit, but more so in the leaf tissue. The only gene active in the leaf is *Crt*W, and therefore the carotenoids available for ketolation are minimal. Tomato leaf tissue is higher in the xanthophylls than the fruit, and therefore, similarly to what has been seen in ZWRIUU/U0/00, there is predominant ketolation of these xanthophylls. This explains the presence of adonixanthin epoxide in the leaf. The presence of adonixanthin epoxide in the fruit is probably due to formation before the overexpression of the hydroxylase occurs. Adonixanthin epoxide cannot be further hydroxylated. In the $P^{MT/WT}$ZWRI line adonixanthin epoxide is only seen in the flowers, and not in the fruit. This coincides with a general increase in epoxy carotenoids, such as violaxanthin, associated with the petals and stamen. The localisation of adonixanthin epoxide to the flowers in this line may also explain why it was not identified in the parent line (Nogueira, *et al.*, 2017). While adonixanthin epoxide is not currently of commercial value, having a sustainable approach to synthesise it could prove beneficial in the future. With the production of adonixanthin epoxide predominantly in the leaf, it is synthesised without negatively impacting the other ketocarotenoids of interest.

Having plant factories which can accumulate different carotenoids in different tissue gives the bio-renewable sector another advantage against chemical synthesis.

6.2.1.2 Genetic modification

The production of ketocarotenoids in tomato requires genetic modification (GM). Bacterial or algal genes are required to synthesise ketocarotenoids from the endogenous carotenoids found in tomato. Despite the many advantages of GM, some of which are discussed in section 1.3.3, there is resistance to the use of GM for crop development. Since the advent of GM technologies, increasingly tight legislation has emerged to control its use (European Parliament, 2003). The legislation has varied country to country, with some areas remaining relatively open to the use of GM technology and other countries shunning it. The United States and Brazil are the top producers of GM crops, here maize, soybean, cotton and others are all grown after the application of GM technologies (Science Literacy Project, 2016). GM can increase yields, provide resistance and improve crop morphology which all allow for the provision of more food. As already shown, GM can also be used to alter the carotenoid content of plants. The European Union (EU) has much tighter restrictions on the use and growth of GM plants, with only GM maize being produced in some EU countries (The Royal Society, 2016). The fears behind GM mostly revolve around concerns that GM varieties will out compete the native varieties. This would lower the genetic diversity available and could limit the natural development of species. There are also concerns that the novel genes inserted into one species could transfer into others, this has the potential to provide weeds with resistance genes against commonly used herbicides. Growth of GM plants in a contained environment could overcome these problems, however this dramatically limits the production areas available for crops and increases the costs.

Different countries also have different views on the import and use of GM crops. Many countries which have banned the growth of GM crops, do allow the importation of GM crops from elsewhere. These GM crops are then used for animal feed, but whether the animal product should then be classified as GM is controversial. With the production of ketocarotenoids for use in aquaculture, this is especially relevant. The aquaculture industry is already using soy protein to replace fish derived protein in the feed (Yang, 2019), most of this soy will be genetically modified. While it may be many years before governments and society accept the direct consumption of GM products, the consumption of meat or fish that have been fed GM

products is hopefully less far away. There is no strong evidence that feeding GM crops to animals has negative effects (Vos; & Swanenburg, 2018). Consumers are currently facing a choice between GM fed fish, and those coloured with synthetic pigments. The synthetic pigments rely on the petrochemical industry, and therefore there are ethical concerns over the sustainability and the impact on the environment the production of synthetic pigments may have. On the other hand, GM products can provide a renewable, green and potentially organic source of pigments, however fear has been created by their 'unnatural' production.

6.2.1.3 Downstream processing

One of the major benefits in using plants as cell factories is the accessibility of the metabolites produced. Downstream processing is something that industries try to minimise because it incurs expensive resources. After chemical synthesis the product often requires substantial purification before it can be used. Any purification step requires both time and resources, furthermore, with purification comes potential loss of yield, all of which are detrimental to industrial productivity. Plant hosts require much less, if any, downstream processing. In the case of tomato, the sink organ in which the carotenoids accumulate is also the one which is widely consumed. This provides a direct option for metabolite accessibility. Even in the case of animal feed, tomato can be ground directly into the feed. This removes the need for any downstream processing.

6.2.1.4 Other approaches for ketocarotenoid production in plants

The crossing of different plant lines in order to combine different traits has been performed since plants were cultivated by humans. This approach is established, and with the correct selection process, it works well. However, there are problems with this approach, with every event added, there is another trait upon which the plants will segregate. If the desired trait needs to be hemizygous or heterozygous, this results in large numbers of plants needing to be screened. Furthermore, with every cross another genetic component is potentially included, and this influences the effect of the gene of interest in a positive or negative manner. In the case where specific effects of the transgene are preferable multiple components create a situation away from an isogenic background. The use of a multigene construct can provide the answers to these problems. Multigene constructs have not been used as extensively as crossing approaches, but their use is increasing. They allow for a controlled design, with all gene parts being considered, such as the multiple promoters used. Transformation into a single

background also simplifies the understanding of resulting changes. The multiple genes are linked when inserted into the genome, and therefore, will segregate as one event. This dramatically reduces the amount of time, and plants required for screening subsequent generations. The major disadvantage to a multigene construct is that it is inflexible in terms of iteratively adding one gene at a time, therefore the gradual changes observed by each gene cannot be observed. When using a multigene construct there needs to be a good prior understanding to the bottlenecks and feedback pathways which exist in the area of study. The advantages and disadvantages to these two approached is shown in Figure 6-1.

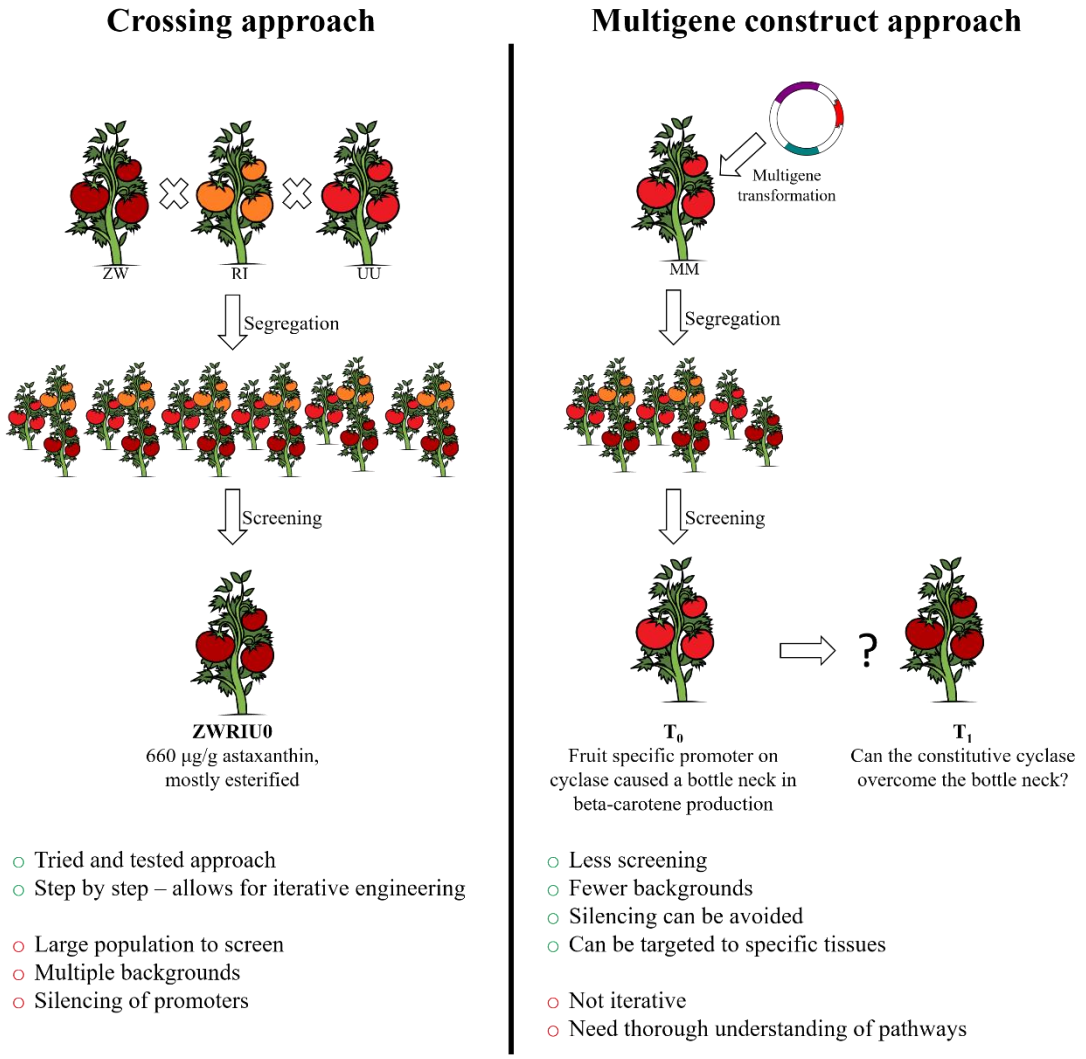

Figure 6-1. Schematic comparing the two different approaches for ketocarotenoid production
The crossing approach is detailed in chapter III, the multigene construct approach is detailed in chapter IV. MM, moneymaker

6.2.1.5 Sequestration

An important part of carotenoid accumulation is carotenoid sequestration. Without a mechanism to store the carotenoids, they are degraded. Within plants the carotenoids are often sequestered by esterification, this changes their lipophilicity and therefore, the storage. The subcellular fractionation performed in chapter III (section 3.2.10) and fractionations performed previously (Enfissi, *et al.*, 2019) confirm that the esterified carotenoids are predominantly stored in the plastoglobuli. This also links with the effect that the absence of carotenoid esters has on the chromoplast formation (Ariizumi, *et al.*, 2014). If less carotenoid esters are made, then it seems that the total carotenoid content is lower, therefore, to achieve high accumulation of carotenoids esterification needs to be promoted.

The production of ketocarotenoid esters is very different between all T_0 plants transformed with the ketocarotenoid construct and ZWRIU0. T_0 plants only have minimal esterification of ketocarotenoids, with phoenicoxanthin being the predominant carotenoid. Meanwhile, almost 50% of the carotenoids found in ZWRIU0 are esterified. This may be due to the relative proportions of ketocarotenoids to carotenoids. ZWRIU0 only has small amounts of the endogenous carotenoids (39.5 µg/g beta-carotene, 0.0 µg/g lycopene) and produces mainly ketocarotenoids. On the other hand, T_0 (PPC2) has comparable levels of endogenous carotenoids to the azygous control, which doesn't produce any esters in the fruit, and has less ketocarotenoids than observed in ZWRIU0. Therefore, it seems that esterification of ketocarotenoids is observed when the endogenous carotenoids are depleted and novel ketocarotenoids are instead produced. This indicates that esterification, may in part, be to sequester unknown carotenoids so as to remove them from the metabolic active site of the cell. The plant therefore recruits the acyltransferase which normally functions in the flower to protect the cell from the perceived threat of the novel ketocarotenoids.

With the absence of the acyltransferase the novel ketocarotenoids cannot be esterified, therefore the amount of free esterified carotenoids increases. Following this there must be an increase in the degradation of the ketocarotenoids, as the total carotenoid content is lower in plants without the acyltransferase. It would therefore seem that if the ketocarotenoids cannot be esterified, degradation increases as a secondary way to remove the novel pigments from the cell. However, the volatile profile for P^{MT}ZWRI compared to P^{WT}ZWRI does not shows this.

Negative regulation could also help to explain the observed decrease in carotenoid content, however Ariizumi, *et al.* (2014) has shown that the carotenoid biosynthetic genes are unaffected in the *pyp* mutants. With esterification playing an important role in carotenoid sequestration, especially in fruit which is synthesising novel carotenoids the presence of an active acyltransferase should be considered in future metabolic engineering approaches. If pigments are to be produced and stored in large quantities, it is important there is a pathway for doing this. Therefore, the overexpression or introduction of an acyltransferase may allow for larger amounts of ketocarotenoids to be accumulated in plants.

Esterification also affects the chromoplast structures. Ariizumi, *et al.* (2014) showed that in flowers without the *pyp* acyltransferase the plastoglobules do not develop fully, they remain flattened, smaller and develop more slowly, these cellular changes are summarised in Figure 6-2. The link between esterified carotenoids and plastoglobule development emphasises how plastic plant cells can be, they react to the presence or absence of a metabolite and can alter the cellular substructure as needed. Furthermore, the plastoglobules seem to only fully form

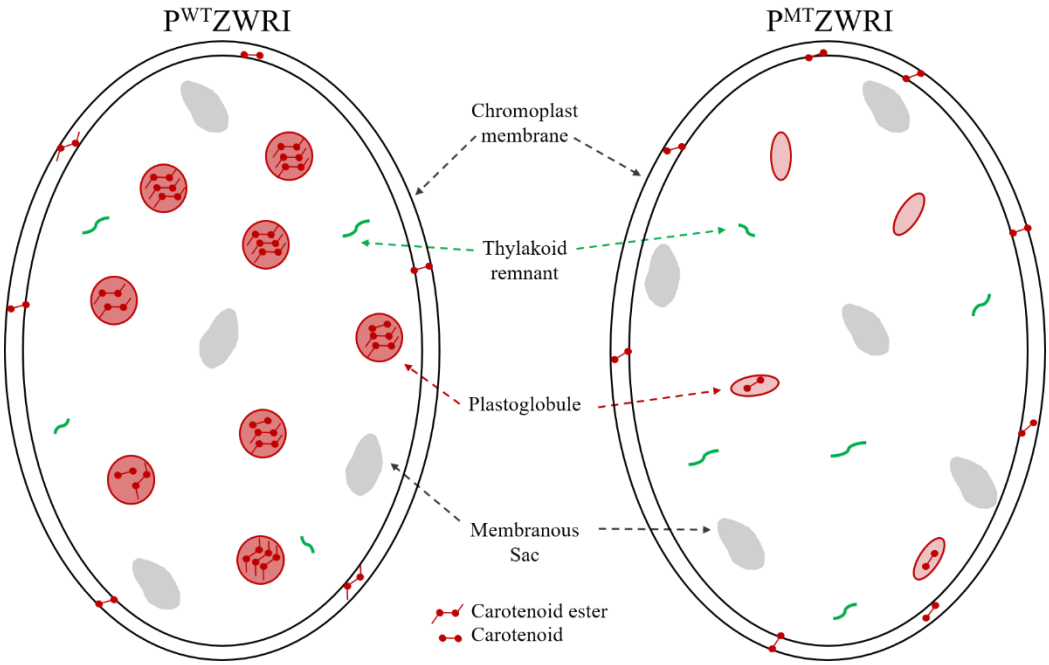

Figure 6-2. Schematic of the predicted changes which occur in the *pyp* mutant fruit chromoplasts
Changes are based on those observed by Ariizumi, *et al.* (2014) in the tomato flower. Without a functioning PYP enzyme, carotenoids are not esterified, accompanying this is a decrease in plastoglobule number, a reduction in plastoglobule size and slower development of plastoglobules resulting in a flattened morphology. There is an absence of esterified carotenoids and a decrease in overall carotenoid content.

when they are required, therefore if plants are metabolically engineered to over accumulate in pigments it should be expected that more plastoglobules, larger plastoglobules or more dense plastoglobules form to provide storage. Conversely, as seen in *pyp*, if the pigments cannot be stored, the plastoglobules are much smaller and less significant.

6.2.2 Other platforms for ketocarotenoid production

Alternative approaches for sustainable ketocarotenoid production are also being investigated. Notably these rely on algal or microbial systems and are discussed in section 1.2.5.2. In summary, *X. dendrorhous* can produce 10 mg/g astaxanthin, with other ketocarotenoids also being synthesised (Gassel, *et al.*, 2013) and *H. pluvialis* can produce 14 mg/g astaxanthin (Hong, *et al.*, 2018). However, these values have not been validated across multiple systems in different environments or through inter-laboratory trials. While *X. dendrorhous* and *H. pluvialis* both produce larger amounts of astaxanthin per dry weight than the best producing plant chassis, the astaxanthin from these cannot be consumed directly, and therefore requires downstream processing. This adds both cost, and chemical processing to the production, therefore the microorganism sources may not appeal to the 'green' market to the same extent as plant sources. The idea of consuming yeast or algal based produce is also alien in the current consumer market, this therefore may hinder the microorganism approach for ketocarotenoid synthesis. Furthermore, in order to scale up production to industrial levels, large scale infrastructure is needed in order to provide fermenters of the required size. The construction of these uses resources, needs investiture, and occupies land which could otherwise be used for food production. Once infrastructure is built the land can no longer be used for crops, on the other hand the use of plant factories allows for crop rotation and can be implemented seasonally.

Adonis is a plant which naturally produces astaxanthin, and therefore may seem like an attractive route for astaxanthin production. However, *Adonis* is not an agriculturally feasible plant and produces toxic metabolites (Woods, *et al.*, 2007), some of which have pharmacological action which may be detrimental to the healthy body (Hosseini, *et al.*, 2019).

The different approaches for astaxanthin production compared to the work presented here is shown in Table 6-2.

Table 6-2. Summary of carotenoid content seen throughout this work, and in the parental ZWRI line
Amounts are in µg/g dry weight. Values show the highest amount produced over the three generations analysed of ZWRIUU/U0/00.

Tomato line	Astaxanthin	Phoenicoxanthin	Canthaxanthin	Ketocarotenoid esters	Total
X. dendrorhous (Gassel, *et al.*, 2013)	10000				
H. pluvialis (Hong, *et al.*, 2018)	14000				
Adonis aestivalis (Maoka, *et al.*, 2011)	23	8	8	1585	1660
ZWRI (Nogueira, *et al.*, 2017)	83	594	899	1052	3287
ZWRI00	131	1554	795	1168	4252
ZWRIU0	215	95	43	1043	2500
ZWRIUU	77	1075	1250	1851	4301
Ketocarotenoid construct fruit specific cyclase	225	286	34.5	113.4	1577
Ketocarotenoid construct constitutive cyclase (ubq)	133	593	160	128	2356

6.3 Future utilisation of the material generated

6.3.1 ZW(Ø)RI(Ø)UU/U0/00

The ZW(Ø)RI(Ø)UU/U0/00 line is reasonably well characterised, with carotenoid analysis having been performed over three generations and over ripening, broader metabolic changes and volatile metabolites assessed, the silencing of *Crt*R-*b2* confirmed, subcellular localisation for carotenoid storage identified, and the effect of the carotenoid composition on photosynthesis ascertained. However, there is more work which could be done to fully understand this line.

The flowers show a clear phenotypic change between ZWRIUU and ZWRIU0. ZWRIUU has much paler flowers than ZWRIU0 which follows the silencing of *Crt*R-*b2* which occurs throughout the ZWRIUU line. The carotenoids responsible for the change in colour have not been assessed. Analysis of this would reveal where the overexpression of *Crt*R-*b2* is acting in the carotenoid pathway, and where an absence of *Crt*R-*b2* has the most impact. Flower tissue is difficult to work with. While it is rich in carotenoids the material is very light, and therefore at least 10 flowers are required per sample. Removal of the flowers also prevents the setting of fruit, and therefore, the number of flowers which can be removed for analysis may be limited.

Which stereoisomer of astaxanthin is produced within this work is an important question that needs answering. There is evidence that it is only the *S* isomer which has biological activity (Yang, *et al.*, 2013), and therefore it is this isomer which is of most value. Previous work has shown that plants produce the more useful *S* isomers of carotenoids. It is assumed this is also the case within this line, with astaxanthin being 3*S*, 3*S*'. The use of a stereoisomer specific column would be able to confirm this. These columns can separate a stereoisomer, and therefore, alongside the use of stereo specific standards the isomers present in a sample can be confirmed. While the analysis of this can be performed on standard HPLC equipment, the sample to be analysed cannot be too complicated. Therefore, fractions of a single carotenoid need to be isolated from the plant extract prior to stereoisomer analysis. If, as expected, the isomer produced in this work is the *S* isomer, this presents a notable advance over chemical synthesis which provides a racemic mixture or *X. dendrorhous* which produces the *R* isomer.

The esters analysed in this work have been putatively identified by the use of LC/MS and the esters produced in ZWRI. The esters of ZWRIUU and ZWRIU0 are assumed to be phoenicoxanthin and adonixanthin C14 and C16. The esters produced in ZWRIU0 are more complicated. The mono-esters have large amounts of co-elution, and therefore identification of each ester is problematic. The di-esters can only be astaxanthin, adonixanthin and adonixanthin epoxide, and based on the spectral characteristics of the di-ester peaks, the di-esters are all astaxanthin. The use of the LC/MS to confirm identification is also difficult due to the contamination with other, non-carotenoid lipids. This makes obtaining an exact mass for each ester problematic. Considering this, the fatty acids which form the di-esters have not been identified. It is likely they are also C14 and C16, but this needs to be confirmed along with the isomer of the fatty acids. A final confirmation of which carotenoids are esterified could be performed by the use of cholesterol esterase to remove the ester group. Analysis of the carotenoid profile both before and after enzymatic treatment reveals which free carotenoids are increased upon the removal of the ester groups.

The main industry which relies on the ketocarotenoids including astaxanthin is the feed and aquaculture industry. It therefore would be of interest to involve these industries to determine the commercial value of the astaxanthin produced in the ZWRIU0 line. A feeding trail using either whole tomatoes or a purified extract from ZWRIU0 would determine the bioavailability of the astaxanthin and other ketocarotenoids from the tomatoes. If this proved to be a feasible feedstuff then this work would have provided a sustainable approach for astaxanthin production in tomato. Furthermore, with one tomato representing a daily dose of astaxanthin, clinical trials are needed to observe the effect this has on human health.

6.3.2 Ketocarotenoid construct

The work presented in chapter IV is data from a T_0 generation. This limits both the statistical power of the dataset, and also the reproducibility of the work. In order to validate the results presented here, the analysis needs to be repeated on at least the T_1 generation. The T_1 generation will provide biological replicates of events, and therefore statistical analysis could be performed. Furthermore, T_1 will produce both hemizygous and homozygous plants which will allow for the optimal zygosity of the construct to be ascertained. In T_0 there was only one plant carrying the alternative construct with the constitutive expression of *lcy*, this needs to be replicated in T_1 to confirm the benefits of the constitutive expression.

The T_0 generation did not produce as much fruit as hoped, and therefore some of the planned analysis could not be performed. Phenotypically it is the jelly of the fruit which shows the largest colour change between transformed fruit and azygous fruit. In the T_1 population the jelly should be analysed for the carotenoid content. The gene expression profile of the inserted genes should also be analysed. With the timing and localisation of each gene being controlled by the relevant promoter, the gene expression of *Crt*W, *lcy* and *Crt*R-*b2* should be profiled in the leaf, the mature green fruit and the ripe fruit. This will confirm that all three genes are active within the construct and also reveal if the promoters express as expected.

What may also be of interest is to look at the effect of the carotenoid profile on the broader metabolism. GC/MS analysis, as performed in section 2.6.6 could be used to identify any changes which have occurred. The effect on the photosynthetic performance can also be measured to identify changes there.

6.3.3 $P^{MT/WT}$ZW(Ø)RI(Ø)

The evidence for the PYP enzymes being responsible for the esterification of carotenoids in tomato fruit is very clear cut, however, some unanswered questions remain. The inability to esterify carotenoids has shown to impact the chromoplast structure in the flowers. The use of microscopy would determine if the same occurs in the fruit. Furthermore, a subcellular fractionation would identify changes in the site of carotenoid storage when esterification cannot occur.

Acyltransferases are involved in other lipid pathways. The preliminary quantitive TLC (section 5.2.7) suggested that the loss of function of *pyp* also affected other lipids. Further investigation into the impact of *pyp* on the lipids is required. Following separation of the fatty acids and ester glycerols by TLC these could then be analysed using GC/MS for both full identification and quantification.

The *pyp* gene is a homologue of the *Arabidopsis pes1/2* genes. Consequently, *pyp* may also play a role in phytol esterification. Determining the phytol levels in P^{MT}ZW(Ø)RI(Ø) would potentially identify if *pyp* was also acting as a phytol ester synthase in the leaf. If phytol esterification is affected, it is expected that the levels of free phytol would be increased. As phytol causes membrane instability, there may also be an impact on the photosynthetic capacity of mutant plants, therefore determining this parameter may also provide information

of the role of *pyp* in the leaves. Tocopherols are also produced upon chlorophyll degradation via phytol (Lippold, *et al.*, 2012). Considering this, carotenoid and tocopherol analysis in the leaf may help understand the pathway further.

Ariizumi, *et al.* (2014) did not identify changes to the carotenoid biosynthetic genes in *pyp* mutants, however, there was an overall reduction in carotenoid content. It therefore seems likely that there is an increase in degradation of carotenoids, and this is performed by the CCDs or NCEDs. Expression analysis of these degradation enzymes has not been performed, but to fully understand how the synthesis and degradation of carotenoids and carotenoid esters work, they should be. Presumably in plants which cannot esterify carotenoids there is an increase in the expression of the CCDs to increase the degradation. CCD4a, CCD4b, CCD1a and CCD1b are of most importance for carotenoid degradation and therefore, it is these which should be focused on.

Considering the importance of esterification for the accumulation of carotenoids, it would be of interest to overexpress *pyp* in both tomato and other non-esterifying plants. Furthermore, to date *pyp* has not been found to esterify zeaxanthin in tomato and the reasons for this are unclear. The overexpression of *pyp* in a high zeaxanthin line would potentially help to elucidate the reasons behind the substrate specificity that *pyp* appears to have against zeaxanthin. Identifying the location of PYP within the cell may also help to answer this question.

6.4 Conclusion

The overall findings presented in this work have shown that plants present a feasible way of producing astaxanthin to industrially viable levels. The levels of astaxanthin approached 1 mg/g with total carotenoid content approaching 2.5 mg/g in both ZWRIU0 and the ketocarotenoid construct with constitutive cyclase (ubq). This is comparable to the ZWRI line used in aquaculture trials (Nogueira, *et al.*, 2017). The importance of the esterification pathway for the sequestration and storage of carotenoids has also been demonstrated with elucidation of the enzyme involved in ketocarotenoid esterification in tomato fruit. The need to consider important factors such as promoter choice when using metabolic engineering have been discussed. In particular the consequences of including multiple identical promoters and homologous genes on silencing of gene expression along with the temporal limits when using

fruit specific promoters. The key results from this work are; astaxanthin has been achieved to high levels (650 μg/g) with the majority being present as a di-ester, fruit specific promoters have been shown to be sub-optimal compared to constitutive promoters, a single transformation event provides an easier and less laborious approach to ketocarotenoid production in tomato, and the *pyp* gene is responsible for esterification of ketocarotenoids in tomato fruit. Overall the technologies exist to produce high value components in a sustainable manner, these technologies could replace traditional petrochemical based manufacturing.

Appendices

7.1.1 Appendix 1 – Parameters for the identification of carotenoid, chlorophylls and tocopherols using UPLC and HPLC-PDA analysis

Table 7-1. Carotenoid, chlorophyll and tocopherol retention times and spectral properties from UPLC and HPLC-PDA analysis
Retention time shown is the modal time of elution. The retention time can sometimes drift by the percentage shown, if no percentage is given the compound was only observed at one retention time. HPLC retention times are also given for compound which were observed on that system. Maxima represents the maximum absorption of the compound, - denotes a maximum of undefined wavelength, * denotes a mixture of compounds, and therefore a mixture of maxima.

Fruit and leaf			
Compound	**UPLC retention time (min)**	**HPLC retention time (min)**	**Maxima (nm)**
Violaxanthin isomer	1.9		-, 442.0, 471.1
Neoxanthin	2.1 ± 5%		414.1, 438.3, 467.4
Violaxanthin	2.2 ± 5%	11.3	-, 442.0, 471.1
Adonixanthin epoxide	2.6 ± 8%	12.7	455.3, 473.5
Neoxanthin isomer	2.9		414.1, 438.3, 467.4
Astaxanthin	3.1 ± 5%	14.7	476.0
Unknown B	3.4		450.4
Unknown A	3.6 ± 6%		454.1
Adonixanthin	3.6 ± 6%		465.0
Unknown D	3.7		455.0, 471.0
Lutein	4.2 ± 5%	15.4	-, 446.8, 474.7
Phoenicoxanthin	4.5 ± 7%	14.7	479.6

Unknown C	4.8		463.0
Canthaxanthin	5.8 ± 3%	18.7	477.2
3'OH echinenone	6.2 ± 2%		465.0
3OH echinenone	6.8 ± 1%		465.0
Chlorophyll B	6.8 ± >1%		465.5
Echinenone	7.1 ± 1%		460.2
Alpha-tocopherol	7.1 ± 1%		293.4
Tocopherol acetate (internal standard)	7.1 ± 1%	14.1	285.0
Chlorophyll A	7.2 ± 1%		429.8
Carotenoid mono-ester group 1 (ZWRIU0)	7.2 ± 10%		*
Lycopene	7.3 ± 1%		-, 472.3, 502.7
Carotenoid mono-ester group 2 (ZWRIU0)	7.3 ± 2%		*
Phytoene	7.5 ± 12%	22.0	286.2
Gamma-carotene	7.5 ± 1%		-, 461.4, 490.5
Carotenoid mono-ester group 3 (ZWRIU0)	7.7 ± 4%		*
Pheophytin	7.9 ± 1%		409.3
Zeta-carotene	7.9		-, 400.8, 425.0
Beta-carotene	8.0 ± 3%	28.5	-, 454.1, 479.6
Phytofluene	8.0 ± 4%		-, 349.0, 368.3

Carotenoid di-ester group 1 (ZWRIU0)		30.0	477.8
Carotenoid di-ester group 2 (ZWRIU0)		30.9	477.8
Carotenoid di-ester group 3 (ZWRIU0)		31.9	477.8
Carotenoid di-ester group 4 (ZWRIU0)		32.9	476.6
Flower carotenoid esters			
Compound	UPLC retention time (min)	HPLC retention time (min)	Maxima (nm)
Violaxanthin mono-esters		20.9, 22.0, 22.6, 23.2, 24.0, 24.8, 27.3, 27.9	- , 442.0, 471.1
Neoxanthin mono-esters		20.9, 21.6, 23.3, 23.7, 25.7	414.1, 438.3, 467.4
Ketocarotenoid mono-esters (P^{WT}ZWRI)		25.2, 26.0, 26.4, 27.1	472 to 479
Violaxanthin di-esters		28.4, 29.0, 29.5, 30.8, 30.5, 30.7, 31.3, 32.3	- , 442.0, 471.1
Neoxanthin di-esters		31.7, 32.7	414.1, 438.3, 467.4
Ketocarotenoid di-esters (P^{WT}ZWRI)		28.5, 29.2, 30.1, 30.5, 31.1, 32.0, 32.2, 33.1	468 to 486

7.1.2 Appendix 2 – The metabolites identified in polar and non-polar extracts using GC/MS analysis

Table 7-2. Identification of all metabolites determined from GC/MS analysis
1 – identified using a standard, 2 – identified using the NIST database, 3 – only the broad classification is known, 4 – unknown. NP, non-polar, P, polar.

Metabolite	Retention time (min)	Retention index	Ref. ion	ID level	Phase
Lactic acid	9.0	1067.9	219	1	NP
Alanine	10.2	1107.9	116	2	P
Methylphosphate	12.8	1178.8	241	2	NP
Valine	13.7	1102.7	72	1	P
Unknown - 21.3 (Ethanolamine (3TMS))	15.2	1259	174	2	P
Unknown - 15.8 min - (Leucine (2TMS))	15.5	1261.5	158	3	P
Leucine (2TMS)	15.6	1273.6	158	1	P
Phosphoric acid	15.7	1269.5	299	2	P
Glycerol	15.7	1272.9	205	1	P
Isoleucine	16.1	1293.8	158	1	P
Glycine	16.4	1304.9	174	1	P
Glyceric acid	17.7	1322.2	292	1	P
Unknown - 18.5	18.0	1343.4	115	4	P
Itaconic acid	18.1	1342.8	259	1	P

Unknown - 18.2 (Itaconic acid)	18.3	1334.1	215	3	NP
Citraconic acid	18.3	1341.3	259	1	P
Mesaconic acid	19.9	1393	259	1	P
Erythrofuranose (3TMS)	20.1	1343.8	218	3	P
Aspartic acid	20.8	1522	232	1	P
Malic acid	22.8	1491.5	335	1	P
Pyroglutamic acid - Proline	23.4	1515.4	156	1	P
GABA	23.7	1520.1	174	1	P
Unknown - 22.1	23.9	1513.6	305	4	P
Unknown - Xylulose	24.1	1546.8	306	3	P
Unknown - 27.5 (Dodecanoic acid (1TMS))	27.1	1638.2	257	3	NP
Gluconic acid	27.2	1984.4	447	1	P
Arabinose/ xylose/ ribose/ lyxose	27.7	1768.6	307	3	P
Lyxopyranose	29.1	1610.2	229	3	P
Aconitic acid	29.8	1751.2	375	2	P
Glycerol-3-P	30.2	1762.3	299	1	P
Unknown Sugar	30.3	1760.6	217	3	P
Unknown Fructose	30.5	1774.1	379	3	P
Fructose isomer	31.3	1791.6	437	2	P

Citric acid	31.6	1821.5	273	2	P
Isocitric acid	31.7	1819	465	2	P
Unknown - 32.7	32.1	1828.1	244	4	P
Unknown Galactose	32.3	1837	319	3	P
Fructose	33.1	1874.2	307	1	P
Mannose/ Glucose	33.9	1887.7	319	3	P
Glucose/ Galactose	34.9	1882.2	217	3	P
Unknown - Turanose	35.0	1947.1	361	3	P
Unknown Sugar derivative glucitol	35.4	1917.6	319	3	P
Galactaric acid/ Galacturonic acid	35.6	1941.7	333	3	P
Galactose	36.2	1902.8	319	2	P
C16:0	36.5	2038.4	313	1	NP
Inositol	38.7	2072.1	305	1	P
C17:0	39.4	2129.9	342	1	NP
Sedoheptulose	40.4	2115.3	319	2	P
Linoleic acid/ octadecadienoic acid	40.8	2197.2	337	3	NP
Unknown - 41.0	41.0	2173.5	339	4	NP
C18:0	41.6	2225.8	356	1	NP
Tricosane	42.8	2289.8	324	1	NP

Unknown - Glycero-1-C14:0	44.8	2387.4	343	3	NP
Unknown - 48.4	48.4	2490.2	455	4	P
Unknown - C16:0 propylester	48.6	2577.3	371	3	NP
Sucrose	50.7	2638.1	361	1	P
Unknown - Glycero-1-C18:2 *cis* 9,12	51.5	2731.6	498	3	NP
Unknown - Glycero-1-C18:0	52.1	2767.8	399	3	NP
Narigenin peak 1	52.6	2782.8	417	2	NP
Nonacosane	54.1	2887.7	408	1	NP
Unknown - 55.3	55.3	2912.7	193	4	NP
Gamma tocopherol derivative	55.5	2958.3	488	2	NP
C26:0	56.3	3013.1	168	2	NP
Hentriacontane	57.4	3086.8	436	1	NP
Alpha tocopherol	57.8	3112.6	502	1	NP
Unknown - 60.6	59.6	3243.9	481	4	NP
Stigmasterol	59.8	3263	484	1	NP
Sitosterol	60.7	3293.5	486	1	NP
Alpha amyrin	61.6	3359.9	498	1	NP

7.1.3 Appendix 3 – Metabolites identified in semi-volatile analysis

Table 7-3. Identification of all semi-volatile metabolites from SPME GC/MS analysis
Identification level is based on in house standards or from the NIST library. 1 – identified using a standard, 2 – identified using the NIST library with a match above 899, 3 – identified using the NIST library with a match lower than 900, 4 – unknown metabolite.

Name	Retention time (min)	Retention index	Ref. ion	Identification level	NIST match
2-Ethylfuran	3.2	704.6	96	2	947
Isopropyl acetate	4.1	716.4	61	2	934
Formic acid	4.2	719.7	46	2	920
1-pentanol	4.4	763.6	42	2	966
3-methyl-butanenitrile	4.5	753.2	43	2	936
Butanoic acid, methyl ester	4.6	720.5	87	2	932
Acetic acid	5.0	721.5	60	2	932
trans-2-pentenal	5.1	770.8	83	2	923
1-penten-3-one	5.2	726.8	55	3	871
Pentanal	5.3	733.9	58	2	922

Dimethyl disulphide	5.4	761.8	94	3	833
n-octane	5.4	800	144	1	
Methylisovalerate	5.6	775.1	85	2	916
2-methyl-1-butanol	5.6	732	57	2	955
Hexanal	5.9	820.8	87	2	914
cis, 2-penten-1-ol	6.0	781.3	68	2	905
2,4-dimethyl-1-heptene	6.6	839.7	70	2	922
2,2,3-trimethylcyclobutanone	7.3	831.3	70	3	868
2-hexenal	7.5	848.9	83	2	943
1-hexanol	7.8	867.4	56	2	940
2-acetyl-5-methylfuran	7.9	855.3	109	2	974
Ethylbenezene	8.1	862.1	106	2	937
2-heptanone	8.3	890.5	114	2	909
2-methyl-1-butanol acetate	8.6	879.2	73	3	883
Pentyl-oxirane	8.8	903.1	73	3	797

2-n-butylfuran	9.0	893.4	81	3	856
Styrene	9.1	888.4	104	2	909
trans-hept-4-enal	9.1	898.7	94	3	816
1-nitropentane	9.2	904.8	71	3	814
trans, trans, 2,4-Hexadienal	9.2	910.1	81	2	907
1-heptanal	9.3	903.2	70	3	892
n-nonane	9.5	900.0	128	1	
Methylhexoate	9.5	924.1	74	3	864
Alpha-pinene	9.7	934.1	93	3	885
5-methyl-3-heptyne	9.8	928.4	151	3	817
1-ethyl-5-methylcyclopentene	10.0	928.3	11	3	853
3-hexenoic acid methyl ester	10.1	930.8	74	3	891
3,5-dimethly-phenol	10.1	932.1	122	3	848
3-ethoxy-pentane	10.2	950.3	94	3	790
4-methyl-2-heptanone	10.6	935.2	93	3	844

cis, 2-heptenal	10.7	953.1	68	2	948
6-methyl-2-heptanone	10.8	953.7	110	2	917
Benzaldehyde	10.9	955.2	105	2	976
2,5-dihydro-thiophene	11.0	960.0	86	2	936
Beta-pinene	11.0	976.5	93	2	936
2-methylnonane	11.1	964.8	98	3	826
2-methyl-1-hepten-6-one	11.2	965.3	108	3	811
Dimethyltrisulphide	11.3	968.6	126	2	900
1-octen-3-one	11.3	976.7	70	3	854
1-octen-3-ol	11.5	979.4	57	2	949
Sulcatone	11.6	987.5	126	3	871
2-pentylfuran	11.7	991.4	138	3	801
2-propyl-furan	11.9	995.1	97	3	874
Delta 2/4 carene	12.3	995.5	121	2	950
Phellandrene	12.4	1006.8	136	2	907

alpha-phellandrene	12.4	1006.8	136	2	907
m-cymene	12.5	1021.5	134	2	909
trans, trans-2,4-heptadienal	12.7	1009.6	81	2	939
2,5-dimethyl-nonane	12.8	1017.6	57	3	886
2,6-dimethylnonane	12.9	1021.5	71	2	909
D-limonene	13.2	1029.8	107	3	861
5-Ethylcyclopent-1-enecarboxaldehyde	13.2	1030.5	95	3	828
Beta-phellandrene	13.2	1031.5	136	3	890
4-propyl-phenol	13.3	1038.6	107	3	849
2,2,6-trimethylcyclohexanone	13.3	1035.8	82	3	896
Phenylacetaldehyde	13.4	1040.2	120	2	963
2,6-dimethyl-2,6-octadiene	13.5	1051.4	95	3	812
1-heptanol	13.6	970.2	56	2	938
Salicylaldehyde	13.6	1044.3	122	3	880
trans 2-octenal	13.8	1058.2	97	2	901

1-octanol	14.0	1071.6	84	2	941
Methyl-2-oxohexanoate	14.1	1061	85	3	812
trans, 2-octen-1-ol	14.3	1066.7	105	3	824
Citral	14.5	1073.7	69	3	803
p-thymol	14.5	1103.4	866	3	866
4-methyl-benzaldehyde	14.6	1083.2	119	2	938
p-cymenene	14.8	1090.1	132	3	895
2-methoxyphenol	14.8	1084.5	109	2	951
Perillene	15.0	1095.7	150	3	736
Sulcatol	15.1	995.5	128	2	945
n-undecane	15.2	1100.0	156	1	
Phenylethyl alcohol	15.2	1110.0	122	2	951
n-decane	15.3	1000.0	142	1	
Beta-isophorone	15.4	1078.6	138	3	833
Octanal	15.6	1003.6	84	2	941

trans, trans, 2,4-octadienal	15.6	1110.3	81	3	805
trans, trans, octadienal	15.6	1110.3	81	3	805
Methyloctanonate	15.8	1122.3	74	3	816
*trans, trans,*2,6-nonadienal	15.9	1152.2	70	3	843
cis,trans, 2,7-dimethyl-3,5-octadiene	16.3	828.5	138	3	856
Benzyl cyanide	16.4	1137.2	117	2	935
5-ethyl-6-methyl-3-hepten-2-one	16.5	1140.1	112	3	864
*trans,*2-nonenal	16.8	1159.4	96	2	909
Octanoic acid	17.0	1165.7	101	3	851
trans, 2-nonenal	17.1	1159.4	96	2	909
4-ethyl-benzaldehyde	17.2	1162.8	134	3	822
Pinocarvone	17.2	1163.7	135	3	823
2-isobutylthiazole	17.3	1029.0.	99	3	899
Alpha phellandren-8-ol	17.5	1172.2	94	3	858
Benzyl alcohol	17.6	1033.6	108	2	971

3,5-dimethylbenzaldehde	17.6	1175.0.	133	2	939
1,3,4-trimethyl-3-cyclohexene-1-carboxaldehyde	17.7	1178.5	109	3	675
Methyl salicylate	17.9	1189.6	152	2	965
Cryptone	18.0	1188.3	138	3	863
n-dodecane	18.0	1200.0	170	1	
Decanal	18.1	1205.0	112	2	948
trans, trans,2,4-nonadienal	18.4	1213.6	81	3	885
Beta-cyclocitral	18.7	1215.7	152	1	
Nonanoic acid, methyl ester	18.9	1217.6	141	3	812
2,3-epoxygerianial	18.9	1228.0	121	3	877
4,8-dimethyl-1-nonanol	19.2	1224.1	126	3	805
Beta-citral	19.2	1235.1	134	2	946
Acetophenone	19.4	1061.5	105	2	967
Beta-homocyclocitral	19.8	1254.4	151	2	909
trans 2-decenal	20.1	1260.1	70	2	926

2,4-decadienal	20.3	1317.7	81	3	899
Nonanoic acid	20.5	1263.1	129	3	860
Formic acid, (2-methylphenyl) methyl ester	21.7	1297.4	104	3	893
Unknown - 22.2	21.9	1313.8	150	4	
Oxo-cyclocitral	21.9	1305.6	166	3	804
beta-linalool	22.0	1099.9	93	2	907
4,5-epoxy-2-decenal	22.2	1372.8	68	3	825
2-undecen-1-al	23.9	1364.1	97	3	812
2-methylpentanoic acid	24.0	1369.3	99	3	851
Dodecanal	24.2	1408.7	96	2	966
Unknown - 24.2	24.3	1374.4	180	4	
Alpha copaene	24.3	1376.6	161	3	881
Alpha-ionone	25.2	1426.5	192	2	927
geranylacetone / pseudoionone	25.6	1446.7	136	1	
7,8-Dihydro-beta-ionone	26.0	1432.5	161	3	836

Beta-ionone-5,6-epoxide	26.3	1481.7	123	2	940
trans, beta-ionone	27.3	1484.2	192	1	
Dihydroactinidiolide	28.3	1529.5	180	2	923
Delta-cadinene	28.3	1514.9	161	3	794
2,3,5,8-Tetramethyl-1,5,9-decatriene	28.8	1532.4	136	3	816
Psuedoionone	30.0	1580.7	124	3	823
4-oxo-beta-ionone	30.1	1658.4	163	1	
Propanoic acid, 2-methyl-, 1-(1,1-dimethylethyl)-2-methyl-1,3-propanediyl ester	30.1	1584.0	159	3	761
3,3-dimethylhexane	30.5	1598.1	57	3	856
3,5-dimethylundecane	30.5	1598.2	85	3	844
Farnesyl acetone	31.9	1907.6	136	2	920
Undecanal	35.9	1306.1	126	2	965
Hexadecanoic acid, methyl ester	37.7	1921.5	74	2	920
Tridecanal	47.4	1510.6	152	2	958

7.1.4 Appendix 4 - Quantification of semi-volatiles from ZW(Ø)RI(Ø)UU/U0/00

Table 7-4. Relative amounts of volatiles produced by all genotypes of ZW(Ø)RI(Ø)UU/U0/00
All values have been scaled, with the smallest value set at 1 and shown ± the standard deviation.

Metabolite	Azygous	ZWRIUU	ZWRI00	ZWRIU0
Acetic acid	118.84 ±28.10	158.29 ±70.04	129.71 ±88.39	155.48 ±56.83
Formic acid	16.96 ±23.98	0.00 ±0.00	0.00 ±0.00	40.68 ±8.44
Isopropyl acetate	11.62 ±5.69	4.71 ±5.63	0.00 ±0.00	20.71 ±6.71
Pentanal	425.82 ±134.16	479.00 ±225.82	707.46 ±496.49	485.26 ±234.51
1-Penten-3-one	1195.44 ±1336.10	1493.73 ±264.24	909.16 ±908.06	1141.49 ±149.62
2-Ethylfuran	139.46 ±92.66	109.90 ±61.23	133.15 ±37.02	256.87 ±79.71
3-methyl-butanenitrile,	0.00 ±0.00	105.88 ±40.52	252.69 ±151.79	141.76 ±71.38
2,2,3-trimethylcyclobutanone	0.00 ±0.00	182.45 ±159.83	76.17 ±49.10	33.75 ±58.46
2-methyl-1-butanol	53.08 ±8.85	0.00 ±0.00	0.00 ±0.00	0.00 ±0.00
Dimethyl disulphide	34.42 ±16.02	59.26 ±22.58	22.56 ±5.89	44.23 ±18.29
1-pentanol	382.64 ±151.26	224.78 ±135.24	422.40 ±162.01	998.82 ±676.53

trans, 2-pentenal	1003.04	±693.60	962.48	±177.13	645.94	±533.61	518.78	±155.89
cis, 2-penten-1-ol	95.28	±134.74	108.68	±48.67	0.00	±0.00	0.00	±0.00
Hexanal	50360.79	±2131.76	46132.43	±10621.62	53459.51	±6993.16	54383.09	±9780.47
n-octane	0.00	±0.00	0.00	±0.00	0.00	±0.00	309.11	±85.98
n-nonane	0.00	±0.00	0.00	±0.00	122.99	±107.23	0.00	±0.00
2,4-dimethyl-1-heptene	2.55	±3.61	9.38	±8.34	0.00	±0.00	11.71	±11.52
2-hexenal	26460.88	±10628.46	20248.66	±9157.24	19555.94	±1732.98	20714.42	±5396.83
2-acetyl-5-methylfuran	0.00	±0.00	0.00	±0.00	14.68	±13.87	0.00	±0.00
Ethylbenzene	58.48	±23.71	61.76	±29.59	48.36	±12.87	57.86	±33.77
1-hexanol	152.52	±18.98	162.21	±132.46	10096.41	±16360.05	574.39	±618.04
2-methyl-1-butanol acetate	18.89	±6.68	12.55	±21.73	0.00	±0.00	35.29	±42.65
2-heptanone	73.33	±41.23	81.96	±33.07	105.74	±31.28	103.81	±16.69
2-n-butylfuran	7.63	±10.79	0.00	±0.00	37.42	±32.81	0.00	±0.00
Styrene	414.94	±17.45	324.05	±125.57	392.24	±224.32	343.25	±146.23
trans, hept-4-enal	81.97	±85.42	38.17	±2.83	53.73	±59.72	0.00	±0.00

1-heptanal	530.82	±287.98	579.52	±125.88	925.70	±212.00	550.47	±188.39
1-Nitropentane	211.13	±298.58	1081.26	±707.19	6836.89	±1049.24	2007.91	±549.00
Pentyl-oxirane	284.90	±94.95	0.00	±0.00	0.00	±0.00	0.00	±0.00
trans, trans, 2,4-Hexadienal	488.75	±376.62	262.88	±219.29	262.08	±242.02	208.93	±73.97
Methylhexoate	113.26	±2.21	327.78	±221.96	309.28	±17.96	745.85	±416.77
1-ethyl-5-methylcyclopentene	182.29	±257.79	710.69	±403.58	336.34	±291.30	440.10	±175.91
3-Hexenoic acid methyl ester	0.00	±0.00	51.24	±88.74	33.56	±58.12	39.74	±34.73
3,5-dimethyl-phenol	225.54	±107.55	0.00	±0.00	0.00	±0.00	0.00	±0.00
4-methyl-2-heptanone	50.31	±7.65	60.65	±18.35	50.14	±50.35	50.98	±44.71
6-methyl- 2-heptanone	57.68	±39.67	21.43	±25.77	36.54	±15.97	0.00	±0.00
cis, 2-heptenal	8620.09	±3351.38	5636.50	±1175.08	7987.00	±4271.73	6109.31	±3633.47
2,5-dihydro- thiophene	0.00	±0.00	16.47	±28.53	18.79	±32.55	0.00	±0.00
Benzaldehyde	901.52	±265.44	495.60	±7.09	509.49	±268.09	1003.06	±542.56
2-methyl-nonane	0.00	±0.00	0.00	±0.00	52.31	±58.13	0.00	±0.00
n-decane	64.27	±4.34	132.01	±70.29	124.54	±61.13	114.15	±83.23

2-methyl-1-hepten-6-one	24423.43	±13410.16	0.00	±0.00	0.00	±0.00	0.00	±0.00
Dimethyltrisulfide	16.87	±9.43	38.93	±39.41	29.16	±11.89	30.93	±7.29
1-heptanol	0.00	±0.00	0.00	±0.00	411.22	±692.19	0.00	±0.00
alpha-phellandrene	313.55	±91.46	587.69	±431.44	404.14	±450.10	348.75	±394.53
m-Cymene	182.19	±107.35	215.47	±193.02	294.59	±268.09	164.28	±97.14
Sulcatone	36680.22	±3923.56	3065.28	±2230.57	3390.75	±607.07	0.00	±0.00
1-octen-3-one	1562.79	±954.90	1146.09	±445.69	1016.64	±697.40	446.43	±210.36
1-octen-3-ol	271.74	±70.05	367.59	±123.28	705.95	±255.37	885.29	±283.63
2-pentylfuran	3048.84	±1895.31	3215.49	±1496.35	5612.82	±2648.34	3721.36	±306.06
Sulcatol	1016.69	±416.18	0.00	±0.00	0.00	±0.00	0.00	±0.00
(+)-4-Carene	94.33	±88.75	382.31	±252.05	775.09	±336.92	401.21	±185.83
trans, *trans*, 2,4-Heptadienal	544.31	±439.92	789.26	±496.41	666.55	±331.83	583.33	±188.78
delta-4-Carene	181.95	±113.27	401.19	±432.60	737.81	±404.96	495.86	±199.73
Octanal	821.40	±624.37	750.90	±523.19	1519.44	±1120.41	449.97	±363.19
Beta-phellandrene	399.70	±151.41	654.02	±337.07	497.22	±437.64	646.41	±162.66

2,5-dimethyl-nonane	22.47	±31.78	54.08	±17.32	83.34	±73.44	43.80	±39.16
2,6-dimethyl-nonane	97.97	±58.82	94.89	±23.22	99.03	±68.61	99.30	±49.40
D-limonene	869.38	±837.72	0.00	±0.00	33.25	±57.59	0.00	±0.00
5-Ethylcyclopent-1-enecarboxaldehyde	1093.08	±879.88	935.62	±353.06	1499.88	±846.95	2008.13	±772.59
2-isobutylthiazole	2331.29	±891.39	5322.81	±1186.29	12377.22	±2238.67	5344.99	±2873.63
2,2,6-trimethyl-cyclohexanone	158.25	±51.69	0.00	±0.00	0.00	±0.00	0.00	±0.00
Benzyl alcohol	121.40	±171.69	0.00	±0.00	0.00	±0.00	93.19	±161.41
4-propyl-phenol	125.98	±84.19	99.91	±97.94	106.45	±56.12	78.00	±54.12
Phenylacetaldehyde	702.26	±330.79	736.70	±368.90	1122.84	±108.09	1098.21	±430.68
Salicylaldehyde	264.33	±209.06	72.09	±3.24	25.58	±44.30	132.96	±30.73
1-octanol	110.50	±112.75	0.00	±0.00	549.37	±565.09	237.91	±144.86
2,6-dimethyl-2,6-octadiene	1922.27	±927.11	31.29	±36.78	47.04	±42.74	11.35	±9.85
trans, 2-octenal	9333.98	±2330.99	5702.53	±233.34	11431.65	±6961.35	8738.05	±2285.61
Methyl-2-oxohexanoate	273.15	±24.97	160.83	±130.16	198.38	±275.70	93.82	±64.44

Acetophenone	224.88	±67.24	117.93	±102.18	162.56	±109.72	118.63	±90.11
trans, 2-octen-1-ol	131.89	±44.42	0.00	±0.00	565.48	±717.57	265.44	±74.01
Citral	486.03	±340.41	50.92	±88.20	40.25	±46.66	0.00	±0.00
Beta-isophorone	0.00	±0.00	293.45	±194.50	351.34	±43.09	11.78	±20.41
4-methyl-benzaldehyde	256.76	±268.11	825.09	±1267.69	65.25	±57.95	0.00	±0.00
2-methoxyphenol	224.87	±259.83	67.55	±13.97	21.34	±18.69	125.13	±63.06
p-thymol	127.29	±30.50	79.85	±14.97	54.08	±47.76	0.00	±0.00
p-Cymenene	100.36	±68.39	132.13	±171.69	64.31	±14.05	34.20	±15.61
Perillene	1063.56	±269.88	0.00	±0.00	0.00	±0.00	0.00	±0.00
beta-linalool	389.85	±13.40	171.88	±172.95	354.17	±97.44	146.58	±29.71
trans, trans, octadienal	194.34	±57.08	89.45	±29.66	165.95	±109.82	87.97	±24.42
Phenylethyl alcohol	515.76	±627.46	248.72	±232.87	313.44	±99.20	586.57	±132.18
Methyl octanoate	53.33	±29.40	116.16	±92.99	117.29	±103.87	66.63	±16.63
cis, trans, 2,7-dimethyl-3,5-octadiene	689.65	±360.97	42.23	±65.82	0.00	±0.00	0.00	±0.00

Benzyl cyanide	82.79	±61.81	677.64	±643.54	180.88	±135.92	271.64	±349.75
5-ethyl-6-methyl-3-hepten-2-one	32.60	±46.10	55.89	±49.48	159.11	±84.86	70.47	±32.17
trans, trans, 2-6-nonadienal	53.15	±23.31	27.39	±5.55	20.66	±21.32	15.92	±8.67
trans, 2-nonenal	2086.03	±1333.18	980.23	±293.86	1105.87	±308.80	874.59	±330.25
4-ethyl-benzaldehyde	54.54	±77.14	23.87	±41.34	60.74	±32.31	32.54	±30.76
Pinocarvone	0.00	±0.00	79.31	±137.36	29.27	±50.70	0.00	±0.00
Octanoic acid	147.78	±85.56	213.01	±162.93	111.74	±123.17	197.01	±96.58
Alpha phellandren-8-ol	0.00	±0.00	43.89	±76.01	41.63	±44.65	26.60	±24.80
3,5-dimethyl-benzaldehyde	159.93	±38.48	153.21	±47.93	201.81	±118.31	125.90	±91.79
1,3,4-trimethyl-3-Cyclohexene-1-carboxaldehyde	176.69	±89.70	0.00	±0.00	0.00	±0.00	0.00	±0.00
Cryptone	386.74	±314.37	481.69	±758.12	359.92	±153.37	157.45	±106.83
Methyl salicylate	429.43	±41.72	287.41	±201.15	62.22	±10.26	161.06	±229.21
n-dodecane	51.10	±72.27	96.55	±26.00	79.97	±28.91	69.51	±30.51
trans, trans, 2,4-Nonadienal	339.97	±295.06	255.43	±137.25	560.28	±108.32	601.56	±314.27

Beta-cyclocitral	1179.85	±755.35	650.08	±448.05	570.33	±146.48	309.69	±110.17
Nonanoic acid, methyl ester	39.66	±15.34	47.30	±25.99	38.71	±12.75	48.58	±17.19
4,8-dimethyl-1-nonanol	81.63	±115.45	0.00	±0.00	20.64	±35.75	0.00	±0.00
2,3-epoxygerianial	941.89	±394.13	0.00	±0.00	7.64	±13.24	0.00	±0.00
Beta-citral	4612.08	±1518.04	138.33	±172.52	256.22	±118.62	42.43	±73.49
Beta-homocyclocitral	43.58	±28.26	±30.24	±21.14	17.32	±16.61	0.00	±0.00
trans, 2-decenal	1033.93	±1052.55	349.72	±245.80	707.88	±236.38	893.97	±308.21
Nonanoic acid	0.00	±0.00	457.85	±300.52	375.81	±306.07	511.75	±352.56
Formic acid, (2-methylphenyl)methyl ester	435.79	±90.55	416.19	±144.31	3175.29	±699.58	1511.67	±761.88
Oxo-cyclocitral	0.00	±0.00	1363.48	±1249.70	2261.46	±677.52	145.73	±188.80
2,4-Decadienal	1470.60	±1035.23	691.46	±491.51	1302.83	±1240.20	1303.74	±367.82
Undecanal	183.65	±259.72	57.26	±99.17	143.79	±129.53	0.00	±0.00
2-undecen-1-al	420.21	±478.66	62.02	±77.21	211.18	±55.99	149.70	±114.56
2-methyl-pentanoic acid	0.00	±0.00	18.05	±20.69	21.86	±11.68	4.77	±8.26

4,5-epoxy-2-decenal	774.93	±505.28	193.16	±87.12	385.04	±242.18	614.54	±139.04
Alpha copaene	0.00	±0.00	0.00	±0.00	151.84	±215.55	294.09	±346.09
Dodecanal	88.35	±115.26	80.20	±74.56	133.75	±33.58	25.92	±4.14
Alpha-Ionone	54.17	±52.25	0.00	±0.00	0.00	±0.00	0.00	±0.00
Geranylacetone	20537.64	±5880.85	1784.34	±1216.88	2699.01	±688.54	644.37	±136.50
7,8-Dihydro-beta-ionone	0.00	±0.00	0.00	±0.00	10.38	±11.63	4.46	±7.72
Pseudoionone	23128.07	±2217.44	1784.34	±1216.88	2699.01	±688.54	644.37	±136.50
Beta-ionone-5,6-epoxide	379.28	±266.72	231.91	±219.98	242.52	±71.50	78.02	±57.64
Tridecanal	29.59	±41.85	15.76	±27.29	0.00	±0.00	0.00	±0.00
Dihydroactinidiolide	180.79	±122.88	149.75	±106.77	174.36	±100.71	34.20	±12.66
1,5,9-Decatriene, 2,3,5,8-tetramethyl-	82.07	±61.66	0.00	±0.00	0.00	±0.00	0.00	±0.00
Propanoic acid, 2-methyl-, 1-(1,1-dimethylethyl)-2-methyl-1,3-propanediyl ester	74.94	±37.28	54.43	±10.68	72.03	±11.02	51.48	±21.30
3,3-dimethyl-hexane	0.00	±0.00	7.24	±7.78	0.00	±0.00	0.00	±0.00

3,5-dimethyl-undecane	0.00 ±0.00	3.50 ±6.06	1.00 ±1.73	0.00 ±0.00
4-oxo-beta-Ionone	0.00 ±0.00	46.53 ±70.51	76.01 ±74.65	2.50 ±4.33
Farnesyl acetone	1623.57 ±1128.50	0.00 ±0.00	0.00 ±0.00	0.00 ±0.00
Hexadecanoic acid, methyl ester	0.00 ±0.00	0.00 ±0.00	11.50 ±19.92	28.84 ±49.95

7.1.5 Appendix 5 - Detailed carotenoid analysis of ZWØRIØUU/U0/00 leaf material (F_2)

Table 7-5. Carotenoid profile of ZWØRIØUU/U0/00 leaves
Amounts calculated from a minimum of three biological and three technical replicates ± standard deviation.

Carotenoid	Azygous	ZWRI00	ZWRIU0	ZWRIUU
Neoxanthin	229.41 ±12.63	3.06 ±1.35	59.82 ±17.09	57.42 ±23.81
Violaxanthin	486.08 ±1.01	9.60 ±4.32	151.56 ±68.20	160.31 ±58.98
Adonixanthin epoxide	0.00 ±0.00	140.41 ±111.49	2763.44 ±1391.77	3159.30 ±683.30
Astaxanthin	0.00 ±0.00	322.83 ±199.91	1613.44 ±595.21	2087.83 ±208.40
Adonixanthin	0.00 ±0.00	32.94 ±7.93	1273.26 ±338.07	1243.03 ±643.05
Unknown	0.00 ±0.00	1008.17 ±598.41	1749.59 ±645.02	2191.66 ±139.54
Lutein	1042.83 ±27.40	248.53 ±73.96	203.89 ±85.91	236.70 ±58.74
Antherxanthin	1554.66 ±249.07	309.22 ±91.86	265.47 ±118.72	300.44 ±84.26
Phoenicoxanthin	0.00 ±0.00	1457.65 ±566.07	127.77 ±63.94	497.36 ±133.70
Canthaxanthin	0.00 ±0.00	603.31 ±172.03	0.00 ±0.00	67.88 ±21.93
3OH	0.00 ±0.00	0.00 ±0.00	30.78 ±15.87	26.47 ±7.77
Echinenone	0.00 ±0.00	67.07 ±31.85	5.71 ±2.46	37.92 ±9.51
Beta-carotene	6877.24 ±1178.19	0.00 ±0.00	0.00 ±0.00	0.00 ±0.00

7.1.6 Appendix 6 - Quantification of metabolites analyses from the broader metabolism of ZWØRIØUU/U0/00

Table 7-6. Relative amounts of significant metabolites from the broader metabolism
Each value is an average of six biological replicates ± the standard deviation. Values have been scaled to the smallest, non-zero value.

Metabolite	Azygous	ZWRI00	ZWRIU0
Aconitic acid	497.59 ±145.35	613.02 ±118.07	455.86 ±91.57
Alanine	130.11 ±64.74	45.37 ±73.76	108.09 ±41.16
Alpha amyrin	8951.11 ±3385.27	5791.81 ±2989.05	6332.90 ±2071.85
Alpha tocopherol	17312.52 ±1559.80	29939.34 ±2199.12	32488.52 ±4089.36
Arabinose/xylose/ribose/lyxose	215.19 ±83.65	71.23 ±36.49	421.60 ±542.40
Aspartic acid	958.65 ±589.38	378.43 ±226.55	297.73 ±191.82
Beta-Amyrin	17995.17 ±2618.84	11190.11 ±4173.53	11622.00 ±2691.91
C16:0	30075.27 ±3343.97	35850.78 ±4762.78	32628.10 ±6965.88
C17:0	241.56 ±51.75	212.26 ±141.70	229.23 ±134.81
C18:0	16639.92 ±2208.00	21344.14 ±3765.05	12940.82 ±2196.43
C23H48, Tricosane	251.73 ±391.32	444.47 ±649.50	0.00 ±0.00
C24:0	1547.54 ±203.20	1262.48 ±211.19	1834.12 ±676.71

C26:0	67.98	±166.52	0.00	±0.00	142.41	±318.44
C29H60, Nonacosane	0.00	±0.00	0.00	±0.00	1729.52	±3867.32
C31H64, Hentriacontane	10723.57	±5973.02	7271.13	±6879.28	12351.83	±9010.18
C32-ol	739.61	±639.51	430.60	±415.07	256.01	±354.05
Carbamic acid	46.47	±16.23	78.76	±24.27	76.49	±46.86
Citraconic acid	360.98	±443.71	165.86	±39.60	160.45	±101.44
Citric acid	25026.70	±6253.37	35632.92	±5512.09	30033.63	±4510.75
Cyclohexaneacetic acid, trimethylsilyl ester	32.14	±38.38	19.37	±25.81	18.86	±22.58
D-(-)-Ribofuranose	626.46	±263.59	804.79	±235.84	779.47	±348.55
D-Ribose	44.06	±18.52	53.23	±15.52	46.95	±28.77
Erythrofuranose	29.18	±10.47	32.01	±13.77	44.86	±13.56
Fructose	94107.00	±6433.05	100232.20	±5618.53	120301.77	±7671.21
Fructose isomer	5167.39	±5699.91	2063.53	±2514.43	721.26	±507.84
GABA	3645.68	±2103.49	1894.38	±2188.03	714.37	±591.61
Galactaric acid/Galacturonic acid	81.53	±47.14	30.25	±17.16	167.46	±112.89

Galactose	0.00	±0.00	439.31	±982.33	30.45	±68.10
Gluconic acid	354.71	±45.13	287.67	±55.89	340.56	±47.28
Glucose/Galactose	6505.63	±7601.92	3266.53	±4841.58	2313.93	±2270.64
Glyceric acid	10.40	±5.92	0.00	±0.00	0.00	±0.00
Glycerol	4464.56	±4773.20	8543.99	±4516.66	9486.20	±1517.23
Glycerol-3-P	1.46	±3.59	0.00	±0.00	2.00	±4.46
Glycine	49.79	±35.70	13.34	±13.52	9.53	±16.01
Inositol	1623.52	±619.38	684.73	±442.08	1277.43	±669.20
Isocitric acid	206.59	±179.83	48.66	±108.82	433.73	±77.64
Isoleucine	162.97	±81.85	2.81	±6.29	16.40	±19.33
Itaconic acid	872.97	±294.72	279.21	±191.58	272.36	±74.89
Leucine 2tms	162.97	±81.85	20.36	±15.52	23.34	±14.98
Linoleic acid/ octadecadienoic acid	24319.93	±6752.29	17868.08	±2955.31	20571.08	±3397.59
Lyxopyranose	6378.30	±7722.59	2149.48	±3277.75	2323.62	±2258.36
Lyxose isomer	11004.03	±26741.84	0.00	±0.00	68.75	±153.74

Malic acid	792.51	±381.64	2389.93	±513.23	1289.57	±610.14
Mannose/Glucose	102844.97	±13934.25	114319.62	±10174.90	125713.15	±8833.37
Mesaconic acid	21.33	±11.87	32.69	±30.56	16.24	±16.30
Methylphosphate	122.09	±143.07	138.99	±95.04	960.13	±376.18
Narigenin peak 1	10756.27	±3650.88	11972.64	±7937.45	9866.48	±4524.28
Phosphoric acid	4354.47	±2901.38	4502.88	±1095.66	3454.97	±1812.17
Propanoic acid, 3,3'-thiobis-, didodecyl ester	98250.00	±46538.63	145314.66	±114438.09	153869.34	±55837.92
Pyroglutamic acid - Proline	4708.05	±2042.21	501.16	±582.01	917.31	±444.57
Sedoheptulose	95.31	±42.79	72.64	±25.28	146.12	±119.87
Sitosterol	1044.99	±1846.89	7076.49	±2774.09	7377.07	±4930.18
Narigenin peak 2	10401.88	±17668.89	57356.79	±43232.67	21550.93	±10774.80
Stigmasterol	11165.82	±2002.63	19253.11	±3583.60	17823.98	±3481.19
Sucrose	305.43	±493.81	718.99	±775.55	902.73	±690.61
Gamma tocopherol tms-derivative	2385.33	±1438.42	304.66	±98.88	848.60	±692.36

Unknown 4',5,7-Trihydroxyflavanone, tris(trimethylsilyl) ether	1009.71	±1753.47	5122.52	±2095.75	3031.35	±877.50
Unknown C16:0 propylester	5229.73	±4153.50	1747.68	±2413.91	1953.46	±4223.53
Unknown Galactose	590.13	±680.57	230.40	±462.30	103.55	±177.50
Unknown Glycero-1-C14:0	338.47	±125.70	144.55	±99.99	251.14	±140.01
Unknown Glycero-1-C18:0	11170.29	±2517.84	9639.72	±5912.12	5457.68	±6448.85
Unknown Glycero-1-C18:2 *cis* 9,12	4459.89	±3501.95	2287.71	±3212.07	5958.99	±2137.55
Unknown Me-Fructose	809.40	±256.04	279.19	±105.50	327.14	±106.38
Unknown 55.3	7783.68	±4001.62	11012.71	±3653.26	10235.20	±2953.97
Unknown 59.40	2796.69	±4352.83	0.00	±0.00	3656.99	±5106.22
Unknow 41.0	7228.24	±4752.46	5745.60	±742.07	4549.12	±1279.20
Unknown Sugar	41.22	±45.79	15.47	±34.59	70.09	±39.94
Unknown Sugar derivative glucitol	0.00	±0.00	0.00	±0.00	33.64	±39.10
Unknown Turanose	373.84	±104.40	532.61	±106.33	646.02	±255.77
Unknown Xylulose	43.38	±20.04	32.79	±18.69	28.43	±21.24

Unknown 60.6	346.60 ±229.59	112.30 ±102.65	336.48 ±276.08
Unknown 9.2 tromethamine	2.18 ±3.45	1.16 ±2.60	1.00 ±2.24
Unknown - 18.2 Itaconic acid	69.67 ±78.14	104.96 ±183.91	33.07 ±45.92
Unknown - 18.5	94.04 ±51.39	97.96 ±47.92	29.69 ±53.69
Unknown - 21.3 (Ethanolamine (3TMS))	4.20 ±6.80	23.44 ±4.12	10.01 ±14.71
Unknown - 27.5 (Dodecanoic acid (1TMS))	79.52 ±87.59	122.62 ±73.09	265.83 ±278.43
Unknown 15.8 - Leucine 2-TMS	96.32 ±34.15	17.39 ±18.05	16.06 ±15.87
Unknown 32.7	169.06 ±31.93	342.96 ±76.31	395.86 ±56.78
Unknown 47.6	37.51 ±12.65	35.41 ±20.40	55.31 ±15.40
Unknown 2.1	22.07 ±19.19	24.18 ±14.40	33.35 ±7.19
Unknown 33.5m 2-Thiobarbituric acid 3-TMS	424.42 ±75.99	617.33 ±121.42	460.05 ±66.27
Unknown Glucaric acid	11.28 ±14.26	0.00 ±0.00	32.88 ±28.12
Valine	43.56 ±38.92	2.91 ±6.51	5.22 ±7.19

7.1.7 Appendix 7 - Genetic map and digestion of the ketocarotenoid construct

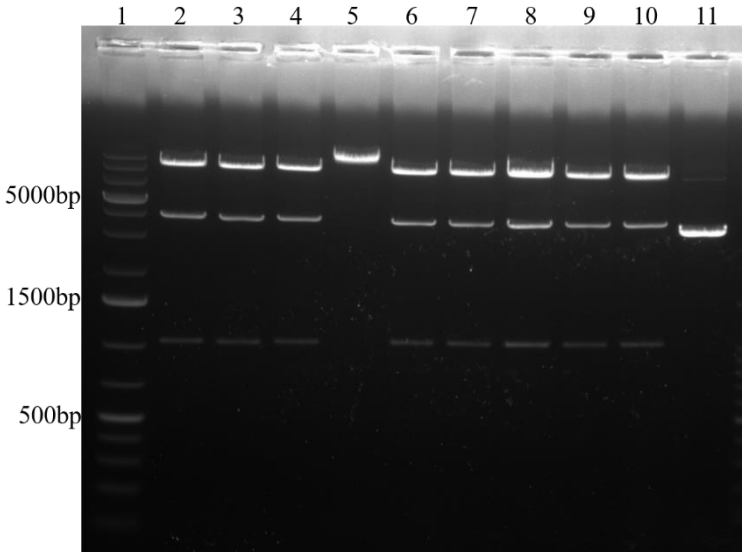

Figure 7-1. Agarose gel of the ketocarotenoid construct digested by XbaI
Lane 1 is the GeneRuler 1kb Plus ladder (Thermoscientific). Lanes 2-4 and 6-10 are correctly assembled plasmids. Lanes 5 and 11 are incorrect. Plasmids were also confirmed by sequencing.

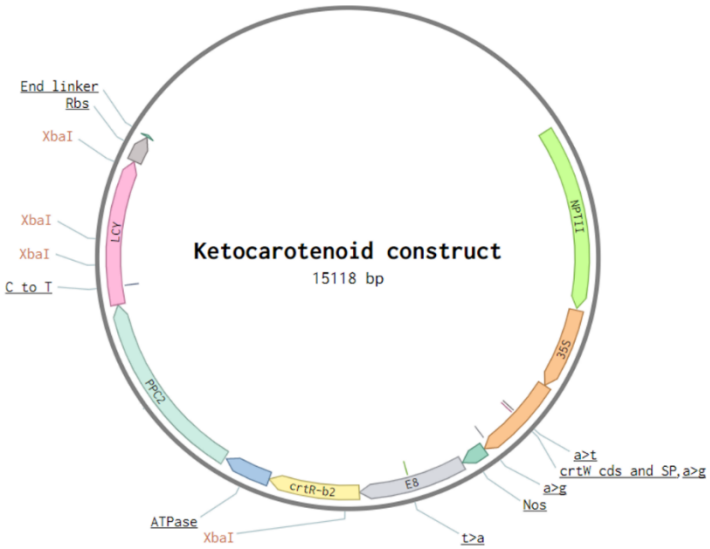

Figure 7-2. Genetic map of the ketocarotenoid construct
Contains, NPTII, 35S-*Crt*W-nos, E8-*Crt*R-*b2*-ATPase, PPC2-*lcy*-Rbs. XbaI was used to confirm the construct was correct.

7.1.8 Appendix 8 - Carotenoid content of plant with the ketocarotenoid construct including the pPAtUbq10 promoter

Table 7-7. Carotenoid content of the plant with *lcy* under the pPAtUbq10 promoter
Amounts in µg/g with ± standard deviation for the azygous control. S11 is a single copy plant with the ketocarotenoid construct (PPC2), U5 is the single copy plant with the alternative (Ubq) construct.

Metabolite	Azygous	S11 (PPC2)	U5 (Ubq)
Adonixanthin epoxide	0.00 ±0.00	0.00	0.00
Astaxanthin	0.00 ±0.00	130.48	132.72
Unknown A	0.00 ±0.00	12.33	28.21
Lutein	9.80 ±0.73	0.85	0.00
Phoenicoxanthin	0.00 ±0.00	213.41	592.63
Canthaxanthin	0.00 ±0.00	34.52	160.05
3OH' echinenone	0.00 ±0.00	1.84	3.93
Alpha-tocopherol	308.42 ±22.23	274.57	358.13
Echinenone	0.00 ±0.00	8.76	87.57
Lycopene	491.98 ±49.22	417.45	337.61
Phytoene	28.76 ±10.97	27.74	40.93
Gamma-carotene	10.93 ±1.70	7.24	8.21
Beta-carotene	78.56 ±5.69	41.62	692.87
Phytofluene	200.63 ±71.99	132.84	143.28
Total esters	0.00 ±0.00	44.31	128.13
Total free carotenoid	820.66 ±110.01	1073.39	2356.14
Total carotenoid	820.66 ±110.01	1117.70	2484.27

7.1.9 Appendix 9 - Quantification of semi-volatiles from $P^{WT/MT}ZW(Ø)RI(Ø)$

Table 7-8. Relative amounts of volatiles produced by all genotypes of $P^{WT/MT}ZW(Ø)RI(Ø)$
All values have been scaled, with the smallest value set at 1 and shown ± the standard deviation.

Metabolite	$P^{WT}ZWØRIØ$	$P^{MT}ZWØRIØ$	$P^{WT}ZWRI$	$P^{MT}ZWRI$
Octanal	312.03 ±171.18	219.89 ±70.68	157.19 ±20.36	213.65 ±64.53
delta-2/4-Carene	229.52 ±161.22	142.41 ±111.05	1255.10 ±161.93	625.14 ±400.38
alpha/beta Phellandrene	259.33 ±148.65	221.83 ±178.25	2104.54 ±639.41	832.47 ±613.98
2,4-Heptadienal, (E,E)	233.08 ±260.08	39.39 ±16.27	84.59 ±11.85	127.09 ±40.36
m-Cymene	57.09 ±15.25	65.64 ±22.01	307.81 ±63.08	138.35 ±88.15
2-Isobutylthiazole	1395.20 ±1434.26	236.11 ±74.79	146.33 ±102.79	508.12 ±300.19
4-propyl phenol	22.98 ±21.79	10.50 ±10.06	16.11 ±1.17	11.79 ±8.45
Phenylacetaldehyde	97.32 ±57.40	72.61 ±12.61	60.87 ±27.27	130.27 ±55.27
2,6-dimethyl-2,6-octadiene	336.26 ±151.33	289.63 ±54.81	0.00 ±0.00	5.11 ±7.58
trans, 2-octenal	3503.33 ±2416.36	1580.82 ±854.34	1160.96 ±454.97	2007.53 ±963.26
1-octanol	96.80 ±72.41	22.25 ±5.22	0.00 ±0.00	24.09 ±25.77

p-thymol	62.46	±36.59	40.70	±8.01	0.00	±0.00	1.16	±2.59
beta-Isophorone	0.00	±0.00	0.00	±0.00	62.15	±21.22	64.57	±55.04
4-methylbenzaldehyde	43.16	±31.53	12.83	±22.21	18.65	±18.24	39.94	±6.74
p-Cymenene	10.02	±4.62	13.70	±1.00	25.25	±6.43	9.32	±9.97
Perilline	191.08	±90.43	136.41	±9.90	0.00	±0.00	0.00	±0.00
n-undecane	394.88	±152.97	582.82	±117.50	432.24	±118.26	403.41	±107.79
Phenylethyl Alcohol	12.92	±25.84	18.78	±9.08	5.77	±10.00	21.13	±21.36
Methyloctanoate	187.87	±128.19	84.13	±45.88	83.12	±16.03	137.92	±58.36
trans, trans, 2-6-Nonadienal	17.82	±3.90	0.00	±0.00	6.35	±6.81	4.50	±3.15
trans, 2-Nonenal	426.45	±152.40	497.26	±338.70	159.02	±83.15	199.72	±143.24
Octanoic acid	52.37	±29.88	15.97	±27.65	11.44	±19.82	29.23	±14.96
Cryptone	0.00	±0.00	17.47	±15.81	52.86	±18.21	46.87	±56.90
Methyl salicylate	328.62	±534.47	101.97	±49.87	663.43	±562.23	117.40	±62.38
n-Dodecane	0.00	±0.00	9.32	±10.16	19.74	±7.09	3.07	±4.69
Decanal	213.03	±99.72	151.65	±21.10	113.99	±22.19	113.25	±40.09

trans, trans-2,4-Nonadienal	55.89	±81.59	3.07	±5.32	14.85	±13.70	20.04	±15.54
Beta-cyclocitral	313.46	±163.15	263.52	±21.00	103.28	±40.98	100.29	±34.81
Nonanoic acid, methyl ester	54.97	±21.84	18.71	±15.63	24.44	±6.42	50.27	±25.40
2,3-epoxygerianial	152.22	±112.97	86.68	±57.29	0.00	±0.00	0.00	±0.00
Beta-citral	971.84	±592.22	727.37	±303.85	0.00	±0.00	0.00	±0.00
Beta-homocyclocitral	4.04	±8.08	8.00	±6.93	0.00	±0.00	1.62	±3.63
trans, 2-Decenal	204.29	±138.20	63.35	±5.88	59.20	±55.71	105.12	±67.00
2,4-decadienal	515.69	±625.41	86.32	±78.59	93.54	±36.72	163.04	±76.88
Oxo-cyclocitral	0.00	±0.00	0.00	±0.00	548.12	±152.64	494.93	±377.79
Unknown 22.2	405.51	±342.64	139.73	±54.05	120.77	±23.73	325.23	±164.60
4,5-Epoxy-2-decenal	89.07	±103.89	8.11	±14.05	9.74	±9.24	10.53	±3.43
Unknown 24.2	56.03	±112.05	292.80	±245.47	24.12	±24.21	35.30	±52.42
Dodecanal	19.48	±17.10	12.98	±9.43	6.33	±8.63	5.54	±6.83
Alpha-ionone	29.71	±20.72	0.00	±0.00	0.00	±0.00	0.00	±0.00
Geranylacetone	4810.52	±2993.26	3082.76	±1356.96	276.21	±170.74	414.59	±307.59

Beta-ionone-5,6-epoxide	83.81	±44.86	84.85	±36.50	19.01	±6.78	33.83	±16.70
trans, beta-ionone	404.41	±224.85	326.50	±39.39	140.60	±36.46	142.21	±61.55
Delta-cadinene	36.22	±20.65	41.44	±28.23	27.59	±14.85	15.97	±9.46
Dihydroactinidiolide	42.19	±18.06	41.59	±9.15	0.00	±0.00	5.19	±11.60
Propanoic acid, 2-methyl-, 1-(1,1-dimethylethyl)-2-methyl-1,3-propanediyl ester	28.13	±9.73	24.39	±24.42	11.48	±10.40	0.00	±0.00
4-oxo-beta-ionone	0.00	±0.00	0.00	±0.00	9.05	±3.79	6.35	±3.42
Farnesyl acetone	170.64	±164.89	51.40	±89.02	0.00	±0.00	0.00	±0.00
2-Ethylfuran	41.46	±31.83	36.07	±10.10	98.86	±64.14	49.75	±22.23
Butanoic acid, methyl ester	5.32	±1.19	8.11	±1.83	10.15	±1.63	7.46	±2.09
Acetic acid	96.28	±35.88	25.40	±5.39	50.73	±26.81	84.97	±9.37
1-Penten-3-one	221.92	±109.03	159.51	±110.21	340.71	±78.89	218.08	±74.43
1-Pentanol	142.88	±45.56	90.23	±66.88	120.06	±40.14	163.48	±38.59
1-Butanol, 2-methyl	29.52	±37.07	22.66	±23.86	20.31	±9.59	28.53	±22.96

Pentanal	103.89	±45.44	104.59	±97.64	129.63	±33.49	182.91	±85.80
Butanenitrile, 3-methyl	51.73	±62.81	0.00	±0.00	4.47	±3.88	14.02	±16.35
trans, 2-Pentenal	166.77	±69.28	127.76	±60.47	167.83	±54.56	169.27	±46.95
Methyl isovalerate	18.24	±27.39	0.00	±0.00	0.00	±0.00	6.71	±9.99
cis, 2-Penten-1-ol	38.41	±21.46	5.03	±8.71	0.00	±0.00	23.17	±21.20
Hexanal	7745.84	±864.90	8488.13	±1071.95	9641.68	±1404.38	8249.90	±2336.46
2,4-Dimethyl-1-heptene	37.73	±16.20	18.42	±4.65	35.76	±34.61	48.46	±21.19
2-Hexenal	8836.98	±694.16	8085.97	±440.39	7563.97	±289.40	8575.98	±956.52
1-Hexanol	189.24	±256.33	150.25	±92.29	141.79	±81.03	546.36	±627.62
2-Heptanone	23.22	±14.03	21.36	±8.72	19.98	±1.21	30.47	±10.86
pentyloxirane	0.00	±0.00	0.00	±0.00	0.00	±0.00	28.38	±38.87
1-Heptanal	228.56	±54.76	207.65	±100.90	137.11	±20.89	204.14	±46.58
1-Nitropentane	1138.55	±1594.45	0.00	±0.00	0.00	±0.00	168.13	±171.94
trans, trans, 2,4-Hexadienal	44.54	±25.97	31.72	±28.22	0.00	±0.00	0.00	±0.00
Methyl hexoate	159.93	±65.93	113.06	±91.16	395.58	±303.76	418.78	±320.21

3-Heptyne, 5-methyl	693.14	±362.47	464.33	±71.89	494.20	±71.28	554.54	±150.48
Alpha-pinene	75.39	±48.22	120.05	±85.96	648.02	±489.63	256.42	±262.97
2-Heptanone, 4-methyl	18.54	±12.99	15.42	±7.13	24.50	±26.45	33.72	±18.67
3-ethoxypentane	26.03	±15.50	34.78	±16.46	27.21	±7.30	23.74	±12.20
cis, 2-Heptenal	1270.64	±824.31	819.61	±280.29	743.03	±148.56	1099.56	±308.84
Benzaldehyde	229.98	±142.58	114.67	±34.62	131.11	±21.69	138.26	±48.91
beta-pinene	361.51	±215.26	150.32	±134.50	1677.78	±1002.48	418.82	±213.62
1-Octen-3-one	205.64	±52.81	413.42	±401.83	180.16	±72.19	137.54	±105.56
1-Octen-3-ol	129.07	±90.01	97.88	±49.23	56.40	±35.58	110.96	±46.35
Sulcatone	6630.58	±2646.20	5459.10	±1494.90	522.05	±101.77	520.30	±180.72
2-Pentylfuran	1102.33	±803.90	458.43	±63.05	550.82	±169.89	735.47	±351.99
2-propylfuran	89.53	±119.06	38.87	±15.92	51.27	±8.64	57.82	±27.50
Sulcatol	179.21	±121.05	250.82	±113.76	0.00	±0.00	0.00	±0.00

References

Abramczyk, H., & Surmacki, J. (2016). Antitumor Activity of Dietary Carotenoids, and Prospects for Applications in Therapy. Chichester, UK: John Wiley & Sons, Ltd.

Aghajanpour, M., Nazer, M. R., Obeidavi, Z., Akbari, M., Ezati, P., & Kor, N. M. (2017). Functional foods and their role in cancer prevention and health promotion: a comprehensive review. *Am J Cancer Res, 7*(4), 740-769.

Ahmad, F. T., Mather, D. E., Law, H.-Y., Li, M., Yousif, S. A.-J., Chalmers, K. J., Asenstorfer, R. E., & Mares, D. J. (2015). Genetic control of lutein esterification in wheat (Triticum aestivum L.) grain. *Journal of Cereal Science, 64*, 109-115.

Alqudah, A. M., Sallam, A., Stephen Baenziger, P., & Börner, A. (2019). GWAS: Fast-forwarding gene identification and characterization in temperate Cereals: lessons from Barley - A review. *Journal of advanced research, 22*, 119-135.

Ambati, R. R., Siew Moi, P., Ravi, S., & Aswathanarayana, R. G. (2014). Astaxanthin: Sources, Extraction, Stability, Biological Activities and Its Commercial Applications—A Review. *Marine Drugs, 12*(1), 128-152.

Aracri, B., Bartley, G. E., Scolnik, P. A., & Giuliano, G. (1994). Sequence of the phytoene desaturase locus of tomato. *Plant Physiology, 106*(2), 789-789.

Ariizumi, T., Kishimoto, S., Kakami, R., Maoka, T., Hirakawa, H., Suzuki, Y., Ozeki, Y., Shirasawa, K., Bernillon, S., Okabe, Y., Moing, A., Asamizu, E., Rothan, C., Ohmiya, A., & Ezura, H. (2014). Identification of the carotenoid modifying gene PALE YELLOW PETAL 1 as an essential factor in xanthophyll esterification and yellow flower pigmentation in tomato (Solanum lycopersicum). *Plant J, 79*(3), 453-465.

Arunkumar, R., Gorusupudi, A., & Bernstein, P. S. (2020). The macular carotenoids: A biochemical overview. *Biochimica et Biophysica Acta (BBA) - Molecular and Cell Biology of Lipids*, 158617.

Asker, D. (2018). High throughput screening and profiling of high-value carotenoids from a wide diversity of bacteria in surface seawater. *Food Chemistry, 261*, 103-111.

Asker, D., Awad, T. S., Beppu, T., & Ueda, K. (2018). Screening and profiling of natural ketocarotenoids from environmental aquatic bacterial isolates. *Food Chemistry, 253*, 247-254.

ATBC. (1994). The Effect of Vitamin E and Beta Carotene on the Incidence of Lung Cancer and Other Cancers in Male Smokers. *New England Journal of Medicine, 330*(15), 1029-1035.

Azizi, M., Moteshafi, H., & Hashemi, M. (2020). Distinctive nutrient designs using statistical approach coupled with light feeding strategy to improve the Haematococcus pluvialis growth performance and astaxanthin accumulation. *Bioresource Technology, 300*, 122594.

Bai, C., Berman, J., Farre, G., Capell, T., Sandmann, G., Christou, P., & Zhu, C. (2017). Reconstruction of the astaxanthin biosynthesis pathway in rice endosperm reveals a metabolic bottleneck at the level of endogenous β-carotene hydroxylase activity. *Transgenic Research, 26*(1), 13-23.

Bai, Y. L., P. (2007). Domestication and Breeding of Tomatoes: What have We Gained and What Can We Gain in the Future? *Annals of Botany, 100*(5), 1085-1094.

Barredo, J. L., García-Estrada, C., Kosalkova, K., & Barreiro, C. (2017). Biosynthesis of Astaxanthin as a Main Carotenoid in the Heterobasidiomycetous Yeast Xanthophyllomyces dendrorhous. *Journal of fungi (Basel, Switzerland), 3*(3), 44.

Bergougnoux, V. (2014). The history of tomato: From domestication to biopharming. *Biotechnology Advances, 32*, 170-189.

Berry, H. M., Rickett, D. V., Baxter, C. J., Enfissi, E. M. A., & Fraser, P. D. (2019). Carotenoid biosynthesis and sequestration in red chilli pepper fruit and its impact on colour intensity traits. *Journal of Experimental Botany, 70*(10), 2637-2650.

Bhosale, P., Serban, B., Zhao, D. Y., & Bernstein, P. S. (2007). Identification and Metabolic Transformations of Carotenoids in Ocular Tissues of the Japanese Quail Coturnix japonica. *Biochemistry, 46*(31), 9050-9057.

Blasco, F., Kauffmann, I., & Schmid, R. D. (2004). CYP175A1 from Thermus thermophilus HB27, the first β-carotene hydroxylase of the P450 superfamily. *Applied Microbiology and Biotechnology, 64*(5), 671-674.

Bohn, T., Desmarchelier, C., El, S. N., Keijer, J., van Schothorst, E., Rühl, R., & Borel, P. (2019). β-Carotene in the human body: metabolic bioactivation pathways – from digestion to tissue distribution and excretion. *Proceedings of the Nutrition Society, 78*(1), 68-87.

Bouvier, F., D'Harlingue, A., Backhaus, R. A., Kumagai, M. H., & Camara, B. (2000). Identification of neoxanthin synthase as a carotenoid cyclase paralog. *The FEBS Journal, 267*(21), 6346-6352.

Bovy, A., Schijlen, E., & Hall, R. D. (2007). Metabolic engineering of flavonoids in tomato (Solanum lycopersicum): the potential for metabolomics. *Metabolomics, 3*, 399-412.

Bowen, P. E., Herbst-Espinosa, S. M., Hussain, E. A., & Stacewicz-Sapuntzakis, M. (2002). Esterification does not impair lutein bioavailability in humans. *J Nutr, 132*(12), 3668-3673.

Breitenbach, J., Bai, C., Rivera, S. M., Canela, R., Capell, T., Christou, P., Zhu, C., & Sandmann, G. (2014). A novel carotenoid, 4-keto-α-carotene, as an unexpected by-product during genetic engineering of carotenogenesis in rice callus. *Phytochemistry, 98*, 85-91.

Breithaupt, D. E. (2007). Modern application of xanthophylls in animal feeding – a review. *Trends in Food Science & Technology, 18*(10), 501-506.

Breithaupt, D. E., Weller, P., Wolters, M., & Hahn, A. (2003). Plasma response to a single dose of dietary beta-cryptoxanthin esters from papaya (Carica papaya L.) or non-esterified beta-cryptoxanthin in adult human subjects: a comparative study. *Br J Nutr, 90*(4), 795-801.

Breithaupt, D. E., Weller, P., Wolters, M., & Hahn, A. (2004). Comparison of plasma responses in human subjects after the ingestion of 3R,3R′-zeaxanthin dipalmitate from wolfberry (Lycium barbarum) and non-esterified 3R,3R′-zeaxanthin using chiral high-performance liquid chromatography. *British Journal of Nutrition, 91*(5), 707-713.

Breseghello, F., & Coelho, A. S. G. (2013). Traditional and Modern Plant Breeding Methods with Examples in Rice (Oryza sativa L.). *Journal of Agricultural and Food Chemistry, 61*(35), 8277-8286.

Britton, G., Liaaen-Jensen, S., & Pfander, H. (2004). Carotenoids Handbook: Birkhauser.

Britton, G., Liaaen-Jensen, S., & Pfander, H. (2009). Carotenoids Volume 5: Nutrition and Health (Vol. 5): Birkhäuser Base.

Bunea, A., Socaciu, C., & Pintea, A. (2014). Xanthophyll esters in fruits and vegetables. *Notulae Botanicae Horti Agrobotanici Cluj-Napoca, 42*(2), 310-324.

Camara, B., Hugueney, P., Bouvier, F., Kuntz, M., & Monéger, R. (1995). Biochemistry and Molecular Biology of Chromoplast Development. In K. W. Jeon & J. Jarvik (Eds.), *International Review of Cytology*, vol. 163 (pp. 175-247): Academic Press.

Campbell, R., Morris, W. L., Mortimer, C. L., Misawa, N., Ducreux, L. J. M., Morris, J. A., Hedley, P. E., Fraser, P. D., & Taylor, M. A. (2015). Optimising ketocarotenoid

production in potato tubers: Effect of genetic background, transgene combinations and environment. *Plant Science, 234*, 27-37.

Cazzonelli, C. I., & Pogson, B. J. (2010). Source to sink: regulation of carotenoid biosynthesis in plants. *Trends in Plant Science, 15*(5), 266-274.

Cheng, Y., Bian, W., Pang, X., Yu, J., Ahammed, G. J., Zhou, G., Wang, R., Ruan, M., Li, Z., Ye, Q., Yao, Z., Yang, Y., & Wan, H. (2017). Genome-Wide Identification and Evaluation of Reference Genes for Quantitative RT-PCR Analysis during Tomato Fruit Development. *Frontiers in Plant Science, 8*, 1440-1440.

Chew, B. P., Park, J. S., Wong, M. W., & Wong, T. S. (1999). A comparison of the anticancer activities of dietary beta-carotene, canthaxanthin and astaxanthin in mice in vivo. *Anticancer Res, 19*(3a), 1849-1853.

Choi, S. K., Harada, H., & Misawa, N. (2007). Characterization of two beta-carotene ketolases, CrtO and CrtW, by complementation analysis in Escherichia coli. - Abstract - Europe PMC. *Applied Microbiology and biotechnology, 75*(6), 1335-1341.

Cunningham, F. X., & Gantt, E. (2001). One ring or two? Determination of ring number in carotenoids by lycopene ε-cyclases. *PNAS, 98*(5), 2905-2910.

Cunningham, F. X., & Gantt, E. (2005). A study in scarlet: enzymes of ketocarotenoid biosynthesis in the flowers of Adonis aestivalis. *The Plant Journal, 41*(3), 478-492.

Cunningham, F. X., Jr., & Gantt, E. (2011). Elucidation of the pathway to astaxanthin in the flowers of Adonis aestivalis. *The Plant cell, 23*(8), 3055-3069.

D'Ambrosio, C., Stigliani, A. L., & Giorio, G. (2011). Overexpression of CrtR-b2 (carotene beta hydroxylase 2) from S. lycopersicum L. differentially affects xanthophyll synthesis and accumulation in transgenic tomato plants. *Transgenic Res, 20*(1), 47-60.

D'Ambrosio, C., Giorio, G., Marino, I., Merendino, A., Petrozza, A., Salfi, L., Stigliani, A. L., & Cellini, F. (2004). Virtually complete conversion of lycopene into β-carotene in fruits of tomato plants transformed with the tomato lycopene β-cyclase (tlcy-b) cDNA. *Plant Science, 166*(1), 207-214.

D'Ambrosio, C., Stigliani, A. L., & Giorio, G. (2018). CRISPR/Cas9 editing of carotenoid genes in tomato. *Transgenic Research, 27*(4), 367-378.

Davinelli, S., Nielsen, M. E., & Scapagnini, G. (2018). Astaxanthin in Skin Health, Repair, and Disease: A Comprehensive Review. *Nutrients, 10*(4), 522.

Davuluri, G. R., van Tuinen, A., Fraser, P. D., Manfredonia, A., Newman, R., Burgess, D., Brummell, D. A., King, S. R., Palys, J., Uhlig, J., Bramley, P. M., Pennings, H. M. J., & Bowler, C. (2005). Fruit-specific RNAi-mediated suppression of DET1 enhances carotenoid and flavonoid content in tomatoes. *Nature Biotechnology, 23*(7), 890-895.

DellaPenna, D., & Pogson, B. (2006). Vitamin synthesis in plants: Tocopherols and Carotenoids | Annual Review of Plant Biology. *Annual Review of Plant Biology, 57*, 711-738.

Diretto, G., Frusciante, S., Fabbri, C., Schauer, N., Busta, L., Wang, Z., Matas, A. J., Fiore, A., K.C. Rose, J., Fernie, A. R., Jetter, R., Mattei, B., Giovannoni, J., & Giuliano, G. (2019). Manipulation of β-carotene levels in tomato fruits results in increased ABA content and extended shelf life. *Plant Biotechnology Journal, n/a*(n/a).

Eckerstorfer, M. F., Dolezel, M., Heissenberger, A., Miklau, M., Reichenbecher, W., Steinbrecher, R. A., & Waßmann, F. (2019). An EU Perspective on Biosafety Considerations for Plants Developed by Genome Editing and Other New Genetic Modification Techniques (nGMs). *Frontiers in bioengineering and biotechnology, 7*, 31-31.

Egea, I., Barsan, C., Bian, W., Purgatto, E., Latché, A., Chervin, C., Bouzayen, M., & Pech, J.-C. (2010). Chromoplast Differentiation: Current Status and Perspectives. *Plant and Cell Physiology, 51*(10), 1601-1611.

Eisenreich, W., Rohdich, F., & Bacher, A. (2001). Deoxyxylulose phosphate pathway to terpenoids. *Trends in Plant Science, 6*(3), 78-84.

Eisenreich, W., Schwarz, M., Cartayrade, A., Arigoni, D., Zenk, M. H., & Bacher, A. (1998). The deoxyxylulose phosphate pathway of terpenoid biosynthesis in plants and microorganisms. *Chemistry & Biology, 5*(9), R221-R233.

Elmayan, T., & Vaucheret, H. (1996). Expression of single copies of a strongly expressed 35S transgene can be silenced post-transcriptionally. *The Plant Journal, 9*(6), 787-797.

Enfissi, E. M., Nogueira, M., D'Ambrosio, C., Stigliani, A. L., Giorio, G., Misawa, N., & Fraser, P. D. (2019). The road to astaxanthin production in tomato fruit reveals plastid and metabolic adaptation resulting in an unintended high lycopene genotype with delayed over-ripening properties. *Plant Biotechnol J, 17*(8), 1501-1513.

Engler, C., Youles, M., Gruetzner, R., Ehnert, T. E., Werner, S., Jones, J. D. G., Patron, N. J., & Marillonnet, S. (2014). A Golden Gate Modular Cloning Toolbox for Plants. *Synthetic Biology, 3*(11), 839-843.

Ernst, W. K. K. H. J. P. H. (1995). Preparation of astaxanthin. In, vol. US5654488A). United States: BASF SE.

European Parliament, C. o. t. E. U. (2003). Regulation (EC) No 1829/2003 of the European Parliament and of the Council of 22 September 2003 on genetically modified food and feed (Text with EEA relevance). In *COD 2001/0173*).

Failla, M. L., ; Rodrigues, D. B.,; Chitchumroonchokchai, C. (2019). Bioavailability and Metabolism of Carotenoid Esters. In A. Z. Mercadante (Ed.), *Carotenoid Esters in Foods: Physical, Chemical and Biological Properties*, (pp. 390-420): Royal Society of Chemistry.

Fantini, E., Falcone, G., Frusciante, S., Giliberto, L., & Giuliano, G. (2013). Dissection of tomato lycopene biosynthesis through virus-induced gene silencing. *Plant Physiology, 163*(2), 986-998.

FAOSTAT. (2017). FAOSTAT crops. In, vol. 2020). http://www.fao.org/faostat/en/#data/QC: FAO.

Farré, G., Perez-Fons, L., Decourcelle, M., Breitenbach, J., Hem, S., Zhu, C., Capell, T., Christou, P., Fraser, P. D., & Sandmann, G. (2016). Metabolic engineering of astaxanthin biosynthesis in maize endosperm and characterization of a prototype high oil hybrid. *Transgenic Research, 25*(4), 477-489.

Fernandez, A. I., Viron, N., Alhagdow, M., Karimi, M., Jones, M., Amsellem, Z., Sicard, A., Czerednik, A., Angenent, G., Grierson, D., May, S., Seymour, G., Eshed, Y., Lemaire-Chamley, M., Rothan, C., & Hilson, P. (2009). Flexible Tools for Gene Expression and Silencing in Tomato. *Plant Physiology, 151*(4).

Finn, T. E., Wang, L., Smolilo, D., Smith, N. A., White, R., Chaudhury, A., Dennis, E. S., & Wang, M.-B. (2011). Transgene expression and transgene-induced silencing in diploid and autotetraploid Arabidopsis. *Genetics, 187*(2), 409-423.

Fraser, P. D., & Bramley, P. M. (2004). The biosynthesis and nutritional uses of carotenoids. *Progress in Lipid Research, 43*(3), 228–265.

Fraser, P. D., Enfissi, E. M., & Bramley, P. M. (2009). Genetic engineering of carotenoid formation in tomato fruit and the potential application of systems and synthetic biology approaches. *Archives of Biochemisty and Biophysics, 483*(2), 196-204.

Fraser, P. D., Miura, Y., & Misawa, N. (1997). In vitro characterization of astaxanthin biosynthetic enzymes. *J Biol Chem, 272*(10), 6128-6135.

Fraser, P. D., Romer, S., Shipton, C. A., Mills, P. B., Kiano, J. W., Misawa, N., Drake, R. G., Schuch, W., & Bramley, P. M. (2002). Evaluation of transgenic tomato plants expressing an additional phytoene synthase in a fruit-specific manner. *Proceedings of the National Academy of Sciences, 99*(2), 1092.

Fray, R. G., Wallace, A., Fraser, P. D., Valero, D., Hedden, P., Bramley, P. M., & Grierson, D. (1995). Constitutive expression of a fruit phytoene synthase gene in transgenic tomatoes causes dwarfism by redirecting metabolites from the gibberellin pathway. *The Plant Journal, 8*(5), 693-701.

Fujisawa, M., Takita, E., Harada, H., Sakurai, N., Suzuki, H., Ohyama, K., Shibata, D., & Misawa, N. (2009). Pathway engineering of Brassica napus seeds using multiple key enzyme genes involved in ketocarotenoid formation. *Journal of Experimental Botany, 60*(4), 1319-1332.

Galpaz, N., Ronen, G., Khalfa, Z., Zamir, D., & Hirschberg, J. (2006). A Chromoplast-Specific Carotenoid Biosynthesis Pathway Is Revealed by Cloning of the Tomato white-flower Locus. *The Plant cell, 18*(8).

Galpaz, N., Wang, Q., Menda, N., Zamir, D., & Hirschberg, J. (2007). Abscisic acid deficiency in the tomato mutant high-pigment 3 leading to increased plastid number and higher fruit lycopene content - Galpaz - 2008 - The Plant Journal - Wiley Online Library. *The Plant Jounal, 53*(5).

Galpaz, N., Wang, Q., Menda, N., Zamir, D., & Hirschberg, J. (2008). Abscisic acid deficiency in the tomato mutant high-pigment 3 leading to increased plastid number and higher fruit lycopene content. *The Plant Journal, 53*(5), 717-730.

Gassel, S., Schewe, H., Schmidt, I., Schrader, J., & Sandmann, G. (2013). Multiple improvement of astaxanthin biosynthesis in Xanthophyllomyces dendrorhous by a combination of conventional mutagenesis and metabolic pathway engineering. *Biotechnology Letters, 35*(4), 565-569.

Gerjets, T., & Sandmann, G. (2006). Ketocarotenoid formation in transgenic potato. *Journal of Experimental Botany, 57*(14), 3639-3645.

Gerjets, T., Sandmann, M., Zhu, C., & Sandmann, G. (2007). Metabolic engineering of ketocarotenoid biosynthesis in leaves and flowers of tobacco species. *Biotechnology Journal, 2*(10), 1263-1269.

Ghatak, A., Chaturvedi, P., Paul, P., Agrawal, G. K., Rakwal, R., Kim, S. T., Weckwerth, W., & Gupta, R. (2017). Proteomics survey of Solanaceae family: Current status and challenges ahead. *Journal of Proteomics, 169*, 41-57.

Goto, S., Kogure, K., Abe, K., Kimata, Y., Kitahama, K., Yamashita, E., & Terada, H. (2001). Efficient radical trapping at the surface and inside the phospholipid membrane is responsible for highly potent antiperoxidative activity of the carotenoid astaxanthin. *Biochimica et Biophysica Acta (BBA) - Biomembranes, 1512*(2), 251-258.

Griffiths, K., Aggarwal, B. B., Singh, R. B., Buttar, H. S., Wilson, D., & De Meester, F. (2016). Food Antioxidants and Their Anti-Inflammatory Properties: A Potential Role in Cardiovascular Diseases and Cancer Prevention. *Diseases, 4*(3).

Hahn, F., Eisenhut, M., Mantegazza, O., & Weber, A. P. M. (2018). Homology-Directed Repair of a Defective Glabrous Gene in Arabidopsis With Cas9-Based Gene Targeting. *Frontiers in Plant Science, 9*, 424-424.

Harker, M., & Hirschberg, J. (1998). Molecular biology of carotenoid biosynthesis in photosynthetic organisms. *Methods in Enzymology, 297*, 224-263.

Hashimoto, H., Uragami, C., & Cogdell, R. J. (2016). Carotenoids and Photosynthesis. In C. Stange (Ed.), *Carotenoids in Nature: Biosynthesis, Regulation and Function*, (pp. 111-139). Cham: Springer International Publishing.

Hasunuma, T., Miyazawa, S. I., Yoshimura, S., Shinzaki, Y., Tomizawa, K. I., Shindo, K., Choi, S. K., Misawa, N., & Miyake, C. (2008). Biosynthesis of astaxanthin in tobacco leaves by transplastomic engineering. *The Plant Journal, 55*(5), 857-868.

Hasunuma, T. M., S. I.; Yoshimura, S.; Shinzaki, Y.; Tomizawa, K. I.; Shindo, K.; Choi, S. K.; Misawa, N.; Miyake, C. (2008). Biosynthesis of astaxanthin in tobacco leaves by transplastomic engineering. *The Plant Jounal*.

Hemmerlin, A., Harwood, J. L., & Bach, T. J. (2012). A raison d'être for two distinct pathways in the early steps of plant isoprenoid biosynthesis? *Progress in Lipid Research, 51*(2), 95–148.

Hernández-Alvarez, E., Blanco-Navarro, I., Pérez-Sacristán, B., Sánchez-Siles, L. M., & Granado-Lorencio, F. (2016). In vitro digestion-assisted development of a β-cryptoxanthin-rich functional beverage; in vivo validation using systemic response and faecal content. *Food Chemistry, 208*, 18-25.

Higuera-Ciapara, I., Félix-Valenzuela, L., & Goycoolea, F. M. (2006). Astaxanthin: A Review of its Chemistry and Applications. *Critical Reviews in Food Science and Nutrition, 46*(2), 185-196.

Hiwasa-Tanase, K., Kuroda, H., Hirai, T., Aoki, K., Takane, K., & Ezura, H. (2012). Novel promoters that induce specific transgene expression during the green to ripening stages of tomato fruit development. *Plant Cell Reports, 31*(8), 1415-1424.

Holland and Barrett Retail Limited. (2020). Pretty Gorgeous Astaxanthin 30 Capsules. In, vol. 2020).

Hong, M. E., Choi, H. I., Kwak, H. S., Hwang, S.-W., Sung, Y. J., Chang, W. S., & Sim, S. J. (2018). Rapid selection of astaxanthin-hyperproducing Haematococcus mutant via azide-based colorimetric assay combined with oil-based astaxanthin extraction. *Bioresource Technology, 267*, 175-181.

Hornero-Méndez, D., & Mínguez-Mosquera, M. I. (2000). Xanthophyll Esterification Accompanying Carotenoid Overaccumulation in Chromoplast of Capsicum annuum Ripening Fruits Is a Constitutive Process and Useful for Ripeness Index. *Journal of Agricultural and Food Chemistry, 48*(5), 1617-1622.

Hosseini, M., Taherkhani, M., & Ghorbani Nohooji, M. (2019). Introduction of Adonis aestivalis as a new source of effective cytotoxic cardiac glycoside. *Natural Product Research, 33*(6), 915-920.

Hou, X., Rivers, J., León, P., McQuinn, R. P., & Pogson, B. J. (2016). Synthesis and Function of Apocarotenoid Signals in Plants. *Trends in Plant Science, 21*(9), 792-803.

Howitt, C. A., & Pogson, B. J. (2006). Carotenoid accumulation and function in seeds and non-green tissues. *Plant, Cell & Environment, 29*(3), 435-445.

Huang, J.-C., Chen, F., & Sandmann, G. (2006). Stress-related differential expression of multiple β-carotene ketolase genes in the unicellular green alga Haematococcus pluvialis. *Journal of Biotechnology, 122*(2), 176-185.

Huang, J., Zhong, Y., Sandmann, G., Liu, J., & Chen, F. (2012). Cloning and selection of carotenoid ketolase genes for the engineering of high-yield astaxanthin in plants. *Planta, 236*(2), 691-699.

Huang, J. C., Zhong, Y. J., Liu, J., Sandmann, G., & Chen, F. (2013). Metabolic engineering of tomato for high-yield production of astaxanthin. *Metabolic engineering, 17*, 59-67.

Ilg, A., Bruno, M., Beyer, P., & Al-Babili, S. (2014). Tomato carotenoid cleavage dioxygenases 1A and 1B: Relaxed double bond specificity leads to a plenitude of dialdehydes, mono-apocarotenoids and isoprenoid volatiles. *FEBS Open Bio, 4*, 584-593.

Isaacson, T., Ohad, I., Beyer, P., & Hirschberg, J. (2004). Analysis in vitro of the enzyme CRTISO establishes a poly-cis-carotenoid biosynthesis pathway in plants. *Plant Physiology, 136*(4), 4246-4255.

Isaacson, T., Ronen, G., Zamir, D., & Hirschberg, J. (2002). Cloning of tangerine from tomato reveals a carotenoid isomerase essential for the production of beta-carotene and xanthophylls in plants. *The Plant cell, 14*(2), 333-342.

Jarvis, P., & López-Juez, E. (2013). Biogenesis and homeostasis of chloroplasts and other plastids. *Nature Reviews Molecular Cell Biology, 14*(12), 787-802.

Jayaraj, J., Devlin, R., & Punja, Z. (2008). Metabolic engineering of novel ketocarotenoid production in carrot plants. *Transgenic Research, 17*(4), 489-501.

Joyard, J., Ferro, M., Masselon, C., Seigneurin-Berny, D., Salvi, D., Garin, J., & Rolland, N. (2009). Chloroplast Proteomics and the Compartmentation of Plastidial Isoprenoid Biosynthetic Pathways. *Molecular Plant, 2*(6), 1154-1180.

Karimi, M. (2010). pEN-L4-PPC2-R1. In, vol. 2020): VIB-UGENT center for plant systems biology.

Karniel, U., Koch, A., Zamir, D., & Hirschberg, J. (2020). Development of zeaxanthin-rich tomato fruit through genetic manipulations of carotenoid biosynthesis. *Plant Biotechnology Journal, n/a*(n/a).

Kaunda, J. S., & Zhang, Y. J. (2019). The Genus Solanum: An Ethnopharmacological, Phytochemical and Biological Properties Review. *Nat Prod Bioprospect, 9*(2), 77-137.

Khan, M. Z., Takemure, M., Maoka, T., Otani, M., & Misawa, N. (2016). Carotenoid analysis of sweetpotato *Ipomoea batatas* and functional identification of its lycopene β- and ε-cyclase genes. *Zeitschrift für Naturforschung C, 71*(9).

Khoo, K. S., Lee, S. Y., Ooi, C. W., Fu, X., Miao, X., Ling, T. C., & Show, P. L. (2019). Recent advances in biorefinery of astaxanthin from Haematococcus pluvialis. *Bioresource Technology, 288*, 121606.

Kishimoto, S., Oda-Yamamizo, C., & Ohmiya, A. (2020). Heterologous expression of xanthophyll esterase genes affects carotenoid accumulation in petunia corollas. *Scientific reports, 10*(1), 1299-1299.

Klimov, V. V. (2002). Discovery of pheophytin function in the photosynthetic energy conversion as the primary electron acceptor of Photosystem II. *Photosynthesis Research, 76*, 247-253.

Knapp, S. (2002). Tobacco to tomatoes: a phylogenetic perspective on fruit diversity in the Solanaceae. *Journal of Experimental Botany, 53*(377), 2001-2022.

Kohlen, W., Charnikhova, T., Lammers, M., Pollina, T., Tóth, P., Haider, I., Pozo, M. J., de Maagd, R. A., Ruyter-Spira, C., Bouwmeester, H. J., & López-Ráez, J. A. (2012). The tomato CAROTENOID CLEAVAGE DIOXYGENASE8 (SlCCD8) regulates rhizosphere signaling, plant architecture and affects reproductive development through strigolactone biosynthesis. *New Phytologist, 196*(2), 535-547.

Kothari, D., Lee, J.-H., Chon, J.-W., Seo, K.-H., & Kim, S.-K. (2019). Improved astaxanthin production by Xanthophyllomyces dendrorhous SK984 with oak leaf extract and inorganic phosphate supplementation. *Food Science and Biotechnology, 28*(4), 1171-1176.

Kurowska, M., Daszkowska-Golec, A., Gruszka, D., Marzec, M., Szurman, M., Szarejko, I., & Maluszynski, M. (2011). TILLING: a shortcut in functional genomics. *Journal of applied genetics, 52*(4), 371-390.

Li, R., Links, M. G., Gjetvaj, B., Sharpe, A., & Hannoufa, A. (2008). Development of an Adonis aestivalis expressed sequence tag population as a resource for genes of the carotenoid pathway. *Genome, 51*(11), 888-896.

Li, X., Wang, Y., Chen, S., Tian, H., Fu, D., Zhu, B., Luo, Y., & Zhu, H. (2018). Lycopene Is Enriched in Tomato Fruit by CRISPR/Cas9-Mediated Multiplex Genome Editing. *Frontiers in Plant Science, 9*(559).

Lignell, Å., & Böttiger, P. (2001). Use of xanthophylls, astaxanthin e.g., for treatment of autoimmune disease, chronic viral and intracellular bacterial infections. In Astacarotene (Ed.)). World.

Lim, K. C., Yusoff, F. M., Shariff, M., & Kamarudin, M. S. (2018). Astaxanthin as feed supplement in aquatic animals. *Reviews in Aquaculture, 10*(3), 738-773.

Linden, H. (1999). Carotenoid hydroxylase from Haematococcus pluvialis: cDNA sequence, regulation and functional complementation. *Biochimica et Biophysica Acta (BBA) - Gene Structure and Expression, 1446*(3), 203-212.

Lindqvist, A., & Andersson, S. (2002). Biochemical Properties of Purified Recombinant Human β-Carotene 15,15′-Monooxygenase. *Journal of Biological Chemistry, 277*(26), 23942-23948.

Lippold, F., vom Dorp, K., Abraham, M., Hölzl, G., Wewer, V., Yilmaz, J. L., Lager, I., Montandon, C., Besagni, C., Kessler, F., Stymne, S., & Dörmann, P. (2012). Fatty Acid Phytyl Ester Synthesis in Chloroplasts of Arabidopsis. *The Plant cell, 24*(5), 2001-2014.

Liu, Z., Yan, H., Wang, K., Kuang, T., Zhang, J., Gui, L., An, X., & Chang, W. (2004). Crystal structure of spinach major light-harvesting complex at 2.72 Å resolution. *Nature, 428*(6980), 287-292.

Lobo, V., Patil, A., Phatak, A., & Chandra, N. (2010). Free radicals, antioxidants and functional foods: Impact on human health. *Pharmacognosy Review, 4*(8), 118-126.

Mann, V., Harker, M., Pecker, I., & Hirschberg, J. (2000). Metabolic engineering of astaxanthin production in tobacco flowers. *Nature Biotechnology, 18*(8), 888-892.

Mann, V., Pecker, I., & Hirschberg, J. (1994). Cloning and characterization of the gene for phytoene desaturase (Pds) from tomato (Lycopersicon esculentum). *Plant Mol Biol, 24*(3), 429-434.

Manshardt, R. (2004). Crop Improvement by Conventional Breeding or Genetic Engineering: How Different Are They? *Cooperative extension service*.

Maoka, T. (2020). Carotenoids as natural functional pigments. *Journal of natural medicines, 74*(1), 1-16.

Maoka, T., Etoh, T., Kishimoto, S., & Sakata, S. (2011). Carotenoids and Their Fatty Acid Esters in the Petals of Adonis aestivalis. *Journal of Oleo Science, 60*(2), 47-52.

Markets and Markets. (2020). Carotenoids Market. In M. a. Markets (Ed.), *Market research reports*).

Masamoto, K., Misawa, N., Kaneko, T., Kikuno, R., & Toh, H. (1998). rβCarotene Hydroxylase Gene from the Cyanobacterium Synechocystis sp. PCC6803. *Plant and Cell Physiology, 39*(5), 560-564.

McWilliams, A. (2018). The Global Market for Carotenoids. In *FOD025F*). BCC Research: BCC publishing.

Menin, B., Santabarbara, S., Lami, A., Musazzi, S., Villafiorita Monteleone, F., & Casazza, A. P. (2019). Non-endogenous ketocarotenoid accumulation in engineered Synechocystis sp. PCC 6803. *Physiologia Plantarum, 166*(1), 403-412.

Mercadante, A. Z., Rodrigues, D. B., Petry, F. C., & Mariutti, L. R. B. (2017). Carotenoid esters in foods - A review and practical directions on analysis and occurrence - ScienceDirect. *Food research international, 99*(2), 830-850.

Minguez-Mosquera, M. I., & Hornero-Mendez, D. (1994). Changes in Carotenoid Esterification during the Fruit Ripening of Capsicum annuum Cv. Bola. *Journal of Agricultural and Food Chemistry, 42*(3), 640-644.

Minoia, S., Petrozza, A., D'Onofrio, O., Piron, F., Mosca, G., Sozio, G., Cellini, F., Bendahmane, A., & Carriero, F. (2010). A new mutant genetic resource for tomato crop improvement by TILLING technology. *BMC research notes, 3*, 69-69.

Misawa, N., Kajiwara, S., Kondo, K., Yokoyama, A., Satomi, Y., Saito, T., Miki, W., & Ohtani, T. (1995). Canthaxanthin Biosynthesis by the Conversion of Methylene to Keto Groups in a Hydrocarbon β-Carotene by a Single Gene. *209*(3), 867–876.

Misawa, N., Nakagawa, M., Kobayashi, K., Yamano, S., Izawa, Y., Nakamura, K., & Harashima, K. (1990). Elucidation of the Erwinia uredovora carotenoid biosynthetic pathway by functional analysis of gene products expressed in Escherichia coli. *J Bacteriol, 172*(12), 6704-6712.

Misawa, N., Satomi, Y., Kondo, K., Yokoyama, A., Kajiwara, S., Saito, T., Ohtani, T., & Miki, W. (1995). Structure and functional analysis of a marine bacterial carotenoid biosynthesis gene cluster and astaxanthin biosynthetic pathway proposed at the gene level. *J Bacteriol, 177*(22), 6575-6584.

Mochimaru, M., Masukawa, H., & Takaichi, S. (2005). The cyanobacterium Anabaena sp. PCC 7120 has two distinct β-carotene ketolases: CrtO for echinenone and CrtW for ketomyxol synthesis. *FEBS Letters, 579*(27), 6111-6114.

Mohan, V., Pandey, A., Sreelakshmi, Y., & Sharma, R. (2016). Neofunctionalization of Chromoplast Specific Lycopene Beta Cyclase Gene (CYC-B) in Tomato Clade. *PLOS, 11*(4).

Morris, W. L., Ducreux, L. J. M., Fraser, P. D., Millam, S., & Taylor, M. A. (2006). Engineering ketocarotenoid biosynthesis in potato tubers. *Metabolic engineering, 8*(3), 253-263.

Mortimer, C. L. (2010). Metabolic engineering of ketocarotenoids in Solanaceae; their biosynthesis and sequestration. *Royal Holloway University of London*.

Mortimer, C. L., Misawa, N., Ducreux, L., Campbell, R., Bramley, P. M., Taylor, M., & Fraser, P. D. (2016). Product stability and sequestration mechanisms in Solanum tuberosum engineered to biosynthesize high value ketocarotenoids. *Plant Biotechnol J, 14*(1), 140-152.

Mortimer, C. L., Misawa, N., Perez-Fons, L., Robertson, F. P., Harada, H., Bramley, P. M., & Fraser, P. D. (2017). The Formation and Sequestration of Nonendogenous Ketocarotenoids in Transgenic Nicotiana glauca. *Plant Physiology, 173*(3), 1617-1635.

Mueller, L. A., Solow, T. H., Taylor, N., Skwarecki, B., Buels, R., Binns, J., Lin, C., Wright, M. H., Ahrens, R., Wang, Y., Herbst, E. V., Keyder, E. R., Menda, N., Zamir, D., & Tanksley, S. D. (2005). The SOL Genomics Network. A Comparative Resource for Solanaceae Biology and Beyond. *Plant Physiology, 138*(3), 1310-1317.

NBRP. (2012). TOMATOMA Tomato Mutants Archive. In, vol. 2020).

Neuman, H., Galpaz, N., Cunningham Jr, F. X., Zamir, D., & Hirschberg, J. (2014). The tomato mutation nxd1 reveals a gene necessary for neoxanthin biosynthesis and demonstrates that violaxanthin is a sufficient precursor for abscisic acid biosynthesis. *The Plant Journal, 78*(1), 80-93.

Nogueira, M. (2013). Optimisation of high-value isoprenoid production in plants. Potential strategies and insight into carotenoid sequestration. *Royal Holloway University of London*.

Nogueira, M., Berry, H., Nohl, R., Klompmaker, M., Holden, A., & Fraser, P. D. (2016). Subchromoplast Fractionation Protocol for Different Solanaceae Fruit Species. *Bio-protocol, 6*(13), e1861.

Nogueira, M., Enfissi, E. M. A., Almeida, J., & Fraser, P. D. (2018). Creating plant molecular factories for industrial and nutritional isoprenoid production. *Current Opinion in Biotechnology, 49*, 80-87.

Nogueira, M., Enfissi, E. M. A., Martínez Valenzuela, M. E., Menard, G. N., Driller, R. L., Eastmond, P. J., Schuch, W., Sandmann, G., & Fraser, P. D. (2017). Engineering of tomato for the sustainable production of ketocarotenoids and its evaluation in aquaculture feed. *Proceedings of the National Academy of Sciences*, 201708349.

Nogueira, M., Enfissi, E. M. A., Welsch, R., Beyer, P., Zurbriggen, M. D., & Fraser, P. D. (2019). Construction of a fusion enzyme for astaxanthin formation and its characterisation in microbial and plant hosts: A new tool for engineering ketocarotenoids. *Metabolic engineering, 52*, 243-252.

Nogueira, N., Berry, H., Nohl, R., Klompmaker, M., Holden, A., & Fraser, P. D. (2016). Subchromoplast Fractionation Protocol for Different ... *Bio-protocol, 8*(13).

Omenn, G. S., Goodman, G. E., Thornquist, M. D., Balmes, J., Cullen, M. R., Glass, A., Keogh, J. P., Meyskens, F. L., Valanis, B., Williams, J. H., Barnhart, S., & Hammar, S. (1996). Effects of a Combination of Beta Carotene and Vitamin A on Lung Cancer and Cardiovascular Disease. *New England Journal of Medicine, 334*(18), 1150-1155.

Ordonez, N., Seidl, M. F., Waalwijk, C., Drenth, A., Kilian, A., Thomma, B. P. H. J., Ploetz, R. C., & Kema, G. H. J. (2015). Worse Comes to Worst: Bananas and Panama Disease--When Plant and Pathogen Clones Meet. *PLoS pathogens, 11*(11), e1005197-e1005197.

Paine, J. A., Shipton, C. A., Chaggar, S., Howells, R. M., Kennedy, M. J., Vernon, G., Wright, S. Y., Hinchliffe, E., Adams, J. L., Silverstone, A. L., & Drake, R. (2005). Improving the nutritional value of Golden Rice through increased pro-vitamin A content. *Nat Biotechnol, 23*(4), 482-487.

Park, H., Kreunen, S. S., Cuttriss, A. J., DellaPenna, D., & Pogson, B. J. (2002). Identification of the Carotenoid Isomerase Provides Insight into Carotenoid Biosynthesis, Prolamellar Body Formation, and Photomorphogenesis. *The Plant cell, 14*(2), 321.

Pérez-Gálvez, A., Martin, H. D., Sies, H., & Stahl, W. (2007). Incorporation of carotenoids from paprika oleoresin into human chylomicrons. *British Journal of Nutrition, 89*(6), 787-793.

Pierce, E. C., LaFayette, P. R., Ortega, M. A., Joyce, B. L., Kopsell, D. A., & Parrott, W. A. (2015). Ketocarotenoid Production in Soybean Seeds through Metabolic Engineering. *PloS one, 10*(9), e0138196-e0138196.

Polivka, T., & Frank, H. A. (2010). Molecular factors controlling photosynthetic light harvesting by carotenoids. *Acc Chem Res, 43*(8), 1125-1134.

Quinet, M., Angosto, T., Yuste-Lisbona, F. J., Blanchard-Gros, R., Bigot, S., Martinez, J. P., & Lutts, S. (2019). Tomato Fruit Development and Metabolism. *Front Plant Sci, 10*.

Racsko, J., & Schrader, L. E. (2012). Sunburn of Apple Fruit: Historical Background, Recent Advances and Future Perspectives. *Critical Reviews in Plant Sciences, 31*(6), 455-504.

Ralley, L., Enfissi, E. M., Misawa, N., Schuch, W., Bramley, P. M., & Fraser, P. D. (2004). Metabolic engineering of ketocarotenoid formation in higher plants. *Plant J, 39*(4), 477-486.

Rapacz, E. (2019). Development of tomato genotypeswith enhanced xanthophyll content in ripe fruit. *Royal Holloway University of London*.

Richaud, D., Stange, C., Gadaleta, A., Colasuonno, P., Parada, R., & Schwember, A. R. (2018). Identification of Lycopene epsilon cyclase (LCYE) gene mutants to potentially increase β-carotene content in durum wheat (Triticum turgidum L.ssp. durum) through TILLING. *PloS one, 13*(12), e0208948.

Rockholm, D. C., & Yamamoto, H. Y. (1996). Violaxanthin De-Epoxidase (Purification of a 43-Kilodalton Lumenal Protein from Lettuce by Lipid-Affinity Precipitation with Monogalactosyldiacylglyceride). *Plant Physiology, 110*(2), 697.

Rohmer, M. K., M.; Simonin, P.; Sutter, B.; Sahm, H. (1993). Isoprenoid biosynthesis in bacteria: a novel pathway for the early steps leading to isopentenyl diphosphate. *Biochemical Journal, 295*, 517-524.

Ronen, G., Carmel-Goren, L., Zamir, D., & Hirschberg, J. (2000). An alternative pathway to β-carotene formation in plant chromoplasts discovered by map-based cloning of Beta and old-gold color mutations in tomato. *PNAS, 97*(20), 11102-11107.

Rottet, S., Devillers, J., Glauser, G., Douet, V., Besagni, C., & Kessler, F. (2016). Identification of Plastoglobules as a Site of Carotenoid Cleavage. *Frontiers in Plant Science, 7*, 1855-1855.

Rowles, J. L., & Erdman, J. W. (2020). Carotenoids and their role in cancer prevention. *Biochimica et Biophysica Acta (BBA) - Molecular and Cell Biology of Lipids*, 158613.

Science Literacy Project. (2016). Where are GMO crops and animals approved and banned? In, vol. 2020).

Seppanen, C. M., Song, Q., & Csallany, A. S. (2010). The Antioxidant Functions of Tocopherol and Tocotrienol Homologues in Oils, Fats, and Food Systems | SpringerLink. *Journal of the American Oil Chemists' Society, 87*(5), 469-481.

Seybold, A., & Goodwin, T. W. (1959). Occurrence of Astaxanthin in the Flower Petals of Adonis annua L. *Nature, 184*(4700), 1714-1715.

SGN. (2014). International Tomato Genome Sequencing Project. In, vol. 2020).

Sheludko, Y. V. (2010). Recent advances in plant biotechnology and genetic engineering for production of secondary metabolites. *Cytology and Genetics, 44*(1), 52-60.

Shindo, K., Hasunuma, T., Asagi, E., Sano, A., Hotta, E., Minemura, N., Miyake, C., Maoka, T., & Misawa, N. (2008). 4-Ketoantheraxanthin, a novel carotenoid produced by the combination of the bacterial enzyme β-carotene ketolase CrtW and endogenous carotenoid biosynthetic enzymes in higher plants. *Tetrahedron Letters, 49*(20), 3294-3296.

Silletti, M. F., Petrozza, A., Stigliani, A. L., Giorio, G., Cellini, F., D'Ambrosio, C., & Carriero, F. (2013). An increase of lycopene content in tomato fruit is associated with a novel Cyc-B allele isolated through TILLING technology. *Molecular Breeding, 31*(3), 665-674.

Simkin, A. J., Schwartz, S. H., Auldridge, M., Taylor, M. G., & Klee, H. J. (2004). The tomato carotenoid cleavage dioxygenase 1 genes contribute to the formation of the flavor

volatiles β-ionone, pseudoionone, and geranylacetone. *The Plant Journal, 40*(6), 882-892.
Singh, D. P., Khattar, J. S., Rajput, A., Chaudhary, R., & Singh, R. (2019). High production of carotenoids by the green microalga Asterarcys quadricellulare PUMCC 5.1.1 under optimized culture conditions. *PloS one, 14*(9), e0221930-e0221930.
Siti, H., N., Kamisah, Y., & Kamsiah, J. (2015). The role of oxidative stress, antioxidants and vascular inflammation in cardiovascular disease (a review). *Vascular Pharmacology, 71*, 40-56.
Stahl, W., & Sies, H. (2007). Carotenoids and Flavonoids Contribute to Nutritional Protection against Skin Damage from Sunlight. *Molecular Biotechnology, 37*(1), 26-30.
Stålberg, K., Lindgren, O., Ek, B., & Höglund, A.-S. (2003). Synthesis of ketocarotenoids in the seed of Arabidopsis thaliana. *The Plant Journal, 36*(6), 771-779.
Stam, M., Mol, J. N. M., & Kooter, J. M. (1997). Review Article: The Silence of Genes in Transgenic Plants. *Annals of Botany, 79*(1), 3-12.
Stigliani, A. L., Giorio, G., & D'Ambrosio, C. (2011). Characterization of P450 Carotenoid β- and ε-Hydroxylases of Tomato and Transcriptional Regulation of Xanthophyll Biosynthesis in Root, Leaf, Petal and Fruit. *Plant and Cell Physiology, 52*(5), 851-865.
Sun, L., Yuan, B., Zhang, M., Wang, L., Cui, M., Wang, Q., & Leng, P. (2012). Fruit-specific RNAi-mediated suppression of SlNCED1 increases both lycopene and beta-carotene contents in tomato fruit. *J Exp Bot, 63*(8), 3097-3108.
Sun, S., Wang, X., Wang, K., & Cui, X. (2019). Dissection of complex traits of tomato in the post-genome era. *Theoretical and Applied Genetics*.
Sun, T., & Li, L. (2020). Toward the 'golden' era: The status in uncovering the regulatory control of carotenoid accumulation in plants. *Plant Science, 290*, 110331.
Sun, T., Yuan, H., Cao, H., Yazdani, M., Tadmor, Y., & Li, L. (2018). Carotenoid Metabolism in Plants: The Role of Plastids. *Molecular Plant, 11*(1), 58-74.
Suzuki, S., Nishihara, M., Nakatsuka, T., Misawa, N., Ogiwara, I., & Yamamura, S. (2007). Flower color alteration in Lotus japonicus by modification of the carotenoid biosynthetic pathway. *Plant Cell Reports, 26*(7), 951-959.
Tandon, K. S., Baldwin, E. A., Scott, J. W., & Shewfelt, R. L. (2003). Linking Sensory Descriptors to Volatile and Nonvolatile Components of Fresh Tomato Flavor. *Journal of Food Science, 68*(7), 2366-2371.
Tang, G., Qin, J., Dolnikowski, G. G., Russell, R. M., & Grusak, M. A. (2009). Golden Rice is an effective source of vitamin A. *Am J Clin Nutr, 89*(6), 1776-1783.
The Royal Society. (2016). What GM crops are currently being grown and where? In T. R. Society (Ed.), vol. 2020).
Tieman, D., Zhu, G., Resende, M. F. R., Lin, T., Nguyen, C., Bies, D., Rambla, J. L., Beltran, K. S. O., Taylor, M., Zhang, B., Ikeda, H., Liu, Z., Fisher, J., Zemach, I., Monforte, A., Zamir, D., Granell, A., Kirst, M., Huang, S., & Klee, H. (2017). A chemical genetic roadmap to improved tomato flavor. *Science, 355*(6323), 391.
Tomato Genome Consortium. (2012). The tomato genome sequence provides insights into fleshy fruit evolution. *Nature, 485*(7400), 635-641.
Tyagi, S., Choudhary, R., Das, A., Won, S. Y., & Shukla, P. (2020). CRISPR-Cas9 system: a genome-editing tool with endless possibilities. *Journal of Biotechnology*.
Van den Berg, R. A., Hoefsloot, H. C. J., Westerhuis, J. A., Smilde, A. K., & Van der Werf, M. J. (2006). Centering, scaling, and transformations: improving the biological information content of metabolomics data. *BMC Genomics, 7*(1), 142.

Vaucheret, H., Béclin, C., Elmayan, T., Feuerbach, F., Godon, C., Morel, J.-B., Mourrain, P., Palauqui, J.-C., & Vernhettes, S. (1998). Transgene-induced gene silencing in plants. *The Plant Journal, 16*(6), 651-659.

Vishnevetsky, M., Ovadis, M., & Vainstein, A. (1999). Carotenoid sequestration in plants: the role of carotenoid-associated proteins. *Trends in Plant Science, 4*(6), 232-235.

Visser, H., van Ooyen, A. J. J., & Verdoes, J. C. (2003). Metabolic engineering of the astaxanthin-biosynthetic pathway of Xanthophyllomyces dendrorhous. *FEMS Yeast Research, 4*(3), 221-231.

Vitagene. (2018). Astaxanthin. In, vol. 2020).

Viuda-Martos, M., Sanchez-Zapata, E., Sayas-Barberá, E., Sendra, E., Pérez-Álvarez, J. A., & Fernández-López, J. (2014). Tomato and Tomato Byproducts. Human Health Benefits of Lycopene and Its Application to Meat Products: A Review. *Critical Reviews in Food Science and Nutrition, 54*(8), 1032-1049.

Vogel, J. T., Walter, M. H., Giavalisco, P., Lytovchenko, A., Kohlen, W., Charnikhova, T., Simkin, A. J., Goulet, C., Strack, D., Bouwmeester, H. J., Fernie, A. R., & Klee, H. J. (2010). SlCCD7 controls strigolactone biosynthesis, shoot branching and mycorrhiza-induced apocarotenoid formation in tomato. *The Plant Journal, 61*(2), 300-311.

Vos;, C. J. d., & Swanenburg, M. (2018). Health effects of feeding genetically modified (GM) crops to livestock animals: A review. *Food and Chemical Toxicology, 117*, 3-12.

Wada, N., Ueta, R., Osakabe, Y., & Osakabe, K. (2020). Precision genome editing in plants: state-of-the-art in CRISPR/Cas9-based genome engineering. *BMC Plant Biology, 20*(1), 234.

Walter, M. H., & Strack, D. (2011). Carotenoids and their cleavage products: Biosynthesis and functions. *Natural Product Reports, 28*(4), 663-692.

Watkins, J. L., Li, M., McQuinn, R. P., Chan, K. X., McFarlane, H. E., Ermakova, M., Furbank, R. T., Mares, D., Dong, C., Chalmers, K. J., Sharp, P., Mather, D. E., & Pogson, B. J. (2019). A GDSL Esterase/Lipase Catalyzes the Esterification of Lutein in Bread Wheat. *The Plant cell, 31*(12), 3092.

Weber, E., Engler, C., Gruetzner, R., Werner, S., & Marillonnet, S. (2011). A Modular Cloning System for Standardized Assembly of Multigene Constructs. *PloS one, 6*(2).

Wei, Y., Wan, H., Wu, Z., Wang, R., Ruan, M., Ye, Q., Li, Z., Zhou, G., Yao, Z., & Yang, Y. (2016). A Comprehensive Analysis of Carotenoid Cleavage Dioxygenases Genes in Solanum Lycopersicum. *Plant Molecular Biology Reporter, 34*(2), 512-523.

Wingerath, T., Sies, H., & Stahl, W. (1998). Xanthophyll Esters in Human Skin. *Archives of Biochemistry and Biophysics, 355*(2), 271-274.

Woods, L. W., George, L. W., Anderson, M. L., Woods, D. M., Filigenzi, M. S., & Puschner, B. (2007). Evaluation of the Toxicity of Adonis Aestivalis in Calves. *Journal of Veterinary Diagnostic Investigation, 19*(5), 581-585.

World Health Organisation. (1997). Vitamin A Supplements: A Guide to Their Use in the Treatment and Prevention of Vitamin A Deficiency and Xerophthalmia: World Health Organisation.

Xu, R.-F., Li, H., Qin, R.-Y., Li, J., Qiu, C.-H., Yang, Y.-C., Ma, H., Li, L., Wei, P.-C., & Yang, J.-B. (2015). Generation of inheritable and "transgene clean" targeted genome-modified rice in later generations using the CRISPR/Cas9 system. *Scientific reports, 5*, 11491-11491.

Yamamoto, H. Y., Nakayama, T. O. M., & Chichester, C. O. (1962). Studies on the light and dark interconversions of leaf xanthophylls. *Archives of Biochemistry and Biophysics, 97*(1), 168-173.

Yang, W. R. G. S. A. Q. (2019). Effects of Replacing Fishmeal with Soybean Products in Fish and Crustaceans Performance. *Journal of Aquaculture Research & Development, 10*(9).

Yang, Y., Kim, B., & Lee, J.-Y. (2013). Astaxanthin structure, metabolism, and health benefits. *J. Hum. Nutr. Food Sci., 1*, 1003-1014.

Ye, X., Al-Babili, S., Kloti, A., Zhang, J., Lucca, P., Beyer, P., & Potrykus, I. (2000). Engineering the provitamin A (beta-carotene) biosynthetic pathway into (carotenoid-free) rice endosperm. *Science, 287*(5451), 303-305.

Zhao, L., Lu, L., Zhang, L., Wang, A., Wang, N., Liang, Z., Lu, X., & Tang, K. (2009). Molecular evolution of the E8 promoter in tomato and some of its relative wild species. *J Biosci, 34*(1), 71-83.

Zheng, X., Guliano, G., & Al-Babili, S. (2020). Carotenoid biofortification in crop plants: citius, altius, fortius. *Biochim Biophys Acta Mol Cell Biol Lipids*, 158664.

Zhong, Y.-J., Huang, J.-C., Liu, J., Li, Y., Jiang, Y., Xu, Z.-F., Sandmann, G., & Chen, F. (2011). Functional characterization of various algal carotenoid ketolases reveals that ketolating zeaxanthin efficiently is essential for high production of astaxanthin in transgenic Arabidopsis. *Journal of Experimental Botany, 62*(10), 3659-3669.

Zhu, C., Gerjets, T., & Sandmann, G. (2007). Nicotiana glauca engineered for the production of ketocarotenoids in flowers and leaves by expressing the cyanobacterial crtO ketolase gene. *Transgenic Research, 16*(6), 813-821.

Zhu, C., Naqvi, S., Capell, T., & Christou, P. (2009). Metabolic engineering of ketocarotenoid biosynthesis in higher plants. *Arch Biochem Biophys, 483*(2), 182-190.

Zhu, G., Wang, S., Huang, Z., Zhang, S., Liao, Q., Zhang, C., Lin, T., Qin, M., Peng, M., Yang, C., Cao, X., Han, X., Wang, X., van der Knaap, E., Zhang, Z., Cui, X., Klee, H., Fernie, A. R., Luo, J., & Huang, S. (2018). Rewiring of the Fruit Metabolome in Tomato Breeding. *Cell, 172*(1), 249-261.e212.

Zhu, Q., Zeng, D., Yu, S., Cui, C., Li, J., Li, H., Chen, J., Zhang, R., Zhao, X., Chen, L., & Liu, Y.-G. (2018). From Golden Rice to aSTARice: Bioengineering Astaxanthin Biosynthesis in Rice Endosperm. *Molecular Plant, 11*(12), 1440-1448.

Ziegler, R. G. (1989). A review of epidemiologic evidence that carotenoids reduce the risk of cancer. *The Journal of Nutrition, 119*(1), 116-122.